



INTERNATIONAL DOCTORAL
SCHOOL OF THE USC

Basma
Al Janabi

PhD Thesis

Transitional metallacycles with
nitrogen and phosphorus
ligands

Santiago de Compostela, 2022

Programa de Doutoramento en Ciencia e Tecnoloxía Química



PhD Thesis

*Transitional metallacycles with
nitrogen and phosphorus
ligands*

Basma Al Janabi

ESCUELA DE DOCTORADO INTERNACIONAL DE LA UNIVERSIDAD DE
SANTIAGO DE COMPOSTELA

PROGRAMA DE DOCTORADO EN CIENCIA Y TECNOLOGÍA QUÍMICA

Santiago de Compostela

2022





DECLARACIÓN DE LA AUTORA DE LA TESIS

TRANSITIONAL METALLACYCLES WITH NITROGEN AND PHOSPHORUS LIGANDS

Dna. Basma Al Janabi

Presento mi tesis, siguiendo el procedimiento adecuado al Reglamento, y declaro que:

- 1) La tesis abarca los resultados de la elaboración de mi trabajo.
- 2) De ser el caso, en la tesis se hace referencia a las colaboraciones que tuvo este trabajo.
- 3) Confirmando que la tesis no incurre en ningún tipo de plagio de otros autores ni de trabajos presentados por mí para la obtención de otros títulos.
- 4) La tesis es la versión definitiva presentada para su defensa y coincide la versión impresa con la presentada en formato electrónico.

En Santiago de Compostela, 21 de outubro de 2022.





AUTORIZACIÓN DO DIRECTOR / TITOR DA TESE

D. José Manuel Vila Abad
En condición de: Titor e Director

D. Juan Manuel Ortigueira Amor
En condición de: Director

INFORMA/N:

Que la presente tesis, se corresponde con el trabajo realizado por Dna Basma Al Janabi, bajo mi dirección/tutorización, y autorizo su presentación, considerando que reúne los requisitos exigidos en el Regulamento de Estudos de Doutoramento da USC, y que como director/titor de esta no incurre en las causas de abstención establecidas en la Lei 40/2015.

De acuerdo con lo indicado en el Regulamento de Estudos de Doutoramento, declara también que la presente tesis de doctoral es idónea para ser defendida sobre la base de la modalidad Monográfica.

En Santiago de Compostela, 21 de outubro de 2022.



Fdo. José Manuel Vila Abad

Fdo. Juan Manuel Ortigueira Amor

Abstract

Cyclometallated compounds are characterized by possessing a σ bond linking a carbon atom to a metal atom, plus a coordination bond between the metal and a donor atom from the ligand, thus giving rise to a metallacycle comprising both the metal and (in part) the ligand. Since the first cyclometallated compounds were found in 1963 by Kleinman and Dubeck the number of such species has come to be overwhelming. They become rather important due to their good stability and because they present the possibility of C–H bond activation. Although many metals are adequate for preparing cyclometallated compounds, one of the most widely used is palladium, mainly because of the easiness of the syntheses, as well as for the numerous applications the ensuing compounds show. Among these are their role as pre-catalysts in carbon-carbon bond formation processes, for LED devices, applications as sensors, and in biomedical research as antineoplastic substances. In the case of palladium the cyclometallated complexes have been coined as the palladacycles.

One of the most frequently used ligands for cyclometallation processes are the Schiff base ligands, also known as imines. They are rather versatile for a number of reasons: the synthetic behavior against transition metals, especially palladium, is outstanding, with the reactions more often than not producing reasonable yields; the number of nitrogen donors, as well as their relative positions on the phenyl ring may be varied at will, as is the present case where one or two donors were used as was appropriate; the C=N double bond may be split quite easily to give the corresponding C=O double bond. Furthermore, the resulting complexes have a number of different bonds at the metal center, which in the case of palladium (this work) may be summarized as follows: a palladium-carbon bond, a palladium-nitrogen bond, palladium-halide bonds, and in the corresponding derivatives palladium-phosphorus bonds. In fact complexes with all four differing bonds at palladium are known.

The main objective of this work was to synthesize and to study the cyclometallated compounds derived from imine ligands and palladium. This also includes synthesis of the phosphine derivatives for which mono- di- and triphosphine ligands were employed.

Initially the research was about reactions including imines with more than one donor, for which purpose the ligands were made from the aldehydes, isophthalaldehyde and terephthalaldehyde. Firstly, the dinuclear acetato-bridged complexes were obtained, which showed a C=O double bond produced after purification by column chromatography from the parent C=N double bond. This is an interesting result because it means a method for functionalization of the complexes. Then, the C=O group could be condensed with a variety of aminophosphines to give new species that behaved as cyclometallated metalloligands, containing either one or two phosphorus donor atoms as was the case.

The complexes where regeneration of the C=N bond was accomplished where then treated with a triphosphine (TRIPHOS) in the hope of again holding tightly the metal atom hindering further reactions and using the resulting compounds as bidentate [P,P] metalloligands. This did not happen and alternatively, the result was the formation of a di-nuclear bis(pentacoordinated) palladium complex, similar to others found earlier in the work of this research group, but from an altogether different reaction route. This puts forward the versatility of the palladacycles to break and form bonds to carbon thus producing either new species or at least new reaction pathways, in the most strict sense of what is known as serendipity. The crystal structure for this complex unequivocally demonstrates the veracity of the spectroscopic data and it confirms the assumption made on the basis of these data.

Chapter 7 deals with the preparation of cyclometallated palladium compounds and their reactions with bidentate phosphines, such as 1,1-bis(diphenylphosphino)ethene (vdpp), a ligand with a C=C double bond. The phosphine vdpp may undergo Michael addition reactions to

the double bond, however, whilst this is rather difficult to obtain on the free phosphine itself, when coordinated in a bidentate fashion (P,P) the double bond is activated and the mentioned addition may proceed smoothly, inclusive at room temperature in some cases. A wide range of nucleophiles may be used to add to the C=C double bond, many of them containing NH or NH₂ groups. In our case the parent complexes were treated with aminophosphines having a PPh₂ group, transforming them into rather large metalloligand-*P* palladacycles. So, this is the second case in the work where the metallacycles give way to new metalloligands, again putting forward the great versatility of these cyclometallated complexes to produce new compounds possessing a yet unknown reactivity.

Chapter 8 is about the palladacycles prepared from potentially tridentate [C,N,S] imines. Their most peculiar characteristic is that reaction between the ligands and the corresponding palladium(II) salt leads to a single nuclear complex with the ligand bonded to the metal through the phenyl carbon, the imine nitrogen and the sulfur atoms, as well as to a terminal chloride ligand. In spite that the sulfur pertains to a non-charged SMe group the tridentate arrangement of the ligand firmly holds the metal, so that reactions can be carried out that involve only one coordination site, leaving the palladium-nitrogen bond intact, and then again only after abstraction of the chloride ligand by treatment with an adequate silver salt. What's more, even strong chelating diphosphines are unable to bond to the metal; this is only possible prior to abstraction of the chloride ligand. An X-ray crystal structural analysis for one of the palladacycles in this chapter shows the geometrical arrangement of the ligand around the palladium atom. It should be noted that in these complexes the metal center is bonded to four different atoms, a rather unusual coordination scheme in this chemistry.

Carbon-carbon bond formation processes are essential for the preparation of bioactive compounds, agrochemicals, and pharmaceuticals. Furthermore, they are employed to create new

organic materials with novel electrical properties. Also, cross-coupling reactions have been one of the most important advances in organic and organometallic synthesis since adequate catalysts were discovered, amongst which palladacycles have emerged as some of the most applicable compounds for such processes, especially in the Suzuki-Miyaura reaction that involves the cross-coupling of organoborane compounds ($\text{Ar}_1\text{-B(OR)}_2$) with electrophiles ($\text{Ar}_2\text{-X}$). In the last chapter, 9, the catalytic activity is commented and the complexes with greater catalytic efficiency are included.

Resumo

Os compostos ciclometalados caracterízanse por posuír unha ligazón s que une un átomo de carbono a un átomo de metal, ademais dunha ligazón de coordinación entre o metal e un átomo donador do ligando, dando lugar así a un metalaciclo que comprende tanto o metal como (en parte) o ligando. Desde que Kleinman e Dubeck atoparon os primeiros compostos ciclometalizados en 1963, o número destas especies chegou a ser abafador. Convertéronse en algo importante debido á súa boa estabilidade e porque presentan a posibilidade de activación da ligazón C-H.

Entre 1965 e 1968, as reaccións de ciclometalación ampliáronse para incluír máis metais de transición. Así, a reacción do paladacíclico foi levada a cabo inicialmente por Cope e Siekman a partir de azobenceno e LiPdCl_4 con activación da ligazón C-H. Posteriormente, utilizouse dimetilbencilamina en metanol para facer un paladacíclico de cinco membros. Os paladaciclos fórmanse cando a ligazón Pd-C se estabiliza por quelación, o que aumenta a estabilidade do produto de organopaladio. Demostrouse que os metais de transición, como Ru, Rh, Os, Pt, Ir, Fe, Ni, Co e Mn, experimentan a reacción de ciclometalación. Debido á activación dos metais, que interactúan facilmente con un par de electróns solitarios do heteroátomo correspondente, considérase que estas reaccións se producen con facilidade. Shaw e Moulton demostraron en 1976 que os complexos de metais de transición de Ni, Pd, Pt, Rh e Ir con ligandos tipo pincer tridentados-[C, P, C] e grupos estéricamente pouco esixentes como o cloruro, o cianuro, o carbonilo ou o fenilacetileno, producen complexos bastante estables. Unha reacción de ciclometalación pode definirse como a formación dun metalaciclo ou un composto organometálico de coordinación intermolecular de cinco membros con, polo menos, unha activación mediada polo metal dunha ligazón de carbono, estabilizado intermolecularmente por dous ou tres átomos doantes neutros. Dispónse dun importante conxunto de coñecementos sobre as súas características e reactividade. A natureza dos ligandos

racionais na química organometálica, en xeral, permite controlar aspectos cinéticos esenciais como a substitución do ligando. Tamén poden ser cinéticamente estables e relativamente lipofílicos, con un estado de oxidación baixo no átomo de metal. Os metais de transición tamén se coñecen como elementos do bloque d porque permiten que os orbitais d contribúan á formación de ligazóns nos seus compostos. Estes elementos teñen unha enerxía de ionización bastante baixa e adoitan estar cargados positivamente, o que os fai dispoñibles para unirse a moitos ligandos. Os compostos ciclometalados obtéñense a partir de substratos con heteroátomos e a activación da ligazón C-H asistida a través dun metal. O termo activación da ligazón C-H utilízase para describir unha reacción na que unha ligazón C-H inerte se substitúe por outro grupo funcional nun só paso. Unha ligazón C-H é un substrato reactivo no que se forma un ligazón carbono-metal ao escindir unha ligazón C-H inerte cunha especie metálica.

Existen tres tipos diferentes de activación de C-H

- i) para a adición oxidativa de ligazóns C-H requírese un centro metálico rico en electróns e de baixo estado de oxidación. Os metais de transición iridio e rodio son os máis comunmente ciclometalados.
- b) A metátesis de ligazóns σ da ligazón C-H realízase con centros metálicos pobres en electróns, como os metais de transición temperáns de elevado estado de oxidación e os lantánidos.
- c) A activación electrofílica da ligazón electrónica obsérvase con metais de transición pobres en electróns. Debido ás aplicacións catalíticas e ao feito de que estas reaccións son sensibles á auga e ao osíxeno, son as máis investigadas na síntese orgánica.

O acetato de paladio(II) é un dos precursores de metalización máis utilizados. Ao reaccionar o trímero cun exceso de NaOAc, pode dividirse facilmente en monomérico $[\text{Pd}(\text{OAc})_2\text{L}_2]$, con todo, a reacción tarda moito tempo. O ácido acético utilízase comunmente como doante débil de disolvente nas reaccións de ciclopaladación, o que lle permite interactuar máis eficientemente co centro de

paladio(II) e dar o produto da activación do C-H. Este proceso dá lugar a un complexo dinuclear con ligandos acetato ponte. Así, o $\text{Pd}(\text{OAc})_2$ demostrou ser un eficaz axente de paladación e un bo reactivo para ligandos que se hidrolizan facilmente. Ademais, crese que é o mellor electrófilo nas reaccións de substitución aromática. Por exemplo, os derivados da anilina son sensibles á hidrólise cando o ligando se coordina co metal en reaccións con $[\text{PdCl}_2(\text{PhCN})_2]$ en metanol ou con PdCl_2 en dioxina acuosa, en contraste co metaciclo que se forma ao utilizar $\text{Pd}(\text{OAc})_2$ en ácido acético glacial.

Os compostos de tipo pincer de paladio foron obxecto de importantes investigacións e estudáronse no contexto da catálise. Os compostos pincer teñen un tipo de deseño que utiliza un novo ligando quiral cun metal de transición para producir unha gran enantioselectividade e eficiencia. Entre eles atópanse os ligandos quirales NCN e PCP con unha columna vertebral de fenilo axustada a dúas unidades quirales. A súa produción comparativamente sinxela permite utilizalos en catálise. Para soste-lo aínda máis a actividade catalítica, varios compostos recentes demostraron ter novas e interesantes capacidades catalíticas mediante a substitución das ligazóns Pd-C por outros elementos, por exemplo, como Pd-Se ou Pd-P, e en raros casos Pd-N. A maioría dos compostos pincer son resistentes ao aire e á humidade, o que facilita o seu almacenamento. Ademais, teñen unha boa estabilidade térmica. Estes puntos críticos permiten unhas fortes propiedades catalíticas e unha ampla gama de posibilidades de reacción. O ligando pincer é importante para a selectividade da catálise porque a xeometría cadrada do composto de pinza só ten un sitio de coordinación libre para a catálise. As aminorfosfinas son compostos que inclúen tanto átomos de fósforo como de nitróxeno, independentemente da súa estrutura específica. Outros nomes, como iminofosfinas, fosfinoamidas, fosfazanos, etc., son máis aplicables para algúns deles. Todos os compostos con un grupo donante máis duro que contén N e unha funcionalidade donante máis branda que contén P denomináronse aminorfosfinas. As

α -aminofosfinas desempeñan un papel fundamental na síntese de

compuestos de metais de transición e son eficaces nas reaccións catalíticas homoxéneas.

Aínda que moitos metais son adecuados para preparar compostos ciclometalados, un dos máis utilizados é o paladio, principalmente pola facilidade das sínteses, así como polas numerosas aplicacións que presentan os compostos resultantes. Entre elas destacan o seu papel como precatalizadores en procesos de formación de ligazóns carbono-carbono, para dispositivos LED, aplicacións como sensores e en investigación biomédica como substancias antineoplásicas. No caso do paladio, os complexos ciclometalados foron acuñados como paladaciclos.

Os complexos obtidos caracterizáronse mediante espectroscopia infravermella (IR), resonancia magnética nuclear (NMR) e, cando foi posible, difracción de raios X (XR). A espectroscopia infravermella é unha técnica que proporciona información estrutural sobre as ligazóns existentes na molécula, así como a disposición dos ligandos ao redor do átomo de metal. Como resultado, a posición dun número de onda de banda maior ou menor está relacionada coa forza da ligazón e a masa dos átomos implicados. A medida que a ligazón é máis débil, a banda desprázase a un número de onda inferior, e cando se comparan dúas ligazóns comparables con átomos de diferente masa, o que ten átomos máis pesados mostrará a banda nun número de onda inferior.

O estudo de RMN de ^1H proporciona información extremadamente útil para entender as estruturas dos compostos e é un dos métodos de caracterización máis utilizados e fiables neste campo da química. A reacción entre os ligandos e o metal provoca unha serie de cambios nos espectros dos complexos. Como resultado, o desprazamento dos sinais, as variacións na súa multiplicidade ou a presenza ou ausencia das mesmas axúdannos a determinar a estrutura dos compostos. Entre todos estes cambios, destaca o estudo da ligazón imina, xa que a presenza do grupo $\text{C}=\text{N}$ provoca un desprazamento anisotrópico dalgúns sinais como consecuencia do desprotección (-) ou apantallamiento (+) en rexións da molécula próximas a el. Con todo,

cando un ligando sofre unha metalización, o sinal do protón aromático inicialmente unido ao carbono metalado desaparece, e hai unha variación resultante na multiplicidade dos protóns aromáticos restantes. Nos compostos que conteñen ligandos de fosfina unidos ao metal, en xeral, o sinal correspondente ao protón da imina desdóbrase por acoplamento ao núcleo ^{31}P da fosfina, o que adoita ocorrer só cando o átomo de fósforo é trans ao nitróxeno da imina. Esta é a disposición máis común, e está causada polo efecto transfóbico. Ademais, a disposición dos aneis fenilos da fosfina pode producir un apantallamento dos núcleos dos aneis aromáticos. A análise de ^{31}P - $\{^1\text{H}\}$ proporciona información relacionada coa xeometría do ligando fosfina, que pode ser especialmente importante para a caracterización do composto. Excepto no caso de certas difosfinas, que actúan como ligandos bidentados quelados, a incorporación deste tipo de ligandos na esfera de coordinación do metal tende a facer que o sinal se desprace a un campo inferior desde a súa posición no espectro do ligando libre. En consecuencia, é útil comparar os datos obtidos para os ligandos libres e coordinados. Os ligandos de fosfina poden coordinarse de maneiras diferentes: monodentados, bidentados ponte, bidentados quelato ou tridentados quelato. Dado que cada átomo de fósforo ten unha contorna química diferente cando a difosfina actúa como ligando monodentado, cabe esperar dous dobretes, un para o núcleo de fósforo coordinado ao metal (o máis desprotexido) e outro para o núcleo de fósforo non coordinado. No modo quelante, os dous doantes da difosfina poden ser equivalentes dependendo da xeometría e obsérvase un sinal singlete. Con todo, isto non adoita ser así e aparecen dous dobretes, como no caso anterior, aínda que ambos están desprazados a campo mais baixo. No modo ponte, ambos os núcleos de ^{31}P son normalmente equivalentes, polo que se espera un único singlete. Os núcleos de fósforo, neste caso, non son equivalentes, polo que se esperan dous sinais distintos. Dado que as monofosfinas (PPh_3) só interactúan como ligandos monodentados, o sinal observado no espectro de $\text{RMN-}^{31}\text{P}$ é obviamente un único singlete.

A difracción de raios-X é unha técnica que permite determinar de forma inequívoca a estrutura dun determinado composto en estado sólido. Utilizáronse diferentes condicións de cristalización para crear as mostras cristalinas. Unha das formas máis eficaces para as substancias químicas producidas neste estudo é a evaporación lenta dunha mostra disolta en diclorometano, ás veces coa adición dunha pequena cantidade de n-hexano. A evaporación lenta en acetona ou cloroformo é outra opción nalgunhas condicións para conseguir monocristais.

Se os factores do acordo son adecuados, a resolución da estrutura dun composto permite determinar as distancias e os ángulos de ligazón. Tamén permite investigar as contornas de coordinación. As interaccións supramoleculares son importantes para obter representacións gráficas máis ricas.

O desenvolvemento do paladio(II) comezou a finais da década de 1960 coa presenza de compostos de arilo, xa sexa estequiométricos ou catalíticos, por Richard Heck a través dun avance na área de reaccións de formación de ligazóns carbono-carbono catalizadas por paladio. Nos anos posteriores, moitos compostos de paladio potenciaron as reaccións de axuste C-C, e as reaccións de axuste catalizadas por paladio foron amplamente empregadas e útiles na síntese orgánica. As reaccións de Heck, Negishi e Suzuki son reaccións significativas que recibiron o Premio Nobel de Química en 2010 "polos axustes cruzados catalizados por paladio en síntese orgánica", o que demostra a importancia e a excelencia da química orgánica. A Suzuki-Miyaura considérase unha das reaccións de axuste cruzado máis utilizadas ($R_1-MR_2 \text{ n} = R_1-B(OH)_2$), debido ás condicións experimentais suaves e á forte estabilidade do ácido borónico substrato ao aire, á auga e ás temperaturas elevadas. Os compostos de paladio catalizan unha serie de reaccións, como a hidroxenación, a oxidación e o axuste carbono-carbono. O paladio está clasificado como un bo catalizador, o máis útil, e ten unha maior actividade que outros metais como o cobre, o níquel e o ferro. Con todo, o paladio comparte propiedades esenciais

con outros metais de transición, como a capacidade de reaccionar facilmente coas ligazóns non polares que se observan nos alquenos, alquinos e arenos. Esta interacción dá lugar a unha adición oxidativa, unha transmetalación e unha eliminación redutora sinxelas, selectivas e a miúdo reversibles.

Un dos ligandos máis utilizados nos procesos de ciclometalación son os ligandos base Schiff, tamén coñecidos como iminas. Son bastante versátiles por unha serie de razóns: o comportamento sintético fronte aos metais de transición, especialmente o paladio, é sobresaliente, e as reaccións adoitan producir rendementos razoables; o número de doantes de nitróxeno, así como as súas posicións relativas no anel de fenilo, poden variarse a vontade, como no presente caso, no que se utilizaron un ou dous doantes segundo conviña; a dobre ligazón C=N pode dividirse con bastante facilidade para dar o correspondente dobre ligazón C=O. Ademais, os complexos resultantes teñen unha serie de ligazóns diferentes no centro metálico, que no caso do paladio (este traballo) poden resumirse como segue: unha ligazón paladio-carbono, unha ligazón paladio-nitróxeno, ligazón-haluro, e nos correspondentes derivados ligazóns paladio-fósforo. De feito coñecense complexos cos catro enlaces sobre o metal diferentes. Os complexos obtidos caracterizáronse mediante espectroscopia de infravermellos (IR), resonancia magnética nuclear (NMR) e, cando foi posible, difracción de raios X (XR).

O obxectivo principal deste traballo foi sintetizar e estudar os compostos ciclometalizados derivados de ligandos imina e paladio. Isto inclúe tamén a síntese dos derivados de fosfina para os que se empregaron ligandos mono-dei e trifosfina.

Inicialmente, a investigación centrouse nas reaccións que incluían iminas con máis dun doador, para o que os ligandos se fixeron a partir dos aldehídos, isoftalaldehído e tereftalaldehído. En primeiro lugar, obtivéronse os complexos dinucleares acetato-bridados, que mostraban unha dobre ligazón C=O que se produce tras a purificación

por cromatografía en columna a partir da dobre ligazón C=N. Este é un resultado interesante porque supón un método de funcionalización dos complexos. Entón, o grupo C=O podería condensarse cunha variedade de aminofosfinas para dar novas especies que se comportasen como metaloligandos ciclometalados, contendo un ou dous átomos doantes de fósforo, como era o caso.

Os complexos nos que se logrou a rexeneración da ligazón C=N tratáronse despois cunha trifosfina (TRIPHOS) coa esperanza de volver unir firmemente o átomo de metal impedindo novas reaccións e de utilizar os compostos resultantes como metaloligandos bidentados [P,P]. Isto non ocorreu e, como alternativa, o resultado foi a formación dun complexo dinuclear de paladio bis(pentacoordinado), similar a outros atopados anteriormente no traballo deste grupo de investigación, pero a partir dun roteiro de reacción totalmente diferente. Isto pon de manifesto a versatilidade dos paladaciclos para romper e formar ligazóns co carbono, producindo así novas especies ou polo menos novas vías de reacción, no sentido máis estrito do que se coñece como serendipia. A estrutura cristalina deste complexo demostra de forma inequívoca a veracidade dos datos espectroscópicos e confirma a suposición realizada a partir destes datos.

O capítulo 7 trata da preparación de compostos de paladio ciclometalados e as súas reaccións con fosfinas bidentadas, como o 1,1-bis(difenilfosfino)eteno (vdpp), un ligando cunha dobre ligazón C=C. A fosfina vdpp pode sufrir reaccións de adición de Michael á dobre ligazón, con todo, mentres que isto é bastante difícil de obter na propia fosfina libre, cando se coordina de forma bidentada (P,P) a dobre ligazón actívase e a mencionada adición pode proceder sen problemas, mesmo a temperatura ambiente nalgúns casos. Pódese utilizar unha ampla gama de nucleófilos para engadir á dobre ligazón C=C, moitos deles conteñen grupos NH ou NH₂. No noso caso, os complexos parentales tratáronse con aminofosfinas que tiñan un grupo PPh₂, transformándoos en paladacíclicos metaloides bastante grandes.

Así pois, este é o segundo caso do traballo no que os metalaciclos dan paso a novos metaloligandos, poñendo de novo de manifesto a gran versatilidade destes complexos ciclometalizados para producir novos compostos que posúan unha reactividade aínda descoñecida.

O capítulo 8 trata dos paladacilos preparados a partir de iminas [C,N,S] potencialmente tridentadas. A súa característica máis peculiar é que a reacción entre os ligandos e o correspondente sal de paladio(II) dá lugar a un único complexo nuclear co ligando unido ao metal a través do carbono fenilo, o nitróxeno da imina e os átomos de xofre, así como a un ligando de cloruro terminal. A pesar de que o xofre pertence a un grupo SMe non cargado, a disposición tridentada do ligando mantén firmemente o metal, de modo que se poden levar a cabo reaccións que implican só un sitio de coordinación, deixando intacto a ligazón paladio-nitróxeno, e de novo só despois da abstracción do ligando de cloruro mediante o tratamento cun sal de prata adecuado. É máis, incluso as difosfinas quelantes fortes son incapaces de unirse ao metal; isto só é posible antes da abstracción do ligando de cloruro. Unha análise estrutural de cristais de raios-X para un dos paladácicos deste capítulo mostra a disposición xeométrica do ligando ao redor do átomo de paladio. Cabe destacar que nestes complexos o centro metálico está unido a catro átomos diferentes, un esquema de coordinación bastante inusual nesta química.

Os procesos de formación de ligazóns carbono-carbono son esenciais para a preparación de compostos bioactivos, agroquímicos e farmacéuticos. Ademais, empréganse para crear novos materiais orgánicos con propiedades eléctricas novas. Así mesmo, as reaccións de axuste cruzado foron un dos avances máis importantes na síntese orgánica e organometálica desde que se descubriron os catalizadores adecuados, entre os que os paladacilos xurdiron como algúns dos compostos máis aplicables para os devanditos procesos, especialmente na reacción de Suzuki-Miyaura que implica o axuste cruzado de compostos organoboránicos ($Ar_1-B(OR)_2$) con electrófilos (Ar_2-X). No último capítulo, o 9, coméntase a actividade catalítica e inclúense

os complexos con maior eficiencia catalítica. Os reactivos organoborónicos están dispoñibles no mercado, son menos tóxicos e son estables ao aire e á humidade, o que dá á reacción de Suzuki-Miyaura varias vantaxes. Outra característica importante é a posibilidade de utilizar auga como disolvente. Como a auga é un bo disolvente para o quecemento por microondas, estudouse o uso da auga como disolvente en combinación co quecemento por microondas. Considérase que o ciclo catalítico da reacción de Suzuki-Miyaura comeza coa adición oxidativa do electrófilo (Ar_2-X) ao catalizador, dando lugar ao intermedio $Ar_2-[Pd]-X$. O composto resultante transmetálase entre $Ar_2-[Pd]-X$ e $(Ar_1-B(OH)_2)$ para dar lugar á especie de paladio disustituída $Ar_1-[Pd]-Ar_2$, tras o cal a fracción de paladio disustituída se elimina reductivamente, liberando un novo produto de axuste (Ar_1-Ar_2) e rexenerando o catalizador, que se incorpora de novo ao ciclo; este último paso verifica o paladaciclo. Diseñáronse paladaciclos que teñen estabilidade térmica, tempos de reacción rápidos, son insensibles ao aire e á auga, teñen un custo mínimo e son beneficiosos para o medio ambiente. Neste artigo ilústranse os resultados dalgúns dos intentos máis importantes na produción de ligandos altamente activos para o seu uso en reaccións de axuste cruzado ao longo da última década.

Index

Chapter 1. Introduction	1
1.1 The beginning of organometallic chemistry	2
1.2 Concept of cyclometallation compounds	3
1.2.1 Reaction of cyclometallated compounds	3
1.2.2 Definition of cyclometallation	8
1.2.3 Synthesis of cyclometallation via C-H activation.....	10
1.2.4 Effect of endo and exo on cyclometallation	12
1.3 Metal precursor	16
1.4 The nature of palladium ligand.....	19
1.4.1 Nature of donor heteroatoms.....	19
1.4.1.1 Mono palladium compounds	19
1.4.1.2 Palladium pincer compounds	22
1.5. Amino phosphines ligands	25
1.5.1 Synthesis of platinum and palladium compounds	27
Chapter 2. Objectives	29
Chapter 3. Experimental part	34
3.1 Reagents and solvents.....	35
3.1.1 Organic reagents.....	35

3.1.2 Inorganic reagents.....	36
3.1.3 Solvents.....	36
Chapter 4. Characterization techniques	38
4.1 Infrared spectroscopy.....	39
4.1.1 Study of band $\nu(\text{C}=\text{N})$	40
4.1.2 Study of band $\nu(\text{C}=\text{O})$	42
4.1.3 Study of the acetate ligand band $\nu(\text{COO})$	42
4.1.4 Study of band $\nu(\text{Pd}-\text{Cl})$	43
4.1.5 Study of band $\nu(\text{C}=\text{O})$ and $\nu(\text{C}=\text{C})$	45
4.2 NMR spectroscopy.....	46
4.2.1 ^1H NMR study.....	47
4.2.2 ^{31}P -NMR study.....	49
4.3 X-ray diffraction.....	51
4.3.1 Bond distances.....	53
4.3.1.1 Hydrogen bond.....	53
4.3.1.2 Molecular stacking π - π interactions.....	54
Chapter 5. Scheme Reactions.....	57
5.1 Cyclopalladation compounds derivatives of Schiff bases from terephthalaldehyde and isophthalaldehyde.....	58

5.1.1 Derivatives compounds of cyclohexylamine Schiff bases ligands.....	58
5.1.2 Derivatives compounds of aminophosphine ligand.....	59
5.2 Cyclopalladated compounds derivatives of imines Schiff bases..	60
5.3 Cyclopalladated compounds derivatives of tridentate [C,N,S] Schiff bases.....	61
Chapter 6. Cyclopalladated compounds from 1,4-(CHO)₂C₆H₄ (terephthalaldehyde) and 1,3-(CHO)₂C₆H₄ (isophthalaldehyde) Schiff bases.....	62
6.1 Introduction.....	63
6.1.1 Synthesis of the Schiff base ligands a and b	66
6.1.2 Synthesis of the acetate-bridged compounds 1a and 1b	67
6.1.3 Synthesis of the halide-bridged compounds 2a and 2b	68
6.1.4 Synthesis of monomer compounds with triphos ligand 3a and 3b	69
6.1.5 Synthesis of monomer compounds 4a and 4b	70
6.1.6 Synthesis of monomer triphos compounds with cyclohexylamine ligand 5a and 5b	71
6.1.7 Synthesis of monomer compounds with acetylacetone 6a and 6b	72

6.1.8 Synthesis of compounds with dppm 7a and 7b	73
6.1.9 Synthesis of monomer compounds with vdpp 8a and 8b	74
6.1.10 Synthesis of monomer compounds with the NH ₂ CH ₂ CH ₂ PPh ₂ ligand 9a and 9b	75
6.1.11 Synthesis of monomer compounds with the NH ₂ CH ₂ CH ₂ PPh ₂ ligand 10a and 10b	76
6.1.12 Attempts the synthesis of monomer compounds using the NH ₂ CH ₂ CH ₂ PPh ₂ ligand with compounds containing acetylacetonate, dppm, and vdpp ligands.....	77
6.1.13 Attempts to synthesize monomer compounds containing triphos and NH ₂ CH ₂ CH ₂ PPh ₂ amino phosphine ligands, with MCl ₂ (PhCN) ₂ [M.= Pt, Pd].....	78
6.2 IR study.....	80
6.3 NMR study.....	82
6.3.1 Study of Schiff base ligands a and b	82
6.3.2 Study of compounds 1a and 1b	83
6.3.3 Study of compounds 2a and 2b	86
6.3.4 Study of compounds 3a and 3b	87
6.3.5 Study of compounds 4a and 4b	91
6.3.6 Study of compounds 5a and 5b	93
6.3.7 Study of compounds 6a and 6b	95
6.3.8 Study of compounds 7a and 7b	97

6.3.9 Study of compounds 8a and 8b	99
6.3.10 Study of compounds 9a and 9b	102
6.3.11 Study of compounds 10a and 10b	105
6.3.12 Study of changes of compounds 3b and 9b in NMR.....	107
6.4 X-ray diffraction study.....	111
6.4.1 Structure of compound 1b	111
6.4.2 Structures of dinuclear compound vi and vi'	114
6.4.3 Structure of compound 4a	121
6.4.4 Structure of compound 6b	124
6.4.5 Structure of compound 7b	128
Chapter 7. Cyclopalladated compounds derivatives of Schiff bases imine ligands	132
7.1 Introduction.....	133
7.1.1 Synthesis of the Schiff base ligands c-j	135
7.1.2 Synthesis of compounds with acetate-bridged 1c-1j	136
7.1.3 Synthesis of compounds with chloride-bridged 2c-2j	137
7.1.4 Synthesis of compounds with triphenylphosphine ligand 3c-3j	138
7.1.5 Synthesis of compounds with chelating dppm 4c-4j	139

7.1.6 Synthesis and Michael Additions to vinylidene diphosphine Complexes of $[M(CO)_4\{(PPh_2P)_2C=CH_2\}]$ (M = Mo, W)	140
7.1.6.1 Preparation of $M(CO)_4[Ph_2PCH(CH_2-NH-(CH_2)_2PPh_2)PPh_2]-P, P]$ (M = Mo, W)	140
7.1.6.2 Synthesis of compounds 5c-5j and 6c-6g	141
7.1.7 Synthesis of compounds with bridging dppm 7e and 7f	142
7.1.8 Synthesis of ligand k	143
7.1.9 Synthesis of compounds 1k and 2k	143
7.1.10 Synthesis of the compound with chelating dppm 3k	144
7.2 NMR study	145
7.2.1 Study of NMR Schiff bases ligands c-j	145
7.2.2 Study of compounds 1c-1j	146
7.2.3 Study of compounds 2c-2j	148
7.2.4 Study of compounds 3c-3j	149
7.2.5 Study of compounds 4c-4j and 3k	151
7.2.6 Cyclopalladated compounds using Michael Additions compounds	153
7.2.6.1 Study of $M(CO)_4[Ph_2PCH(CH_2-NH-(CH_2)_2PPh_2)PPh_2]-P, P]$ (M = Mo, W)	153
7.2.6.2 Study of compounds 5c-5j and 6c-6f	156

7.2.7 Study of compounds 7e and 7f	159
7.3 Study of X-ray diffraction.....	161
7.3.1 Crystal structure of cyclometallated 3c and 3d	161
7.3.2 Crystal structures of cyclometallated 4e , 4f , 4h and 3k	167
7.4 Data additional.....	174
Chapter 8. Palladacycles with tridentate [C, N, S] Schiff base ligands	196
8.1 biographies.....	197
8.1.1 Synthesis of the Schiff base ligands l-n	199
8.1.2 Synthesis of compounds 1l-1n	200
8.1.3 Synthesis of compound 2l	202
8.1.4 Synthesis of compound 2n	202
8.2 NMR studying.....	203
8.2.1 Study of compounds l-n	204
8.2.2 Study of compounds 1l-1n	206
8.2.3 Study of compound 2l	208
8.2.4 Study of compound 2n	209
8.3 Study of X-ray diffraction.....	211
8.3.1 Study structure of compounds 1l and 1n	211

Chapter 9. Catalysis	217
9.1 Introduction.....	218
9.1.1 cross coupling-reactions.....	219
9.1.2 The Suzuki-Miyaura cross-coupling reaction.....	220
9.1.3 Oxidative addition.....	223
9.1.4 Transmetallation	224
9.1.5 Reductive elimination.....	226
9.1.6 Catalysts.....	227
9.1.7 Boronic acid derivatives.....	228
9.2 Methodology.....	229
9.2.1 System of reaction.....	229
9.2.2 Method of working.....	231
9.2.2.1 The reaction procedure.....	231
9.2.2.2 Methodology of experimentation.....	231
9.2.2.3 ¹ H NMR detection of reactions.....	232
9.2.3 Compounds used as catalysts.....	234
Chapter 10. Conclusions	240

Abbreviations:

A.E	Elemental Analysis
Ac	Acetate
acac	Acetylacetonate
<i>ca.</i>	Approximately
cat.	Catalyst
CDCl ₃	Deuterated Chloroform
CHCl ₃	Chloroform
cm ³	Cubic centimeters
Cy	Cyclohexyl
DCM	Dichloromethane
dppm	Bis(diphenylphosphine)methane
eq.	Equivalents
EtOH	Ethanol
g	Grams
IR	Infrared
MeOH	Methanol
mL	Milliliter
mmol	Millimole
NMR	Nuclear Magnetic Resonance
OMe	Methoxy
Me	Methyl
Ph	Phenyl
PPh ₃	Triphenylphosphine
ppm	Parts per million

r.t	Room Temperature
t	Temperature
T	Time
THF	Tetrahydrofuran
triphos	Bis(2-diphenylphosphinoethyl)phenylphosphine
vdpp	Bis(diphenylphosphine)ethene
δ	Displacement
ν	Wave number

CHAPTER 1

Introduction



1.1 The beginning of organometallic chemistry

Since the second part of the twentieth century, organometallic chemistry has gained popularity in a variety of domains, including the academic and the industrial applications. Organometallic compounds include a variety of metals and many stereochemistry, related to the coordination of metals with organic chemistry.¹

The main organometallic compounds that have been discovered over the last two decades are worth mentioning. Cadet de Gassicourt prepared the first organometallic compound in 1760, tetramethyldiarsine, $[(\text{CH}_3)_4\text{As}_2]$. Sir Edward Frankland reported the synthesis of Zeise's salt $\text{K}[\text{PtCl}_3(\text{C}_2\text{H}_4)]$ in 1827 and produced derivatives of metal alkyls such as $[\text{Zn}(\text{CH}_3)_2]$ in 1840. Reppe's study in 1890 was showed that L. Mond's $\text{Ni}(\text{CO})_4$ could be useful in catalysis. Grignard coined the $[\text{RMgX}]$ reagent in 1900, which led to the expansion of the field of organometallic chemistry by a large number of chemists, reaching over 500 species in 1908.

Chemists' innovations in organometallics have been carried on at various levels until the twenty-first century. Hieber reported with substantial effort $[\text{C}_4\text{H}_6\text{Fe}(\text{CO})_3]$ in the early twentieth century, namely in 1930. Later, Hien announced a benzene-bonded chromium aromatic molecule. Many main group metal organometallics, such as organoarsenic and organomercury compounds, have been found to exhibit biological activity.²

¹ H. Nakazawa, **2021**.

² T.J. Colacot, V. Sivakumar, *Springer*, **2019**.

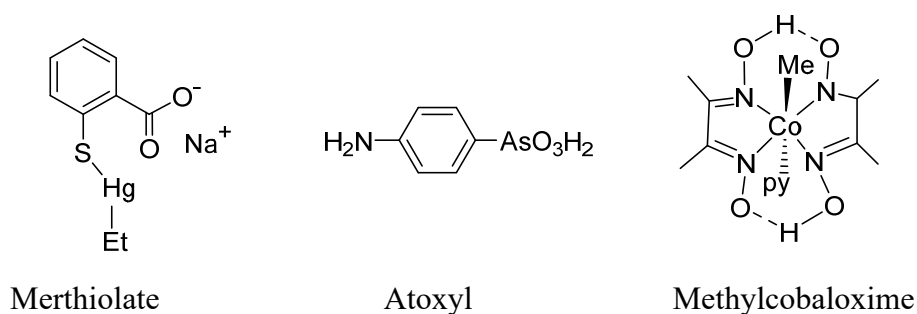


Figure 1. Biologically active organometallic compounds.

1.2 Concept of cyclometallation compounds

1.2.1 Reaction of cyclometallated compounds

The synthesis of new symmetric cyclometallated compounds using transition metals, which established a suitable pathway for producing metal-carbon bonds, revealed the concepts of cyclometallation compounds in the early 1960s.

Kleinman and Dubeck reported the first cyclometallated compound using as starting materials azobenzene and NiCp_2 in 1963, obtaining a five-membered metallacycle complex. The Ni(II) atom was used as a transition metal to activate the C-H bond, leading to the formation of a five-membered ring complex.³

³ J.P. Kleinman, M. Dubeck, *Journal of the American Chemical Society*, 85 (1963) 1544-1545.

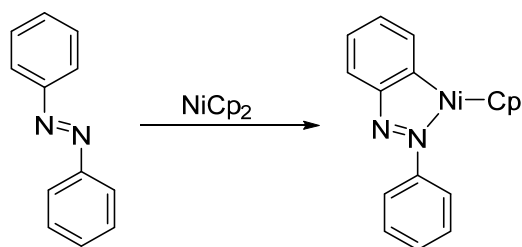


Figure 2. Synthesis of the first metallacycle.

Between 1965 and 1968, cyclometallation reactions were extended to include more transition metals. Thus, the palladacycle reaction was initially carried out by Cope and Siekman from azobenzene and LiPdCl_4 with C-H bond activation.⁴ Later, dimethylbenzylamine in methanol was used to make a five-membered palladacycle. Palladacycles are formed when the Pd-C bond is stabilized by chelation, increasing the stability of the organopalladium product.

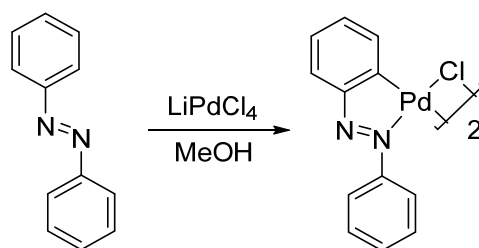


Figure 3. Synthesis of a dinuclear metallacycle.

⁴ A.C. Cope, R.W. Siekman, *Journal of the American Chemical Society*, 87 (1965) 3272-3273.

Hartwell *et al.* reported the first C(sp³)-Pd compound in 1970, by activating the benzylic C–H bond of 8-methyl quinoline with Li₂PdCl₄. The insoluble dinuclear chloride-bridged compound gave the mononuclear species after reaction with triphenylphosphine.⁵

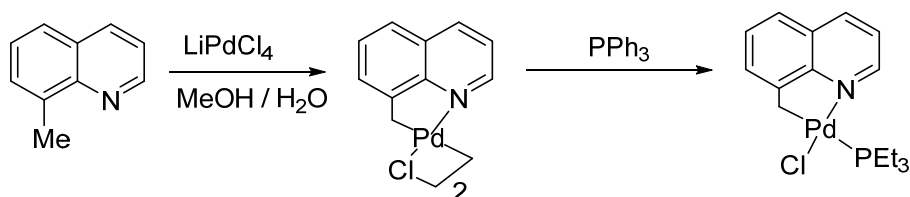


Figure 4. Synthesis of a mononuclear metallacycle.

Many transition metals, such as Ru, Rh, Os, Pt, Ir, Fe, Ni, Co, and Mn, have been shown to undergo the cyclometallation reaction.⁶ Due to the activation of metals, which easily interact with a lone electron pair of the corresponding heteroatom, these reactions are considered to proceed readily. Shaw and Moulton showed in 1976 that Ni, Pd, Pt, Rh, and Ir transition metal complexes with tridentate-[C, P, C] pincer ligands and sterically few demanding groups such as chloride,

⁵ G.E. Hartwell, R.V. Lawrence, M.J. Smas, *Journal of the Chemical Society D: Chemical Communications*, (1970) 912-912.

⁶ M. Albrecht, *Chemical reviews*, 110 (2010) 576-623.

cyanide, carbonyl, or phenylacetylene, render quite stable, complexes.⁷

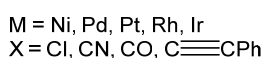
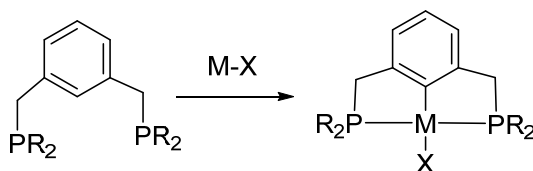


Figure 5. Metallacycles with pincer ligands.

Mononuclear species have been used to present the majority of chemicals. Despite the high stability and tenability of tridentate ligands, which facilitate a wide application in catalysis and medicinal chemistry, there are a limited number of Pd(II), Pt(II), Ru(III), and Re(I) binuclear and trinuclear complexes combining numerous pincer motifs in their structures. For example, in acetone with a silver salt AgX and subsequent reaction with organometallic linkers, dinuclear Pt(II) cyclometallated complexes containing an organometallic assembly ligand have been observed.⁸

⁷ C.J. Moulton, B.L. Shaw, *Journal of the Chemical Society, Dalton Transactions*, (1976) 1020-1024.

⁸ H. Sesolis, C.K.-M. Chan, G. Gontard, H.L.-K. Fu, V.W.-W. Yam, H. Amouri, *Organometallics*, 36 (2017) 4794-4801.

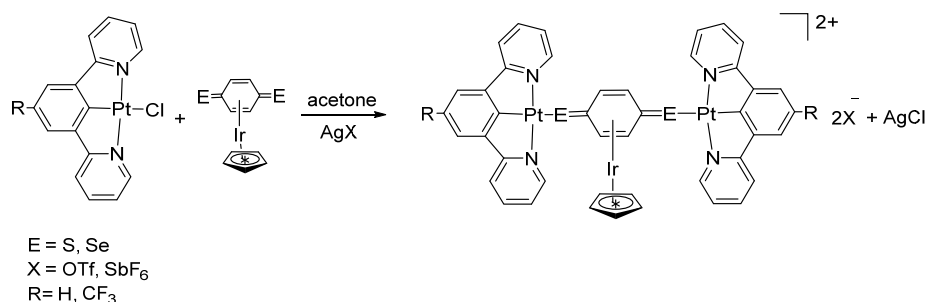


Figure 6. Multinuclear metallacycles with pincer ligands.

Chirality-organized quinone diimine derivatives, containing amino acid moieties that react with $\text{Pd}(\text{OAc})_2$ in acetonitrile to form the chiral homobimetallic $\text{Pd}(\text{II})$ compound, which is another example of a dinuclear cyclometallated compound.⁹

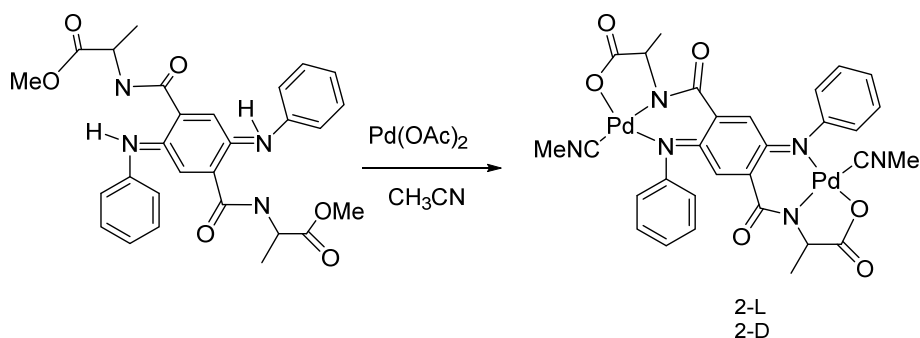


Figure 7. Chiral palladacycles.

Zhao and colleagues prepared a neutral $\text{Pt}(\text{II})$ compound with a tridentate pincer ligand by reacting 1,3-bis(*N*-substituted benzimidazole-2-yl)benzene ligands with K_2PtCl_4 in refluxing acetic

⁹ S.D. Ohmura, T. Moriuchi, T. Hirao, *Journal of Inorganic and Organometallic Polymers and Materials*, 23 (2013) 251-255.

acid and then treating the compound with KI and aromatic terminal alkenes in methanolic NaOH.¹⁰

¹⁰ Z. Wang, Z. Sun, X.-Q. Hao, J.-L. Niu, D. Wei, T. Tu, J.-F. Gong, M.-P. Song, *Organometallics*, 33 (2014) 1563-1573.

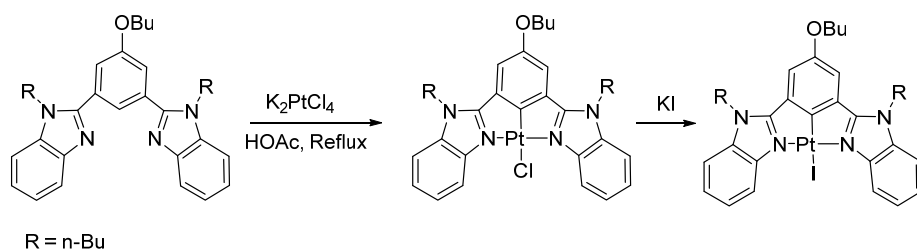


Figure 8. Benzimidazole platinumacycles.

1.2.2 Definition of cyclometallation.

A cyclometallation reaction may be defined as the formation of a metallacycle or organometallic intermolecular-coordination five-membered ring compound with at least one metal-mediated activation of a carbon bond, intermolecularly stabilized by two or three neutral donor atoms. A significant body of knowledge regarding their characteristics and reactivity is available. The activated bonds are known for donor heteroatoms such as N, O, P, S, Se, and As, and the cyclometallation reaction can occur *via* C-H, C-C, and C-O activation bonds. C-H activation is the most well-known and it has also received much attention in organic synthesis, but C-C, C-O, and C-Si reactions have also been studied.¹¹ Four or six electron donors [C-Y, C-Y-Y, Y-C-Y] from chelating ligands are used in the reactions. After being linked to the metal ion [M⁺], these chelating ligands produce stable compounds. Due to the high dissociation energy of C-H activation and

hence limited chemical reactivity, C-H bond activation has grown in popularity as a research topic.¹²

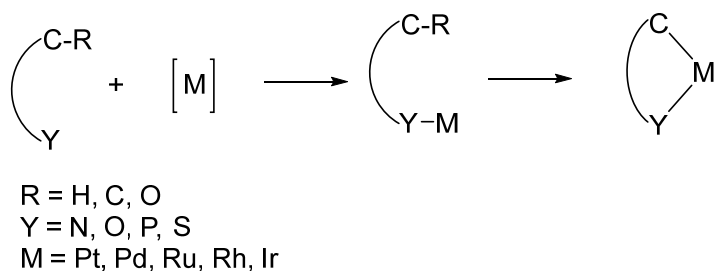


Figure 9. The cyclometallation reaction.

The nature of rational ligands in organometallic chemistry, in general, provides control over essential kinetic aspects such as ligand substitution. They can also be kinetically stable and relatively lipophilic, with a low oxidation state on the metal atom. Transition metals are also known as *d* block elements¹³ because they allow *d* orbitals to contribute to the formation of bonds in their compounds. These elements have fairly low ionization energy and are usually positively charged, making them available for bonding to many ligands.

¹² T. Gensch, M. Hopkinson, F. Glorius, J. Wencel-Delord, *Chemical Society Reviews*, 45 (2016) 2900-2936.

¹³ A. Earnshaw, N.N. Greenwood, *Butterworth-Heinemann Oxford*, 1997.

1.2.3 Synthesis of cyclometallation *via* C-H activation.

Cyclometallated compounds are made from substrates with heteroatoms and C-H bond activation assisted *via* a metal. The term C-H bond activation is used to describe a reaction in which an inert C-H bond is replaced with another functional group in a single step. A C-H bond is a reactive substrate where a carbon-metal link is formed by cleaving an inert C-H bond with a metal species.^{14,15}

There are three different types of C-H activation:¹⁶

i) an electron-rich low valent late metal center is required for oxidative addition of C-H bonds. Iridium and rhodium transition metals are the most commonly cyclometallated transition metals.

b) σ -bond metathesis of the C-H bond is accomplished with electron-poor metal centers such as high-valent early transition metals and lanthanides.

c) electrophilic electron bond activation is observed with electron-poor late transition metals. Due to the catalytic applications and the fact that these reactions are sensitive to water and oxygen, they are the most extensively researched in organic synthesis.

¹⁴ D. Balccells, E. Clot, O. Eisenstein, *Chemical reviews*, 110 (2010) 749-823.

¹⁵ A.E. Shilov, G.B. Shul'pin, *Chemical Reviews*, 97 (1997) 2879-2932.

¹⁶ D. Gallego, E.A. Baquero, *Open Chemistry*, 16 (2018) 1001-1058.

The C-H bond activation improves the oxidation state of the substrates, but it necessitates oxidative reaction conditions. There are several exceptions, such as hydroarylation and electrophilic unsaturated bonds. As a result, the catalytic system works under oxidative conditions by using C-H bond functionalization.

High-valent metal catalysts are the most common type of transition metal. Pd(II),¹⁷ Ru(II),¹⁸ Rh(III),¹⁹ Ir(III),²⁰ Cu(II),²¹ Ni(II) and Co(III),²² were all investigated for C-H bond functionalization. The activation of a strong C-H bond by transition metals is one of the most important steps in the cyclometallation reaction. Electrophilic activation¹⁰ was named after these late high valent electrophilic transition metals.

The intermolecular C-H activation, which occurs through an agostic interaction with the assistance of the internal Lewis base, is particularly easy in cyclometallation reactions with conventional substrates that contain a heteroatom called a directing group that experiences a C-H activation. The metal atom is then linked to a heteroatom, forming a five-membered metallacycle ring (Scheme 1).²³

¹⁷ R. Giri, S. Thapa, A. Kafle, *Advanced Synthesis & Catalysis*, 356 (2014) 1395-1411.

¹⁸ L. Ackermann, *Organic Process Research & Development*, 19 (2015) 260-269.

¹⁹ B. Ye, N. Cramer, *Accounts of chemical research*, 48 (2015) 1308-1318.

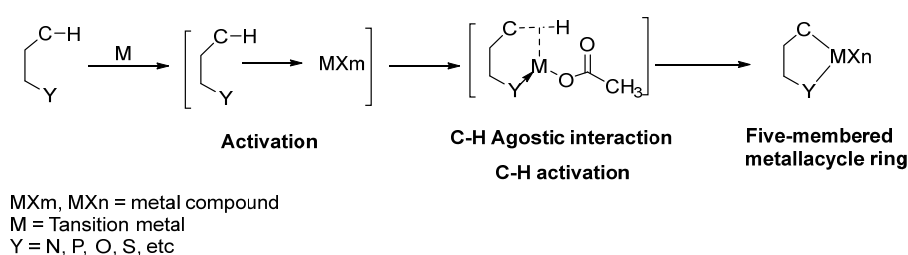
²⁰ T. Kang, Y. Kim, D. Lee, Z. Wang, S. Chang, *Journal of the American Chemical Society*, 136 (2014) 4141-4144.

²¹ W.-H. Rao, B.-F. Shi, *Organic Chemistry Frontiers*, 3 (2016) 1028-1047.

²² T.K. Hyster, *Catalysis Letters*, 145 (2015) 458-467.

²³ I. Omae, *Journal of Organometallic Chemistry*, 696 (2011) 1128-1145.

The metallated carbon in the vast majority of known complexes is usually an aromatic sp^2 carbon,²⁴ with sp^3 aliphatic,²⁵ benzylic, or sp^2 vinylic carbons being less frequent.²⁶



Scheme 1. Mechanism of C-H activation.

1.2.4 Effect of endo and exo substitutions on cyclometallation.

Through endo or exo directing mechanisms, the synthesis of metallacycles by C-H activation can be highly selective.²⁷ With many types of imines and oxazolines, the endo effect has been found. For example, when *N*-benzylbenzaldimine reacts with Li_2PdCl_4 , it generates a chloro-bridged *endo*-palladacycle, which has undergone ligand exchange to become a led monomer, as determined by X-ray

²⁴ A.C. Cope, E.C. Friedrich, *Journal of the American Chemical Society*, 90 (1968) 909-913.

²⁵ J. Dupont, N.R. Basso, M.R. Meneghetti, R.A. Konrath, R. Burrow, M. Horner, *Organometallics*, 16 (1997) 2386-2391.

²⁶ B. Fedorov, N. Golovina, G. Strukov, V. Kedrov, V. Arakcheeva, R. Trofimova, G. Shilov, L. Atovmyan, *Russian chemical bulletin*, 46 (1997) 1626-1627.

²⁷ Y. Xu, G. Dong, *Chemical Science*, 9 (2018) 1424-1432.

diffraction.²⁸ The *endo*-metallacycle was also formed exclusively in nearly quantitative yield when 4-phenyl-2-oxazoline was treated with stoichiometric Pd(OAc)₂.²⁹

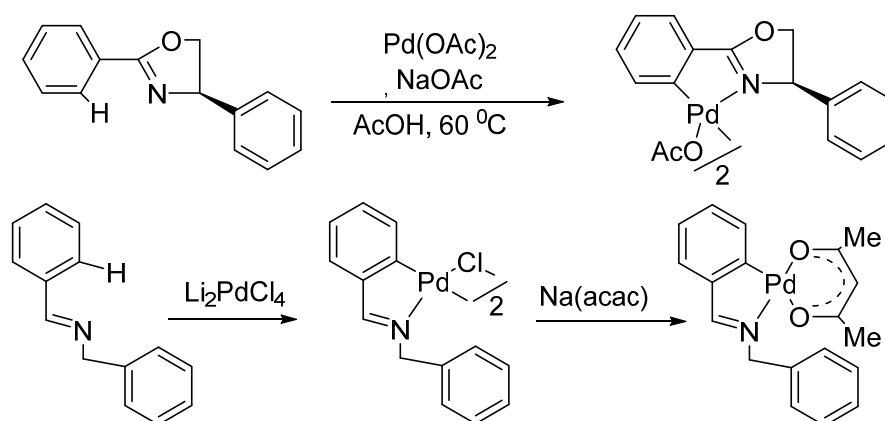


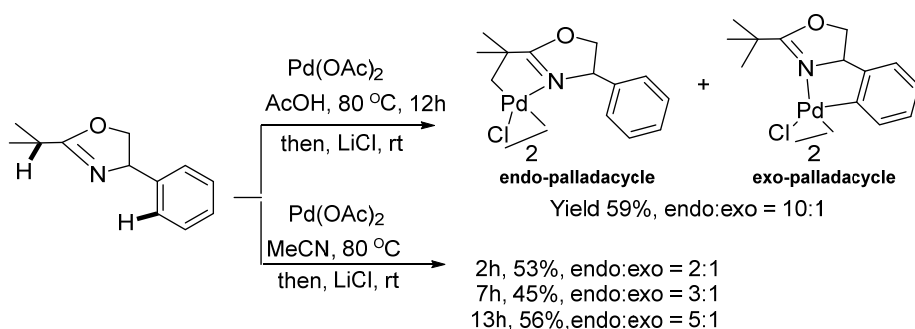
Figure 10. The synthesis of endo-metallacycle

In other cases, endo activation is preferred because it allows the activation of an endo C(sp³)-H bond even when a more active exo C(sp³)-H bond is present. The endo sp³ palladated compound was produced as the main product of the reaction of (*S*)-2-tert-butyl-4-phenyl-2-oxazoline with a stoichiometric amount of Pd(OAc)₂ under different conditions.³⁰

²⁸ P. Clark, S. Dyke, G. Smith, C. Kennard, *Journal of organometallic chemistry*, 330 (1987) 447-460.

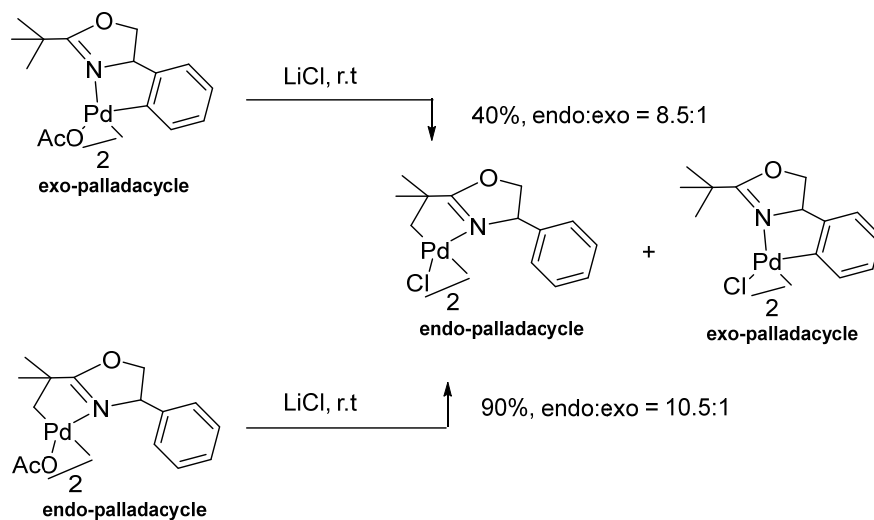
²⁹ O.N. Gorunova, K.J. Keuseman, B.M. Goebel, N.A. Kataeva, A.V. Churakov, L.G. Kuz'mina, V.V. Dunina, I.P. Smoliakova, *Journal of organometallic chemistry*, 689 (2004) 2382-2394.

³⁰ R.Y. Mawo, S. Mustakim, V.G. Young, M.R. Hoffmann, I.P. Smoliakova, *Organometallics*, 26 (2007) 1801-1810.



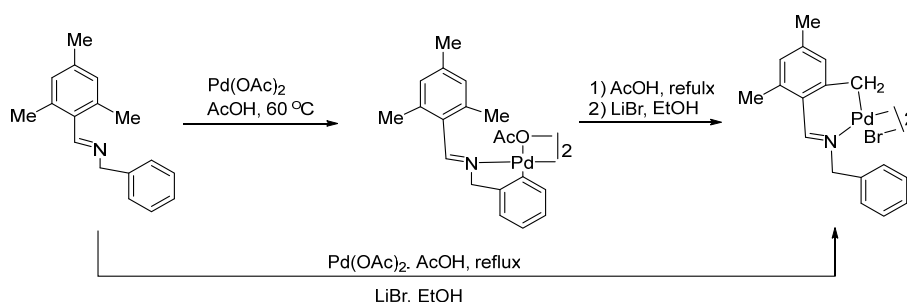
Scheme 2. Synthesis of Cyclopalladation of (S)-2-tert-butyl-4-phenyl-2-oxazoline

At 80 °C, the reaction of pure *exo*-complex with acetic acid produced an approximately 8.5:1 mixture of *endo* and *exo* isomers. Under the same conditions, the reaction of pure *endo*-complex produced a mixture of *endo* and *exo* isomers of up to 10.5:1.



Scheme 3. Effect of endo and exo-cyclopalladation of (S)-2-tert-Butyl-4-phenyl-2-oxazoline

In some situations, the exo complex is a kinetic product that may be separated and isomerized to generate a more thermodynamically stable endo complex, such as when N-mesityl-benzylidene amine reacts with Pd(OAc)₂ at 60°C to form a five-membered exo palladacycle.³¹



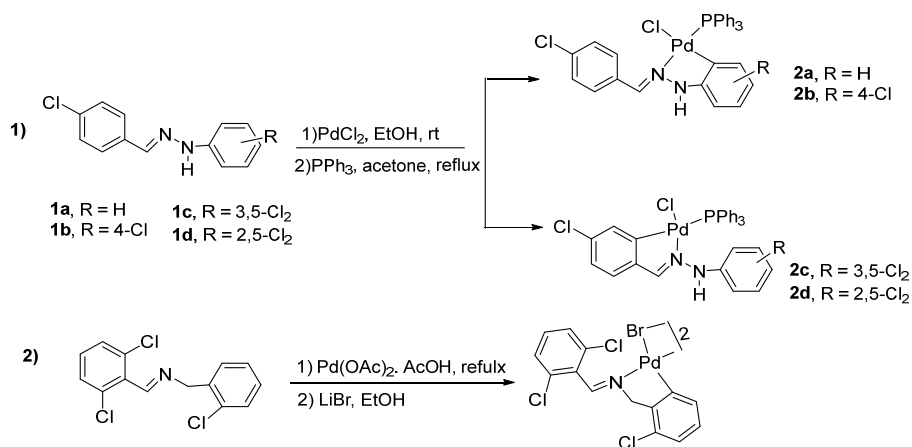
Scheme 4. Synthesis of cyclopalladated of endo and exo-N-mesitylbenzylideneamines.

The exo-metallacycle can sometimes become the major product when there is a strong electronic or steric bias. For example, exo-palladacycles were produced at ambient temperature when benzaldehyde phenylhydrazones (**1a** and **1b**) were reacted with PdCl₂, owing to the substantial difference in electron density between the endo- and exo-rings caused by the highly electron-donating amine moiety (Scheme 5). Only the endo-metallacycles were obtained when stronger electron-withdrawing (and thus more sterically demanding) chlorine substituents were added at the ortho- and meta-positions of the phenylhydrazine rings (**1c** and **1d**), as expected.³² Furthermore, the

³¹ J. Albert, R.M. Ceder, M. Gomez, J. Granell, J. Sales, *Organometallics*, 11 (1992) 1536-1541.

³² J. Granell, R. Moragas, J. Sales, M. Font-Bardía, X. Solans, *Journal of the Chemical Society, Dalton Transactions*, (1993) 1237-1244.

endo reaction sites can be blocked to achieve exo-metallation. The exo-palladacycle was produced exclusively when both endo C–H bonds of N-benzylbenzaldimine were replaced by chlorine atoms.³³



Scheme 5. 1) synthesis of exo- and endo-cyclopalladated phenylhydrazones. 2) synthesis of the six-membered exo-cyclopalladated compound of N-benzylideneamines.

1.2.5 Metal precursor

Palladium(II) acetate is one of the most used metallation precursors. By reacting the trimer with an excess of NaOAc, it can be easily divided into monomeric [Pd(OAc)₂L₂], however, the reaction takes a long time.³⁴ Acetic acid is commonly used as a weak solvent donor in cyclopalladation reactions, allowing it to interact more efficiently with

³³J. Albert, M. Gomez, J. Granell, J. Sales, X. Solans, *Organometallics*, 9 (1990) 1405-1413.

³⁴ A.C. Skapski, M.L. Smart, *Journal of the Chemical Society D: Chemical Communications*, (1970) 658b-659.

the palladium(II) center and yield the product of C-H activation. This process renders a dinuclear acetate-bridged complex (Figure 11).³⁵

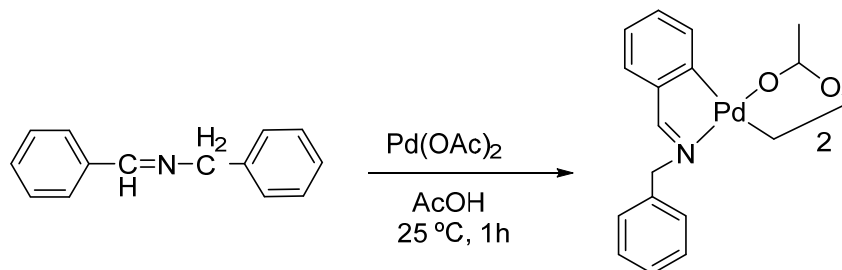


Figure 11. cyclopalladation reaction in acetic acid solvent.

Thus, Pd(OAc)₂ has proven to be an effective palladation agent³⁶ and a good reagent for ligands that are easily hydrolyzed. Additionally, it is thought to be the best electrophile in aromatic substitution reactions.³⁷ For example, aniline derivatives are sensitive to hydrolysis when the ligand is coordinated to the metal in reactions with [PdCl₂(PhCN)₂] in methanol or with PdCl₂ in aqueous dioxin, in contrast to the metallacycle formed when using Pd(OAc)₂ in glacial acetic acid.³⁸

³⁵ M. Gómez, J. Granell, M. Martinez, *European Journal of Inorganic Chemistry*, 2000 (2000) 217-224.

³⁶ Y. Fuchita, K. Hiraki, Y. Kage, *Bulletin of the Chemical Society of Japan*, 55 (1982) 955-956.

³⁷ J. Davidson, C. Triggs, *Journal of the Chemical Society A: Inorganic, Physical, Theoretical*, (1968) 1324-1330.

³⁸ H. Onoue, I. Moritani, *Journal of Organometallic Chemistry*, 43 (1972) 431-436.

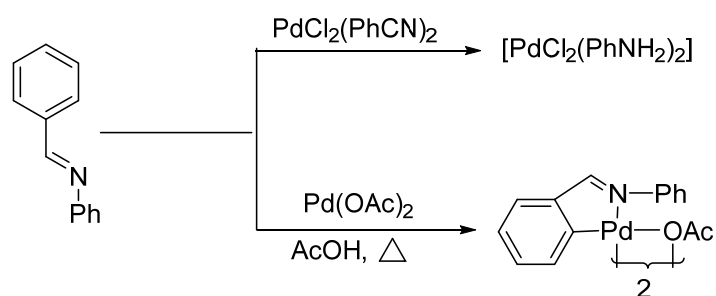


Figure 12. Metalation reactions of N-phenylbenzaldimine.

Another example is a reaction involving benzylideneazines and PdCl_2 , which produced only polymeric dicyclopalladated compounds, whereas a reaction involving $\text{Pd}(\text{OAc})_2$ allows for the isolation of monometallated and metallated derivatives under different conditions.³⁹

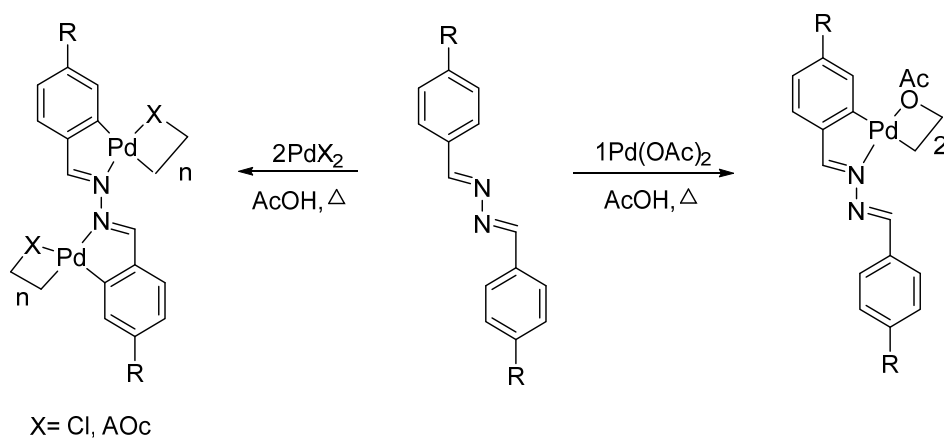


Figure 13. Binuclear mixed metal cyclometallated complexes.

Alternative palladium precursors, such as $[\text{PdX}_4]^{2-}$, $\text{PdX}_2(\text{NCR})_2$ ($X =$ halide, generally chloride), and highly electrophilic $[\text{Pd}(\text{NCR})_4]^{2+}$, can be used. For C-H bond mediated cyclopalladation, $\text{PdCl}_2(\text{cod})$ ($\text{cod} =$ 1,5-cyclooctadiene) or precursor $\text{PdCl}_2(\text{PPh}_3)_2$ have been reported to be less widely used.⁴⁰

1.3 The nature of Palladium ligands.

The majority of cyclopalladation ligands form monoanionic E-C-bidentate or pincer-type monoanionic E-C-E tridentate structures. N, P, and S containing groups such as amines, imines, phosphines, phosphinites, and thioethers are the most prevalent heteroatoms E.⁴¹

1.3.1 Nature of the donor Heteroatoms.

1.3.1.1 Mono palladium compounds.

The stability given by the E donor is usually altered by carefully selecting the heteroatom, such as in wide a variety of bidentate C-N palladacycles of the amine and imine ligands, which are relatively simple to prepare.⁴² Most transition metal ions form stable metal-carbon bonds with strong donating N-donor ligands. Considering that nitrogen-donor ligands, amines, oximes, amides, and azo-compounds, have generated substantial interest in catalysis for the Suzuki-Miyaura cross-coupling, they have been fully researched.

⁴⁰ K.M. Engle, *Pure and Applied Chemistry*, 88 (2016) 119-138.

⁴¹ D. Morales-Morales, *Elsevier*, 2018.

⁴² S. Gründemann, M. Albrecht, A. Kovacevic, J.W. Faller, R.H. Crabtree, *Journal of the Chemical Society, Dalton Transactions*, (2002) 2163-2167.

Bidentate imine ligands give stable molecules with lower toxicity than phosphines, although being less electron-donating. Schiff base metallacycles were found to be good catalysts for Suzuki-Miyaura cross-coupling in cyclopalladated compounds.⁴³

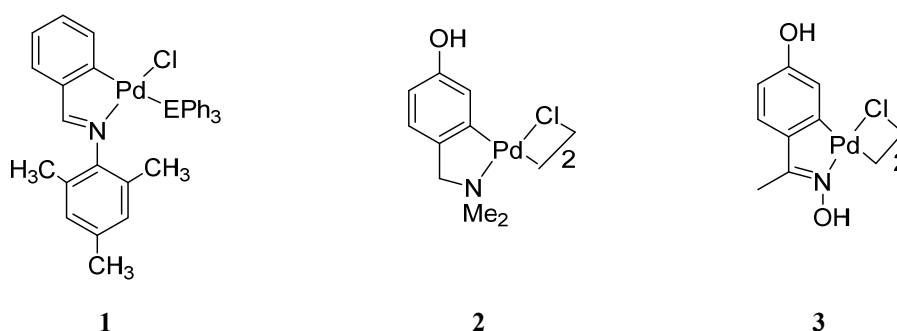


Figure 14. Nitrogen donor palladacycle as active catalysts.

A comparison of benzylphosphines to their amine analogues in metallation shows that the phosphine–palladium bond is stronger than the palladium–nitrogen bond, stabilizing the coordination complex. To achieve successful cyclopalladation, high temperatures were commonly used with extended reaction periods. Mono-, bis- and dinuclear cyclopalladated phosphine compounds have been described. On the other hand, phosphorus-based ligands, are toxic and air-sensitive, and they promote side reactions, decreasing the yield of desired cross-coupled products.⁴⁴

However, the cyclopalladated (**4**) was chosen from a group of related phosphorous donor compounds for its strong activity in aqueous

⁴³ A. Kapdi, D. Maiti, *Elsevier*, 2019.

⁴⁴ P.C. Kamer, P.W. van Leeuwen, *John Wiley & Sons*, 2012.

media at ambient temperature.⁴⁵ Suzuki-Miyaura cross-coupling was performed with cyclopalladated compounds (**5**, **6**) with phosphine ligands.^{46,47,48}

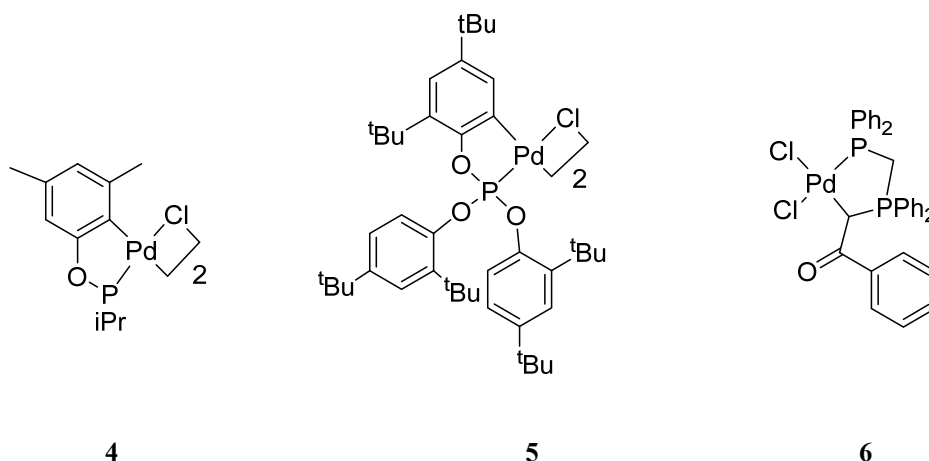


Figure 15. phosphorus donor palladacycle compounds.

Another feature of cyclopalladated compounds is the common usage of organic ligands having a C-S bond. The structural stability of the sulfur-containing cyclopalladated compound is excellent.⁴⁹ Sulfur-containing structures have achieved the pharmacological target and exhibit catalytic activity. Murai has reported the active catalysis of

⁴⁵A.N. Marziale, S.H. Faul, T. Reiner, S. Schneider, J. Eppinger, *Green Chemistry*, 12 (2010) 35-38.

⁴⁶ P. Gautam, B.M. Bhanage, *The Journal of organic chemistry*, 80 (2015) 7810-7815.

⁴⁷ K. Karami, M. Ghasemi, N.H. Naeini, *Tetrahedron Letters*, 54 (2013) 1352-1355.

⁴⁸ S.J. Sabounchei, M. Sayadi, M. Bayat, A. Sedghi, R.W. Gable, *Journal of Coordination Chemistry*, 70 (2017) 3727-3748.

⁴⁹ C. Shen, P. Zhang, Q. Sun, S. Bai, T.A. Hor, X. Liu, *Chemical Society Reviews*, 44 (2015) 291-314.

arylation of thienyl thioamides by $[\text{Pd}(\text{phen})_2](\text{PF}_6)_2$ complexes.⁵⁰ In the Suzuki coupling test, another mononuclear C-S bonded molecule exhibits increased activity.⁵¹

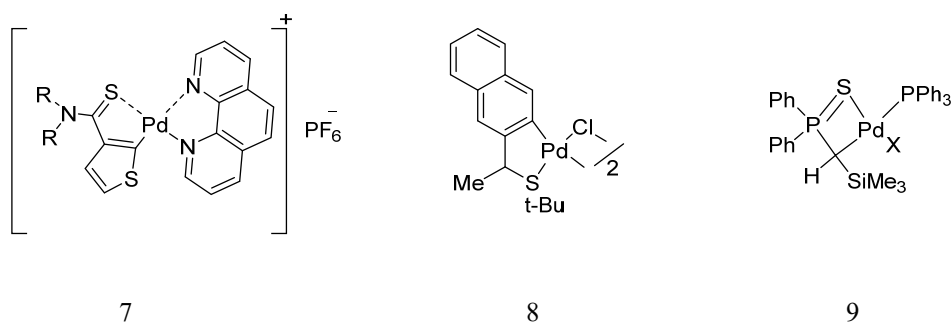


Figure 16. Mono and dinuclear palladacycle exhibiting [S, C] coordination.

1.3.1.2 Palladium pincer compounds.

Palladium pincer compounds have been the subject of substantial research and have been studied in the context of catalysis. Pincer compounds have a type of design that uses a novel chiral ligand with a transition metal to produce great enantioselectivity and efficiency. Chiral NCN, PCP ligands with a phenyl backbone coupled with two chiral units are among them. The comparatively simple production of the chemicals allows them to be used in catalysis. To further sustain the catalytic activity, several recent compounds have been shown to have interesting new catalytic capabilities through the substitution of

⁵⁰ T. Yamauchi, F. Shibahara, T. Murai, *Organic letters*, 17 (2015) 5392-5395.

⁵¹ S. Molitor, C. Schwarz, V.H. Gessner, *Organometallics*, 35 (2016) 159-167.

Pd-C bonds by other elements, for example, such as Pd-Si or Pd-P^{52, 53} and in rare cases Pd-N.^{54,55}

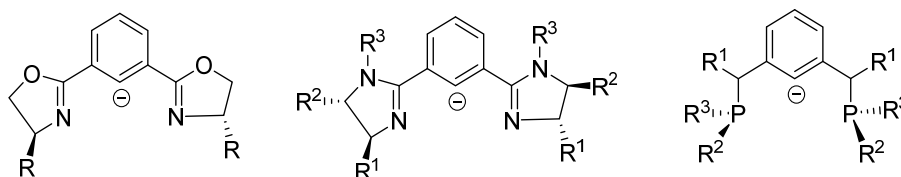


Figure 17. Types of design pincer compounds.

Most pincer compounds are air and moisture resistant, making them simple to store. Furthermore, they have good thermal stability. These critical sites enable strong catalytic properties and a wide range of reaction possibilities. The pincer ligand is important for catalysis selectivity because the square-planar geometry of the pincer compound only has one free coordination site for catalysis. The reactivity of the pincer compound is altered by changing the heteroatom, E, of the pincer ligand and using different donor groups. Pincer compounds with aromatic backbones also present electronic phenomena to be induced by *para* substitution of the aryl moiety.⁵⁶

⁵² M. Mazzeo, M. Lamberti, A. Massa, A. Scettri, C. Pellicchia, J.C. Peters, *Organometallics*, 27 (2008) 5741-5743.

⁵³ J. Takaya, N. Iwasawa, *Organometallics*, 28 (2009) 6636-6638.

⁵⁴ R.A. Begum, D. Powell, K. Bowman-James, *Inorganic chemistry*, 45 (2006) 964-966.

⁵⁵ B. Ines, R. SanMartin, M.J. Moure, E. Dominguez, *Advanced Synthesis & Catalysis*, 351 (2009) 2124-2132.

⁵⁶ I.G. Jung, S.U. Son, K.H. Park, K.-C. Chung, J.W. Lee, Y.K. Chung, *Organometallics*, 22 (2003) 4715-4720.

The activity of several pincer palladacycles as catalysts in Suzuki coupling has been achieved. The oxazoline group in compound (11)⁵⁷ is more active than the pyridine or amine groups. Compounds (12⁵⁸,13⁵⁹) with phosphorus and nitrogen/selenium or sulfur donors, respectively, also work well as catalysts and are air-stable.

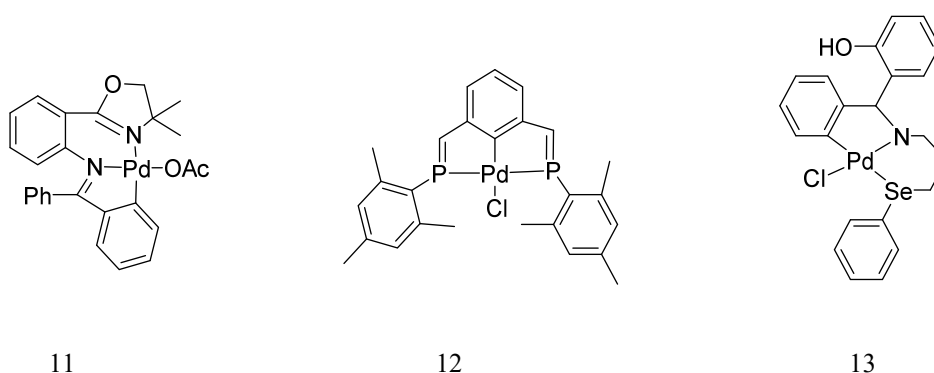


Figure 18. palladium pincer compound as active catalysts.

Modifications in the donor sites [N, C, N], [N, C, P], and [N, C, S] with palladium and platinum pincer compounds are extremely stable and allow functionalization after ligand metalation,⁶⁰ making them particularly suited and ideal building blocks for the synthesis of novel

⁵⁷ K.-M. Wu, C.-A. Huang, K.-F. Peng, C.-T. Chen, *Tetrahedron*, 61 (2005) 9679-9687.

⁵⁸ B. Deschamps, X. Le Goff, L. Ricard, P. Le Floch, *Heteroatom Chemistry*, 18 (2007) 363-371.

⁵⁹ G.K. Rao, A. Kumar, S. Kumar, U.B. Dupare, A.K. Singh, *Organometallics*, 32 (2013) 2452-2458.

⁶⁰ M.Q. Slagt, G. Rodríguez, M.M. Grutters, R.J. Klein Gebbink, W. Klopper, L.W. Jenneskens, M. Lutz, A.L. Spek, G. van Koten, *Chemistry-A European Journal*, 10 (2004) 1331-1344.

catalysis.⁶¹ Compounds (14,⁶² 15,⁶³ 6,⁶⁴) were found to be extremely effective catalysts.

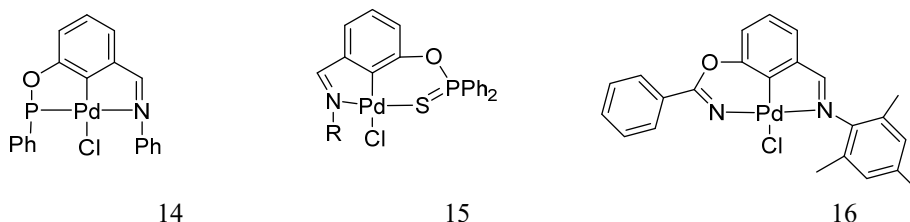


Figure 19. Nonsymmetrical [N, C, P], [N, C, S] and [N, C, N] palladium pincer compounds.

1.5 Aminophosphine ligands

In the 1980s, organometallic chemists became interested in the use of α -aminophosphine ligands in transition metals complexes. Since then, this area has received much attention, with about half of the publications in the last few years.

Aminophosphines are compounds that include both phosphorus and nitrogen atoms, independent of their specific structure. Other names, such as iminophosphines, phosphinoamides, phosphazanes, and so on, are more applicable for some of them.

⁶¹ S. Gründemann, M. Albrecht, J.A. Loch, J.W. Faller, R.H. Crabtree, *Organometallics*, 20 (2001) 5485-5488.

⁶² B.-S. Zhang, C. Wang, J.-F. Gong, M.-P. Song, *Journal of Organometallic Chemistry*, 694 (2009) 2555-2561.

⁶³ V. Kozlov, D. Aleksanyan, Y.V. Nelyubina, K. Lyssenko, A. Vasil'ev, P. Petrovskii, I. Odinet, *Organometallics*, 29 (2010) 2054-2062.

⁶⁴ A. Avila-Sorrosa, H.A. Jiménez-Vázquez, A. Reyes-Arellano, J.R. Pioquinto-Mendoza, R.A. Toscano, L. González-Sebastián, D. Morales-Morales, *Journal of Organometallic Chemistry*, 819 (2016) 69-75.

All compounds with a harder *N*-containing donor group and a softer *P*-containing donor functionality will be referred to as aminophosphine.⁶⁵

α -aminophosphines play a key role in the synthesis of transition metal compounds and are effective in homogenous catalytic reactions. Pt, Pd, Rh, and Ru are the most important platinum group derivatives in catalysis due to their unique features as compared to other transition metals.⁶⁶ For example, Pt and Ru compounds have shown medical properties through biological activation.⁶⁷

Phosphine ligands include phosphinoamines (P–N),⁶⁸ aminophosphines (P–C–N),⁶⁹ and other miscellaneous aminophosphines (P–C_n–N).⁷⁰ Aminophosphines are a type of phosphine that can be synthesized through the condensation of an amine, an oxo-compound, and a secondary phosphine.⁷¹ The method for synthesizing aminophosphines with transition metals Pt, Pd, and

⁶⁵ M.M. Pereira, M.J. Calvete, R.M. Carrilho, A.R. Abreu, *Chemical Society Reviews*, 42 (2013) 6990-7027.

⁶⁶ A. Fauq, R. Singh, D. Meshri, *Paquette*, LA, Ed, (2006).

⁶⁷ U. Ndagi, N. Mhlongo, M.E. Soliman, *Drug design, development and therapy*, 11 (2017) 599.

⁶⁸ V. A. Stepanova, I. P. Smoliakova, *Current Organic Chemistry*, 16 (2012) 2893-2920.

⁶⁹ W. Li, J. Zhang, *Chemical Society Reviews*, 45 (2016) 1657-1677.

⁷⁰ J. Gopalakrishnan, *Applied Organometallic Chemistry*, 23 (2009) 291-318.

⁷¹ L.A. Labios, C.J. Weiss, J.D. Egbert, S. Lense, R.M. Bullock, W.G. Dougherty, W.S. Kassel, M.T. Mock, *Zeitschrift für anorganische und allgemeine Chemie*, 641 (2015) 105-117.

Rh has been established using a variety of aminophosphine ligands, including linear, cyclic, mono-, and bidentate ligands.⁷²

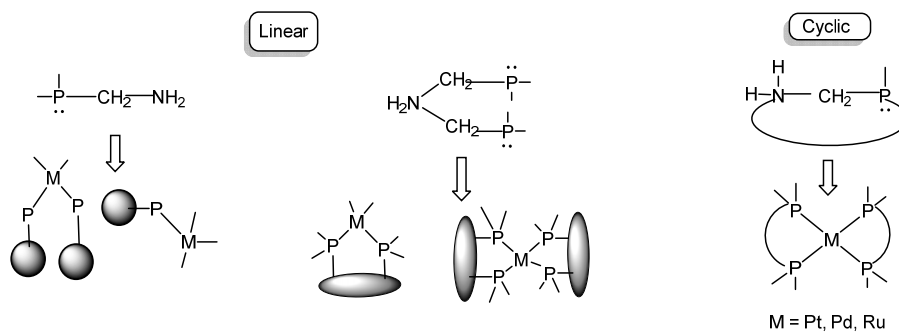


Figure 20. Types of aminophosphines synthesizing.

1.5.1 Platinum and palladium pincer compounds.

The attempts to obtain palladium and platinum complexes by treatment of $M(\text{cod})X_2$ [$M = \text{Pd}$, $X = \text{Cl}$]; [$M = \text{Pt}$, $X = \text{Br}$] with [N, N, N] ligands resulted in the formation of cationic, tetracoordinate, square-planar palladium and platinum complexes.⁷³

Palladium PNP complexes can catalyze the Suzuki coupling of phenylboronic acid with aryl and alkyl bromides. As a result, only palladium complex with PNP-Ph was used as a catalyst.

⁷² E. Bálint, Á. Tajti, A. Tripolszky, G. Keglevich, *Dalton Transactions*, 47 (2018) 4755-4778.

⁷³ D. Benito-Garagorri, E. Becker, J. Wiedermann, W. Lackner, M. Pollak, K. Mereiter, J. Kisala, K. Kirchner, *Organometallics*, 25 (2006) 1900-1913.

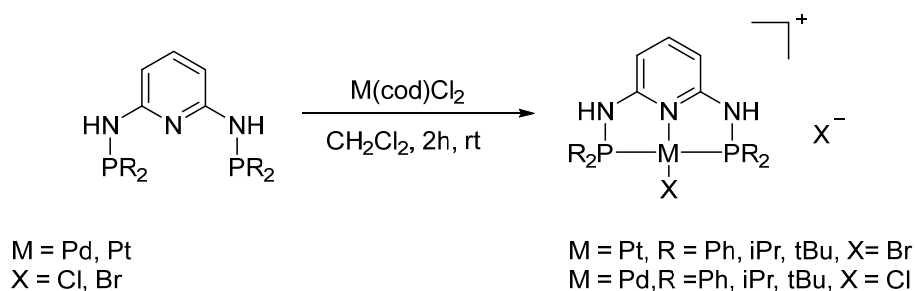


Figure 21. Cyclometallation catalysts PNP compounds.

Direct metalation of the ligands with Pd(COD)Cl₂, and Pt(COD)Br₂ resulted in neutral, tetracoordinated, square-planar palladium, and platinum PCP complexes. In the Suzuki coupling of aryl and alkyl bromides with phenylboronic acid, palladium PCP complexes are far more effective catalysts than their PNP analogues.⁷⁴

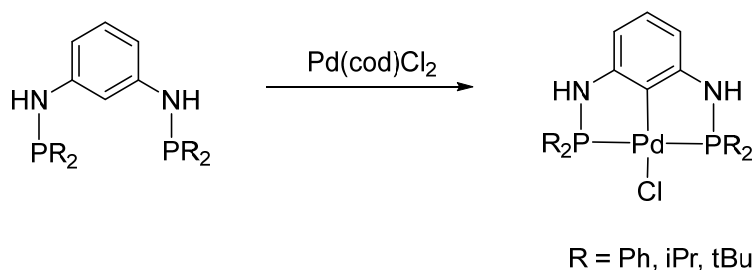


Figure 22. Cyclopalladation catalyst PCP compound.

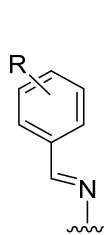
⁷⁴ D. Benito-Garagorri, V. Bocokić, K. Mereiter, K. Kirchner, *Organometallics*, 25 (2006) 3817-3823.

CHAPTER 2

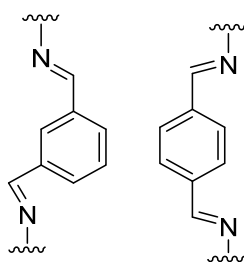
Objectives

In the Inorganic Chemistry Department of the University of Santiago of Compostela exists lines of investigation. One of the lines is the synthesis and preparation of cyclometallation compounds. In recent years, chemistry has expanded toward innovations in mysteriously many fields, especially inorganic chemistry, which has given an important role in the design and synthesis of wide compounds, which confirms in many fields of applications.

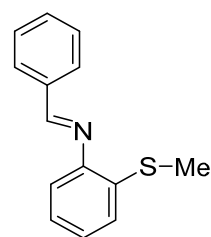
These compounds have been shown their interest in catalytic behavior. Moreover, in the research area, studies have been aimed at improving, growing, and preparing new compounds, which efficiently catalyze reactions in a highly enantioselective manner. In addition to taking into consideration a high potential of aminophosphine compounds derivatives in symmetric synthesis and catalysis. In this investigation, compounds have been done with different types of Schiff bases, and phosphines ligands. The Schiff bases have been synthesized with bidentate [C, N] and tridentate [C, N, S] donors such as mono imines and diimine ligands.



monoimine



diimine



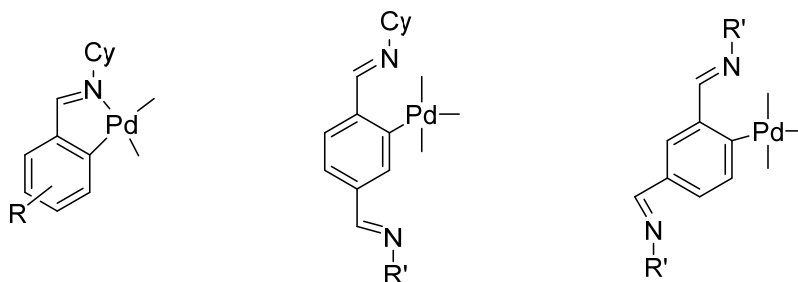
monoimine C, N, S

Schiff bases have created cyclometallated compounds of palladium(II) having a five-membered cyclometallated through intramolecular ortho-Csp² activation bond with acetate or halogen bridging ligands to study the cyclometallation of numerous differently substituted ligands. Otherwise, Schiff base of tridentate ligand [C, N, S] coordinated to palladium(II) chloride produced a mononuclear compound.

The cyclometallation of variously substituted ligands has been examined using tertiary diphosphines or triphosphines, depending on the case. The reactivity of these compounds against monodentate neutral ligands, such as tertiary phosphines (PRR), and ligands with two or three donor atoms formed in cyclometallated and non-cyclometallated monomer compounds of significant structural importance. The study of multifunctional ligands, such as diimines or aminophosphines, in which the ligand can attach to the metal via multiple donor atoms, has recently been expanded.

The first part of the study focused on cyclometallation reactions involving Schiff bases with numerous donors. In the experiment, two ligands derived from isophthalaldehyde and terephthalaldehyde were used simultaneously, yielding monocyclometallated compounds with which interactions with diphosphines, or triphosphines, were carried out. The possibility of regenerating one or both bonds, depending on the case, was explored by treating the relevant compound with a diimine or an aminophosphine. Moreover, the triphosphines compounds, reactions with diimine and aminophosphine ligands were carried out to functionalize them with new donor atoms and investigate the possibility that these latter ligands species coordinate

to another metal center, the same or different from the one linked to the ligand by a sigma bond, resulting in homo- or heteroatom complexes, respectively.

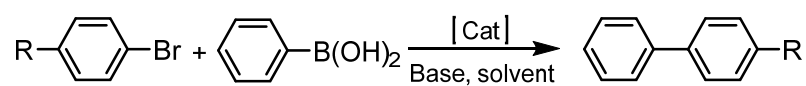


The second part of the study aimed to synthesize cyclopalladated compounds of derived Schiff bases [C, N]. They synthesized Pd(II) dimer compounds with acetate bridges and then used them to make compounds with halogen bridges. Reactions of the latter were carried out with mono and diphosphine ligands. In contrast, we described Michael additions to the C=CH₂ moiety of the coordinated ligand, which were then treated with cyclopalladated compounds.

The third part of the study focused on the synthesis of simple cyclopalladated compounds with a σ [Csp², N, S] tridentate ligand and a strong Pd-S bond, as well as to investigate their reactivity towards phosphine ligands.

Finally, a catalytic study was carried out to describe a possible application for the compounds synthesized. In the Suzuki reaction, which is an example of a carbon-carbon coupling process, the catalytic activity of these compounds was investigated. The aim of

these tests is to look into reaction efficiency, see whether structural features of these catalysts have an effect on reaction results, and, to the extent possible, optimize reaction settings for optimal efficiency.



CHAPTER 3

Experimental part

3. Experimental Part

3.1 Reagents and solvents

3.1.1 Organic Reagents

All reagents and solvents used in this study were used without further purification.

Isophthalaldehyde (Aldrich 97 %)

Terephthalaldehyde (Aldrich 98 %)

4-Bromobenzylaldehyde (Aldrich 99 %)

3-Bromobenzylaldehyde (Aldrich 97 %)

4-Bromoacetofenone (Aldrich 98 %)

2-Bromobenzylaldehyde (Aldrich 98 %)

2-Chlorobenzylaldehyde (Aldrich 98 %)

2-Florobenzylaldehyde (Aldrich 98 %)

2,3,4-Methoxybenzylaldehyde (Aldrich 99 %)

2,4-Methoxybenzylaldehyde (Aldrich 99 %)

3,4-Methoxybenzylaldehyde (Aldrich 99 %)

2-Methoxybenzylaldehyde (Aldrich 98 %)

4-Methoxybenzylaldehyde (Aldrich 98 %)

Boronic acid (Fluka)

Amine

Cyclohexylamine (Aldrich 99 %)

2(diphenylphosphino)Ethan-1-amine (Fluka 97 %).

Aniline

2-(methylthio)aniline (Avocado 98 %)

3.1.2 Inorganic Reagents

Palladium acetate(II) (Fluka 97 %).

Palladium chloride. (ABCR 97 %).

Bis(benzonitrilo)platinum(II) dichloride.

Bis(benzonitrilo)palladium(II) dichloride

Thallium acetaylacetone (Aldrich)

Lithium chloride (Aldrich 99 %)

Sodium chloride (Panreac 99,5 %)

Sodium bromide (Panreac 99,5 %)

Sodium sulfate anhydrous (Panreac).

Silica gel 60 for column chromatography (MERCK) (70-230 mesh 15 ASTM)

Ammonium hexafluorophosphate (Aldrich 99,5 %).

Phosphines

Triphenylphosphine (Avocado 99 %).

Bis(diphenylphosphine)methane (Aldrich 98 %)

Bis(diphenylphosphine)ethene (Aldrich 98 %)

Bis(2-diphenylphosphinoethyl)phenylphosphine (Aldrich 98 %)

3.1.3 Solvents

Acetone (Panreac 99.5 %)

Hydrochloric acid (T3 chemistry, S.C.C.L. 35 %)

Chloroform (Scharlau)

Ethanol (Absolute, Sacharlau 99.5 %)

Diethyl ether (technical grade)

Ethyl acetate

Dichloromethane (Scharlau)

Acetic acid glacial (Scharlau)

Toluene (Aldrich 99.8 %)

n-Hexane (SDS)

Methanol (Panreac)

Dry Tetrahydrofuran (THF) (Panreac) was dried by sodium metal in the presence of benzophenone and was freshly distilled under Argon before use.

Deuterated solvents

Chloroform-d (SDS, Aldrich 99.8 %)

Acetone-d₆ (Aldrich 99.8 %)

DMSO-d₆ (Aldrich)

CHAPTER 4

Characterization techniques

4. Characterization Techniques

The obtained complexes were characterized using infrared (IR) spectroscopy, magnetic resonance nuclear (NMR), and, where possible, X-ray diffraction (XR).

4.1 Infrared spectroscopy.

Infrared spectra were collected using a Varian spectrophotometer. Spectra were taken in the 4000-400 cm^{-1} and in the 100-500 cm^{-1} ranges. Wavenumbers were used to represent infrared data (cm^{-1}).

Infrared spectroscopy is a technique that provides structural information on the existing bonds in the molecule as well as the arrangement of the ligands around the metal atom. As a result, the position of a higher or lower band wavenumber is related to the bond strength and mass of the atoms involved.

As the bond is weaker the band is shifted to a lower wavenumber, and when two comparable bonds with atoms of different mass are compared, the one with the heavier atoms will display the band at a lower wavenumber. Next follows a study of the most characteristic vibration frequencies of the complexes prepared.^{75,76}

⁷⁵ K. Nakamoto, *organometallic, and bioinorganic chemistry*, John Wiley & Sons, 2009.

⁷⁶ S.L. Palencia, A. García, M. Palencia, *Journal of the Chilean Chemical Society*, 65 (2020) 5015-5022.

4.1.1 Study of $\nu(\text{C}=\text{N})$ band

The assignment of this vibration is more often than not difficult since its strength and position alter dramatically with changes in the environment of the $\text{C}=\text{N}$ group. Because of their low intensity, their assignment is usually difficult. This becomes more confusing if it happens to overlap with other bands, such as the aromatic ring vibration $\nu(\text{C}=\text{C})$. Due to aromatic conjugation, which causes the signal to shift to lower wavenumbers, this band is found between 1674 and 1664 cm^{-1} for unconjugated imines of the $\text{R}-\text{CH}=\text{N}-\text{R}$ type, while in the case of conjugated imines of type $\text{Ar}-\text{CH}=\text{N}-\text{Ar}$ it is found between 1637 and 1613 cm^{-1} .⁷⁷ As a result, it is to be predicted that in a partially conjugated imine system, such as $\text{Ar}-\text{CH}=\text{N}-\text{Me}$, this band will appear halfway between the two preceding values.

The position of this band in the spectrum of the free ligand in comparison to the position in the spectrum of the complexes can be used to assess whether or not a bond was established between this group and the metal atom, as well as the sort of connection. There are two options, as shown in the accompanying diagram Figure 23.

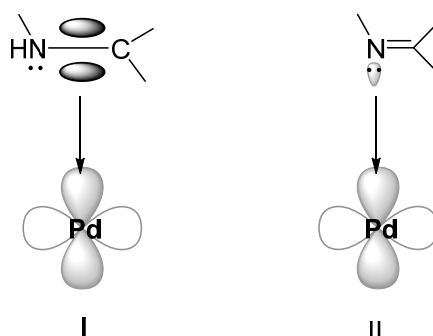


Figure 23. Coordination possibilities of the C=N group.

In either case, the coordination of the metal weakens the bond, resulting in a decrease in the wavenumber of the vibration band of that link (of varying magnitude depending on the type of bonding of the metal atom to the group C=N). In instance I, the metallic atom will also share the C=N group's bonding orbital. This reduces the electron density between carbon and nitrogen, resulting in a decrease in bond strength and displacement of the band $\nu(\text{C}=\text{N})$ at lower wavenumbers of the order of 150 cm^{-1} .

In case II, the electronic pair allows coordination. The metal is linked to nitrogen in a non-bonding orbital, and this does not affect the bond order. However, if there is a retrodonation of charge from the metal to the orbital $\pi^*(\text{C}=\text{N})$, the force constant of that bond will decrease, resulting in a shift of the band $\nu(\text{C}=\text{N})$ to lower wavenumbers *ca.* of $15 - 45\text{ cm}^{-1}$.

4.1.2 Study of $\nu(\text{C}=\text{O})$ band

All carbonyl compounds have a strong absorption band that corresponds to $\nu(\text{C}=\text{O})$ stretch between $1820\text{--}1670\text{ cm}^{-1}$. Its position varies relatively little depending on the functional group to which the carbonyl belongs in each case, the intensity, and the absence of other bands that interfere with it make it one of the easiest bands to assign in the spectrum. When determining whether or not the imine bond has been formed, this band can provide information regarding the synthesis of ligands having a carbonyl group (aldehyde) as a precursor.

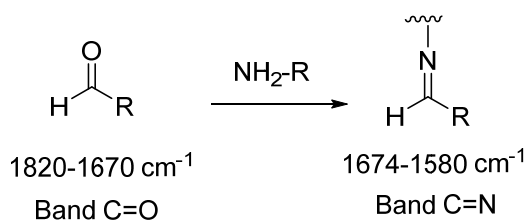


Figure 24. The C=O and C=N bands appear at different wavenumbers.

4.1.3 Study of the acetate ligand $\nu(\text{COO})$ band

The acetate ligand displays a variety of coordination modes.

Examining the differences observed in the IR spectra in the bands assigned to the symmetric $\nu_s(\text{COO})$ and asymmetric $\nu_{as}(\text{COO})$ vibrations determining which of the possibilities occurs can be quite straightforward.

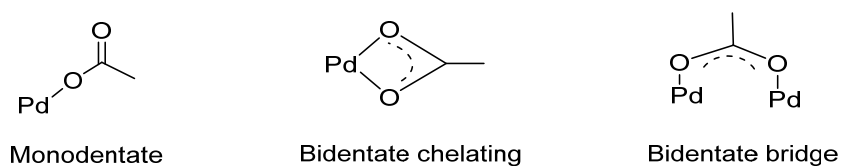


Figure 25. possibility of acetate ligand coordination.

As a result, the separation between these two bands—symmetric and asymmetric—can be used to indicate the type of coordination of the acetate ligand. The $\nu_{as}(\text{COO})$ and $\nu_s(\text{COO})$ vibrations are shifted to lower wavenumbers and higher wavenumbers, respectively. If the acetate ligand is monodentate, the $\nu_{as}(\text{COO})$ vibration shifts to a higher wavenumber, while the $\nu_s(\text{COO})$ vibration shifts to a lower wavenumber, increasing the difference between the two with respect to the free ligand to $290\text{--}230\text{ cm}^{-1}$. In case it behaves as a chelated bidentate ligand, and the separation between the two is *ca.* $80\text{--}40\text{ cm}^{-1}$. While when it is a bridging bidentate ligand, the separation between the bands is *ca.* 170 and 140 cm^{-1} . When two acetate bridging ligands are present in the compound there should be four bands, two corresponding to $\nu_{as}(\text{COO})$ and two corresponding to $\nu_s(\text{COO})$, for the in-phase opposition and out-of-phase modes. However, due to the width of the (COO) bands, only two bands are detected that can be assigned to $\nu_{as}(\text{COO})$ and $\nu_s(\text{COO})$.

4.1.4 Study of band $\nu(\text{Pd-Cl})$

Halogens can be used as bridging or terminal ligands.^{76,77} The ligand or donor atom *trans* to the chloride ligand determines the position of the band in the spectra. With a strong *trans* effect ligand, the metal-chloride bond is weakened, resulting in a band shift to lower

wavenumbers. Also, depending on the type of coordination, distinct bands may appear in complexes with chlorine ligands.^{78, 79}

Table 1. Chloro ligands position bands.

Type of coordination	$\nu(\text{Pd-Cl-trans-N})$ in cm^{-1}	$\nu(\text{Pd-Cl-trans-C, S})$ in cm^{-1}
Terminal Position	360-300	310-270
Bridge Position	370-300	270-210

When the chloride ligand is at the terminal position, a single band appears *ca.* 310–270 cm^{-1} . When confronted with strong *trans* influence atoms, such as the phenyl carbon⁸⁰ or sulfur, and *ca.* 300–360 cm^{-1} when *trans* to of weaker *trans* influence, such as the imine nitrogen. The chlorine-bridged complexes show two bands in the spectra, one due to the *trans*-Pd-Cl bond to nitrogen and the other due to the *trans*-Pd-Cl bond to carbon. Because the *trans* influence of a nitrogen atom is less than that of a phenyl carbon atom, the band observed at higher wavenumbers corresponds to $\nu(\text{Pd-Cl})$ *trans*-N, while the band observed at lower wavenumbers corresponds to $\nu(\text{Pd-Cl})$ *trans*-C. Thus, the former band appears *ca.* 370–300 cm^{-1} , while the latter band appears *ca.* 270–210 cm^{-1} . Furthermore, it should be noted that when the chloride ligand acts as a bridging ligand between two metal centers, *cisoid* and *transoid* isomers may appear, making the assignment even more difficult.

⁷⁸ M. Nonoyama, *Journal of Inorganic and Nuclear Chemistry*, 42 (1980) 297-299.

⁷⁹ R.M. Cedar, J. Sales, X. Solans, M. Font-Altava, *Journal of the Chemical Society, Dalton Transactions*, (1986) 1351-1358.

⁸⁰ F. Hartley, *Chemical Society Reviews*, 2 (1973) 163-179.

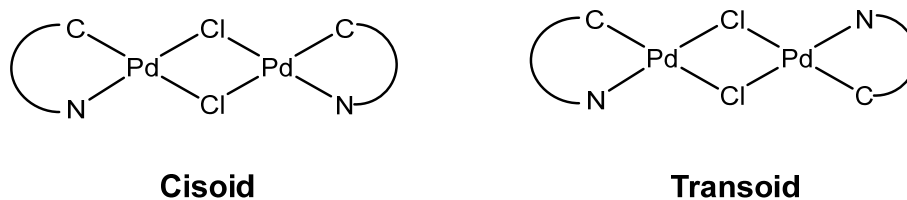


Figure 26. Cyclometallated compounds with Halogen bridges.

Furthermore, it is possible to carry out in the case of compounds containing Br bridges, however the interval in which the $\nu(\text{Pd-Br})$ bands appear is $210\text{--}140\text{ cm}^{-1}$.

4.1.5 Study of band $\nu(\text{C=O})$ and $\nu(\text{C=C})$

The ligand acetylacetonate can act as a bridging or bidentate chelate to coordinate to a metal ion. Studying the tension vibrations of $\nu(\text{C=O})$ and $\nu(\text{C=C})$ using IR spectroscopy can clarify the type of coordination that takes place.

The presence of bands at 1580 and 1390 cm^{-1} , typical of $\nu(\text{C=O})$, is an unmistakable indication that the acetylacetonate ion is coordinated to the metal atom acting as a ligand bidentate chelate through oxygen atoms,⁸¹ which is further supported by the presence of a band *ca.* 1515 cm^{-1} due to $\nu(\text{C=C})$. Around 1270 cm^{-1} , a band should also be particularly noticeable, but the phenyl ring bands $\nu(\text{C=C})$ cover this band.

⁸¹ K. Nakamoto, IR and Raman spectra of inorganic and coordination compounds,

4.2 NMR Spectroscopy.

Instrumentation: ^1H and ^{31}P NMR spectra were obtained using the Bruker DPX 250 and Varian Inova 400 spectrometers, respectively. The samples were dissolved in CDCl_3 , acetone- d_6 , DMSO- d_6 and then recorded. The MestreNova program was used to process the spectra.⁸²

The ^{31}P -NMR spectra were $^{31}\text{P}\{-^1\text{H}\}$.

The conditions of NMR spectra are given in parenthesis (resonance frequency, solvent, acquisition temperature). ^1H NMR, *e.g.*, (250 MHz, CDCl_3 , 298 K).

- NMR data for ^1H or ^{31}P -NMR is presented as follows: chemical shift (multiplicity, integration, assignment, and coupling constant, if applicable).
- The coupling constants J are measured in hertz (Hz). The following abbreviations are used to indicate multiplicity: s, singlet; br s, broad singlet; d, doublet; dd, doublet of doublet; t, triplet; tt, triplet of triplet and m, multiplet.
- Chemical shifts of residual solvent signals: chloroform- d , +7.28 ppm; DMSO- d_6 , +2.50 ppm; and acetone- d_6 , +2.05 ppm.⁸³

⁸² C. Cobas et al. Mestre Lab Research S.L

⁸³ G.R. Fulmer, A.J. Miller, N.H. Sherden, H.E. Gottlieb, A. Nudelman, B.M. Stoltz, J.E. Bercaw, K.I. Goldberg, *Organometallics*, 29 (2010) 2176-2179.

4.2.1 ^1H NMR Study.

The ^1H NMR study provides extremely useful information for understanding compound structures and is one of the most widely used and reliable characterization methods in this field of chemistry.⁸⁴

The reaction between the ligands and the metal causes a series of changes in the spectra of the complexes. As a result, the shift of the signals, variations in their multiplicity, or the presence or absence of the signals assists us in determining the structure of the compounds. Among all of these changes, the study of the imine bond is noteworthy, since the presence of the $\text{C}=\text{N}$ group causes anisotropic displacement of some signals as a result of deshielding (-) or shielding (+) in regions of the molecule close to it. Figure 27.

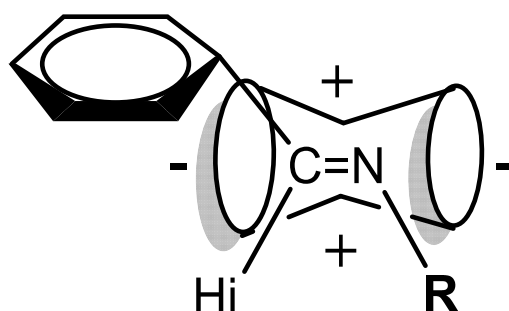


Figure 27. Shielding (+) and deshielding (-) of the imine bond.

This effect may be seen in the imine proton, whose signal is observed at a low field because it is located in the anisotropic deshielding zone of the $\text{C}=\text{N}$ double bond. Furthermore, the protons bonded to the

⁸⁴ S.F. Ontaneda, R.N. Martín, I.V.A. Laplana, Grado en Química 27219-Determinación estructural.

carbon in the *ortho* position of the phenyl ring are also affected by the imine group.

When a ligand undergoes metallation, however, the signal of the aromatic proton initially bonded to the metallated carbon disappears, and there is a resulting variation in the multiplicity of the remaining aromatic protons. In compounds produced from thiosemicarbazone ligands, the signal of the hydrazine proton present in the free ligand is absent as a result of the bonding to the metal atom. In compounds containing phosphine ligands bonded to the metal, in general, the signal corresponding to the imine proton is split by coupling to the ^{31}P nucleus of phosphine, which usually occurs only when the phosphorous atom is *trans* to the imine nitrogen. This is the most common disposition, and it is caused by the transphobic effect.⁸⁵ Furthermore, the arrangement of the phosphine phenyl rings can produce shielding of the aromatic ring nuclei. As a result, the signal of the H5 proton and the substituents found in the H4 and H5 positions are shielded from its position in the ligand spectrum.

⁸⁵ J. Vicente, J.A. Abad, A.D. Frankland, M.C. Ramírez de Arellano, *Chemistry–A European Journal*, 5 (1999) 3066-3075.

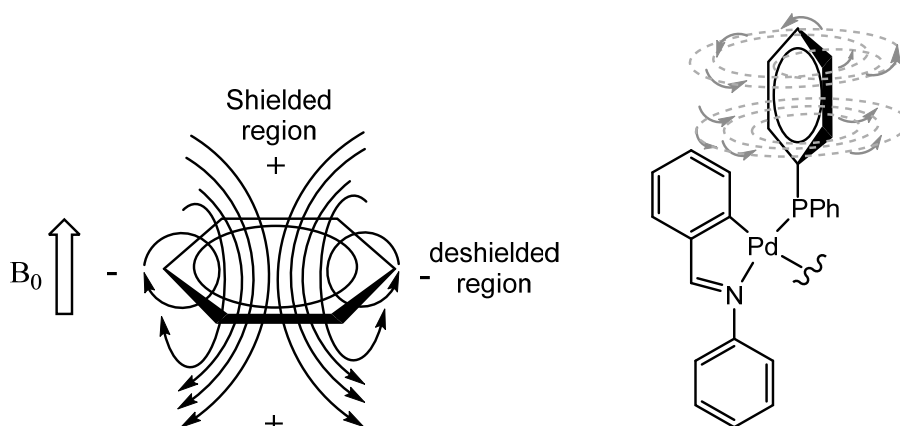


Figure 28. The effect of the ring current, shielding (+), and deshielded (-) areas created by the phenyl ring. a) After applying a magnetic field B_0 to a phenyl ring, a ring current emerges. The applied magnetic field is weakened both above and below the molecule in shielding areas (+ sign), but it appears reinforced in unshielded areas.

4.2.2 ^{31}P - $\{^1\text{H}\}$ NMR Study.

The ^{31}P - $\{^1\text{H}\}$ NMR analysis gives information related to the phosphine ligand geometry, which can be particularly important for compound characterization. Except in the case of certain diphosphines, which act as chelated bidentate ligands, the incorporation of this type of ligands in the metal coordination sphere tends to cause the signal to shift to a lower field from its position in the free ligand spectrum.^{86,87} As a result, it is useful to compare the data obtained for the free and coordinated ligands.

Phosphine ligands can be coordinated in three different ways: monodentate, bridge bidentate, chelate bidentate or chelate tridentate.

⁸⁶ R. Ares, M. López-Torres, A. Fernández, S. Castro-Juiz, A. Suarez, G. Alberdi, J.J. Fernández, J.M. Vila, *Polyhedron*, 21 (2002) 2309-2315.

⁸⁷ A. Miedaner, D.L. DuBois, *Inorganic Chemistry*, 27 (1988) 2479-2484.

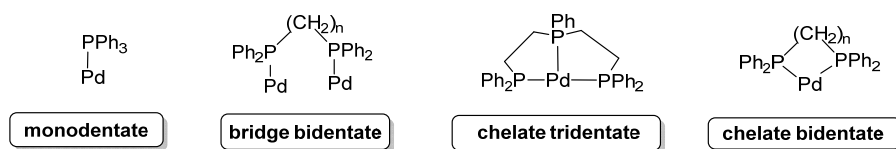


Figure 29. The principal coordinative possibilities for phosphine ligands.

Since each phosphorus atom has a different chemical environment when the diphosphine acts as a monodentate ligand, two doublets can be expected, one for the coordinated phosphorus nucleus to the metal (the most deshielded) and the other for the uncoordinated phosphorus nucleus. In the chelating mode, the two donors of the diphosphine may be equivalent depending on the geometry and one singlet signal is observed. However, this is not usually the case and two doublets appear, as in the former case, albeit both shifted to lower field. In the bridging mode, both ^{31}P nuclei are normally equivalent, hence a single singlet is expected. The phosphorus nuclei, in this case, are not equivalent, so two distinct signals are expected. Because monophosphines (PPh_3) interact only as monodentate ligands, the signal observed in the ^{31}P -NMR spectrum is obviously a single singlet.

Table 2. The chemical shift of phosphine signals in the spectrum of ^{31}P - $\{^1\text{H}\}$ NMR.

Phosphine	abbreviation	$\delta^{31}\text{P}-\{^1\text{H}\} / \text{ppm}$
Triphenylphosphine	PPh_3	-7
Bis(diphenylphosphine)methane	dppm	-24.2
1,1-Bis(diphenylphosphine)ethane	vdpp	-3.27
Bis(2-diphenylphosphinoethyl)phenylphosphine	Triphos	-12.35

4.3 X-ray diffraction.

Suitable crystals for X-ray diffraction studies were obtained for some of the compounds synthesized in this work. X-ray diffraction data were collected using an automatic diffractometer ENRAF-NONIUS model MACH3, a BRUKER SMART 1000 CCD, a Bruker KAPPA-APEX II, and a NONIUS FR591-KAPPACCD2000. The CAD4-Express software (Nonius, 1994), BRUKER SMART⁸⁸, and Nonius Collect-HKL2000 were used to control the diffractometers. In all of the measured reflections, the Lorentz and polarization effects were adjusted.⁸⁹ A semi-empirical technique (SADABS)⁹⁰ based on repeated measurement of equivalent reflections by symmetry was also used to adjust for absorption. Direct methods were used to resolve structures, and F² full-matrix least-squares methods were used to refine them. Hydrogen atoms were added to the models in geometrically calculated positions and refined while attached to the atom to which they were attached. The refinement was continued until all of the refined parameters converged, taking into account the anisotropic nature of all non-hydrogen atoms.

The calculations were carried out using the SHELXS-86 program package,⁹¹ SHELXL-97,⁹² SIR-92,⁹³ SIR-97, SIR-2004,⁹⁴ and

⁸⁸ V. SMART, Oxford Diffraction Ltd., Version.

⁸⁹ A. Dawson, D.R. Allan, S. Parsons, M. Ruf, *Journal of applied crystallography*, 37 (2004) 410-416.

⁹⁰ G. Sheldrick, University of Göttingen, Germany, (1996).

⁹¹ G. Sheldrick, Institut für Anorganische Chemie der Universität Göttingen, Germany, (1986).

DIRDIF-99,⁹⁵ all of which are included in the winGX software package,⁹⁶ the Ortep3v2 programs,⁹⁷ PLUTON,⁹⁸ Mercury 3.6, and POVRay v3.62. The atomic scattering factors were calculated using the International Tables for X-ray Crystallography.⁹⁹

X-ray diffraction is a technique for unmistakably determining the structure of a given compound in the solid-state. Different crystallization conditions were used to create the crystalline samples. One of the most effective ways for chemicals produced in this study is the slow evaporation of a sample dissolved in dichloromethane, sometimes with the addition of a little amount of n-hexane. Slow evaporation in acetone or chloroform is another option in some conditions to achieve single crystals.

If the factors of the agreement are suitable, the resolution of a compound's structure allows for the determination of distances and bond angles. It also enables the investigation of coordinating environments. Supramolecular interactions are important, in obtaining richer graphical representations.

⁹² G.M. Sheldrick, A: *Found. Crystallogr*, 64 (2008) 112.

⁹³ L.J. Farrugia, *Journal of Applied Crystallography*, 45 (2012) 849-854.

⁹⁴ M.C. Burla, R. Caliandro, M. Camalli, B. Carrozzini, G.L. Cascarano, L. De Caro, C. Giacovazzo, G. Polidori, R. Spagna, *Journal of Applied Crystallography*, 38 (2005) 381-388.

⁹⁵ L.J. Farrugia, *Journal of Applied Crystallography*, 32 (1999) 837-838.

⁹⁶ L.J. Farrugia, *Journal of Applied Crystallography*, 45 (2012) 849-854.

⁹⁷ L.J. Farrugia, *Journal of Applied Crystallography*, 30 (1997) 565-565.

⁹⁸ A. L. Spek; *J. Appl. Crystallogr*, 36 (2003) 7.

⁹⁹ I. Suh, J. Suh, T. Ko, K. Aoki, H. Yamazaki, *J. Appl. Cryst*, 19 (2006) 6.

4.3.1 Bond distances.

The bond distance is one of the things to look into once a compound's crystalline structure is known; this helps to find the type and characteristics of the bonds.

The covalent radii of the atoms involved in the bond must be known, which can be obtained directly from the corresponding single homonuclear bond or indirectly through the difference of the covalent radii. The covalent radii of the atoms corresponding to the compounds that appear in this work are shown in Table 3.¹⁰⁰

Table 3. Atomic Covalent Radii reported in solved structures.

Element	Radios of covalent bond/ pm	Element	Radios of covalent bond/ pm
H	37	S	102
C	77	Cl	99
N	75	Pd	131
O	73	P	128

4.3.1.1 Hydrogen bonding.

Hydrogen bonding is one of the most important interactions and has received a lot of attention. It is important in biological systems because, in conjunction with other interactions, it is responsible for the secondary and tertiary structure of proteins. It is an interaction

¹⁰⁰ Tables of Interatomic Distances and Configuration in Molecules and Ions. Special Publication N° 11; Supplement 1956-1959, Special Publication N°18, Chemical Society London 1958.

between a donor and a proton acceptor $D-H\cdots A$, where D is the donor and A is the acceptor; it is a dipole-dipole interaction. Strong, moderate, and weak connections can be identified from hydrogen based on the distances and angles formed during these interactions. In the first case, the distances $D-H$ and $H\cdots A$ are similar, and the angle $D-H\cdots A$ is close to 180° , indicating that the hydrogen bond has a strong covalent character; in the second case, $H\cdots A$ is greater than $D-H$, with bond angles ranging from 90° to 150° .

The Platon software, which is part of the WinGX package, was used to investigate these types of interactions here. It considers the presence of a hydrogen bond when $d(D\cdots A) < R(D) + R(A) + 0.50$; $d(H\cdots A) < R(H) + R(A) - 0.12$; $d-H-A > 100^\circ$. Where $R(D)$ and $R(A)$ are the atomic radii for D and A, respectively.

4.3.1.2 Molecular stacking π - π interactions.

Non-covalent intermolecular forces are defined as π - π or aromatic-aromatic interactions. These forces are responsible for the development of some molecular structures in key structures such as nucleic acids. They are referred to as electrostatic and van der Waals forces, within a σ and a π framework existing in aromatic systems. The electrostatic attraction σ - π favors this type of interaction and determines the best geometry to make it possible. There are two types of interactions: type T and face-to-face interactions.

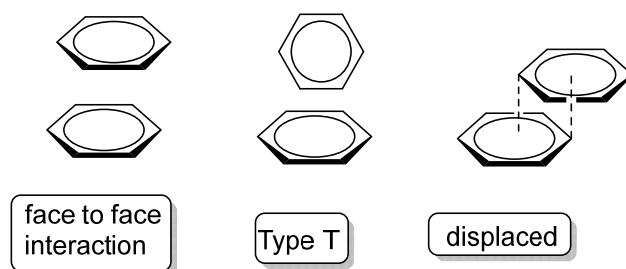


Figure 30. Several sorts of π - π interactions.

Face-to-face interactions can occur between two overlapping rings, which is known as a sandwich-type, or between two parallel rings that are displaced from each other.¹⁰¹ The angles β , γ , and the distance between planes can be used to measure the relative displacement of one ring on another. It can be assumed that there are stronger or weaker interactions depending on the values of these parameters.¹⁰² For simplicity when the distance between centroids ($dC_{g(I)} - C_{g(I)}$) is less than 3.9 and the angles are less than 40, the interaction π - π is considered to exist.

¹⁰¹ M.O. Sinnokrot, E.F. Valeev, C.D. Sherrill, *Journal of the American Chemical Society*, 124 (2002) 10887-10893.

¹⁰² C. Janiak, *Journal of the Chemical Society, Dalton Transactions*, (2000) 3885-

3896.

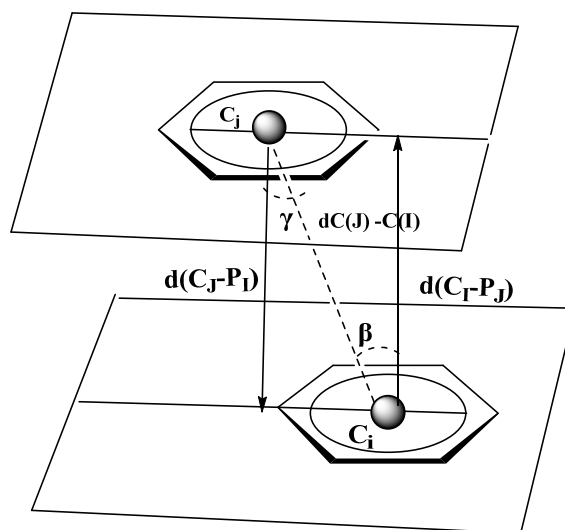


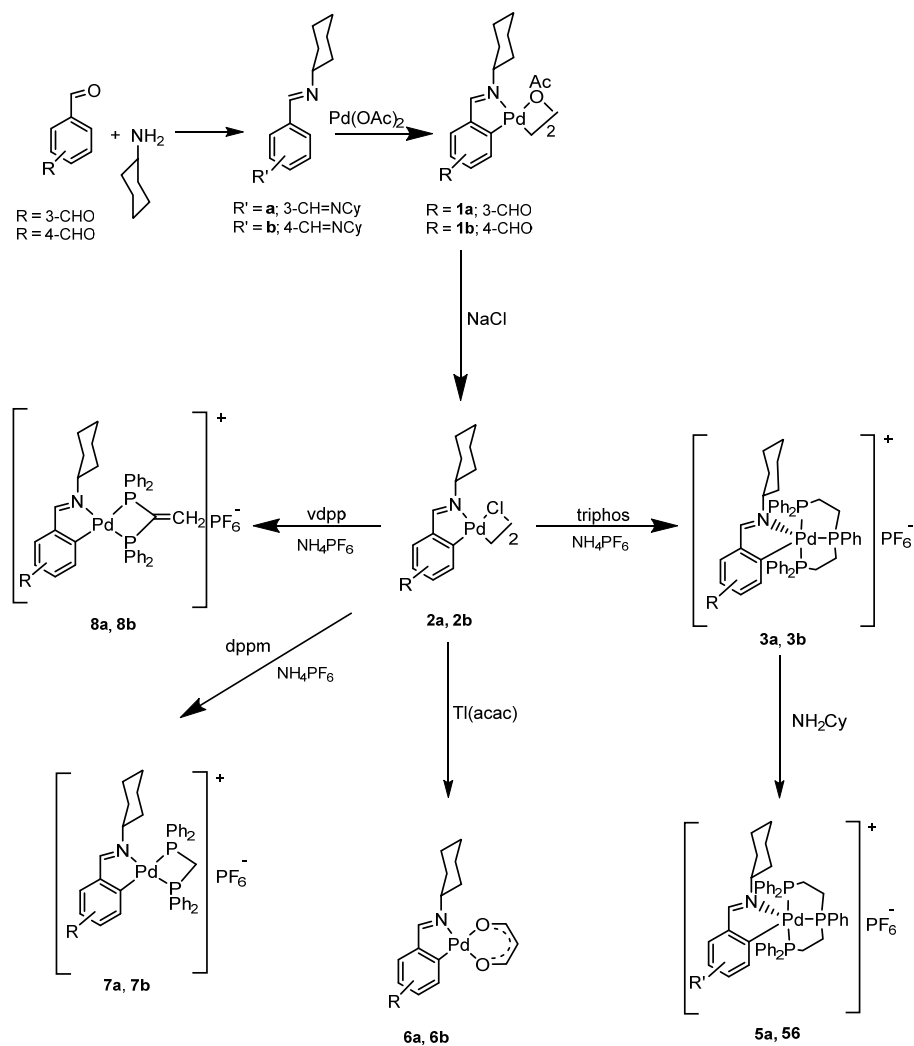
Figure 31. Interaction parameters π - π .

CHAPTER 5

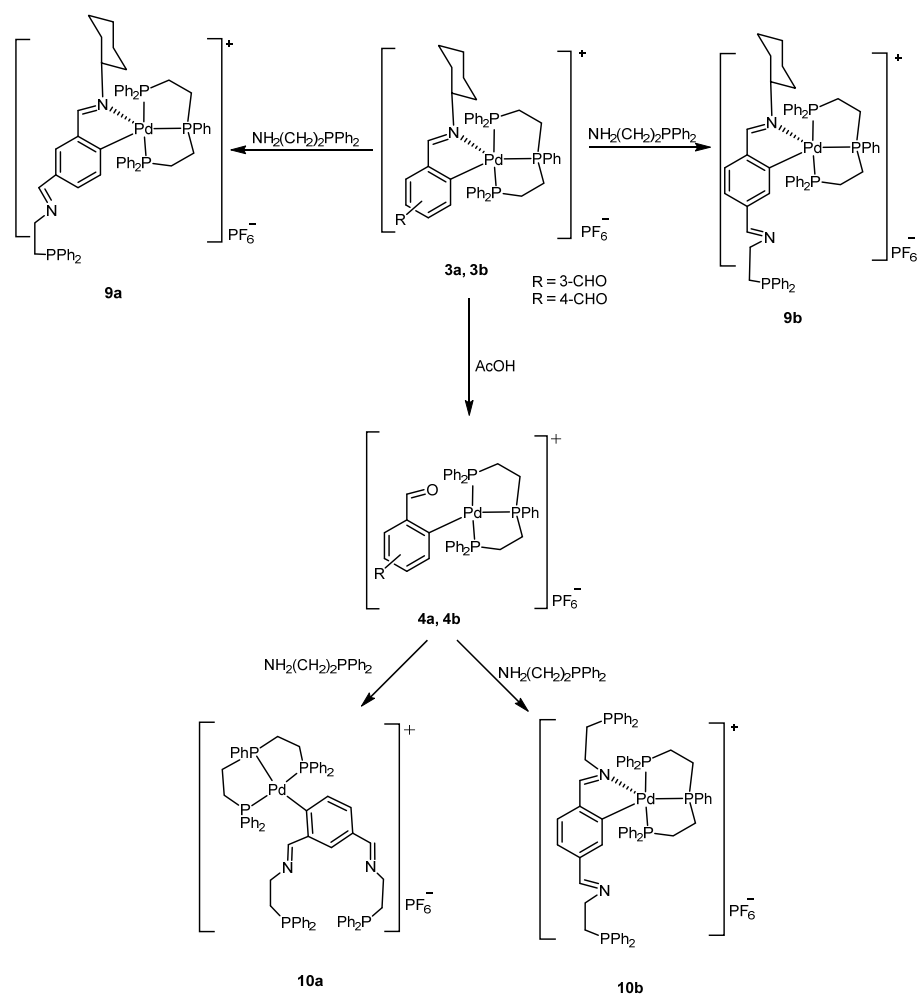
Schemes Reactions

5.1 Cyclopalladation compounds derivatives of Schiff bases from terephthalaldehyde and isophthalaldehyde

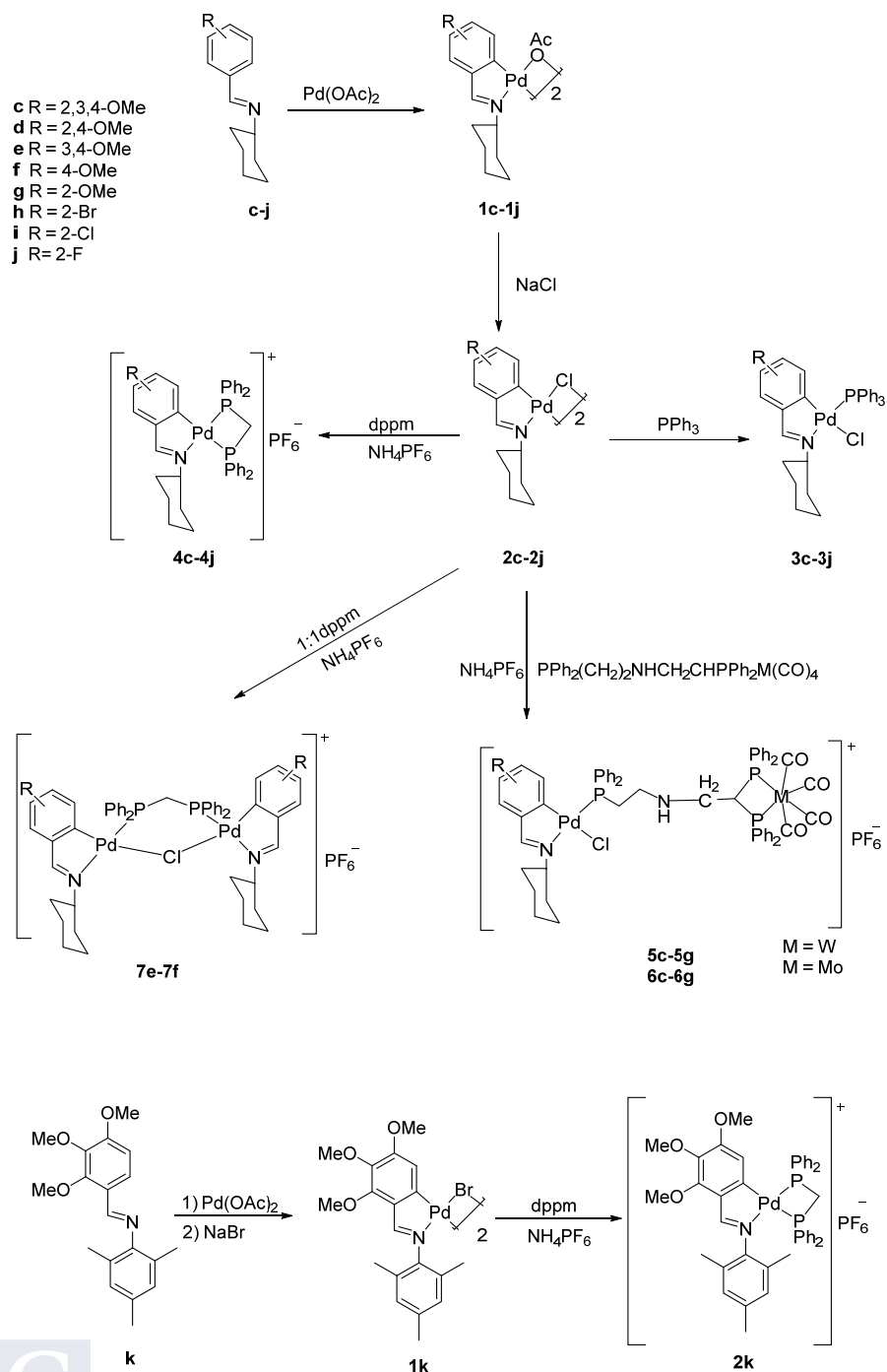
5.1.1 Derivatives compounds of cyclohexylamine Schiff bases ligands.



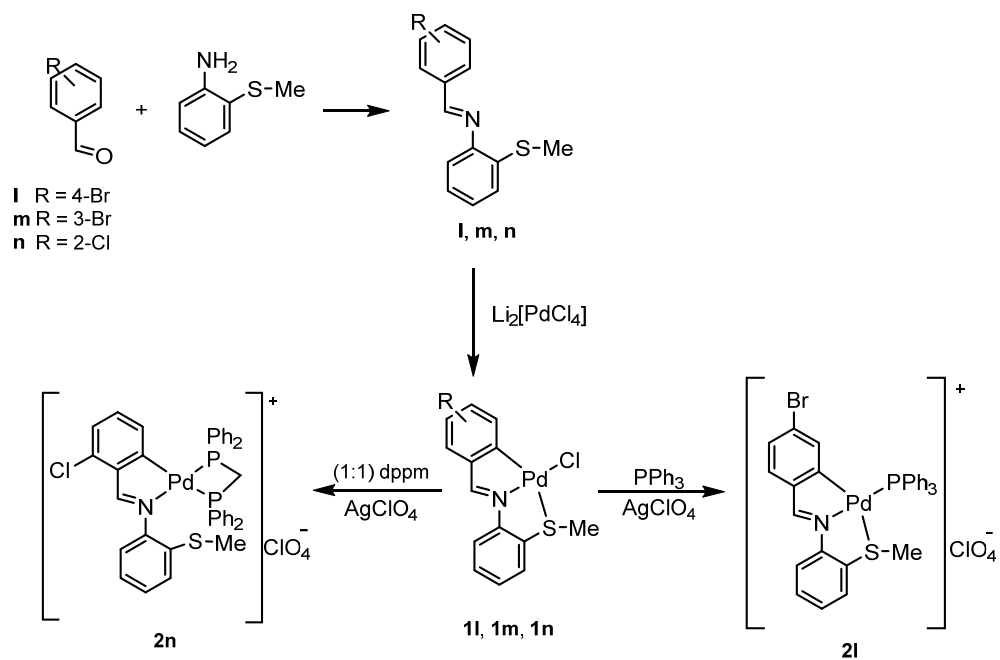
5.1.2 Derivatives compounds of aminophosphine ligand.



5.2 Cyclopalladated compounds derivatives of imines Schiff bases.



5.3 Cyclopalladated compounds derivatives of tridentate [C,N,S] Schiff bases.



CHAPTER 6

**Cyclopalladated compounds from 1,4-(CHO)₂C₆H₄
(terephthalaldehyde) and 1,3-(CHO)₂C₆H₄
(isophthalaldehyde) Schiff bases.**

6.1 Introduction

Palladium(II) compounds with bidentate [C,N] and tridentate [C,N,X] (X= N, O, S) Schiff bases have been considered in this dissertation. In accordance with previous work metalation of the ligands is said to take place by the electrophilic attack of palladium(II) acetate on a C-H bond.^{103, 104}

Compounds derived from diamines with two metal atoms linked to the same organic moiety have also been described. The reaction conditions in the former case influence the cyclometallation process, and it was shown that theoretically tetradentate Schiff bases produced from 1,4-(CHO)₂C₆H₄ (terephthalaldehyde) and 1,3-(CHO)₂C₆H₄ (isophthalaldehyde) produce distinct products. treatment of 1,3-(CyN=CH)₂C₆H₄ with Pd(OAc)₂ can result in a mixture of mono- and dicyclometallated compounds II and III, the formation of the former suggests that the meta disposition of the imine groups and subsequent coordination of the C=N group to the palladium atom obstructs hydrolysis.¹⁰⁵ Only by oxidatively adding [Pd₂(dba)₃] to the dichloro derivative 1,4-(CyN=CH)₂-2,5-Cl₂-C₆H₂ in benzene can the

¹⁰³ B. Tejjido, A.A. Fernández, M. López-Torres, A. Suárez, J.M. Vila, R. Mosteiro, J.J. Fernández, *Organometallics*, 21 (2002) 1304-1307.

¹⁰⁴ B. Tejjido, A. Fernández, M. López-Torres, S. Castro-Juiz, A. Suárez, J.M. Ortigueira, J.M. Vila, J.J. Fernández, *Journal of Organometallic Chemistry*, 598 (2000) 71-79.

¹⁰⁵ J. Vila, M. Gayoso, M.T. Pereira, M.L. Torres, J.J. Fernández, A. Fernández, J.M. Ortigueira, *Journal of organometallic chemistry*, 506 (1996) 165-174.

dicyclopalladated molecule IV be obtained.¹⁰⁶ Compound V can be achieved with Pd(OAc)₂ using reflux CHCl₃.¹⁰⁷ Mono- or dicyclopalladated compounds I, II, and VI can be prepared by reacting [MeMn(CO)₅] in n-octane, depending on the molar ratio.

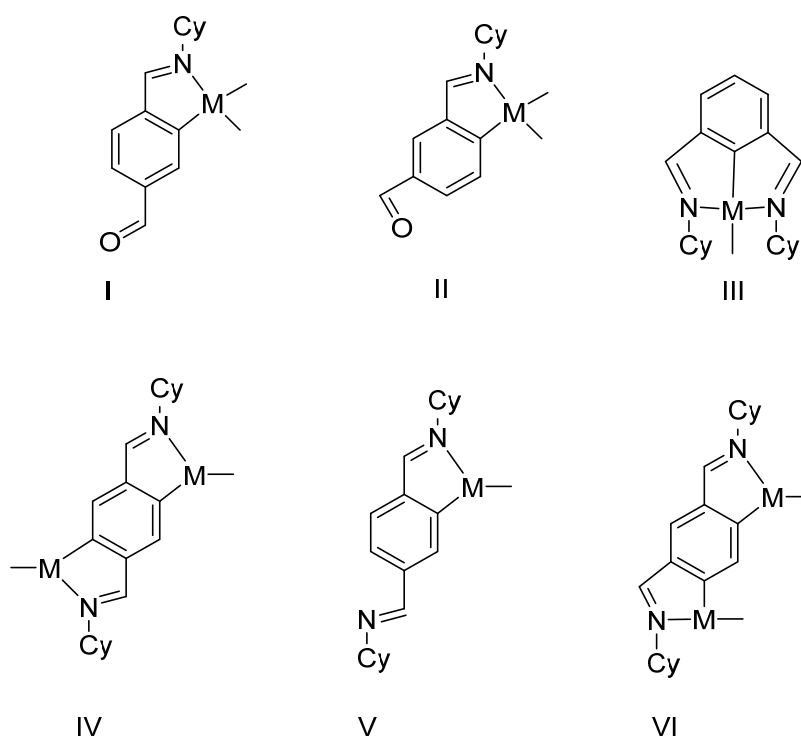


Figure 32. Cyclometallated compounds prepared from diimines derived.

¹⁰⁶ J.M. Vila, M. Gayoso, M.T. Pereira, M.L. Torres, J.J. Fernández, A. Fernández, J.M. Ortigueira, *Zeitschrift für anorganische und allgemeine Chemie*, 623 (1997) 844-848.

¹⁰⁷ J.M. Vila, M. Gayoso, M.T. Pereira, M. López, G. Alonso, J.J. Fernández, *Journal of organometallic chemistry*, 445 (1993) 287-294.

Different compounds were prepared by the most usual palladation procedures using the Schiff bases derived from 1,4-(CHO)₂-C₆H₄ (terephthalaldehyde) and 1,3-(CHO)₂-C₆H₄ (isophthalaldehyde). For example, the mono-cyclopalladated compound was obtained by reacting 1,4-(CyN=CH)₂C₆H₄ with Pd(OAc)₂ in glacial acetic acid, where the acidic nature of the solvent promoted hydrolysis of one of the C=N double bonds whilst palladium coordination stabilized the second imine group.¹⁰⁷ Furthermore, the presence of a free formyl group in these complexes allows for a novel and interesting functionalization that allows for the synthesis of new cyclopalladated compounds with heterobidentate ligands, which could be used for active catalysis. As a result, the cyclopalladated compounds have been produced using the corresponding heterobidentate ligand having phosphorus and nitrogen atoms in an attempt to make homo and heteronuclear compounds with transition metals.

6.1.1 Synthesis of the Schiff base ligands **a** and **b**.

In a 100 mL round bottom flask containing 40 cm³ of dry chloroform, 0.5 g (3.727 mmol) of isophthalaldehyde or terephthalaldehyde, and 0.8129 g (8.187 mmol) of cyclohexylamine (10 % excess) were added, the mixture was refluxed in a modified Dean-Stark apparatus for 8 h, then allowed to cool at room temperature. The solution was evaporated and dried in a *vacuum*. The compounds gave brown solids with yields for ligand **a** (94 %) and for ligand **b** (96 %).

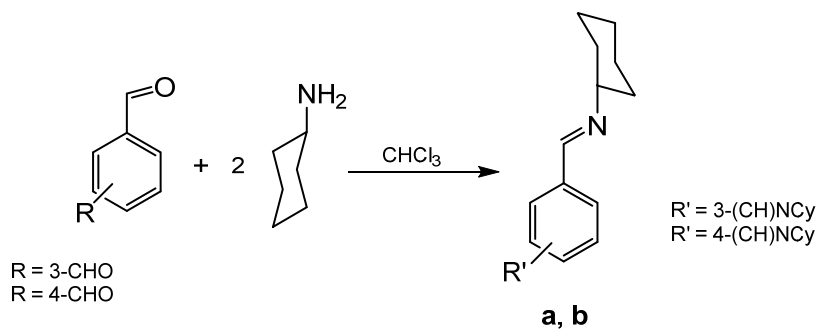


Table 4. Quantities of materials used in ligand synthesis.

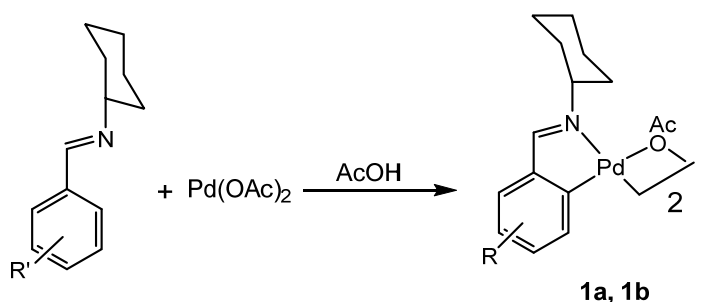
ligand	aldehyde's		cyclohexylamine	
	g	mmol	g	mmol
a	0.5	3.727	0.8129	8.187
b	0.5	3.727	0.8129	8.187

6.1.2 Synthesis of the acetate-bridged compounds **1a** and **1b**.

These reactions were carried out under dry nitrogen in glacial acetic acid. Although the final products are air-stable, it has been found that reaction intermediates could be air-sensitive.

In a 100 mL Schlenk flask, a suspension of 0.2 g (0.890 mmol) Pd(OAc)₂, 0.263 g (0.890 mmol) Schiff base **a** or **b**, and 40 cm³ of glacial acetic acid was heated under dry nitrogen for 3 h at 55 °C. After cooling to room temperature, some of the Pd(II) in the residue was converted to Pd(0), resulting in a black powder. The residue was filtered to remove Pd(0) to give pure a yellow solution for compound **1a** and an orange solution for **1b**, then reduced to low volume, and diluted with H₂O and extracted with CH₂Cl₂. The extracts were mixed, dried over anhydrous sodium sulphate, filtered, and vacuum concentrated.

Compounds **1a** and **1b** were eluted with CH₂Cl₂/EtOH (1 %) on a silica gel 60 chromatography column, yielding a yellow band for compound **1a** and an orange band for compound **1b**, which were collected and concentrated under vacuum.



R' = 3-(CH)NCy
R' = 4-(CH)NCy

R = 3-CHO
R = 4-CHO

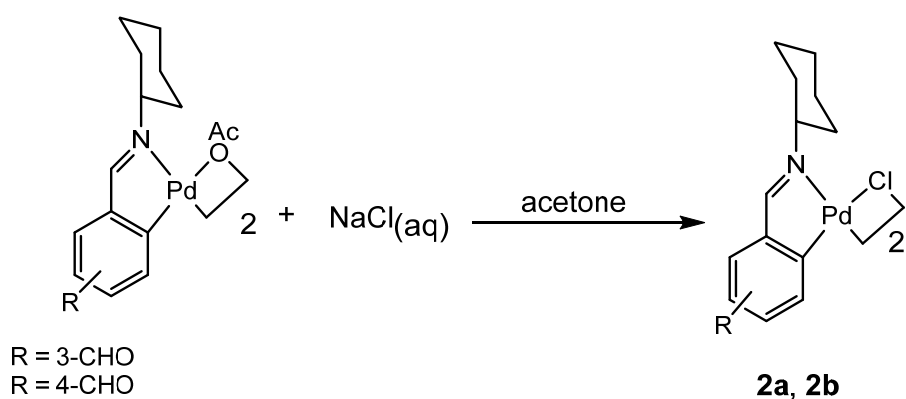
Table 5. The quantity of materials used to make cyclometallated compounds.

compound	Pd(OAc) ₂		ligand	
	g	mmol	g	mmol
a	0.2	0.890	0.263	0.890
b	0.2	0.890	0.263	0.890

6.1.3 Synthesis of the halide-bridged compounds **2a** and **2b**.

The cyclopalladated compounds **2a** and **2b** were prepared from the dinuclear cyclopalladated compound with acetate-bridging ligands in acetone as solvent.

To a solution of **1a** or **1b** (0.2 g, 0.263 mmol) in 10 cm³ of acetone, was added aqueous NaCl (20 cm³, 0.05 M) and the mixture was stirred at room temperature for 2 h. Afterward, the solid was filtered and dried under vacuum to give compound **2a** (75 %) and compound **2b** (59 %).



6.1.4 Synthesis of monomer compounds with triphos ligand **3a** and **3b**.

In a 50 mL Schlenk flask containing 10 cm³ of acetone, **2a** or **2b** 0.05 g (0.070 mmol) was added with 0.0750 g (0.140 mmol) triphos ligand in 1:2 molar ratio. After stirring at room temperature for 2 h, aqueous ammonium hexafluorophosphate 0.0228 g (0.140 mmol) was added and stirred for further 1 h. The compound was precipitated by adding water, filtered off, and dried in a vacuum. Recrystallization of compounds **3a** and **3b** from dichloromethane/hexane produced a yellow solid with yields for **3a** (95 %) and for **3b** (96 %).

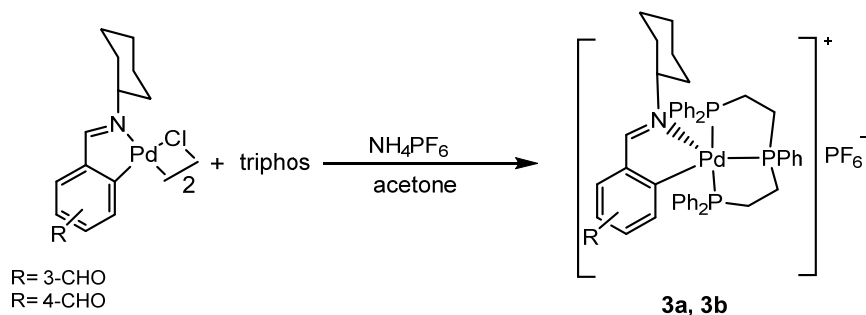


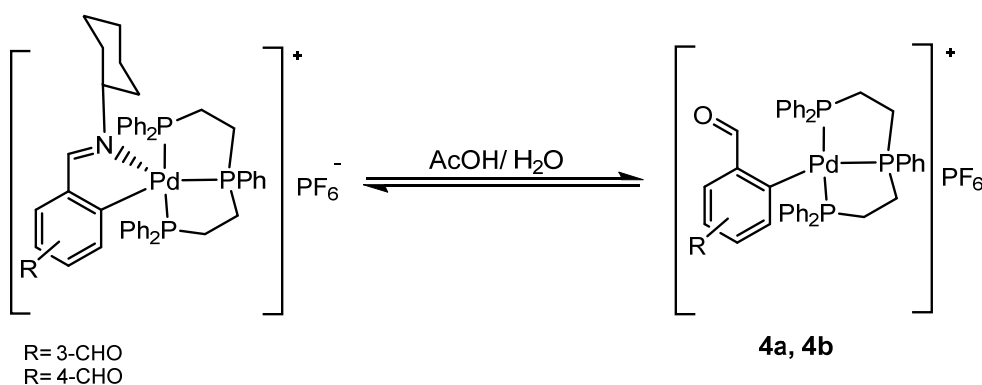
Table 6. The quantity of materials used to prepare compounds with triphos ligands.

	compound		triphos ligand		NH ₄ PF ₆	
	g	mmol	g	mmol	g	mmol
2a	0.05	0.070	0.0750	0.140	0.0228	0.140
2b	0.05	0.070	0.0750	0.140	0.0228	0.140

6.1.5 Synthesis of monomer compounds **4a** and **4b**.

Compounds **3a** or **3b** 0.05 g (0.049 mmol) was treated with 15 cm³ of glacial acetic acid and 2 cm³ of water for 2 days at room temperature.

Water was added to the residue after the acetic acid was vacuumed out, and the product was extracted with dichloromethane. To get the final product, the mixed extracts were dried over anhydrous sodium sulfate, filtered, and the solvent was removed under vacuum to yield compounds **4a** (80 %) and **4b** (90 %).



6.1.6 Synthesis of monomer triphos compounds with cyclohexylamine ligands **5a** and **5b**.

In a 50 mL round bottom flask, 0.05 g (0.049 mmol) of **3a** or **3b** was treated with 0.005 g (0.049 mmol) of cyclohexylamine in 15 cm³ of CHCl₃. The mixture was refluxed for 8 h and cooled to room temperature, and the solvent was eliminated under vacuum to dryness.

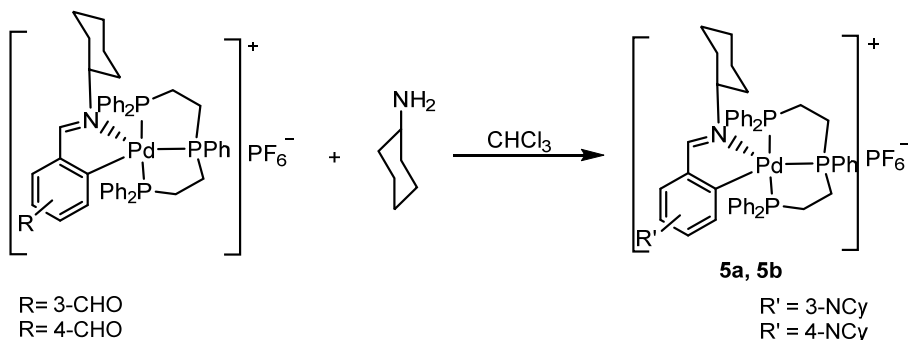


Table 7. The quantity of materials used to prepare compounds contains cyclohexylamine.

	compound		cyclohexylamine	
	g	mmol	g	mmol
3a	0.05	0.049	0.005	0.049
3b	0.05	0.049	0.005	0.049

6.1.7 Synthesis of monomer compounds with acetylacetone **6a** and **6b**.

In a 50 mL Schlenk flask containing 20 cm³ of CHCl₃, 0.05 g (0.0701 mmol) of **2a** or **2b** was treated with 0.0425 g (0.140 mmol) of Tl(acac)₂ in molar ratio 1:2 and the mixture was stirred for 24 h at r.t. The compound was centrifuged to ensure complete precipitation of the TlCl salt. The final solution was reduced to a low volume to give a yellow solid in the case of **6a** (86 %) and an orange solid in the case of **6b** (78 %)

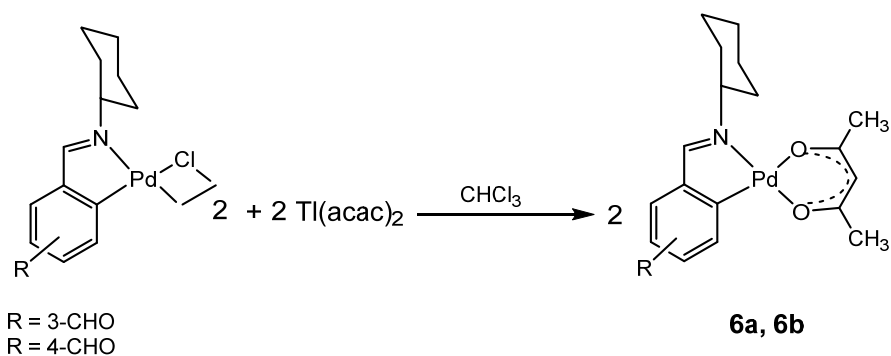


Table 8. The quantity of materials used to prepare cyclometallated compounds with acac.

	compound		Tl(acac) ₂	
	g	mmol	g	mmol
2a	0.05	0.0701	0.0425	0.140
2b	0.05	0.0701	0.0425	0.140

6.1.8 Synthesis of compounds with dppm **7a** and **7b**.

In a 50 mL Schlenk flask containing 10 cm³ of acetone, **2a** or **2b** 0.05 g (0.070 mmol) was added with 0.0538 g (0.140 mmol) of dppm in molar ratio 1:2 and the mixture was stirred for 2 h at r.t. Then, ammonium hexafluorophosphate 0.0228 g (0.140 mmol) was added to the resulting solution and stirred for further 1 h. The compound was precipitated by adding water, filtered off, and dried under a vacuum. The yellow compounds of **7a** and **7b** were dried under vacuum to give yields of (73%) and (82%), respectively.

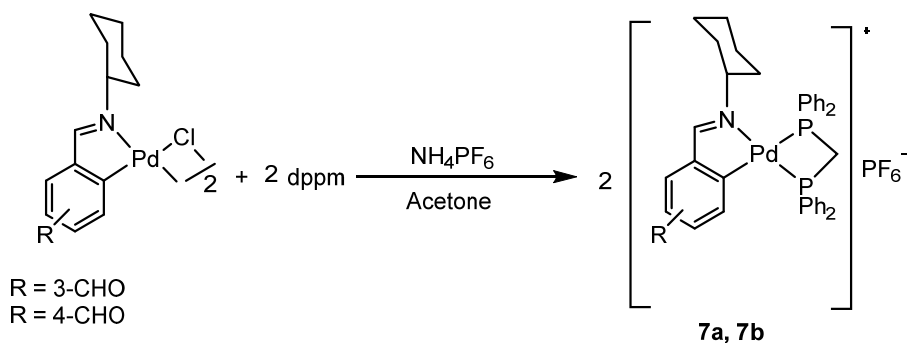


Table 9. The quantity of materials used to prepare cyclometallated compounds with dppm.

	compound		dppm ligand		NH ₄ PF ₆	
	g	mmol	g	mmol	g	mmol
2a	0.05	0.070	0.0538	0.140	0.0228	0.140
2b	0.05	0.070	0.0538	0.140	0.0228	0.140

6.1.9 Synthesis of monomer compounds with vdpp **8a** and **8b**.

In a 50 mL Schlenk flask containing 10 cm³ of acetone, **2a** or **2b** 0.05 g (0.070 mmol) was added together with 0.055 g (0.140 mmol) of vdpp ligand in molar ratio 1:2 and the mixture was stirred for 2 h. Then, 0.0228 g (0.140 mmol) ammonium hexafluorophosphate was added to the solution and stirred further for 1 h. The compound was precipitated by adding water, filtered off, and dried under a vacuum. The yellow **8a** and orange **8b** compounds were dried under vacuum to give yields of (82 %) and (73 %), respectively.

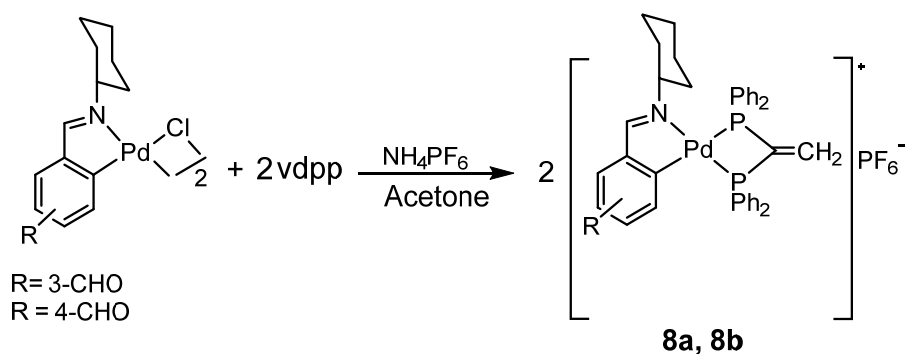


Table 10. The quantity of materials used to prepare cyclometallated compounds with vdpp.

	compound		vdpp ligand		NH ₄ PF ₆	
	g	mmol	g	mmol	g	mmol
2a	0.05	0.070	0.0555	0.140	0.0228	0.140
2b	0.05	0.070	0.0555	0.140	0.0228	0.140

6.1.10 Synthesis of monomer compounds with the $\text{NH}_2\text{CH}_2\text{CH}_2\text{PPh}_2$ ligand **9a** and **9b**.

The addition of aminophosphine to the monomer compounds (**3a**, **3b**) was performed under argon. In a 50 mL round bottom flask, **3a** or **3b** was added 0.05 g (0.049 mmol) with 0.0114 g (0.049 mmol) of the aminophosphine ligand ($\text{NH}_2\text{CH}_2\text{CH}_2\text{PPh}_2$) in 15 cm^3 of CHCl_3 . The mixture was refluxed for 8 h. After reducing to low volume and drying under vacuum, compounds **9a** (75 %) and **9b** (83 %) were obtained.

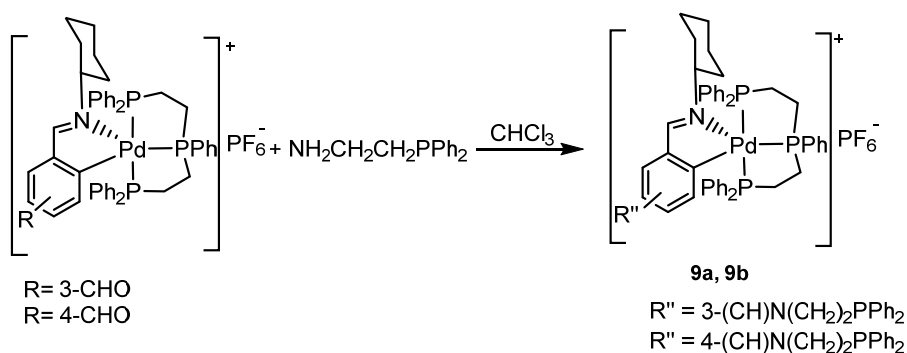


Table 11. The quantity of materials used to prepare compounds contains an aminophosphine ligand.

	compound		$\text{NH}_2\text{CH}_2\text{CH}_2\text{PPh}_2$ ligand	
	g	mmol	g	mmol
3a	0.05	0.049	0.0114	0.049
3b	0.05	0.049	0.0114	0.049

6.1.11 Synthesis of monomer compounds with the $\text{NH}_2\text{CH}_2\text{CH}_2\text{PPh}_2$ ligand **10a** and **10b**.

The addition of aminophosphine to the monomer compounds (**10a**, **10b**) was performed under argon. In a 50 mL round bottom flask, **3a** or **3b** 0.05 g (0.054 mmol) was added with 0.0250 g (0.108 mmol) of the aminophosphine ligand ($\text{NH}_2\text{CH}_2\text{CH}_2\text{PPh}_2$) in 1:2 molar ratio in 15 cm^3 of CHCl_3 . The mixture was refluxed for 8 h. The solvent of the resulting solution was evaporated by rotary vapor and dried in a vacuum. After reducing to low volume and drying under vacuum, compounds **10a** (86 %) and **10b** (69 %) were obtained.

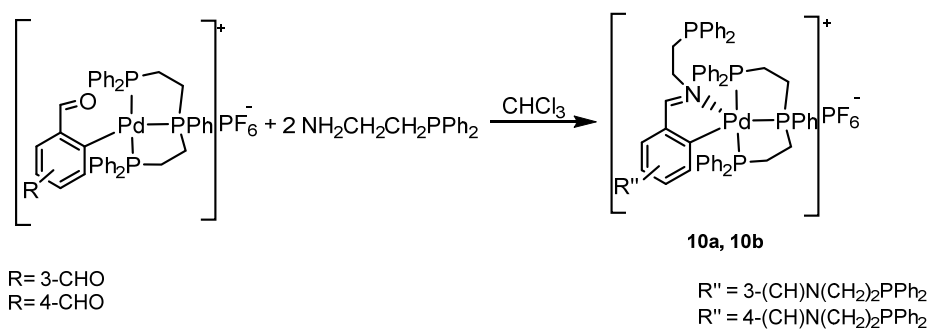


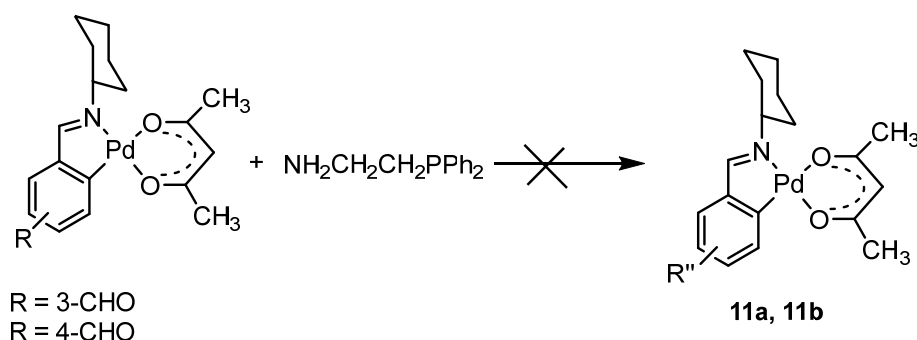
Table 12. The quantity of materials used to prepare compounds contains aminophosphine ligands.

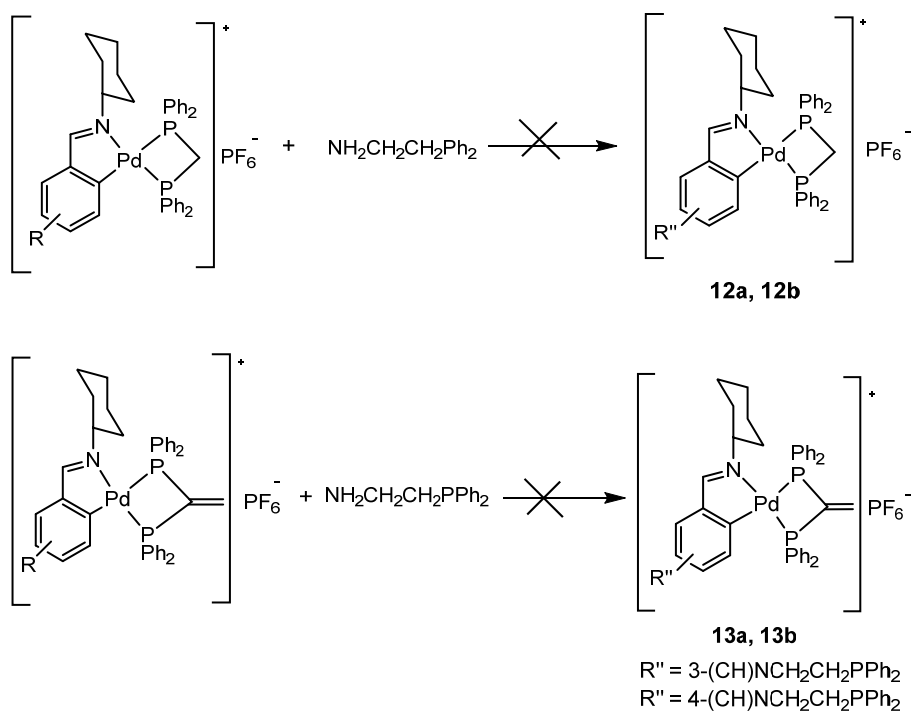
	compound		$\text{NH}_2\text{CH}_2\text{CH}_2\text{PPh}_2$ ligand	
	g	mmol	g	mmol
4a	0.05	0.049	0.0250	0.108
4b	0.05	0.049	0.0250	0.108

6.1.12 Attempts the synthesis of monomer compounds using the $\text{NH}_2\text{CH}_2\text{CH}_2\text{PPh}_2$ ligand with compounds containing acetylacetonate, dppm, and vdpp ligands.

The addition of aminophosphine to the monomer compounds (6a, 6b, 7a, 7b, 8a, 8b) was undergone under argon gas. In a 50 mL round bottom flask, 0.0114 g (0.049 mmol) of aminophosphine ligand ($\text{NH}_2\text{CH}_2\text{CH}_2\text{PPh}_2$) was treated with the corresponding amount of compounds **6a**, **6b**, **7a**, **7b**, **8a**, and **8b** in molar ratio 1:1 in 15 cm^3 of CHCl_3 . The reaction was refluxed for 8 h. The resulting solution solvent was then evaporated by rotary vapor and dried in vacuum.

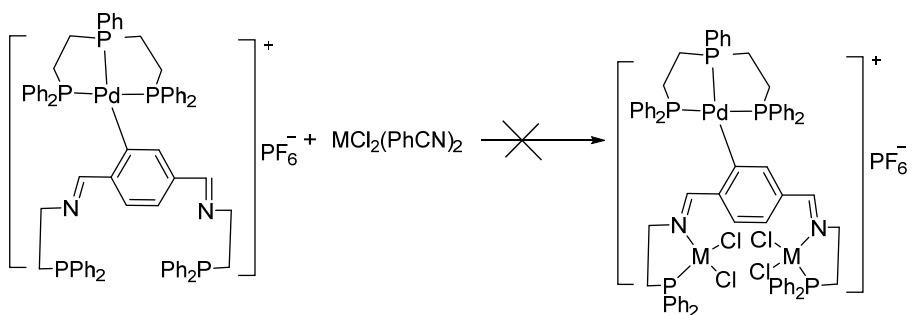
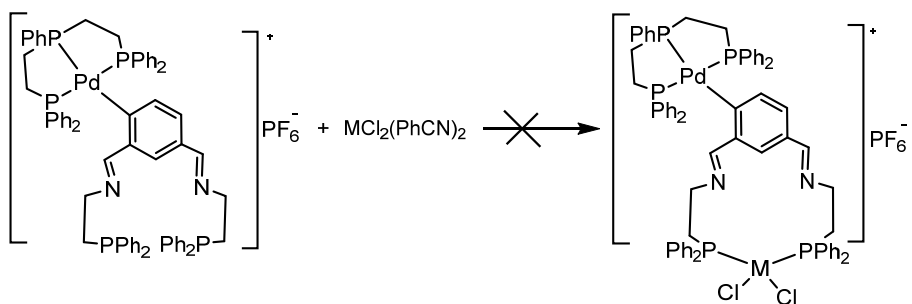
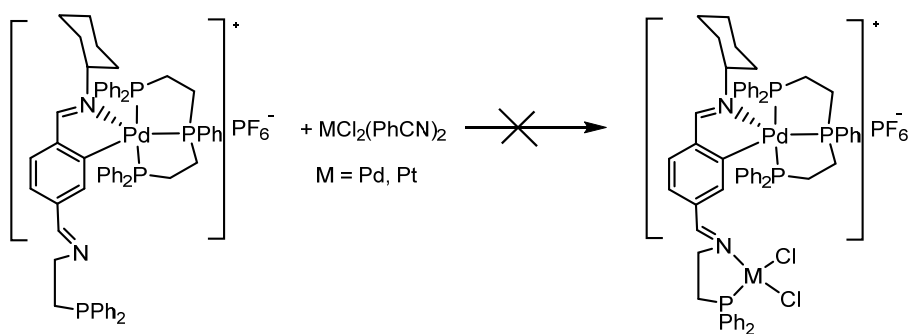
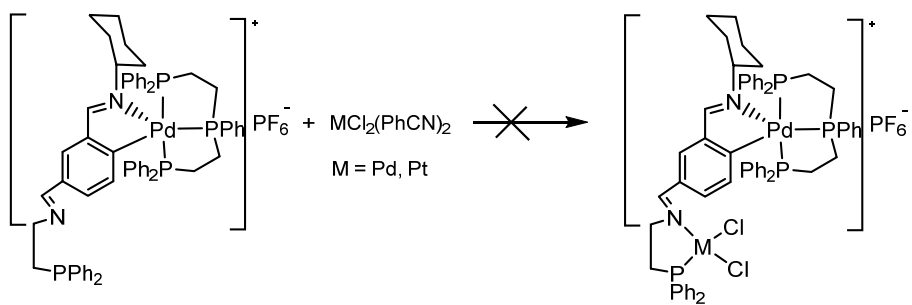
Compounds with the acetylacetonate, dppm, and vdpp ligand **11a-13b**, were unsuccessfully synthesized. Compounds **11a** and **11b** resulted in substituting acetylacetonate with amino phosphine ligand, which was not an expected compound. Whilst compounds **12a**, **12b**, **13a**, and **13b** produced a mixture of products that could not be separated by column chromatography.





6.1.13 Attempts to synthesize monomer compounds containing triphos and NH₂CH₂CH₂PPh₂ amino phosphine ligands, with MCl₂(PhCN)₂ [M.= Pt, Pd].

Compounds **9a**, **9b**, **10a**, and **10b** were tried to synthesize homo and heteronuclear compounds without success using PtCl₂(PhCN)₂ and PdCl₂(PhCN)₂ under different conditions. The conditions were used in different solvents; dry CHCl₃, CH₂Cl₂, and acetone for 2 h at room temperature. The desired compounds were not detected by ¹H NMR and ³¹P-¹H NMR spectroscopy.



6.2 IR study

Table 13 shows the IR data for the compounds, which includes the more important bands for the complexes. The data show that the shift of the $\nu(\text{C}=\text{N})$ band in the complexes, always to lower frequencies, is in agreement with the bonding of the metal to the lone pair of the C=N nitrogen atom. Also, a band *ca.* 1695-1670 cm^{-1} appears that was assigned to the $\nu(\text{C}=\text{O})$ stretch, so compounds **1a-3a** and **1b-3b** have two distinct stretches, $\nu(\text{C}=\text{N})$ and $\nu(\text{C}=\text{O})$, in agreement with cleavage of one C=N double bond. For compounds, **4a** and **4b** hydrolysis of the remaining C=N bond is evidenced by the absence of any band assignable to $\nu(\text{C}=\text{N})$, and by the presence of two $\nu(\text{C}=\text{O})$ bands. In the case of the $\nu(\text{Pd}-\text{Cl})$ stretches in the spectra of compounds **2a** and **2b**, the data are in accordance with bridging chloride ligands. Thus, two bands were assigned *ca.* 280 and 250 cm^{-1} , for the $\nu(\text{Pd}-\text{Cl})$ *trans* to nitrogen and for the $\nu(\text{Pd}-\text{Cl})$ *trans* to carbon vibrations.

Table 14 shows the bands corresponding to the vibrations $\nu_{\text{as}}\text{COO}$ and $\nu_{\text{s}}\text{COO}$ of the acetate ligands of the synthesized compounds **1a** and **1b**. The acetate ligand acts as a bidentate bridge ligand, and the bands corresponding to vibrations $\nu(\text{C}=\text{O})_{\text{acac}}$ and $\nu(\text{C}=\text{C})_{\text{acac}}$ in compounds **6a** and **6b** containing the acetylacetonate ligand, which the ligand acts as a bidentate ligand.

Table 13. IR data (in cm^{-1}) of compounds derivatives from Schiff bases **a** and **b**.

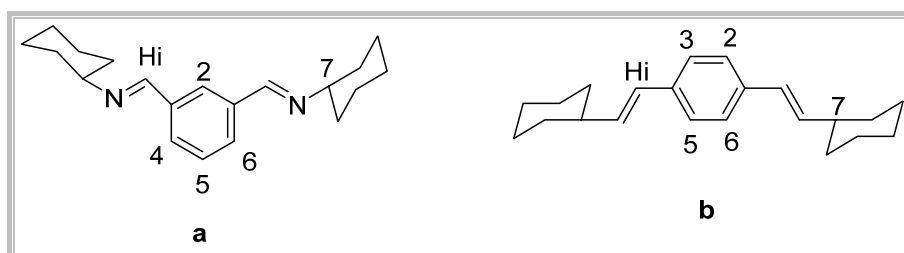
Compound	$\nu(\text{C=O})$	$\nu(\text{C=N})$	$\Delta\text{C=N}$	$\nu(\text{Pd-Cl})$
a		1640		
b		1639		
1a	1695	1605	35	
1b	1690	1605	34	
2a	1692	1616	24	281 257
2b	1694	1609	30	282 248
3a	1688	1624	16	
3b	1691	1619	20	
4a	1689 1666			
4b	1693 1668			
6a	1690	1611	29	
6b	1685	1605	34	
7a	1693	1617	23	
7b	1692	1624	15	
8a	1696	1623	17	
8b	1697	1620	19	
9a		1624 1639	16 1	
9b		1618 1638	21 1	
10a		1609 1624	31 16	
10b		1617 1642	22 -3	

Table 14. Assignment of the IR bands (in cm^{-1}) of the acetate ligands and acetylacetonone ligand.

Compound	$\nu_{\text{as}}(\text{COO})$	$\nu_{\text{s}}(\text{COO})$	Δ	$\nu(\text{C=O})_{\text{acac}}$	$\nu(\text{C=C})_{\text{acac}}$
1a	1570	1410	160		
1b	1576	1420	156		
6a				1567/1411	1517
6b				1564/1398	1511

6.3 NMR study

6.3.1 Study of Schiff base ligands **a**, **b**



The ^1H NMR spectra of the diimine ligands (**a**) and (**b**) were recorded in CDCl_3 .

In the ^1H NMR spectrum of ligand **a**, the signal of H5 showed a triplet signal at 7.43 ppm ($^3J(\text{HH}) = 7.7$ Hz), while the signals of H4 and H6 appeared a doublet peak at 7.79 ppm ($^3J(\text{HH}) = 7.7$ Hz). At 8.0 ppm, the H2 signal appeared as a singlet. The protons of diimine Hi showed a singlet at 8.35 ppm. The signals of the group cyclohexylamine observed varied from 1.2 to 1.9 ppm, and the multiplet peak at 3.20 ppm was related to the proton H7 of cyclohexylamine, which is close to the nitrogen atom.

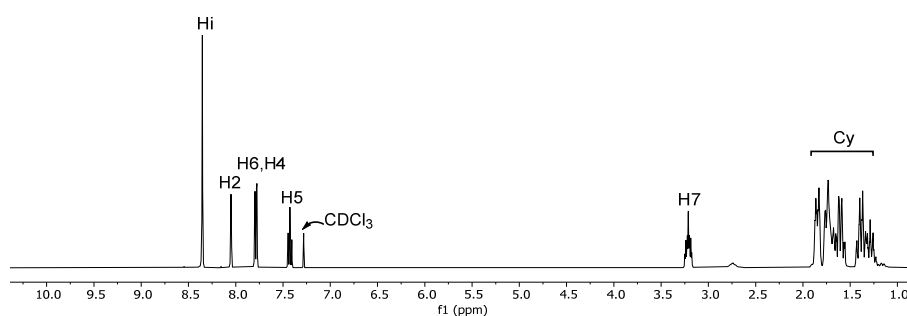


Figure 33. ^1H NMR of Schiff base **a** in CDCl_3 .

While ^1H NMR spectra of ligand **b**, the diimine Hi protons showed a singlet signal peak at 8.24 ppm, and protons H2, H3, H5, and H6 showed a singlet signal at 7.67 ppm. Signals for the cyclohexylamine amine group ranged from 1.18 to 1.77 ppm. A multiplet was found at 3.12 ppm for the proton H7.

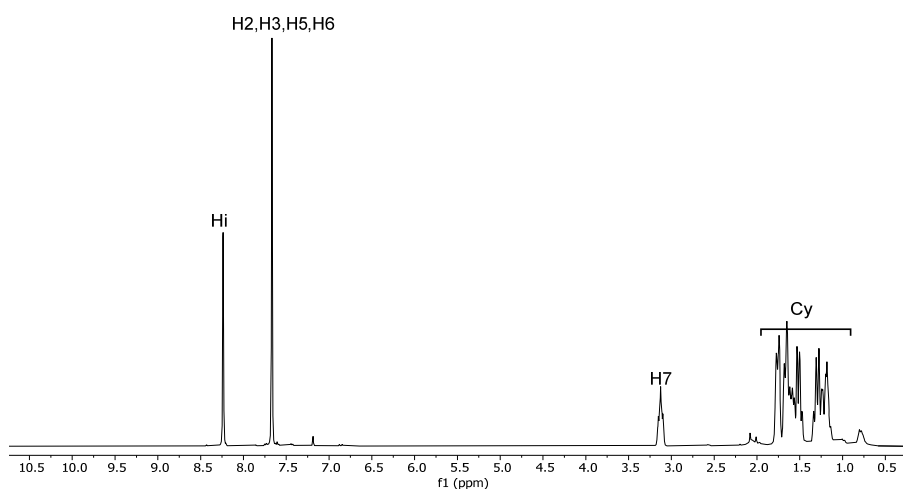
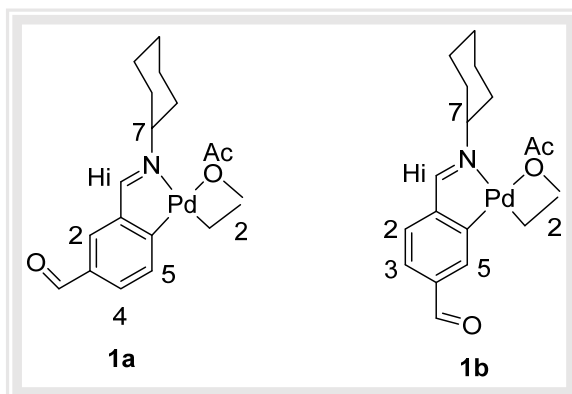


Figure 34. ^1H NMR of Schiff base **b** in CDCl_3 .

6.3.2 Study of compounds **1a** and **1b**.

The preparation of cyclopalladated compounds with acetate bridge **1a** and **1b** were carried out at the same conditions of temperature and reaction time, which were soluble in glacial acetic acid for 3 h at 55 °C. The cyclopalladation process is affected by reaction conditions. We have found that diimine ligands with both derivatives of isophthalaldehyde and terephthalaldehyde gave rise to different products. Thus, the reaction of compounds **a** and **b** with palladium acetate(II) in glacial acetic acid formed dinuclear cyclopalladated compounds, indicating that the nature of acetic acid solvent caused

hydrolysis to the one part of the C=N double bond while stabilizing the palladium coordination to another part of the imine.



^1H NMR spectra of both compounds **1a** and **1b** were recorded in CDCl_3 . The ^1H NMR spectrum of compound **1a** shows a singlet at 9.90 ppm, which was assigned to the $\text{HC}=\text{O}$ resonance. The chemical shift of proton Hi appeared a singlet at 7.60 ppm. It is noted that the chemical shift of the Hi has been shifted to the right concerning the diimine ligand. The proton H2 showed a single peak at 7.47 ppm. While the protons of H4 and H5 formed two doublets. The chemical shift of the proton H4 observed a doublet signal at 7.54 ppm [$^3J(\text{H4H5}) = 8.1 \text{ Hz}$, 1H], which is very close to proton H2 and coupling with the proton H5. The proton H5 showed a doublet signal as well, but with a high field shift at 7.33 ppm [$^3J(\text{H5H4}) = 8.1 \text{ Hz}$, 1H], indicating that it is coupling with the proton H4. The disappearance of the proton H6 in the ^1H NMR spectrum confirms that the carbon atom Csp^2 metallated to Pd^{2+} given cyclometallation compound with acetate bridges. The two equivalent protons of methyl groups were assigned as a singlet at 2.20 ppm. Chemical shifts of the

cyclohexylamine group ranged from 0.5 to 2.5 ppm. The proton of H7 was shown at 3.05 ppm.

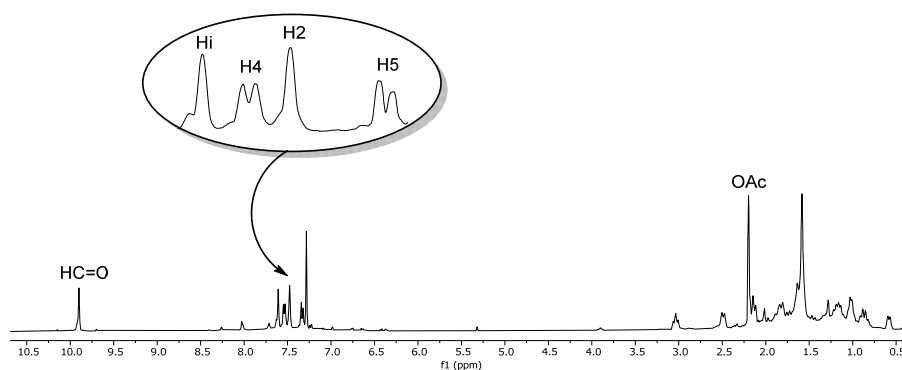


Figure 35. ^1H NMR of compound **1a** in CDCl_3 .

The ^1H NMR spectrum of the compound **1b** show $\delta(\text{ppm}) = 9.97$ (s, 1H, HC=O), 7.60 (s, 1H, HC=N), 7.40 (s, 1H, H5), 7.55 (d, $^3J(\text{H3H2}) = 7.5$ Hz, 1H, H3), 7.24 (d, $^3J(\text{H2H3}) = 7.5$ Hz, 1H, H2), 3.05 (m, 1H, H7), 2.22 (s, 3H, CH_3), 0.5–2.5 (m, 10H, Cy).

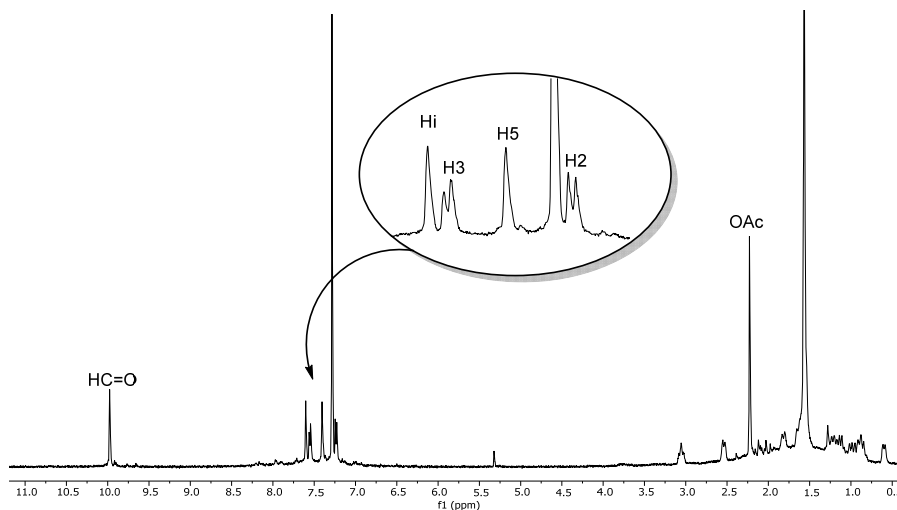
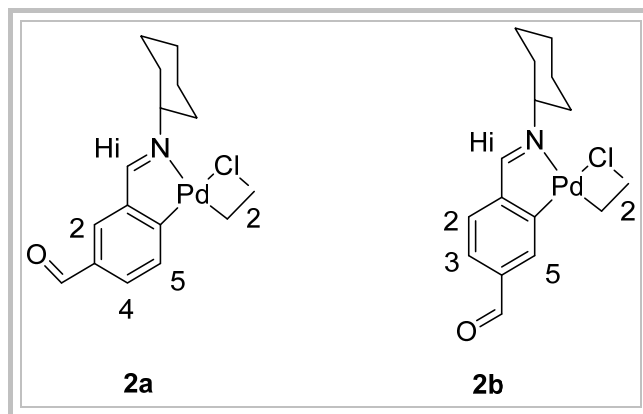


Figure 36. ^1H NMR of compound **1b** in CDCl_3 .

6.3.3 Study of compounds **2a** and **2b**.



The ^1H NMR of compounds **2a** and **2b** were recorded in CDCl_3 .

The ^1H NMR of compound **2a** with halogen bridges, as shown in Figure 37 observed a lack of protons corresponding to the acetate bridge ligands. The proton of $\text{HC}=\text{O}$ showed a singlet at 9.88 ppm. The proton of Hi appeared a singlet at 7.93 ppm. While the H4 and H5 appeared broad signals at 7.60 and 7.55 ppm, respectively. The chemical shift of H2 observed a singlet at 7.68 ppm. The proton H7 was shown a broad signal at 3.70 ppm and protons of the cyclohexylamine group ranged from 0.5 to 2.10 ppm.

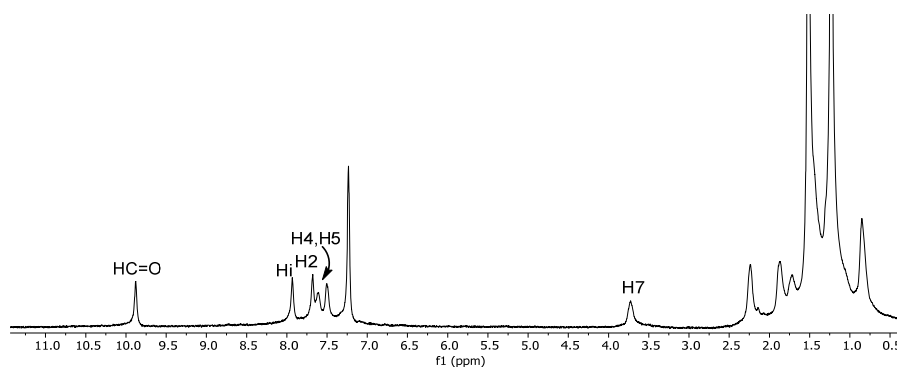


Figure 37. ^1H NMR of compound **2a** in CDCl_3 .

In the ^1H NMR of compound **2b**, the HC=O proton showed a singlet at 9.90 ppm, and a singlet at 7.87 ppm, was assigned to HC=N proton. The proton H5 observed a singlet at 7.80 ppm. At 7.53 [$^3J(\text{H3H2}) = 6.7$ Hz, 1H], the H3 appeared as a doublet. At 7.28 ppm [$^3J(\text{H2H3}) = 6.7$ Hz, 1H], proton H2 showed a doublet. The proton of H7 was found as a broad signal at 3.70 ppm, and the other protons of the cyclohexylamine group were found to be 0.5 to 2.10 ppm.

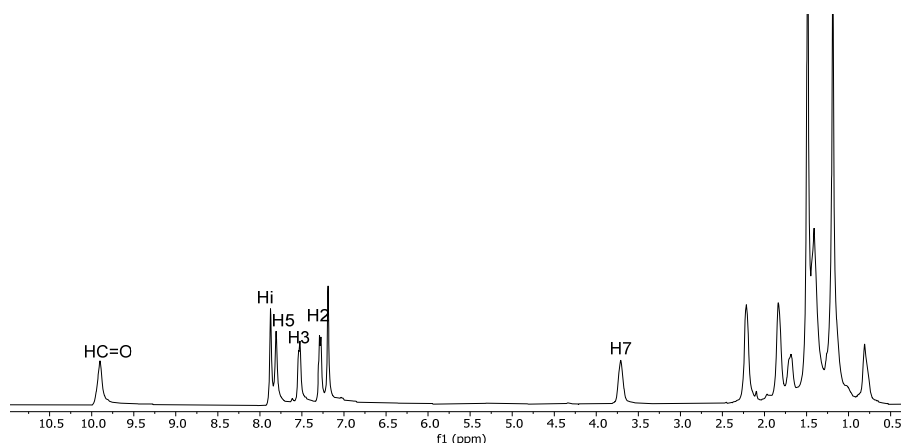
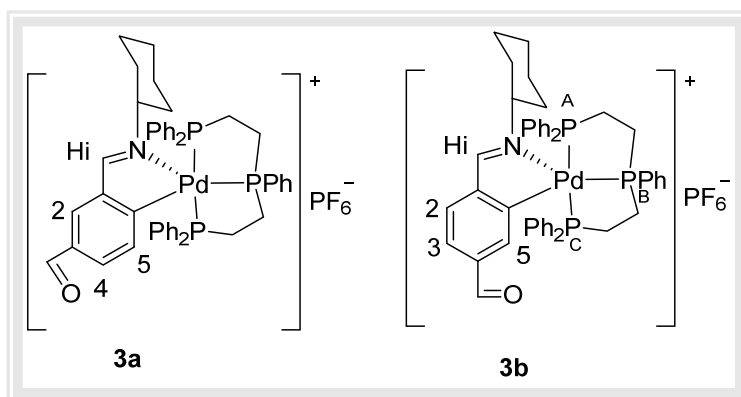


Figure 38. ^1H NMR of compound **2b** in CDCl_3 .

6.3.4 Study of compounds **3a** and **3b**.

Compounds **3a** and **3b** are formed after cleavage of the Pd-Cl bridging bonds by reaction with a tridentate [P,P,P] phosphine. These species are metallated, but not cyclometallated, and it represents a synthetic route to binding a [$\text{Pd}(\text{phosphine-}P,P,P)$] moiety to a phenyl ring. The numerous phenyl proton signal makes it rather difficult to fully analyze proton NMR spectra. Nevertheless, some useful information can still be defined.



The ^1H NMR and $^{31}\text{P}\{-^1\text{H}\}$ NMR of compounds **3a** and **3b** were recorded in CDCl_3 .

In the ^1H NMR spectrum of compound **3a**, a singlet signal at 9.79 ppm was assigned to the $\text{HC}=\text{O}$ resonance; the chemical shift of the proton Hi resonance was at 8.19 ppm; the latter was upfield shifted consequent on palladium-nitrogen interaction formation.¹⁰⁸ The signal for the H2 proton showed a singlet at 7.72 ppm. The proton H5 resonance was observed as a doublet at 6.11 ppm, coupled to the H4 and phosphorus nucleus ($^3J(\text{H5H4}) = ^4J(\text{H5P}) = 7.3$ Hz, 1H), shifted to the higher field with respect to the parent compound **3a** due to shielding of the phosphine phenyl rings. The proton H4 resonance showed a doublet at 6.88 ppm ($^3J(\text{H4H5}) = 7.3$ Hz, 1H), coupled to proton H5.

¹⁰⁸ Y.A. Ustynyuk, V. Chertkov, I. Barinov, *Journal of Organometallic Chemistry*, 29 (1971) C53-C54.

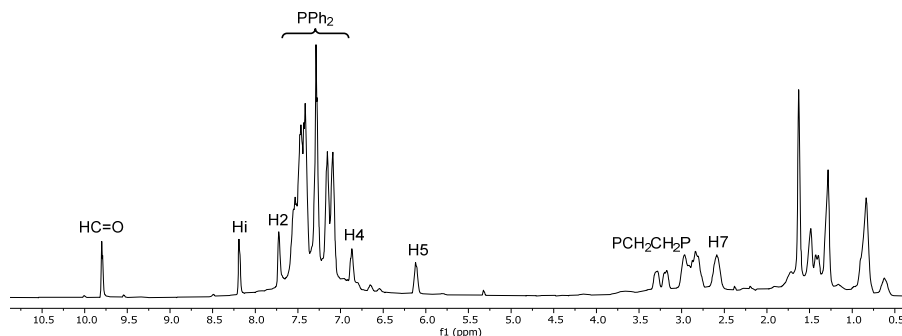


Figure 39. ^1H NMR of compound **3a** in CDCl_3 .

The ^1H NMR spectrum of compound **3b** shows a similar result. Thus, a singlet at 8.94 ppm, was assigned to the proton $\text{HC}=\text{O}$ proton; whilst a singlet at 8.22 ppm was due to the $\text{HC}=\text{N}$ proton. The proton of H5 shows a doublet at 6.11 ppm ($^4J(\text{H5P}) = 7.3$ Hz, 1H), indicating coupling with the phosphorus nucleus; the signals for the H2 and H3 protons were occluded by the phosphine phenyl resonances.

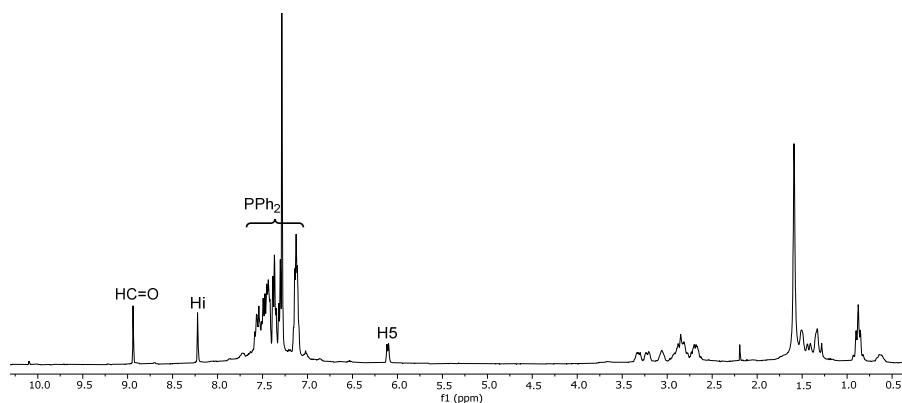


Figure 40. ^1H NMR of compound **3b** in CDCl_3 .

The $^{31}\text{P}\{-^1\text{H}\}$ NMR spectra of the compounds **3a** and **3b** showed doublet and triplet resonances. The former one *ca.* δ 44.47 [d, P_A , P_C], which is assigned to the two equivalents, mutually *trans* phosphorous nuclei, and the latter resonance *ca.* δ 85.50 [t, P_B] assigned to the central ^{31}P nucleus, *trans* to the metallated carbon atom with $J = 27$ Hz, in agreement with the coordination mode of the phosphine ligand. The phosphorous resonance for the anion hexafluorophosphate ion was observed a heptuplet *ca.* -144 ppm.

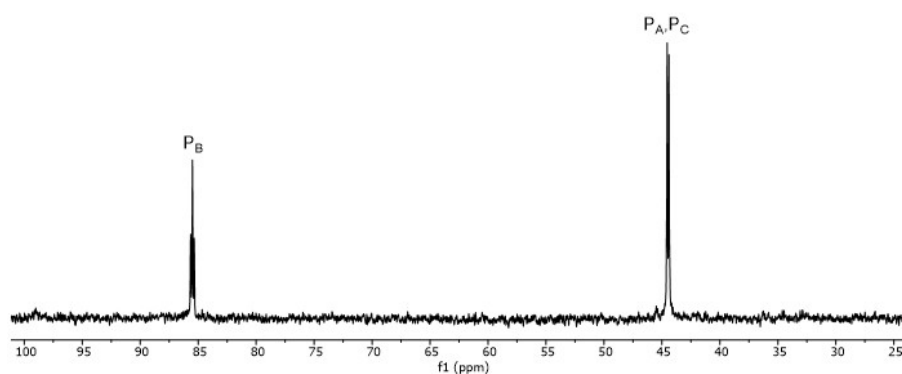
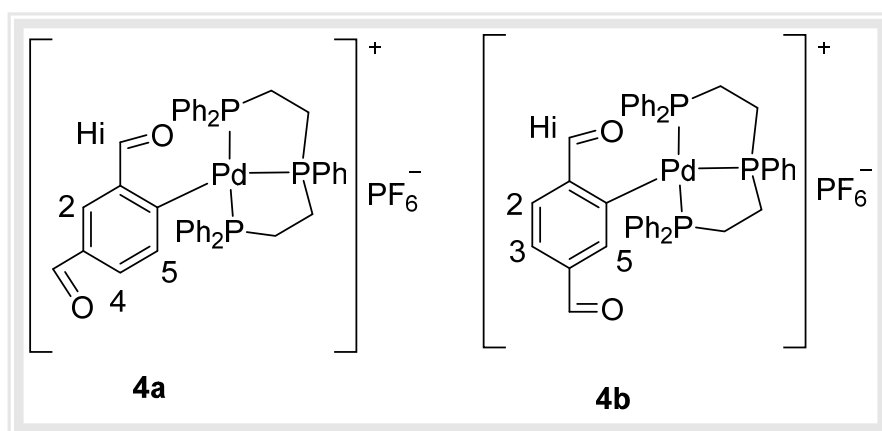


Figure 41. $^{31}\text{P}\{-^1\text{H}\}$ NMR of compound **3b** in CDCl_3 .

6.3.5 Study of compounds **4a** and **4b**.

Compounds **4a** and **4b** were obtained after controlled hydrolysis by treatment with acetic acid of **3a** and **3b**, resulting in the cleavage of the remaining C=N double bond, giving a compound with two non-coordinated formyl groups on the metallated phenyl ring.



The ¹H NMR spectrum for compound **4a** showed two singlets at 9.80 and 9.60 ppm, which were assigned to the two protons HC=O, and the absence of any trace of the HC=N resonance. A broad signal at 8.20 ppm was ascribed to the H4 proton; a doublet resonance at 6.50 ppm [³J(H5H4) = ⁴J(H5P) = 7.6 Hz, 1H] was for the H5 proton. The proton H2 observed a singlet at 7.93 ppm.

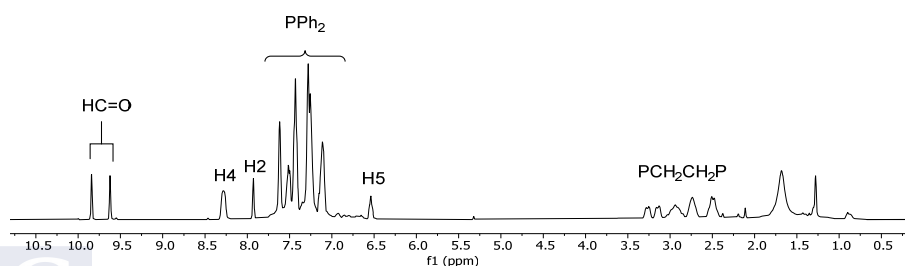


Figure 42. ¹H NMR of compound **4a** in CDCl₃.

As for the ^1H NMR spectrum for compound **4b**, two low field singlets at 9.59 and 9.13 ppm were assigned to the HC=O formyl groups. A broad doublet at 8.13 ppm [d, $^3J(\text{H2H3}) = 7.9$ Hz, 2H], was assigned to H2 and H3 resonances and a doublet at 6.39 ppm [d, $^4J(\text{H5P}) = 6.5$ Hz, 1H], was assigned to H5 proton resonance.

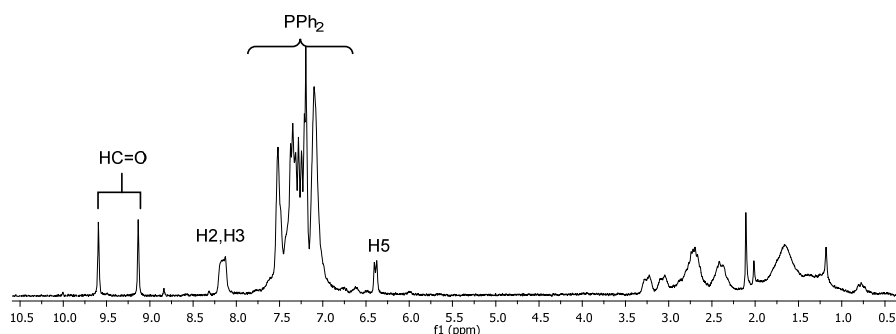


Figure 43. ^1H NMR of compound **4b** in CDCl_3 .

The $^{31}\text{P}\{-^1\text{H}\}$ NMR spectra of compounds **4a** and **4b** each showed doublet and triplet resonances. The former one *ca.* δ 47 [d, P_A , P_C], was assigned to the two equivalent, mutually *trans* phosphorous nuclei, and the latter one *ca.* δ 95 [t, P_B] was assigned to the central ^{31}P nucleus, *trans* to the metallated carbon atom, with $J = 23.4$ Hz. The phosphorus resonance for the anion PF_6^- showed a heptuplet *ca.* -144 ppm.

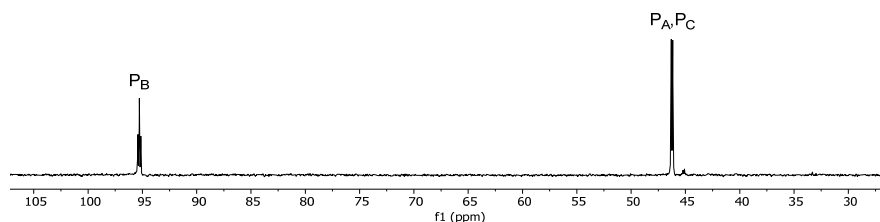
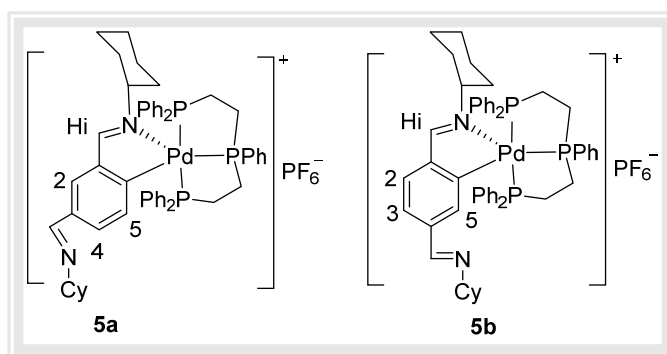


Figure 44. $^{31}\text{P}\{-^1\text{H}\}$ NMR of compound **4a** in CDCl_3 .

6.3.6 Study of compounds **5a** and **5b**.

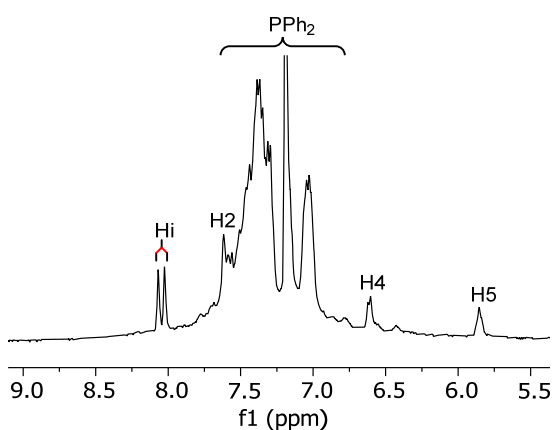
After hydrolysis of compounds **2a** and **2b**, which rendered **4a** and **4b** containing two HC=O moieties on the phenyl ring, the question remained as to whether the initial C=N double bonds could be regenerated. Well, the answer was yes, and thus, treatment of **3a** and **3b** with a primary amine such as cyclohexylamine gave complexes **5a** and **5b** having two -HC=NR substituents.



The ^1H NMR and $^{31}\text{P}\{-\text{H}\}$ NMR of compounds **5a** and **5b** were recorded in CDCl_3 .

Figure 45. ^1H NMR of compound **5a** in CDCl_3

The ^1H NMR spectra for compound **5a** shows two singlet signals at 8.025 and 8.069 ppm assigned to the two non-equivalent HC=N protons and the absence of any signal due to HC=O groups.



The first (higher frequency) is ascribed to the regenerated HC=N proton, and the second HC=N proton (lower frequency) to the nearer palladium atom.¹⁰⁹ A broad signal was ascribed to the proton H5 at 5.85 ppm. The proton H4 showed a doublet at 6.61 ppm [$^3J(\text{H4H5}) = 7.9$ Hz, 1H], indicating coupling with the proton H5. The proton H2 showed a singlet at 7.62 ppm. For compound **5b**, the protons HC=N appeared as a singlet at 8.07 ppm and proton H5 observed a doublet at 5.70 ppm [$^4J = 7.6$ Hz, 1H], indicating coupling with the phosphorus nucleus.

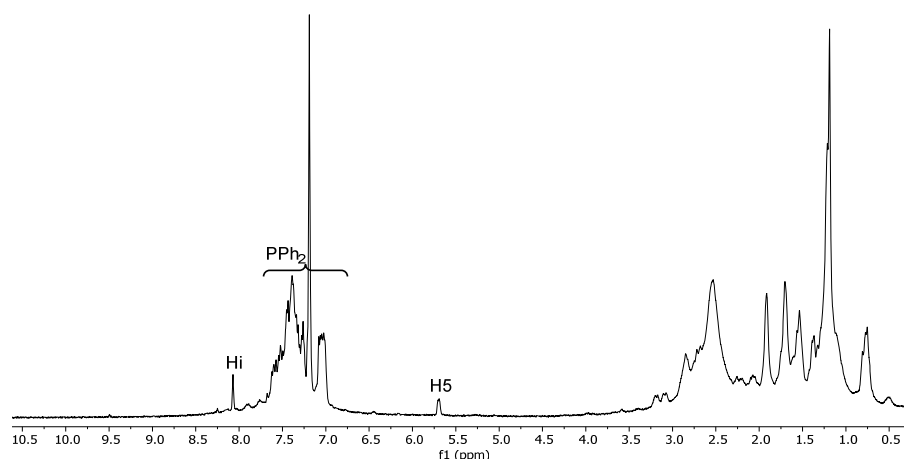
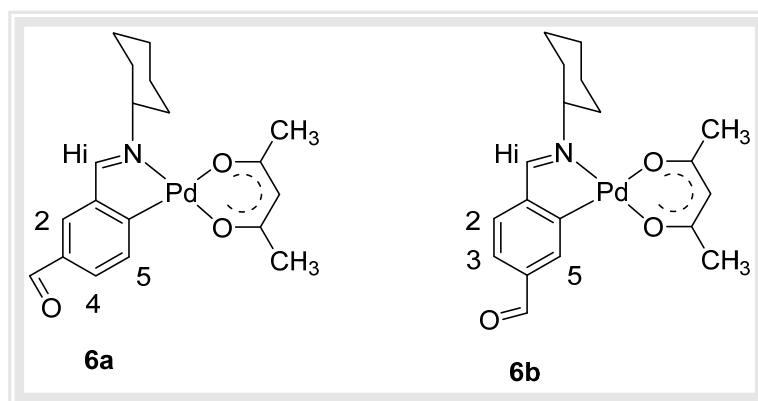


Figure 46. ^1H NMR of compound **5b** in CDCl_3 .

Compounds **5a** and **5b** showed doublet and triplet resonances in their $^{31}\text{P}\{-^1\text{H}\}$ NMR spectra. The two equivalents, mutually trans phosphorous nuclei were assigned *ca.* 45 [d], while the center ^{31}P nucleus, trans to the metallated carbon atom, was assigned *ca.* 95 [t], with $J = 24.7$ Hz. This finding supports the diphosphine ligands' coordination response. The hexafluorophosphate ion's phosphor resonance showed a heptuplet *ca.* -144 ppm.

6.3.7 Study of compounds **6a** and **6b**.

Compounds **6a** and **6b** were prepared by treatment of the parent halide-bridged species with thallium acetylacetonate to render mononuclear non-electrolyte compounds, with a bidentate acac-*O, O* ligand. The good solubility of the compounds and absence of aromatic compounds other than those of the metallated ring allows for a correct assignment of the resonances. The most noticeable difference with the starting NMR materials spectra was the presence of the signals due to the acetylacetonate ligand.



The ^1H NMR of compounds **6a** and **6b** were recorded in CDCl_3 .

In the ^1H NMR spectrum for **6a**, a singlet at 9.83 ppm was assigned to the $\text{HC}=\text{O}$ resonance. The proton $\text{HC}=\text{N}$ assigned as a singlet signal at 7.96 ppm. A singlet at 7.69 ppm was for the proton H2, and two doublets at 7.67 and 7.55 ppm [$^3J(\text{H4H5}) = 7.8$ Hz] were assigned to the protons H5 and H4, respectively. The acac resonances were at 5.35 ppm (-CH) and 1.9 and 2.10 ppm for the two non-equivalent methyl groups. A multiplet at 3.63 ppm was assigned to the cyclohexyl H7 proton.

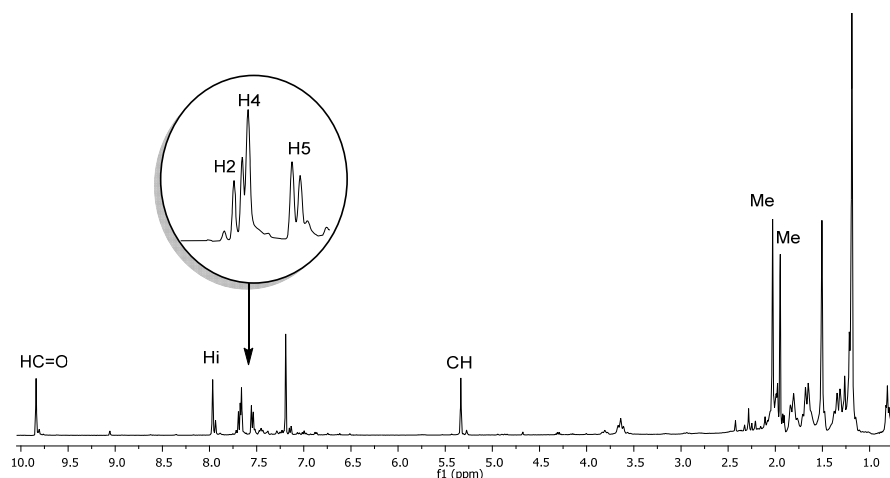


Figure 47. ^1H NMR of compound 6a in CDCl_3 .

In the ^1H NMR spectrum for **6b**, a singlet at 9.96 ppm was assigned to the $\text{HC}=\text{O}$ resonance. The $\text{HC}=\text{N}$ proton signal was a singlet at 7.95 ppm. The H5 resonance was a singlet at 7.92 ppm. Two doublets at 7.52 and 7.30 ppm [$^3J(\text{H}2\text{H}3) = 7.8$ Hz] were assigned to the H2 and H3 protons, respectively. The acac resonances were at 5.30 ppm (-CH) and 1.9 and 2.10 ppm for the two non-equivalent methyl groups. A multiplet at 3.7 ppm was assigned to the cyclohexyl H7 proton.

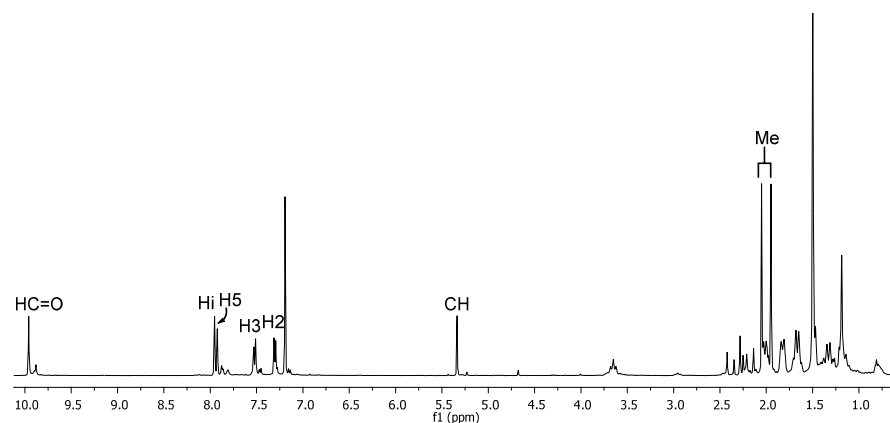
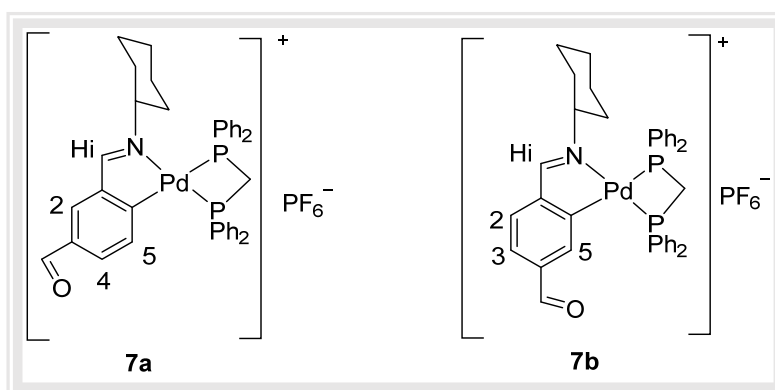


Figure 48. ^1H NMR of compound 6b in CDCl_3 .

6.3.8 Study of compounds **7a** and **7b**.

Compounds **7a** and **7b** were prepared from the parent compounds **2a** and **2b** by reaction with two equivalents of $\text{Ph}_2\text{PCH}_2\text{PPh}_2$ (bis(diphenylphosphino)methane, dppm) resulting in complexes with the diphosphine in the chelating-*P,P* mode.



The ^1H NMR and $^{31}\text{P}\{-^1\text{H}\}$ NMR of compounds **7a** and **7b** were recorded in CDCl_3 . The ^1H NMR spectra of both compounds are quite identical save for the aromatic proton resonance splitting pattern. Singlets at 9.87 (**7a**) and 9.52 (**7b**) ppm were assigned to the $\text{HC}=\text{O}$ resonances. A doublet signal *ca.* 8.4 ppm ($^4J(\text{PHi}) = 7.3$ Hz) in both cases was due to the $\text{HC}=\text{N}$ proton, coupled to the phosphorus nuclei trans to the coordinated nitrogen atom. A doublet at 6.8 ppm was ascribed to the H5 proton ($^3J(\text{H5H4}) = 7.6$ Hz), which was coupled to the H4 and phosphorus nucleus as well in case **7a** and phosphorus nucleus in case **7b** with ($^4J(\text{H5P}) = 6.4$ Hz). Assignment of the remaining aromatic ring protons was not possible due to overlapping with the phosphine phenyl ring proton signals, except for proton H2 of **7a**, which showed a singlet at 7.95 ppm. An apparent triplet at 4.30

ppm in both spectra was for the phosphine CH₂ group, which gives an AA'XX' pattern by coupling to the two-phosphorus nucleus. Additionally, a multiplet at 3.37 ppm was ascribed to the proton H7 resonance.

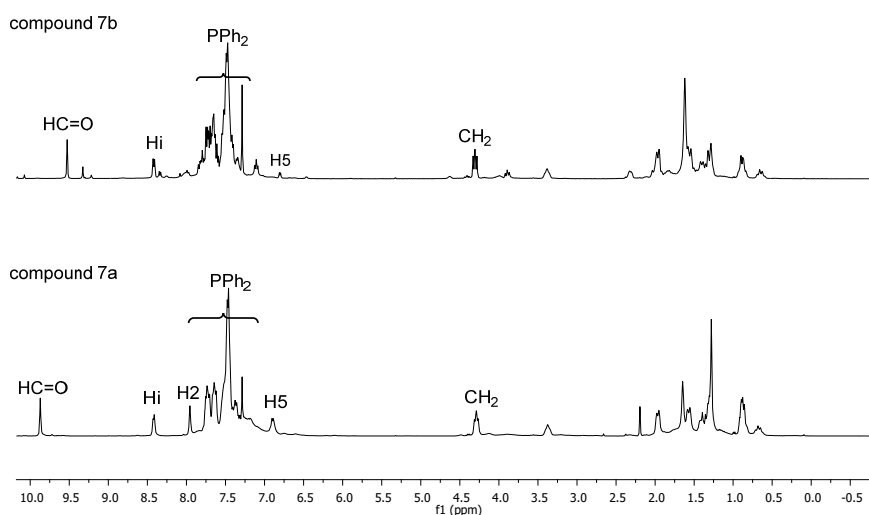


Figure 49. ¹H NMR for compounds 7a and 7b in CDCl₃.

The ³¹P-¹H NMR spectra of compounds **7a** and **7b** showed two doublets, for the two non-equivalent phosphorus. The doublets were assigned based on the idea that a ligand with a higher *trans* influence causes the phosphorus atoms *trans* to it to resonate at a lower frequency.¹⁰⁹ The four-membered ring size of dppm ligand influenced the chemical shifts and gave negative upfield resonances.¹¹⁰

¹⁰⁹ P.S. Pregosin, R.W. Kuntz, *Springer*, Berlin, 1979.

¹¹⁰ P.E. Garrou, *Chemical Reviews*, 81 (1981) 229-266.

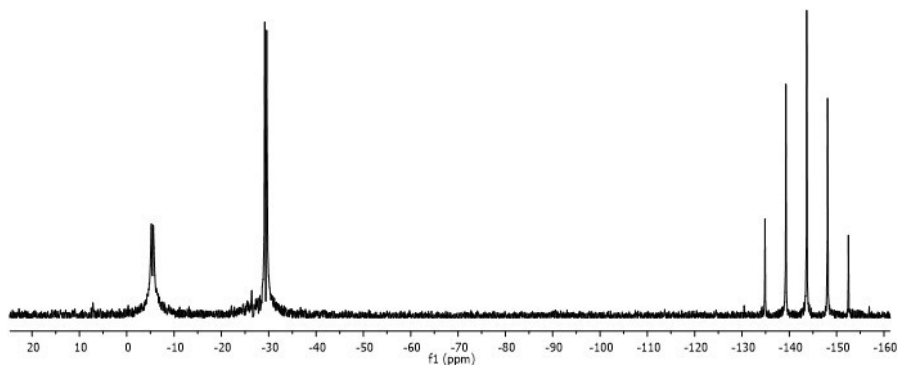
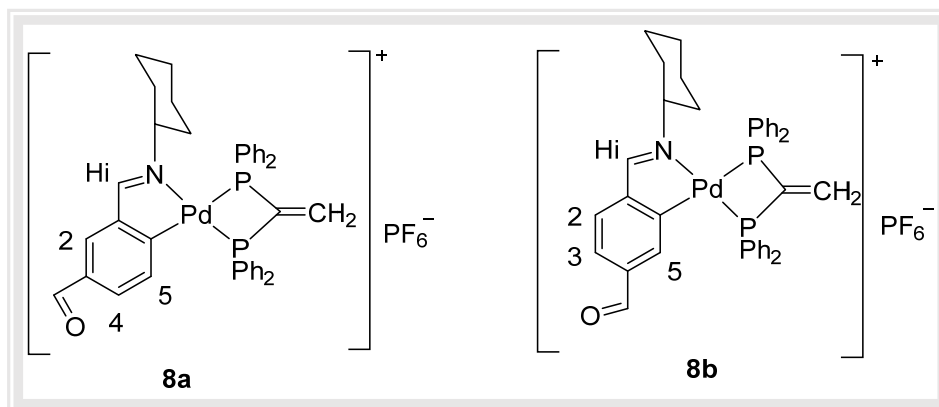


Figure 50. $^{31}\text{P}\{^1\text{H}\}$ NMR of compound **7a** in CDCl_3 .

6.3.9 Study of compounds **8a** and **8b**.

In a similar fashion to complexes **8a** and **8b**, treatment of **2a** and **2b** with two equivalents of $\text{Ph}_2\text{PC}(\text{=CH}_2)\text{PPh}_2$ (1,1-bisdiphenylphosphinoethene, vdpp) resulted in complexes with the diphosphine in the chelating-*P,P* mode.



The ^1H NMR and $^{31}\text{P}\{^1\text{H}\}$ NMR of compounds **8a** and **8b** were recorded in CDCl_3 .

In the ^1H NMR spectra for compound **8a**, a singlet *ca.* 9.8 ppm was assigned to the $\text{HC}=\text{O}$ proton. A triplet of triplets *ca.* 5 ppm was

ascribed to the proton H5, coupled to the H4 and phosphorus nucleus [$^3J(\text{H5H4}) = 7.5 \text{ Hz}$ and $^4J(\text{P}_{\text{trans-NH5}}) \text{ ca. } 14 \text{ Hz, } 1\text{H}$]. A doublet resonance *ca.* 8.4 ppm was for the HC=N proton coupled to the phosphorus nucleus *trans* to the coordinated nitrogen atom [$^4J(\text{PHi}) = 7.5 \text{ Hz}$]. The H2 and H4 protons could not be assigned, due to overlapping with the phosphine phenyl ring proton signals. The vinylidene protons of the vdpp ligand were assigned a multiplet signal *ca.* 6.5 ppm, resulting from the AA'XX' pattern for the HHPP nuclei.

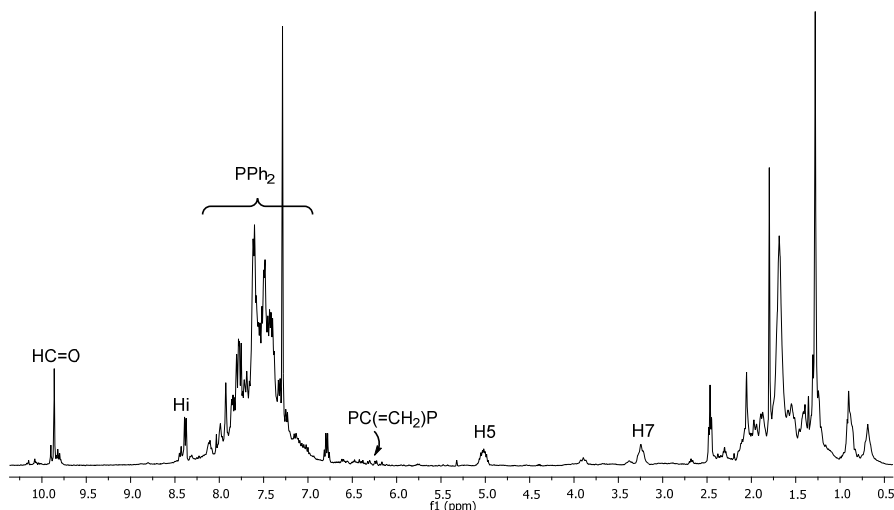


Figure 51. ^1H NMR of compound **8a** in CDCl_3 .

In the ^1H NMR spectra for compound **8b**, a singlet at 9.55 ppm, was assigned to HC=O proton. A doublet resonance *ca.* 8.47 ($^4J(\text{PHi}) = 7.5 \text{ Hz}$), assigned to HC=N proton coupled to the phosphorus nucleus *trans* to the coordinated nitrogen atom. A triplet of doublets at 5.0 ppm was shown to the H5 proton, coupled to both phosphorus nuclei ($^4J(\text{P}_{\text{trans-NH5}}) \text{ ca. } 14 \text{ Hz}$, $^4J(\text{P}_{\text{trans-CH5}}) \text{ ca. } 7.0 \text{ Hz}$). The H2 and H3 protons could not be assigned, due to overlapping with the phosphine phenyl ring proton signals. The AA'XX' pattern for the HHPP nuclei

gave the vinylidene protons of the vdpp ligand a multiplet signal of around 6.3 ppm.

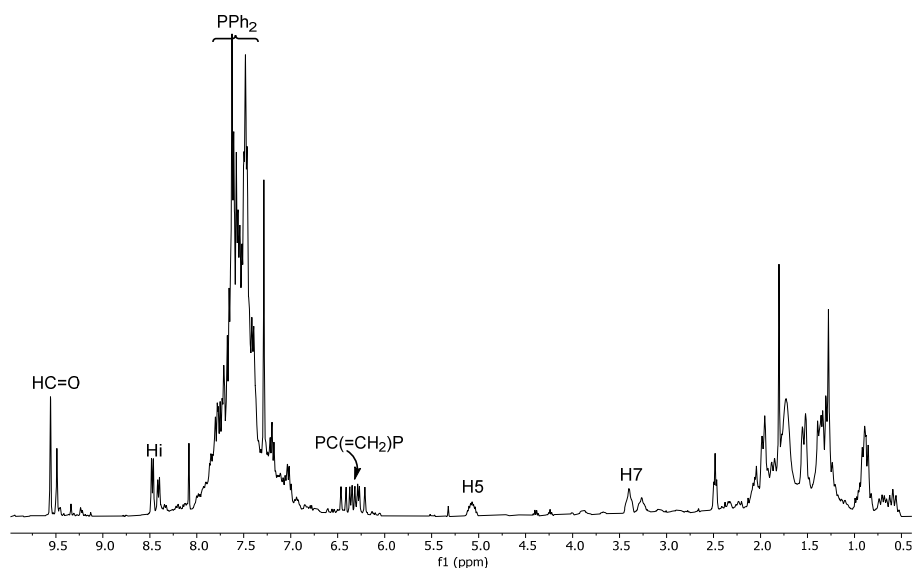


Figure 52. ^1H NMR of compound **8b** in CDCl_3 .

The $^{31}\text{P}\{-^1\text{H}\}$ NMR spectrum of compound **8a** showed two doublets assigned to the two non-equivalent phosphorus nuclei with $J = 57.2$ Hz at 11.8, and -9.97 ppm; also, for compound **8b** doublets with a coupling constant were very different at 11.8, and -9.97 ppm with $J = 55.9$ Hz, and at 13.9, and -3.78 ppm with $J = 13.4$ Hz, due to the different dispositions of diphosphines, the compound **8b** may contain two isomers, resulting in doubled signals.

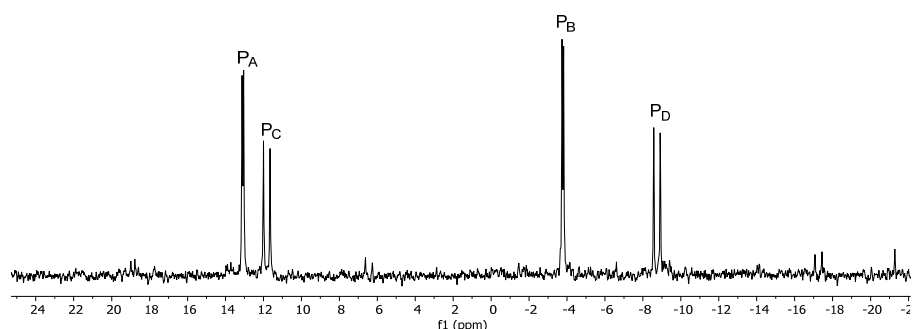
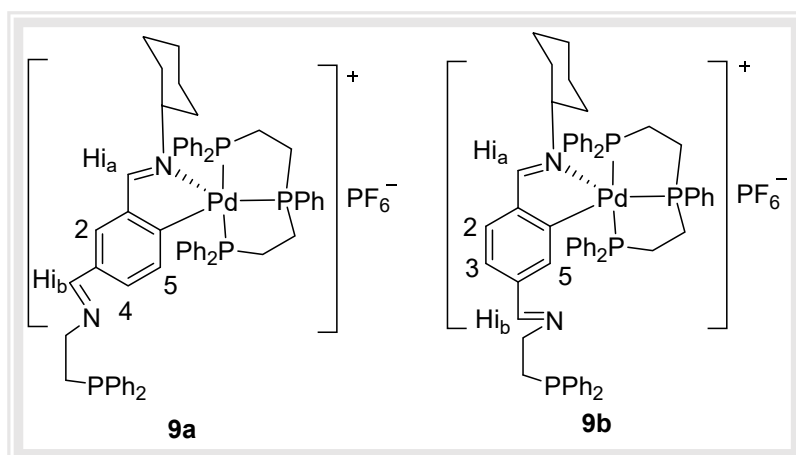


Figure 53. $^{31}\text{P}\{-^1\text{H}\}$ NMR of compound **8a** in CDCl_3 .

6.3.10 Study of compounds **9a** and **9b**.

The use of phosphorus and nitrogen chelating ligands is a widely successful strategy for the synthesis of metal-based catalysts. Compounds of type **3a** and **3b** with a chelating triphosphine ligand may further extend chelation by condensing the free formyl group with a suitable amine precursor, thus enabling coordination of a second metal atom in a $[P,N]$ chelated mode. Hence, the reaction of α -aminophosphines containing 2(diphenylphosphanyl)ethan-1-amine, $\text{H}_2\text{N}(\text{CH}_2)_2\text{PPh}_2$, with compounds **3a** and **3b** was attempted, to give compounds **9a** and **9b** after the condensation reaction of the amino and the carbonyl groups. The ^1H NMR and $^{31}\text{P}\{-^1\text{H}\}$ NMR of compounds **9a** and **9b** were recorded in CDCl_3 .



The ^1H NMR spectra for compounds **9a** showed two nearly overlapped HC=N proton resonances *ca.* 8.1 ppm and two equivalent protons assigned a singlet for **9b**, in accordance with C=N bond formation and absence of the formyl proton signal: The proton of the HC=N group linked to or closer to the palladium atom is allocated to the singlet signal at a higher field, while the proton of the HC=N group that has been regenerated is assigned to the singlet signal at slightly lower field.

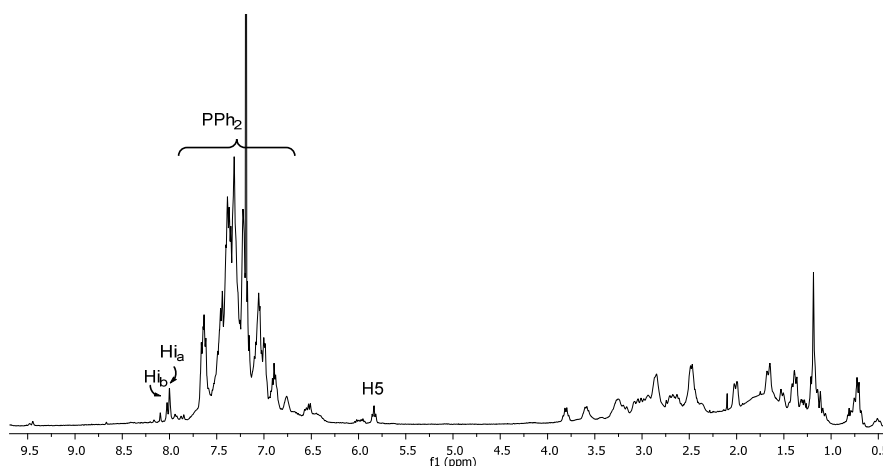


Figure 54. ^1H NMR of Compound **9a** in CDCl_3 .

The proton of H5 (**9a**) showed a triplet signal at 5.83 ppm [$^3J(\text{H5H4}) = ^4J(\text{H5P}) = 7.6$ Hz] and a doublet at 5.65 ppm [$^4J(\text{H5P}) = 7.8$ Hz] for the H5 proton (**9b**) coupled to the trans phosphorus nucleus. The signals for the amine methylene protons were *ca.* 4.0–3.5 ppm.

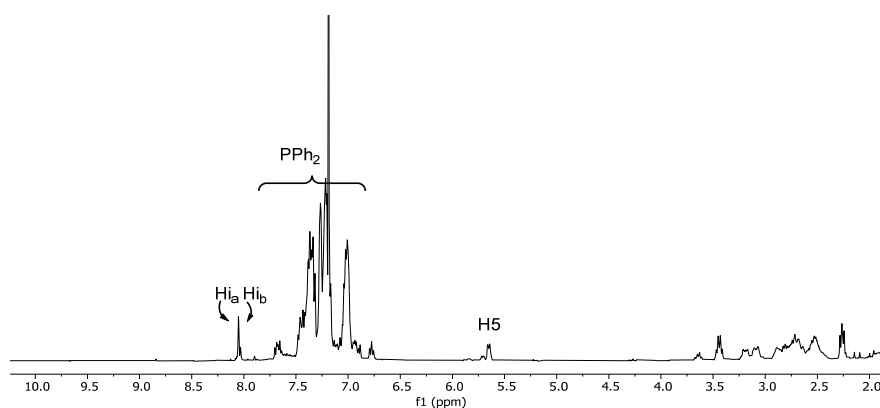


Figure 55. ^1H NMR of Compound **9b** in CDCl_3 .

The $^{31}\text{P}\{-^1\text{H}\}$ NMR spectra of compounds **9a** and **9b** showed the tridentate phosphine resonances *ca.* 84–85 ppm for the central phosphorus nucleus, and *ca.* 45 ppm for the two equivalent terminal phosphorus nuclei with $J = 28$ Hz. Additionally, a third singlet signal was assigned to the non-coordinated phosphorus nucleus from the amino phosphine ligand *ca.* -20 ppm.

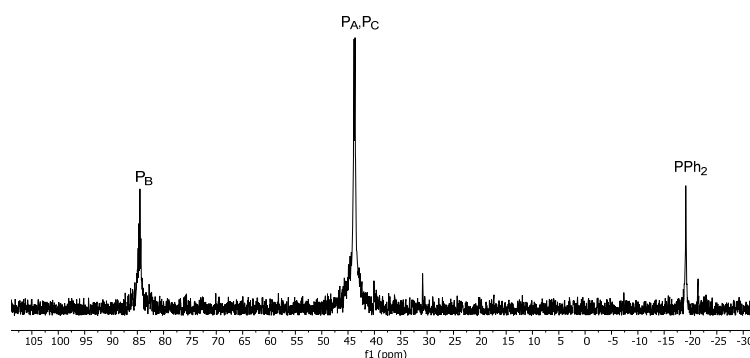
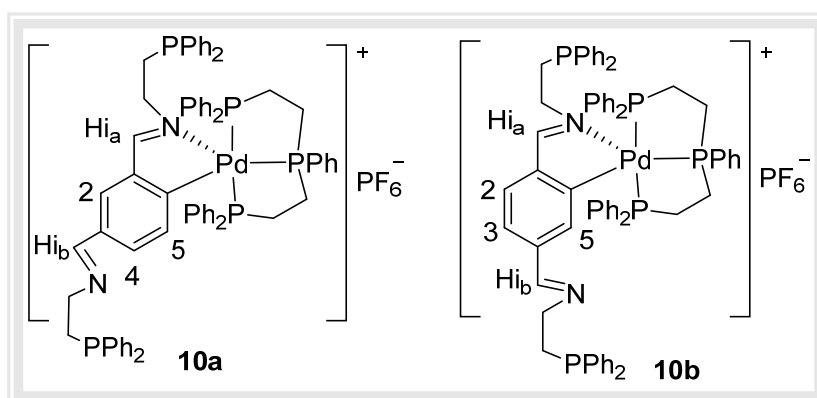


Figure 56. $^{31}\text{P}\{-^1\text{H}\}$ NMR of compound **9b** in CDCl_3 .

6.3.11 Study of compounds **10a** and **10b**.

In a similar manner to the syntheses of compounds **9a** and **9b**, complexes with two non-coordinated phosphorus donors could be produced by the condensation reaction of the mentioned aminophosphine with compounds **4a** and **4b** having two formyl groups on the metallated phenyl ring, thus giving compounds **10a** and **10b**.



The ¹H NMR and ³¹P-¹H NMR of compounds **10a** and **10b** were recorded in CDCl₃. The ¹H NMR spectra data of **10a** and **10b** are consistent with the structures proposed. Thus, two singlet signals of HC=N appeared in both cases at 7.95 and 7.86 ppm and at 9.46 and 9.43 ppm, respectively, as already mentioned, the regenerated HC=N proton is at a higher frequency, whereas the HC=N close to the palladium atom is at a lower frequency, no signal ascribable to the HC=O resonances was observed. Broad signal *ca.* 5.95 ppm for **10a** and doublet at 6.10 ppm (⁴J(PH5) = 6.9 Hz, 1H) for **10b**, were assigned to the H5 resonances. The signals for the amine methylene protons were *ca.* 3.8-2.5 ppm.

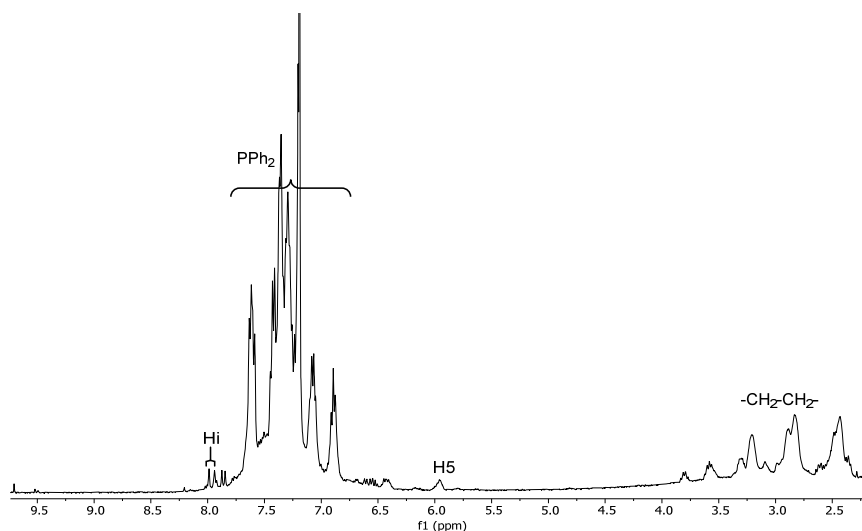


Figure 57. ^1H NMR of compound **10a** in CDCl_3 .

The $^{31}\text{P}\{-^1\text{H}\}$ NMR spectra of compounds **10a** and **10b** showed the tridentate phosphine resonances *ca.* 89 ppm for the central phosphorus nucleus, and *ca.* 43 ppm for the two equivalent terminal phosphorus nuclei with $J \approx 28$ Hz. Additionally, two singlet signals were assigned to the non-coordinated phosphorus nucleus from the apparently non-equivalent aminophosphine ligands *ca.* -19 and -20 ppm.

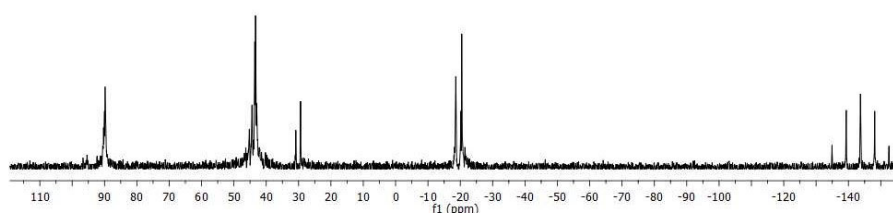
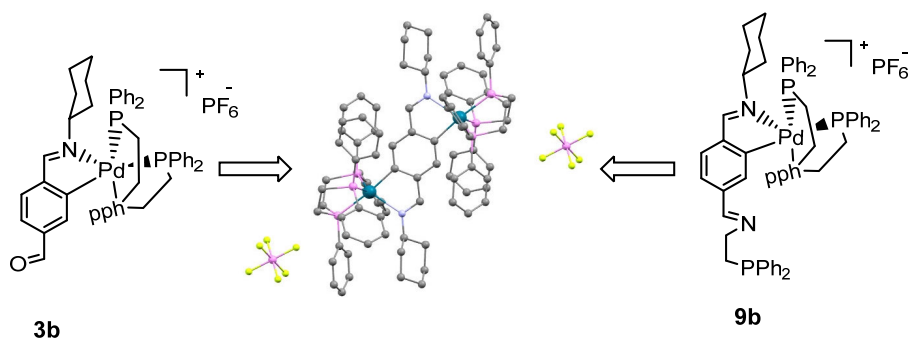


Figure 58. $^{31}\text{P}\{-^1\text{H}\}$ NMR of compound **10a** in CDCl_3 .

6.3.12 Study of changes of compounds **3b** and **9b** in NMR.



The crystal result of compounds **3b** and **9b** obtained was not initially expected, therefore we investigated the compounds **3b** and **9b** in the NMR spectrum after one week of CDCl_3 addition at room temperature. The ^1H NMR and $^{31}\text{P}\{-^1\text{H}\}$ NMR spectra of compound **3b** showed an addition of protons and phosphorus signals. In ^1H NMR, another doublet at 5.7 ppm ($^4J = 7.9$ Hz) was observed, showing further proton coupling with the phosphorus nucleus, and another singlet signal at 8.10 ppm, which is assigned to HC=N proton. In $^{31}\text{P}\{-^1\text{H}\}$ NMR, addition another triplet resonance showed *ca.* 82 ppm, which is assigned to the central ^{31}P nucleus, and doublet signals *ca.* 43 ppm, which are assigned to the two-equivalent phosphorous. This result was in agreement with the result of a dinuclear compound that has been reported.¹¹¹

¹¹¹ M. López-Torres, A. Fernández, J.J. Fernández, A. Suárez, M.T. Pereira, J.M. Ortigueira, J.M. Vila, H. Adams, *Inorganic Chemistry*, 40 (2001) 4583-4587.

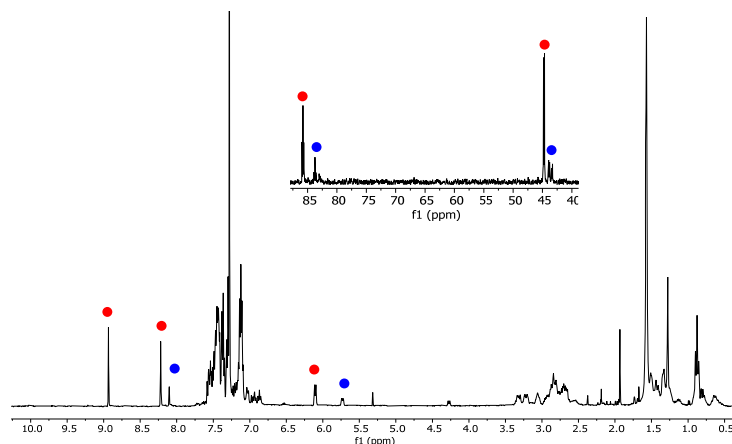


Figure 59. ^1H NMR and $^{31}\text{P}\{-^1\text{H}\}$ NMR of compound **3b** in CDCl_3 after one week. ● Protons and phosphorus correspond to compound **3b**. ● Protons and phosphorus correspond to the dinuclear compound.

NMR spectroscopy of compound **9b** has provided also additional evidence for the hydrolysis $-\text{C}=\text{N}$ of the aminophosphine ligand through the observation of ^1H NMR and $^{31}\text{P}\{-^1\text{H}\}$ NMR signals. The ^1H NMR showed two singlets at 8.13 ppm and 8.85 ppm, which are assigned to protons of $\text{HC}=\text{N}$ and $\text{HC}=\text{O}$, respectively. Two doublets at 6.0 ppm ($^4J = 7.3$ Hz, 1H), 5.7 ppm ($^4J = 7.7$ Hz, 1H) was assigned to the H5 proton of **3b**, **9b**, and another doublet at 5.65 ppm ($^4J = 7.7$ Hz, 2H), is assigned to proton H5 and H2 of a dinuclear compound, respectively. The $^{31}\text{P}\{-^1\text{H}\}$ NMR was also shown to have other couplings constant *ca.* 27 Hz.

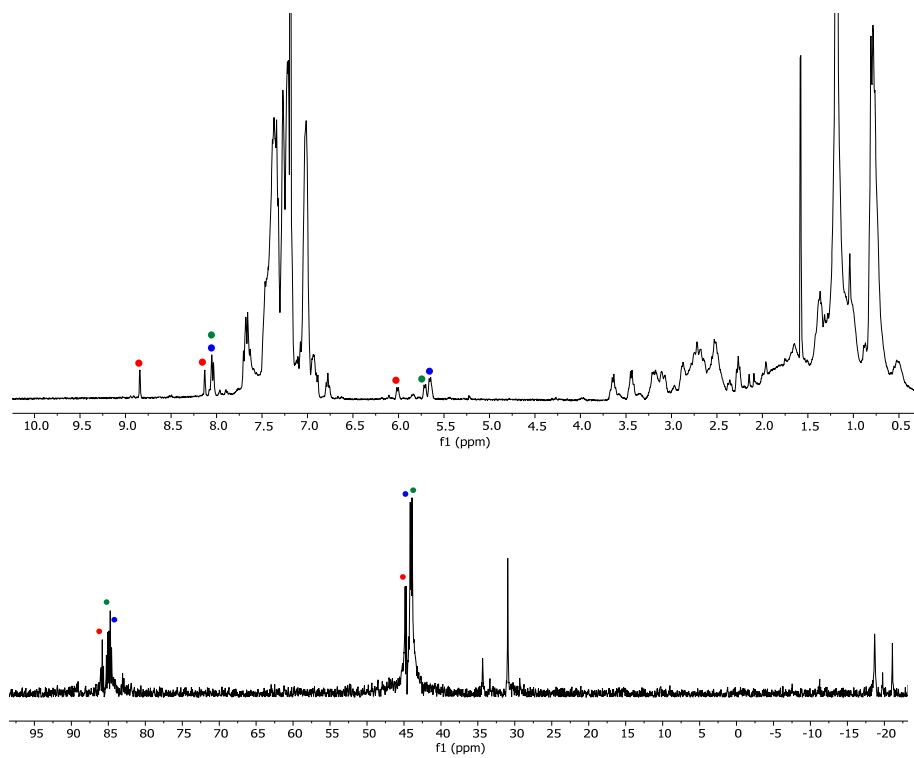


Figure 60. ^1H NMR and $^{31}\text{P}\{-^1\text{H}\}$ NMR of compound 9b in CDCl_3 . ● Protons and phosphorus corresponding to compound 9b. ● protons and phosphorous decomposed to compound 3b. ● Protons and phosphorus correspond to the dinuclear compound.

The suggested mechanism starts with the H-solvent contact and is stabilized by solvent coordination (ii), resulting in chelating ligand dissociation (iii). On the other hand, the existence of H_2O , imine, or aminophosphine ligand can be converted back to the carbonyl compound, thus compound dissociation will occur (iv), resulting in the formation of T-shape Pd(II) cationic compound, which is related to complex stabilized with bulky phosphine ligand and α -solvent

6.4 X-ray diffraction study

6.4.1 Structure of compound **1b**

Suitable crystals of compound **1b** were grown by slow evaporation from an ethyl acetate/n-hexane solution. The structure of **1b** is that of a dinuclear complex with two cyclometallated moieties linked by acetate-bridging ligands and consists of one molecule per asymmetric unit. The most significant bond lengths and angles are shown in Figure 61. The Pd(1)–C(1) bond length of 1.961(3) Å, is less than the expected value of 2.081 Å (based on the sum of the covalent radii for carbon (sp²) and palladium 0.771 and 1.31 Å, respectively), is consistent with those found in related complexes,^{114,115} and with the five-membered cyclometallated ring having a significant aromatic character.¹¹⁶ The Pd(1)–N(2) bond length 2.013(2) Å, is consistent with the 2.011 Å single bond value predicted from the sum of covalent radii for nitrogen (sp²) and palladium, 0.701 and 1.31 Å, respectively.¹¹⁷ The asymmetric character of the Pd(Me-OAc)₂Pd moiety, as evidenced by the Pd–OAc bond lengths [Pd(1)–O(1) 2.146(2); Pd(2)–O(2) 2.037(2); Pd(1)–O(3) 2.035(2); Pd(2)–O(4)

¹¹⁴ J. M. Vila, et al. *Journal of organometallic chemistry* 448.1-2 (1993): 233-239.

¹¹⁵ G. Zhao, Q.-G. Wang, T.C. Mak, *Journal of the Chemical Society, Dalton Transactions*, (1998) 1241-1248.

¹¹⁶ A. Crispini, M. Ghedini, *Journal of the Chemical Society, Dalton Transactions*, (1997) 75-80.

¹¹⁷ A.G. Orpen, L. Brammer, F.H. Allen, O. Kennard, D.G. Watson, R. Taylor, *Journal of the Chemical Society, Dalton Transactions*, (1989) S1-S83.

2.146(2) Å], is due to the differing *trans* influence of the Schiff base ligand donor atoms.¹¹⁸

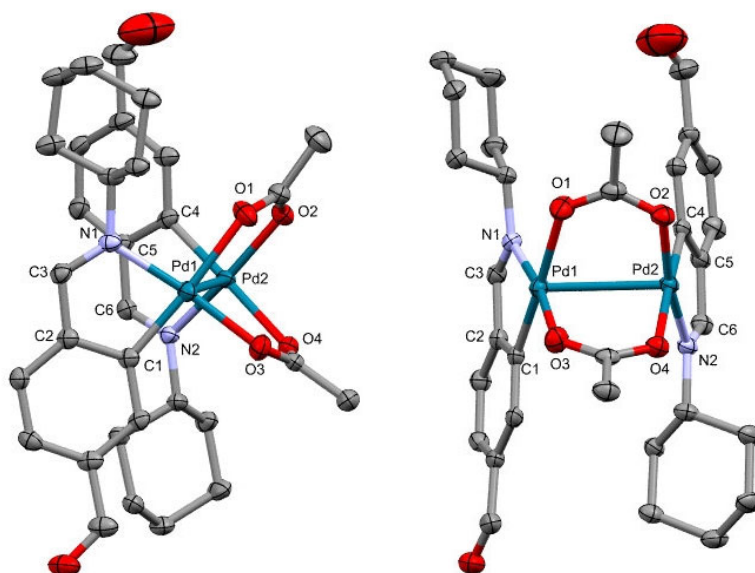


Figure 61. the crystal structure of compound 1b

The acetate bridging ligands span across the two palladium centers separating them by a distance of 2.88 Å, a value greater than the sum of the van der Waals radii for palladium, 2.62 Å, precluding any contact between, although but in some cases some type of interaction has been reported in the literature.¹¹⁹

¹¹⁸ J.M. Vila, et al. *Journal of organometallic chemistry* 471.1-2 (1994): 259-263.

¹¹⁹ J.R. Walensky, C.M. Fafard, C. Guo, C.M. Brammell, B.M. Foxman, M.B. Hall, O.V. Ozerov, *Inorganic chemistry*, 52 (2013) 2317-2322.

Table 15. Complex 1b was obtained from X-ray single-crystal diffraction studies (see drawing below). Bond lengths are given in [Å] and angles in [°].

Pd(1)-C(1)	1.961(3)	Pd(1)-O(1)	2.146(2)
Pd(2)-C(4)	1.967(2)	Pd(2)-O(2)	2.037(2)
Pd(1)-N(1)	2.015(2)	Pd(1)-O(3)	2.035(2)
Pd(2)-N(2)	2.013(2)	Pd(2)-O(4)	2.150(2)

Table 16. Crystal data and structure refinement for compound 1b

Molecular formula	C ₃₂ H ₃₈ N ₂ O ₆ Pd ₂
Formula weight	759.44
Temperature/K	100.0
Crystal system	Monoclinic
Space group	P2 ₁ /n
a/Å	11.5718(4)
b/Å	9.6296(3)
c/Å	27.2380(9)
α/°	90
β/°	91.9690(10)
γ/°	90
Volume/Å ³	3033.39(17)
Z	4
ρ _{calc} /cm ³	1.663
μ/mm ⁻¹	1.232
F(000)	1536.0
Crystal size/mm ³	0.14 × 0.12 × 0.04
Radiation	MoKα (λ = 0.71073)
θ range for data collection/°	4.486 to 55.754
Index ranges	-15 ≤ h ≤ 15, -12 ≤ k ≤ 12, -35 ≤ l ≤ 35
Reflections collected	40301
Independent reflections	7226 [R _{int} = 0.0433, R _{sigma} = 0.0306]
Data/restraints/parameters	7226/0/532
Goodness-of-fit on F ²	1.044
Final R indexes [I ≥ 2σ (I)]	R ₁ = 0.0311, wR ₂ = 0.0726
Final R indexes [all data]	R ₁ = 0.0401, wR ₂ = 0.0770
Largest diff. peak/hole / e Å ⁻³	1.91/-0.76

6.4.2 Structures of dinuclear compound **vi** and **vi'**

Suitable crystals of compounds **3b** and **9b** were grown by slow evaporation from a $\text{CH}_2\text{Cl}_2/\text{CHCl}_3$ and an ethylacetate/acetone solution, respectively. The crystal result of compounds **3b** and **9b** are dinuclear metal complex bis(palladacycle) complexes (**vi** and **vi'**), respectively, which represents a quite surprisingly result because the parent compound in case **3b** only has one $-\text{C}=\text{NCy}$ group and a formyl moiety on the metallated phenyl ring, and two different $-\text{C}=\text{N}-$ group in case **9b**. whereas the crystal structures show two $-\text{C}=\text{NCy}$ groups bonded, each palladium atom is bonded to the $-\text{C}=\text{NCy}$ through the nitrogen lone pair interaction. The symmetric units of **vi** and **vi'** formed a dinuclear metal complex co-crystallizes with two molecules of hexafluorophosphate anions.

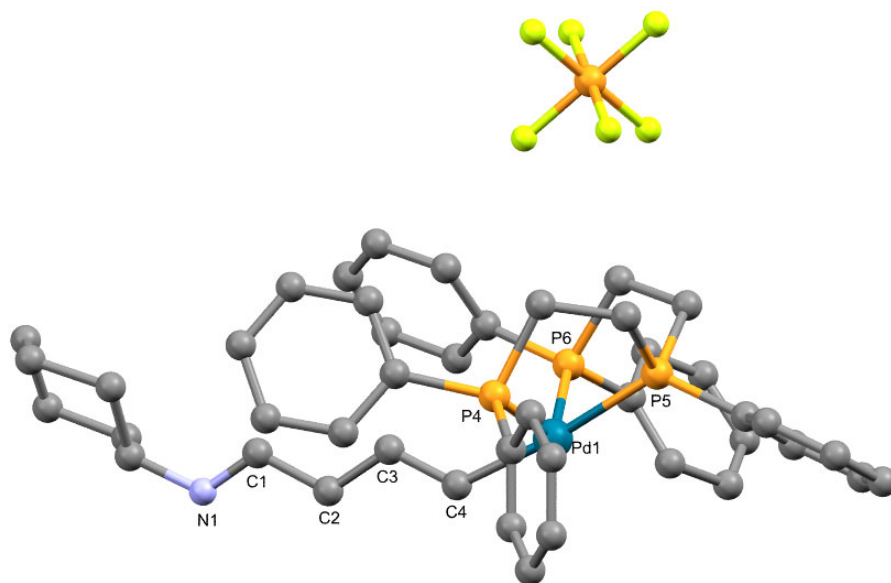


Figure 62. view of the asymmetric unit for compound **vi**.

The palladium atoms are in distorted trigonal bipyramidal environments bonded to the bidentate [C, N] Schiff base ligand and the three phosphorus donor atoms of the tridentate phosphine ligand, with the palladium, nitrogen, and terminal phosphorus atoms in the equatorial plane. In contrast, phosphine-*P,P,P* bonding of the phosphorus donors to the palladium center would cleave the palladium–nitrogen bond, leaving an uncoordinated nitrogen atom; in either case, additional coordination of the nitrogen or phosphorus atoms should be possible to provide bimetallic complexes.

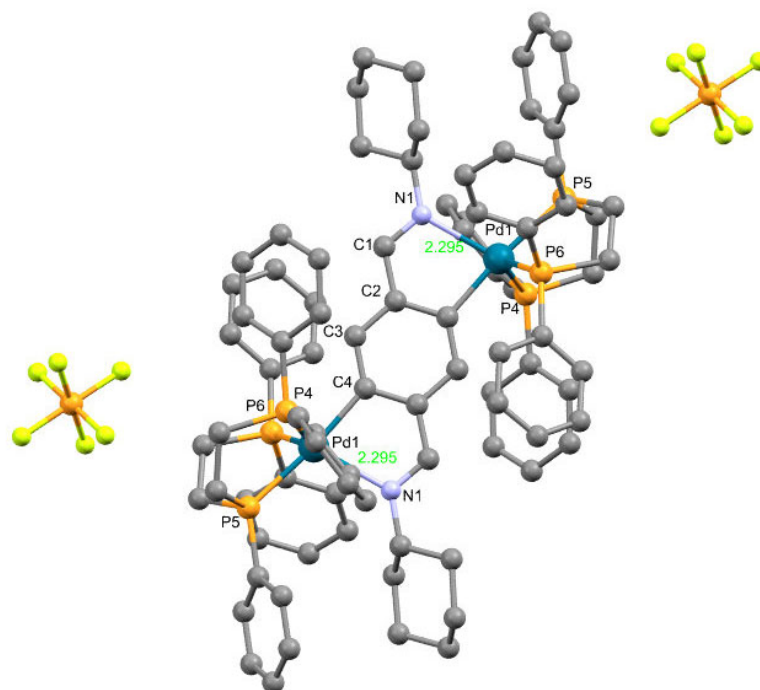


Figure 63. symmetric unit view of compound **vi**.

Compound **vi** and **vi'** contain a doubly cyclopalladated compound having two pentacoordinated palladium centers, with a Pd(1)-N(1) bond length of 2.295(2) Å and 2.285(2) Å respectively, which is quite

near to the Pd-N bond length of 2.23(2) Å discovered in an actual pentacoordinate palladium(II) complex.¹²⁰ These distances are to the best of our knowledge the shortest value given for this type of complex. The [P(4)–Pd(1)–N(1)], [P(6)–Pd(1)–N(1)], and [P(4)–Pd(1)–P(6)] bond angles are all close to the ideal value of 120° expected for planar trigonal geometry, with values of 116.60(9), 119.99(9), and 123.07(4)°, respectively.

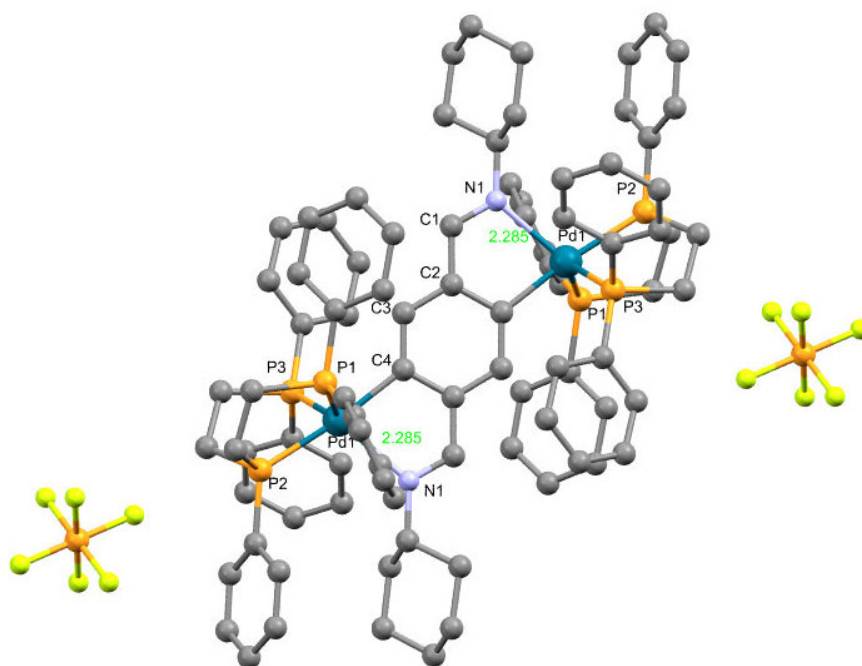


Figure 64. symmetric unit view of compound vi'.

The [C(4)–Pd(1)–P(5)] bond angle is close to 180°, as would be expected for metallated carbon and P(5) atoms in axial positions of a trigonal bipyramid or opposite positions of the base of a square

¹²⁰ F. Cecconi, C.A. Ghilardi, S. Midollini, S. Moneti, A. Orlandini, G. Scapacci, *Journal of the Chemical Society, Dalton Transactions*, (1989) 211-216.

pyramid. The degree of distortion toward square base pyramidal geometry is shown by the mean departure from the C(4)-Pd(1)-P(6) least-squares plane (which might be considered the basal plane for a square pyramid). The Pd(1)-C(4) length of 2.042(3) Å is similar to those found in related cyclometallated compounds with carbon *trans* to phosphorus but longer than palladium-carbon distances found in cyclometallated compounds with carbon *trans* to nitrogen or chlorine, consequent on the presence of a phosphine ligand in the *trans* position.¹²¹ The Pd-P bond lengths are similar to those found in analogous Pd(II) complexes,¹²² implying the presence of a partial double bond between the palladium and phosphorus atoms.¹²³

¹²¹ A. Fernández, M. López-Torres, A. Suárez, JM Ortigueira, T. Pereira, JJ Fernández, JM Vila, and H. Adams, *J. Organomet. Chem*, 598 (2000) 1.

¹²² C.E. Housecroft, B.A. Shaykh, A. Rheingold, B. Haggerty, *Acta Crystallographica Section C: Crystal Structure Communications*, 46 (1990) 1549-1551.

¹²³ J. Vila, M. Gayoso, M.L. Torres, J.J. Fernandez, A. Fernández, J.M. Ortigueira, N.A. Bailey, H. Adams, *Journal of organometallic chemistry*, 511 (1996) 129-138.

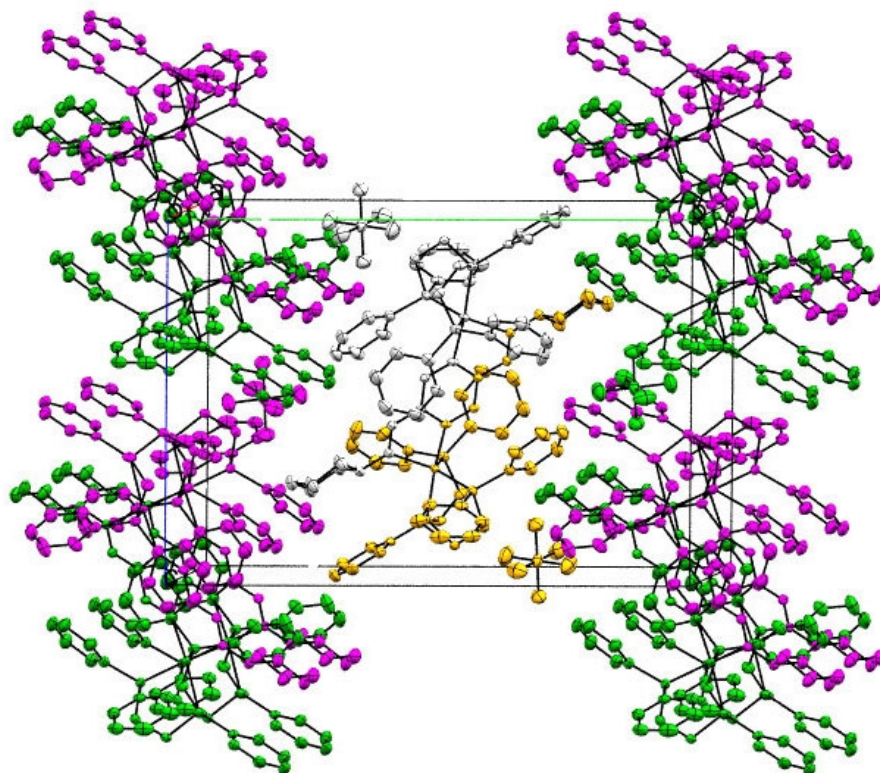


Figure 65. The molecular packing of vi within the unit cell.

Table 17. Asymmetric compound **vi** was obtained from X-ray single-crystal diffraction studies. Bond lengths are given in [Å] and angles in [°].

Pd(1)-N(1)	2.295(2)	P(4)-Pd(1)-P(6)	123.07(4)
Pd(1)-C(4)	2.042(3)	N(1)-Pd(1)-P(4)	116.60(9)
N(1)-C(1)	1.279(4)	C(4)-Pd(1)-P(4)	92.06(12)
C(1)-C(2)	1.455(4)	N(1)-Pd(1)-P(5)	107.26(9)
C(2)-C(3)	1.405(4)	P(4)-Pd(1)-P(5)	85.05(4)
C(3)-C(4)	1.387(4)	P(5)-Pd(1)-P(6)	84.30(4)
Pd(1)-P(4)	2.311(9)	N(1)-Pd(1)-P(6)	119.99(9)
Pd(1)-P(5)	2.337(8)	C(4)-Pd(1)-N(1)	78.43(15)
Pd(1)-P(6)	2.312(8)	Pd(1)-N(1)-C(1)	110.09(3)
C(4)-Pd(1)-P(5)	174.30(12)		

Table 18. Asymmetric compound **vi'** was obtained from X-ray single-crystal diffraction studies. Bond lengths are given in [Å] and angles in [°].

Pd(1)-N(1)	2.285(2)	P(1)-Pd(1)-P(3)	122.76(4)
Pd(1)-C(4)	2.044(3)	N(1)-Pd(1)-P(3)	120.34(9)
N(1)-C(1)	1.282(4)	C(4)-Pd(1)-P(4)	93.45(12)
C(1)-C(2)	1.448(4)	N(1)-Pd(1)-P(2)	107.20(9)
C(2)-C(3)	1.404(4)	P(3)-Pd(1)-P(2)	84.21(4)
C(3)-C(4)	1.387(4)	P(2)-Pd(1)-P(1)	85.04(4)
Pd(1)-P(1)	2.312(9)	N(1)-Pd(1)-P(1)	116.57(9)
Pd(1)-P(2)	2.342(8)	C(4)-Pd(1)-N(1)	78.35(15)
Pd(1)-P(3)	2.315(8)	N(1)-Pd(1)-C(1)	110.10(3)
C(4)-Pd(1)-P(2)	174.24(12)		

Table 19. Crystal data and structure refinement for compound vi.

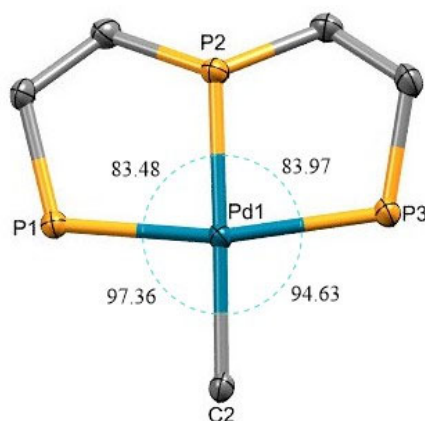
Crystal structure	vi	vi'
Molecular formula	C ₈₈ H ₉₂ F ₁₂ N ₂ P ₈ Pd ₂	C ₈₈ H ₉₂ F ₁₂ N ₂ P ₈ Pd ₂
Formula weight	1866.33	1866.33
Temperature/K	100.0	100.00
Crystal system	monoclinic	monoclinic
Space group	P2 ₁ /n	P2 ₁ /n
a/Å	11.6509(4)	11.6417(9)
b/Å	22.6116(9)	22.6057(17)
c/Å	15.5974(7)	15.6302(13)
α/°	90	90
β/°	96.3390(1)	96.218(3)
γ/°	90	90
Volume/Å ³	4083.9(3)	4089.2(6)
Z	2	2
ρ _{calc} /cm ³	1.518	1.516
μ/mm ⁻¹	0.672	0.671
F(000)	1906.8	1906.8
Crystal size/mm ³	0.11 × 0.07 × 0.03	0.2 × 0.2 × 0.1
Radiation	Mo Kα (λ = 0.71073)	Mo Kα (λ = 0.71073)
θ range for data collection/°	4.16 to 52.74	3.96 to 56.56
Index ranges	-14 ≤ h ≤ 12, -28 ≤ k ≤ 28, -19 ≤ l ≤ 19	15 ≤ h ≤ 15, -30 ≤ k ≤ 30, -20 ≤ l ≤ 20
Reflections collected	86534	135373
Independent reflections	8352 [R _{int} = 0.0539, R _{sigma} = 0.0256]	10139 [R _{int} = 0.0817, R _{sigma} = 0.0339]
Data/restraints/parameters	8352/0/506	10139/0/905
Goodness-of-fit on F ²	1.119	1.040
Final R indexes [I >= 2σ (I)]	R ₁ = 0.0404, wR ₂ = 0.1048	R ₁ = 0.0414, wR ₂ = 0.1175
Final R indexes [all data]	R ₁ = 0.0488, wR ₂ = 0.1135	R ₁ = 0.0550, wR ₂ = 0.1456
Largest diff. peak/hole / e Å ⁻³	0.98/-0.64	1.29/-1.00

6.4.3 Structure of compound **4a**

Suitable crystals of compound **4a** were grown by slow evaporation from an ethyl acetate/n-hexane solution.

Tables 20 and 21, contain crystal information, as well as selected bond distances and angles. In the structure of compound **4a**, there is one molecule of hexafluorophosphate anion. The adjacent ortho carbon of the phenyl ring and the three phosphorous atoms of the tridentate phosphine ligand are bonded to the palladium atom.

The palladium atom is in a square-planar coordination geometry bonded to the carbon atom of the phenyl ring and the three phosphorus donor atoms of the triphosphine ligand. The angles at palladium pertaining to the coordinated rings [P(1)-Pd(1)-P(2)] 83.97(3), and [P(2)-Pd(1)-P(3)] 83.48(3), are smaller than 90°, whilst the outer angles are larger [C(2)-Pd(1)-P(1)] 94.63(8) and [C(2)-Pd(1)-P(3)] 97.36(8).



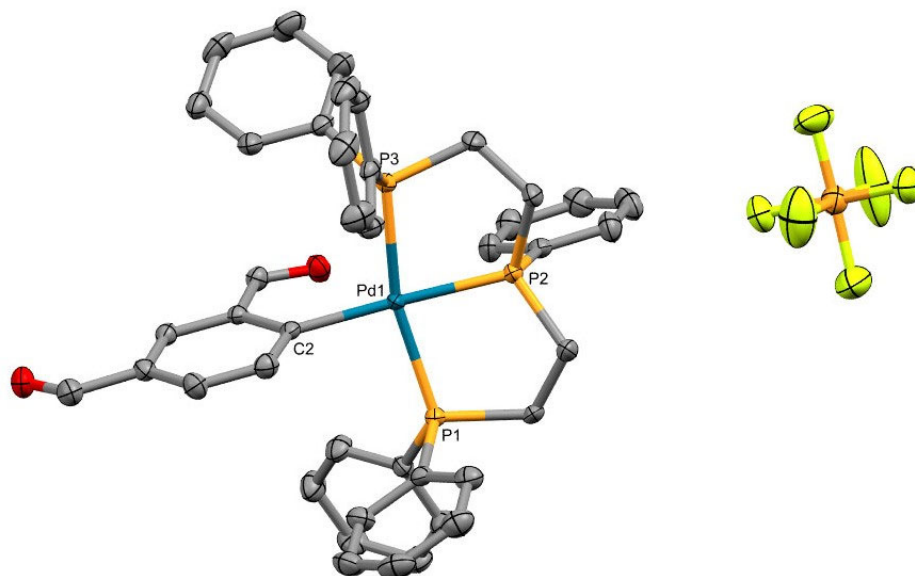


Figure 67. The crystal structure of compound 4a.

Table 20. Complex 4a was obtained from X-ray single-crystal diffraction studies. Bond lengths are given in [Å] and angles in [°].

Pd(1)-C(1)	2.080(3)	C(4)-C(5)	1.391(5)
Pd(1)-P(1)	2.310(8)	C(5)-C(6)	1.381(5)
Pd(1)-P(2)	2.276(1)	C(6)-C(1)	1.398(4)
Pd(1)-P(3)	2.334(8)	C(2)-Pd(1)-P(1)	94.63(8)
C(1)-C(2)	1.430(4)	P(1)-Pd(1)-P(2)	83.97(3)
C(2)-C(3)	1.387(5)	P(2)-Pd(1)-P(3)	83.48(3)
C(3)-C(4)	1.394(4)	C(2)-Pd(1)-P(3)	97.36(8)

Table 21. Crystal data and structure refinement for compound 4a

Molecular formula	C ₄₂ H ₃₈ F ₆ O ₂ P ₄ Pd
Formula weight	919.00
Temperature/K	100.0
Crystal system	monoclinic
Space group	P2 ₁ /n
a/Å	13.1305(4)
b/Å	14.8772(4)
c/Å	20.4043(7)
α /°	90
β /°	102.5510(10)
γ /°	90
Volume/Å ³	3890.6(2)
Z	4
$\rho_{\text{calc}}/\text{cm}^3$	1.569
μ/mm^{-1}	0.707
F(000)	1864.0
Crystal size/mm ³	0.09 × 0.04 × 0.03
Radiation	MoK α (λ = 0.71073)
θ range for data collection/°	4.922 to 52.744
Index ranges	-15 ≤ h ≤ 16, -18 ≤ k ≤ 18, -25 ≤ l ≤ 25
Reflections collected	59817
Independent reflections	7952 [R _{int} = 0.0481, R _{sigma} = 0.0303]
Data/restraints/parameters	7952/0/649
Goodness-of-fit on F ²	1.063
Final R indexes [I ≥ 2 σ (I)]	R ₁ = 0.0403, wR ₂ = 0.0870
Final R indexes [all data]	R ₁ = 0.0497, wR ₂ = 0.0911
Largest diff. peak/hole / e Å ⁻³	1.25/-0.62

6.4.4 Structures of compound **6b**

The structures of the **6b** compound were grown from a slowly evaporating CH_2Cl_2 . Tables 22 and 23 contain crystallographic data as well as selected bond lengths and angles. Discrete dinuclear molecules are separated by normal van der Waals distances in the crystal structure. The created crystal generated four crystal structures with unique distinct molecules per asymmetric unit, corresponding to two distinct conformers, due to the rotation of the formyl group. The bond lengths and angles, however, are within predicted limits.

A phenyl ring ortho carbon, a $\text{C}=\text{N}$ nitrogen atom, and two oxygen atoms from the 2,4-pentanedionate group make up the coordination sphere around the palladium atom. In the coordination sphere, the angles between adjacent atoms are close to the expected value of 90° , $90.99(4)$, $91.67(3)$, $95.11(5)^\circ$, with more pronounced distortions in the 'bite' angle $\text{C}(1)\text{-Pd}(1)\text{-N}(4)$ $82.23(6)^\circ$ as a result of chelation. Palladium has a sum of angles of 360° .

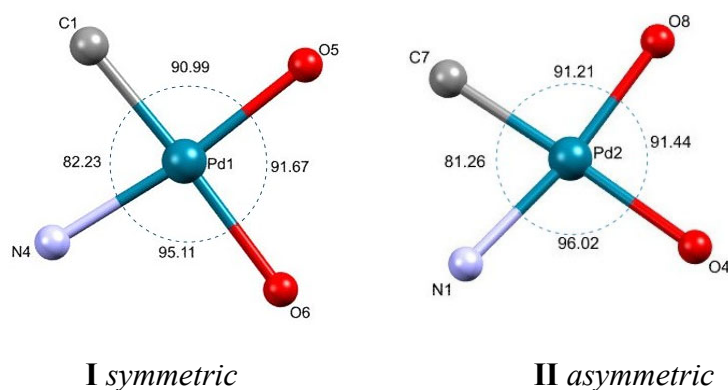


Figure 68. The bonds angles of symmetric and asymmetric conformers of compound **6b**.

The Pd(1)-C(1) bond length, 1.943(12) Å. The Pd1-N4 bond length is 2.015(11) Å. The Pd-O distances [Pd(1)-O(5) 2.011(7) and Pd(1)-O(6) 2.093(8) Å] are within the range of values expected for Pd-O single bonds. The lengthening of the Pd-O distances trans to carbon indicated that the phenyl carbon has a stronger trans influence than the imine nitrogen atom.

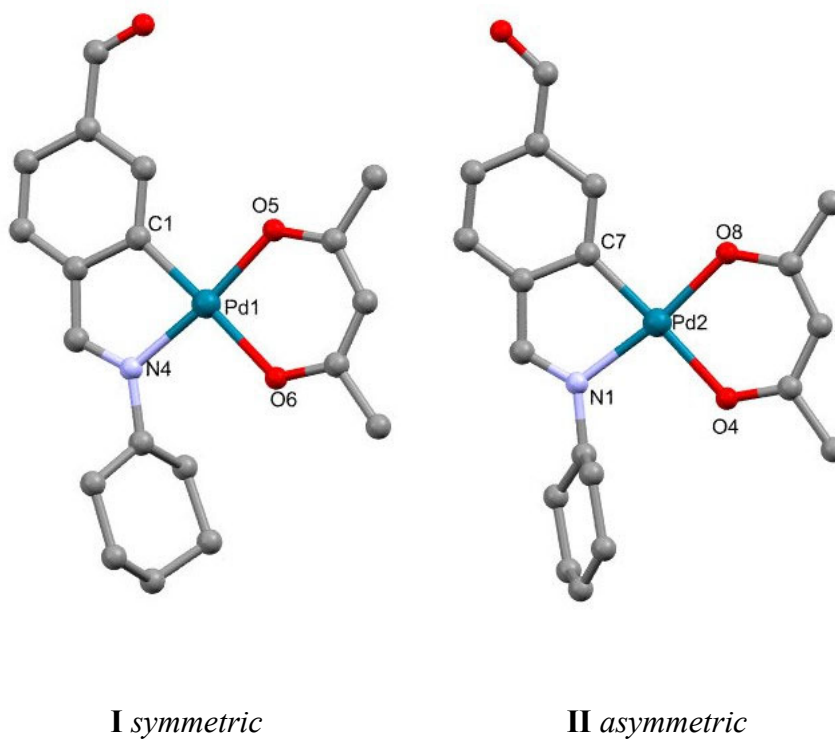


Figure 69. The symmetric and asymmetric conformers of compound 6b.

Table 22. Symmetric conformer 6b was obtained from X-ray single-crystal diffraction studies. Bond lengths are given in [Å] and angles in [°].

Pd(1)-C(1)	1.943(12)	N(2)-Pd(4)	2.018(7)
Pd(1)-N(4)	2.015(11)	Pd(4)-O(9)	2.075(6)
Pd(1)-O(5)	2.011(7)	C(1)-Pd(1)-N(4)	82.23(6)
Pd(1)-O(6)	2.093(8)	C(1)-C(2)-C(3)	113.37(13)
C(1)-C(2)	1.436(18)	O(5)-Pd(1)-N(4)	173.10(5)
C(2)-C(3)	1.406(2)	O(5)-Pd(1)-O(6)	91.67(3)
C(3)-N(4)	1.284(2)	C(2)-C(1)-Pd(1)	112.32(10)
C(43)-C(22)	1.437(15)	C(5)-Pd(3)-N(36)	82.05(4)
C(22)-N(36)	1.294(12)	C(5)-C(43)-C(22)	114.02(9)
N(36)-Pd(3)	2.010(7)	N(36)-Pd(3)-O(1)	93.2(3)
Pd(3)-O(1)	2.073(7)	O(1)-Pd(3)-O(2)	92.29(3)
Pd(3)-O(2)	2.029(6)	O(2)-Pd(3)-C(5)	92.39(3)
Pd(4)-C(37)	1.975(9)	C(37)-Pd(4)-N(2)	81.64(3)
C(37)-C(12)	1.409(12)	N(2)-Pd(4)-O(9)	93.59(3)
C(12)-C(31)	1.444(13)	O(9)-Pd(4)-O(7)	92.62(2)
C(31)-N(2)	1.292(12)	O(7)-Pd(4)-C(37)	92.12(3)
Pd(4)-O(7)	2.016(6)	C(37)-C(12)-C(31)	115.55(8)

Table 23. Asymmetric conformer 6b was obtained from X-ray single-crystal diffraction studies. Bond lengths are given in [Å] and angles in [°].

Pd(2)-C(7)	1.966(10)	Pd(2)-O(8)	2.000(9)
C(7)-C(1M)	1.435(15)	C(7)-Pd(2)-N(1)	81.25(4)
C(1M)-C(18)	1.436(16)	C(7)-C(1M)-C(18)	112.00(11)
C(18)-N(1)	1.282(16)	O(2)-Pd(2)-N(1)	96.02(4)
N(1)-Pd(2)	2.035(12)	O(4)-Pd(2)-O(8)	91.40(4)
Pd(2)-O(4)	2.079(8)	O(8)-Pd(2)-C(7)	91.25(4)

Table 24. Crystal data and structure refinement for 6b.

Molecular formula	C ₁₉ H ₂₃ NO ₃ Pd
Formula weight	419.78
Temperature/K	100.0
Crystal system	triclinic
Space group	P-1
a/Å	11.7133(8)
b/Å	12.6652(8)
c/Å	25.1058(16)
α/°	99.442(2)
β/°	103.334(2)
γ/°	91.289(2)
Volume/Å ³	3567.9(4)
Z	4
ρ _{calc} /cm ³	1.562
μ/mm ⁻¹	1.056
F(000)	1710.0
Crystal size/mm ³	0.13 × 0.09 × 0.02
Radiation	MoKα (λ = 0.71073)
θ range for data collection/°	3.932 to 52.742
Index ranges	-14 ≤ h ≤ 14, -15 ≤ k ≤ 15, -31 ≤ l ≤ 31
Reflections collected	114555
Independent reflections	14579 [R _{int} = 0.0530, R _{sigma} = 0.0347]
Data/restraints/parameters	14579/0/882
Goodness-of-fit on F ²	1.256
Final R indexes [I ≥ 2σ (I)]	R ₁ = 0.0941, wR ₂ = 0.1959
Final R indexes [all data]	R ₁ = 0.1027, wR ₂ = 0.1994
Largest diff. peak/hole / e Å ⁻³	3.40/-2.62

6.4.5 Structures of compound 7b

A suitable crystal of compound 7b was grown by slowly evaporating a CH₂Cl₂/n-hexane. The crystal structure 7b contains a mononuclear molecule and hexafluorophosphate anion. A nitrogen atom from the imine group, an ortho carbon atom from the phenyl ring (C1), and two phosphorus atoms from chelating dppm make up the coordination sphere surrounding the palladium atom.

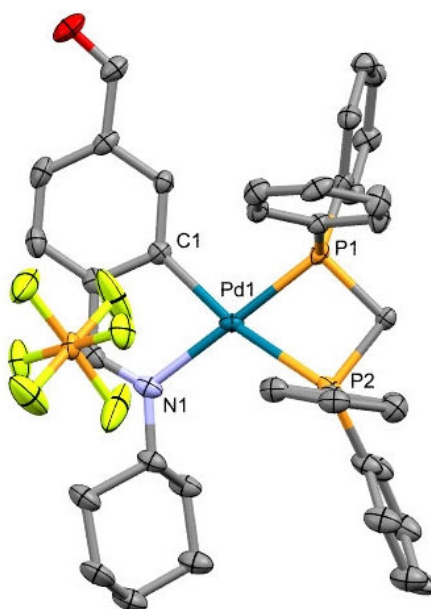


Figure 70. The crystal structure of compound 7b.

At palladium, the sum of angles are approximately 360°, with the distortions being more visible in the slightly reduced "bite" angles C(1)-Pd(1)-N(1) due to chelation 81.02 (16). The Pd(1)-N(1) bond length is around 2.097(4) Å, indicating the trans influence of the phosphorus atom. The length of the Pd(1)-C(1) bond, is 2.02 Å. The Pd-P distance trans to carbon, Pd(1)-P(1), and trans to nitrogen,

Pd(1)–P(2), shows the different impact of the phenyl carbon and imine nitrogen atoms [2.248(11) vs 2.463(13)]. As seen in Figure 71, the C8···H24–C24_{aryl} and O1···H–C intermolecular interaction hydrogen bonding results in weak interactions between adjacent molecules. The crystal structure 7b are connected by weak interaction C8···H24; 2.874 Å, C8–C24; 3.191 Å, O1···H27A; 2.298 Å and O1···H29; 2.658 Å resulting in an extended bifurcated hydrogen bond along the crystallographic direction.

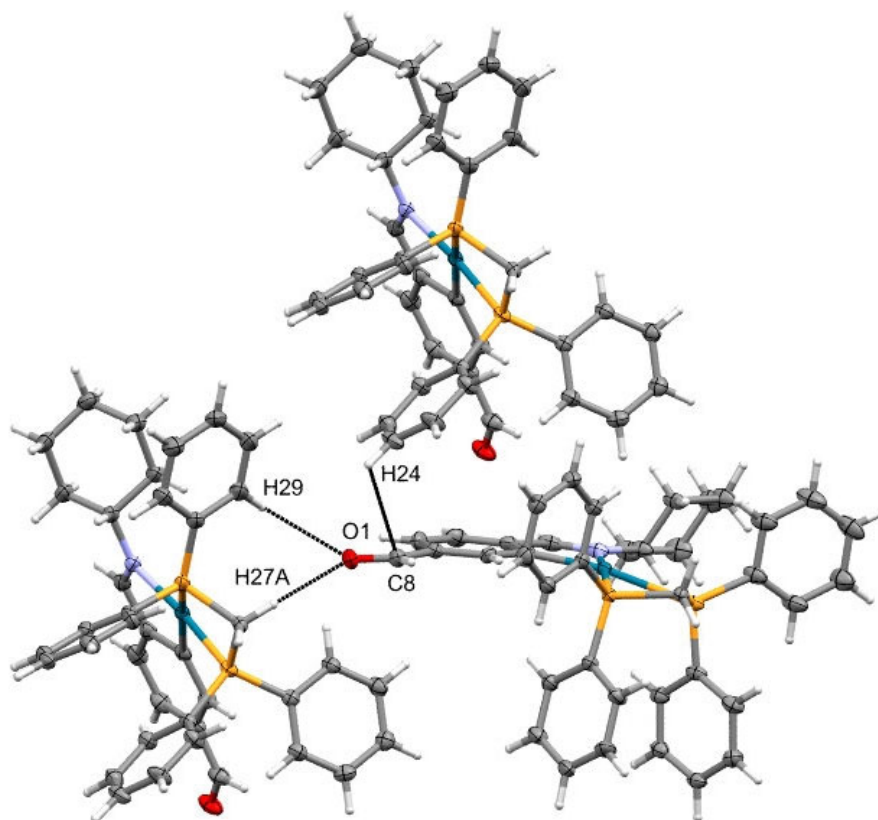


Figure 71. Intermolecular interaction (C–H···C_{aryl}) and (C–H···O) of compound 7b.

Table 25. Compound 7b was obtained from X-ray single-crystal diffraction studies. Bond lengths are given in [Å] and angles in [°].

Pd(1)-N(1)	2.097(4)	C(1)-Pd(1)-N(1)	81.02(16)
Pd(1)-C(1)	2.025(4)	P(1)-Pd(1)-N(1)	175.10(10)
Pd(1)-P(1)	2.248(11)	N(1)-Pd(1)-P(2)	109.25(11)
Pd(1)-P(2)	2.463(13)	P(1)-Pd(1)-C(1)	98.97(12)
P(1)-Pd(1)-P(2)	70.15(4)	C(1)-Pd(1)-P(2)	167.36(12)

Table 26. C-H \cdots C_{aryl} and C-H \cdots O interactions (Å, °) of compound 3j.

C-H \cdots C _{aryl}	C-H	H \cdots C _{aryl}	C-C _{aryl}	\angle (C-H \cdots C _{aryl}) [°]
C8-H18-C24	0.95	2.874	3.191	100.78
C-H \cdots O1	C-H	H \cdots O	C-O	\angle (C-H \cdots O) [°]
C27-H27A-O1	0.99	2.298	3.337	128.91
C29-H29-O1	0.95	2.658	3.288	178.46

Symmetry operation # 0.5 + x, 1.5 - y, -0.5 + z.

Table 27. Crystal data and structure refinement for 7b.

Molecular formula	C ₃₉ H ₃₈ F ₆ NOP ₃ Pd
Formula weight	850.01
Temperature/K	100.00
Crystal system	monoclinic
Space group	P2 ₁ /n
a/Å	10.0932(6)
b/Å	33.4658(18)
c/Å	11.4492(6)
α/°	90
β/°	110.580(2)
γ/°	90
Volume/Å ³	3620.5(3)
Z	4
ρ _{calc} /cm ³	1.559
μ/mm ⁻¹	0.710
F(000)	1728.0
Crystal size/mm ³	0.9 × 0.07 × 0.04
Radiation	MoKα (λ = 0.71073)
θ range for data collection/°	4.48 to 56.554
Index ranges	-13 ≤ h ≤ 13, -44 ≤ k ≤ 44, -15 ≤ l ≤ 15
Reflections collected	149704
Independent reflections	8997 [R _{int} = 0.0551, R _{sigma} = 0.0214]
Data/restraints/parameters	8997/0/461
Goodness-of-fit on F ²	1.194
Final R indexes [I >= 2σ (I)]	R ₁ = 0.0595, wR ₂ = 0.1224
Final R indexes [all data]	R ₁ = 0.0661, wR ₂ = 0.1256
Largest diff. peak/hole / e Å ⁻³	2.50/-1.83

CHAPTER 7

**Cyclopalladated compounds derived from Schiff base
imines.**

7.1 Introduction

This chapter deals with the preparation of palladacycles derived from Schiff base ligands by treatment of the latter with palladium(II) acetate. After C-H bond activation the corresponding ligand is bonded to the metal center in a bidentate [C, N] fashion. As seen in Figure 72, the effect of various substituents next to the carbon atom where metallation is possible only one ortho C-H bond is present in the simplest example (i) but when there are many metallation sites on the ligand, the issue of regioselectivity arises.^{124, 125}

Methoxy groups at the C3 and C5 atoms prevent palladium(II) metallation at the C2 and C6 atoms (ii); with only one methoxy group in the C3 position, the C6 carbon is selectively metallated (iii); and the less sterically demanding methyl group at the position C3 allows palladium(II) attack at the C2 atom (iv). Varied cyclic substituents had different directing effects depending on the size of the substituent ring; benzodioxane derivatives exclusively gave the ortho metallation reaction at the C6 atom (v), whereas piperonal derivatives gave a mixture of the two potential isomers (vi). As a result, cyclopalladation reactions of diverse methoxy group substituted Schiff base ligands produced from [C, N] ligands have piqued our interest. We were able to synthesize a variety of Schiff bases ligands, which have been successfully applied to organic synthesis and catalysis.

¹²⁴ J.M. Vila, M.T. Pereira, E. Gayoso, M. Gayoso, *Transition Metal Chemistry*, 11 (1986) 342-346.

¹²⁵ J.M. Vila, M.T. Pereira, E. Gayoso, M. Gayoso, *Polyhedron*, 6 (1987) 1003.

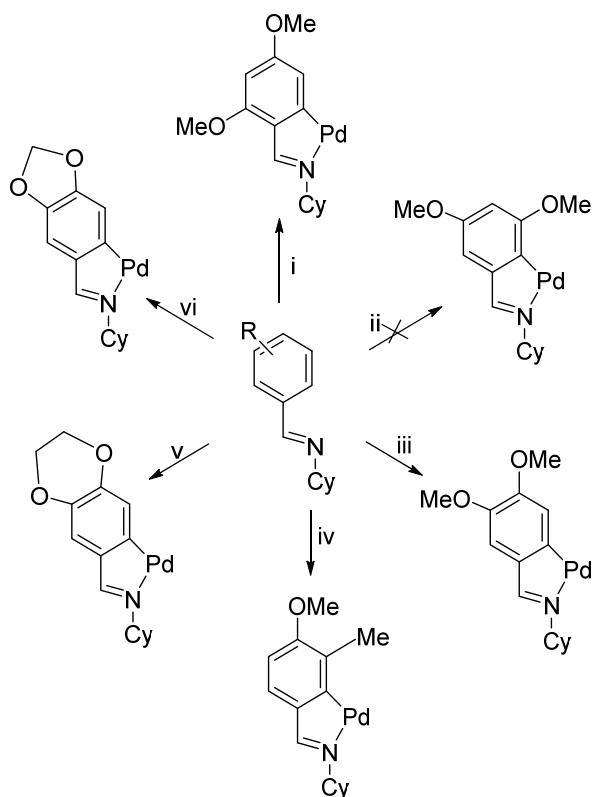


Figure 72. Possibility of metallation

On the other hand, ligands containing mono or diphosphine atoms play an important and growing role in coordination and organometallic chemistry, owing to their broad range of steric and electronic properties that make them suitable for a wide range of applications, such as their use in catalytic processes or their ability to stabilize different oxidation states, as well as to form homo and hetero polymetallic complexes.¹²⁶ Therefore, the ensuing cyclopalladated complexes were then treated with phosphine nucleophiles to give the compounds with the phosphorus ligand bonded to the metal atom.

7.1.1 Synthesis of the Schiff base ligands **c-j**.

In a 100 mL round bottom flask an appropriate substituted benzaldehyde (0.5 g), and cyclohexylamine were added in chloroform (40 cm³) using modified Dean-Stark apparatus. The resulting mixture was stirred under reflux for 8 hours. After that, the solvent was eliminated and the product dried under vacuum.

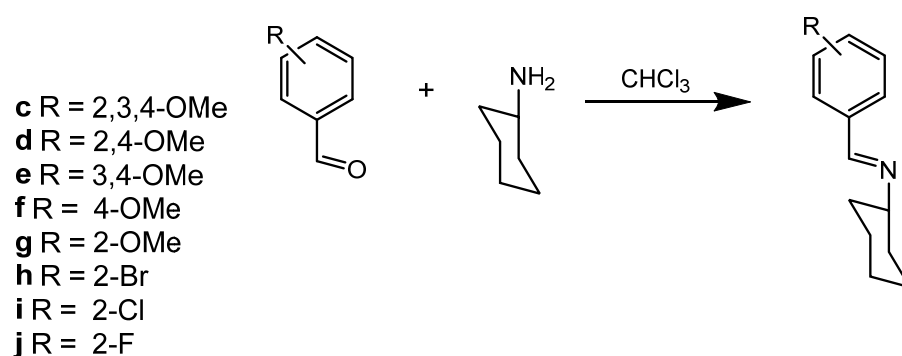


Table 28. Quantities of materials used in ligand synthesis.

ligand	aldehyde's		cyclohexylamine	
	g	mmol	g	mmol
c	0.5	2.54	0.25	2.54
d	0.5	3.00	0.29	3.00
e	0.5	3.00	0.29	3.00
f	0.5	3.67	0.36	3.67
g	0.5	3.67	0.36	3.67
h	0.5	2.70	0.26	2.70
i	0.5	3.55	0.35	3.55
j	0.5	4.02	0.39	4.02

7.1.2 Synthesis of compounds with acetate-bridged **1c-1j**.

These reactions were carried out under Argon. Although the final products are air-stable, it has been found that reaction intermediates could be air-sensitive.

In a 100 mL Schlenk flask, 0.1 g (0.44 mmol) Pd(OAc)₂, and the corresponding amount of ligand (in 1:1 molar ratio) was added to 40 cm³ of toluene and heated for 3 hours at 65 °C. After cooling to room temperature, the solution was filtered to remove the small amount of black palladium that had formed. Under vacuum, the solvent was removed, and the product was recrystallized from CH₂Cl₂/n-hexane, washed with cold ethanol, and filtered to yield the desired compound.

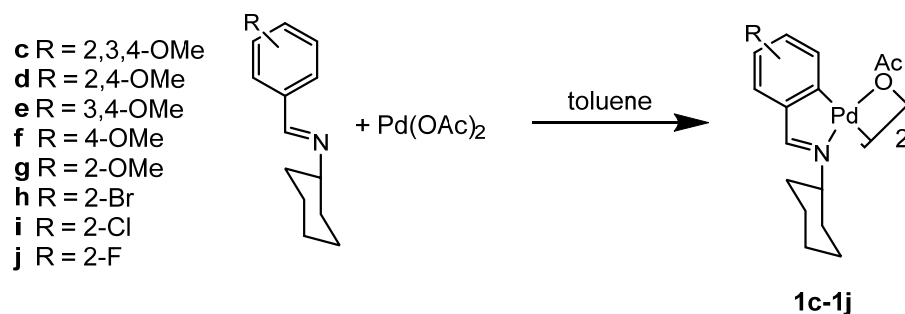


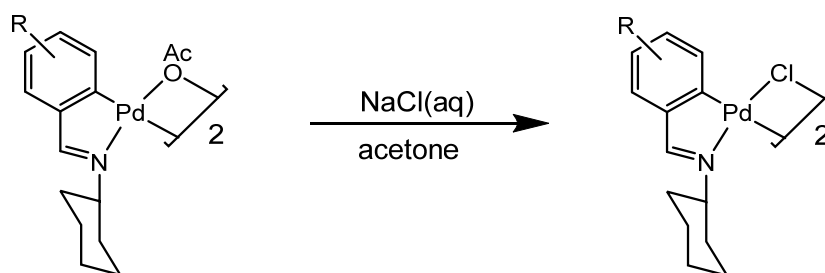
Table 29. Quantities of materials used in cyclometallated synthesis having acetate ligands.

compound	Pd(OAc) ₂		ligand	
	g	mmol	g	mmol
1c	0.1	0.44	0.12	0.44
1d	0.1	0.44	0.11	0.44

1e	0.1	0.44	0.11	0.44
1f	0.1	0.44	0.09	0.44
1g	0.1	0.44	0.09	0.44
1h	0.1	0.44	0.11	0.44
1i	0.1	0.44	0.09	0.44
1j	0.1	0.44	0.09	0.44

7.1.3 Synthesis of compounds with chloride-bridge **2c-2j**

An aqueous solution of sodium chloride (0.05 M, *ca.* 25 cm³) was added dropwise to a solution of compounds **2c-2j** in acetone (*ca.* 15 cm³). After stirring for 2 h, a pale yellow solid precipitated, which was filtered off, washed with H₂O, and dried under vacuum.



- 1c** R = 2,3,4-OMe
1d R = 2,4-OMe
1e R = 3,4-OMe
1f R = 4-OMe
1g R = 2-OMe
1h R = 2-Br
1i R = 2-Cl
1j R = 2-F

2c-2j

7.1.4 Synthesis of compounds with triphenylphosphine ligand **3c-3j**

In a 50 mL Schlenk flask, compound **2c-2j** was added in acetone (10 cm³). The appropriate amount of triphenylphosphine (in a 1:2 molar ratio) was added, and the mixture was stirred at room temperature for 3 hours. The solution was evaporated to low volume, and the resulting solid was recrystallized from CH₂Cl₂/n-hexane and dried under vacuum.

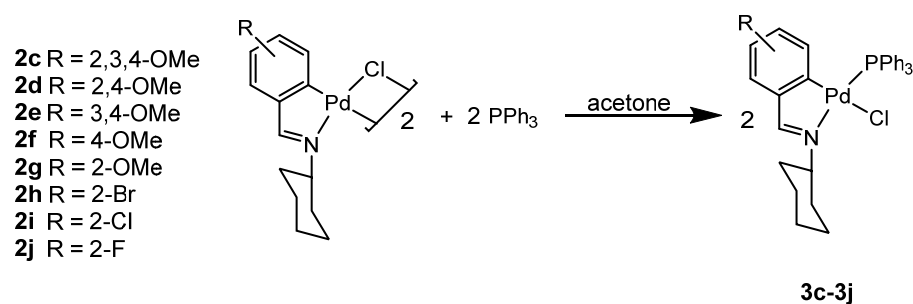


Table 30. Quantities of materials used to prepare cyclometallated compounds with triphenylphosphine ligand.

	compound		triphenylphosphine ligand	
	g	mmol	g	mmol
2c	0.025	0.029	0.015	0.059
2d	0.025	0.032	0.016	0.064
2e	0.025	0.032	0.016	0.064
2f	0.025	0.034	0.018	0.069
2g	0.025	0.034	0.018	0.069
2h	0.025	0.030	0.016	0.061
2i	0.025	0.034	0.018	0.068
2j	0.025	0.036	0.018	0.072

7.1.5 Synthesis of compounds with chelating dppm **4c-4j**

In a 50 mL Schlenk flask, compound (**2c-2j**) was added to acetone (10 cm³). The appropriate amounts of dppm and NH₄PF₆ were added, and the mixture was stirred for 3 hours at room temperature. Then, the NH₄Cl was precipitated by centrifuging, the solvent was evaporated to dryness, and the resulting residue was recrystallized from CH₂Cl₂/n-hexane and dried under vacuum.

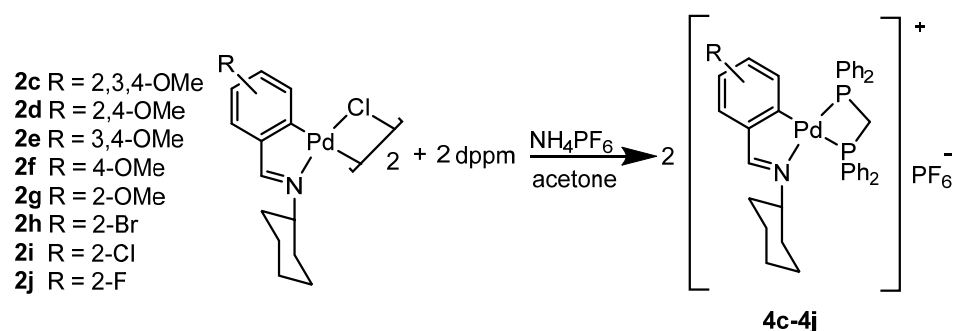


Table 31. Quantities of materials used to prepare cyclometallated compounds with dppm ligand.

	compound		dppm ligand		NH ₄ PF ₆	
	g	mmol	g	mmol	g	mmol
2c	0.03	0.035	0.027	0.070	0.0114	0.070
2d	0.03	0.038	0.029	0.077	0.0125	0.077
2e	0.03	0.038	0.029	0.077	0.0125	0.077
2f	0.03	0.041	0.032	0.083	0.0136	0.083
2g	0.03	0.041	0.032	0.083	0.0136	0.083
2h	0.03	0.036	0.028	0.073	0.0120	0.073
2i	0.03	0.041	0.031	0.0827	0.0134	0.0827
2j	0.03	0.048	0.037	0.097	0.0158	0.097

7.1.6 Synthesis and Michael Additions to vinylidene diphosphine complexes of $[M(CO)_4\{(PPh_2P)_2C=CH_2\}]$ ($M = Mo, W$).

7.1.6.1 Preparation of $M(CO)_4[Ph_2PCH(CH_2-NH-(CH_2)_2PPh_2)PPh_2]-P, P]$ ($M = Mo, W$).

The starting tetracarbonyl metalloligands-*P* were prepared by a Michael addition reaction of the aminophosphine ligand to the tetracarbonyl metal complex thus, 2-(diphenylphosphine)ethylamine (0.05g, 0.218 mmol) and $[M(CO)_4vdpp]$ (Mo , 0.13 g, 0.218 mmol; W , 0.15 g, 0.218 mmol) were added together in dry THF under argon, and the resulting mixture was stirred at 68 °C for 9 hours. Then, the solvent was removed to give an oily yellow and an oily orange residue in good yields which were dried under vacuum.

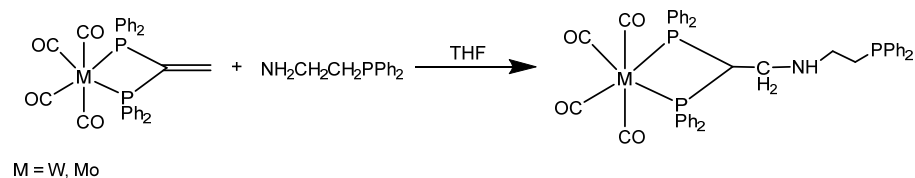


Table 32. Quantities of materials used to synthesize $M(CO)_4vdpp$ with aminophosphine ligand.

	$M(CO)_4vdpp$		aminophosphine	
	g	mmol	g	mmol
$W(CO)_4vdpp$	0.15	0.218	0.05	0.218
$Mo(CO)_4vdpp$	0.13	0.218	0.05	0.218

7.1.6.2 Synthesis of compounds **5c-5j** and **6c-6g**

In a 50 mL Schlenk flask, compound **2c-2j** was dissolved in acetone (10 cm³). The appropriate amounts of NH₄PF₆ were added in appropriate amounts, and the mixture was agitated at room temperature for 4 hours. Following that, the NH₄Cl salt was then precipitated by a centrifuge tube and the solvent was then evaporated to dryness and recrystallized from CH₂Cl₂/n-hexane and dried under vacuum.

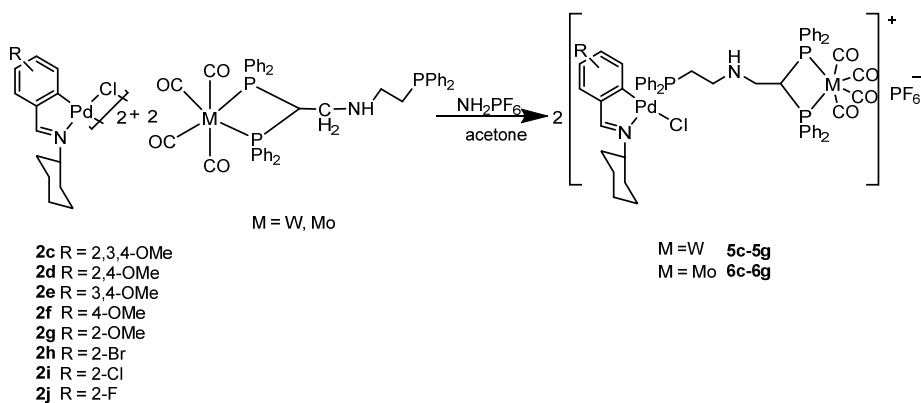


Table 33. Quantities of materials used to prepare cyclometallated compound with W(CO)₄(Ph₂PC(=CH₂)PPh₂)-P, P).

compound	W(CO) ₄ (Ph ₂ PC(=CH ₂)PPh ₂)-P, P)		NH ₄ PF ₆			
	g	mmol	g	mmol		
2c	0.01	0.011	0.022	0.024	0.004	0.024
2d	0.01	0.012	0.023	0.025	0.004	0.025
2e	0.01	0.012	0.023	0.025	0.004	0.025
2f	0.01	0.013	0.025	0.028	0.004	0.028
2g	0.01	0.013	0.025	0.028	0.004	0.028

Table 34. Quantities of materials used to prepare cyclometallated compound with $\text{Mo}(\text{CO})_4(\text{Ph}_2\text{PC}(\text{=CH}_2)\text{PPh}_2)\text{-P, P}$.

compound	$\text{Mo}(\text{CO})_4(\text{Ph}_2\text{PC}(\text{=CH}_2)\text{PPh}_2)\text{-P, P}$		NH_4PF_6			
	g	mmol	g	mmol		
2c	0.01	0.011	0.020	0.024	0.003	0.024
2e	0.01	0.012	0.020	0.025	0.004	0.025
2f	0.01	0.014	0.023	0.027	0.004	0.027
2g	0.01	0.014	0.023	0.027	0.004	0.027

7.1.7 Synthesis of compounds with bridging dppm **7e** and **7f**.

In a 50 mL Schlenk flask, compound **7e** or **7f** was added to acetone (10 cm^3). The appropriate amounts of dppm and NH_4PF_6 were added in a molar ratio (1:1), and the mixture was agitated for 4 hours at room temperature. The NH_4Cl was then separated by centrifugation, the solvent was evaporated to dryness, and the resultant residue was recrystallized from $\text{CH}_2\text{Cl}_2/\text{n-hexane}$ and dried under vacuum.

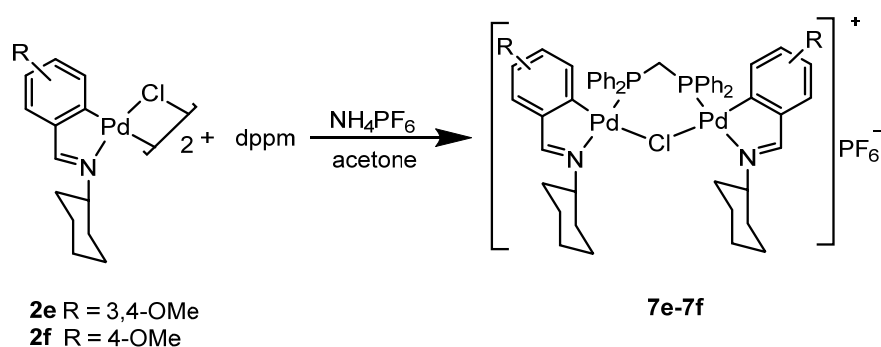
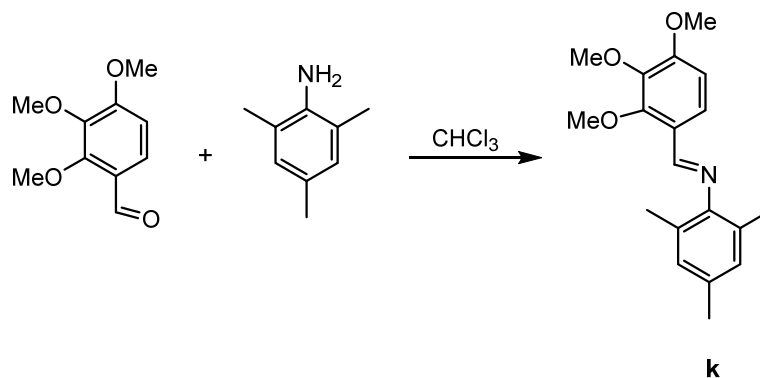


Table 35. Quantities of materials used to prepare cyclometallated compounds with dppm ligand in a molar ratio (1:1).

	compound		dppm ligand		NH ₄ PF ₆	
	g	mmol	g	mmol	g	mmol
2e	0.01	0.012	0.004	0.012	0.0020	0.0128
2f	0.01	0.0130	0.005	0.0130	0.0021	0.0130

7.1.8 Synthesis of ligand **k**.

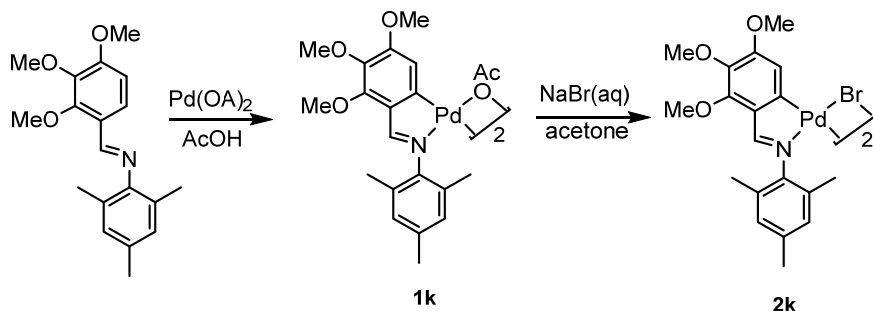
In a 100 mL round bottom flask, 2,3,4-methoxybenzaldehyde (0.3 gm, 1.529 mmol) and 2,4,6-methylaniline (0.2 g, 1.529 mmol), 40 cm³ of CHCl₃ were added. In a Dean-Stark apparatus, the mixture was heated under reflux for 8 hours. The solvent was evaporated and dried under vacuum.



7.1.9 Synthesis of compounds **1k** and **2k**.

(0.14g, 0.445 mmol) ligand **k** and (0.1 g, 0.445 mmol) of Pd(OAc)₂ were added to a Schlenk flask. It is purged with argon for five minutes, then 25 cm³ of glacial acetic acid was added, the mixture was stirred for 4 hours at 65 °C. The resulting orange solid was observed,

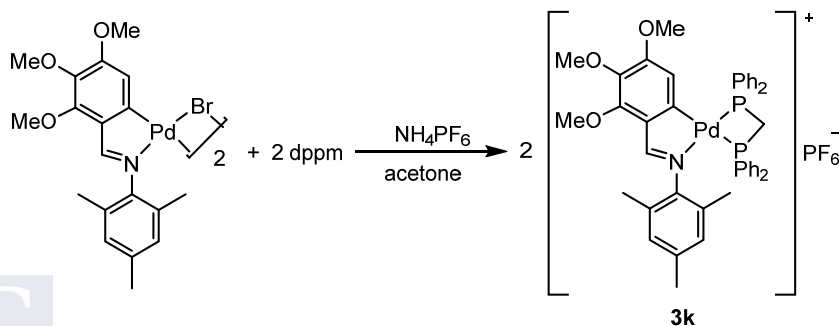
which was then filtered and extracted with dichloromethane and water.



Compound 1k was converted to compound 2k by dissolving (0.1g) in 10 cm³ acetone, then adding 10 cm³ (0.05 M) NaBr solution and stirring for 2 hours. The precipitated solid was filtered, water-washed, and vacuum-dried.

7.1.10 Synthesis of the compound with chelating dppm **3k**.

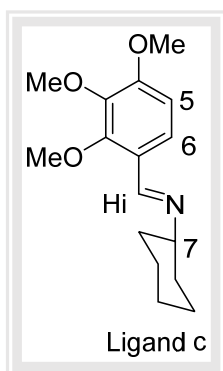
In a 50 mL Schlenk flask, compound 2k (0.025 g, 0.025 mmol) was introduced to acetone (10 cm³). The dppm (0.01, 0.05 mmol) and (0.008 g, 0.05 mmol) NH₄PF₆ were added to the mixture, which was then agitated at room temperature for 3 hours. The resulting orange precipitate was filtered, dried in a vacuum, and recrystallized from dichloromethane/n-hexane.



7.2 NMR study

7.2.1 Study of NMR Schiff bases ligands **c-j**

Schiff base ligands, also known as imines, are readily prepared by treatment of electrophilic carbonyl compounds such as aldehydes, and nucleophilic species, namely primary amines. Enhancement of both electronic aspects results in quite stable compounds. The reaction is favored by acid catalysis and water removal from the reaction medium. Aromatic aldehydes, in contrast to aliphatic aldehydes, form a more stable Schiff base due to efficient conjugation.¹²⁷



The good solubility of the ligands ensures the correct assignment of the signals. The spectra were recorded in CDCl₃. A singlet signal at 8.58 ppm was ascribed to the HC=N resonance. Two doublets at 6.7 and 7.7 ppm were assigned to the AB spin system for the H5 and H6 protons, respectively. Three singlets *ca.* 3.94-3.89 were for the three methoxy groups. The methylene resonances of the cyclohexylamine moiety were the proton resonances of the cyclohexylamine group were *ca.* 1.8-1.2 ppm and the multiplet at 3.18 ppm was assigned to the H7 proton. The assignment of the ¹H NMR resonances for the remaining Schiff base compounds was carried out accordingly in data addition.

¹²⁷ N.K. Bhattacharyya, D. Dutta, J. Biswas, *Indian Journal of Chemistry-Section B (IJC-B)*, 60 (2021) 1478-1489.

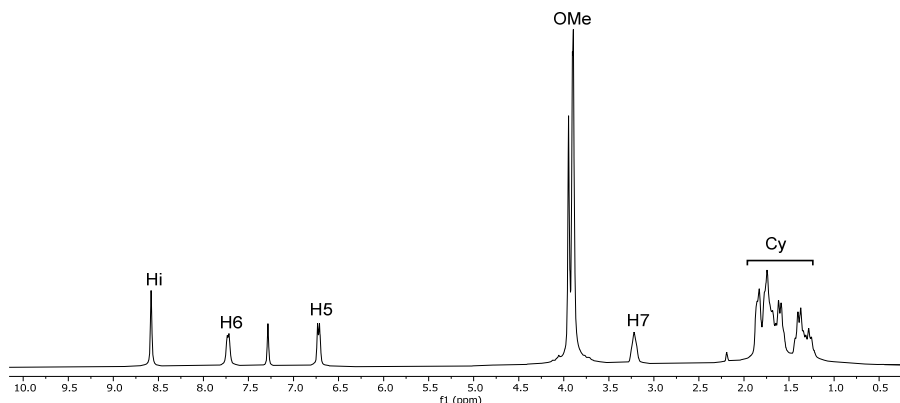
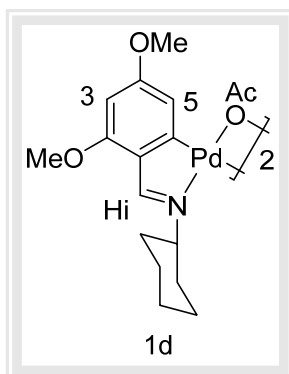


Figure 73. ^1H NMR of compound **c** in CDCl_3 .

7.2.2 Study of compounds **1c-1j**

The ^1H NMR spectra of compounds **1c-1j** were recorded in CDCl_3 .



The spectra of compound **1d** showed the singlet signals at 7.6, 6.20, and 6.0 ppm assigned to the $\text{HC}=\text{N}$, H3, and H5 protons, respectively, and as expected, the absence of the H6 resonance in agreement with ligand metalation at the C6 carbon atom. For compound **1c**, the H5 and Hi protons observed

a singlet at 6.3 and 7.57 ppm, respectively. There was no resonance signal for H6. As predicted, the signal for the H6 nucleus was eliminated after metallation at C6. In the case of ligand **e** derivatives, the electrophilic attack of the palladium atom occurs at any of the two potential metallation sites, the C2 and C6 atoms, which are affected by both electronic and steric factors,¹²⁸ and a mixture of isomers could result. However, in toluene, the reaction between ligand **e** and

¹²⁸ G.W. Parshall, *Accounts of Chemical Research*, 3 (1970) 139-144.

Pd(OAc)₂ gave only one product, which was that obtained from C–H activation at the C6 position, and no product with the metal linked to the C2 atom was observed. Thus, two singlet signals at 6.7 and 6.5 ppm were assigned to the H2 and H5 protons, respectively. The proton was detected as a singlet at 7.3 ppm was for the HC=N resonance.

In the ¹H NMR spectrum of **1f** the parent spin system in the ligand spectrum, AA'XX', was modified to two doublets at 7.0 and 6.5 ppm, assigned to the H2 and H3 protons (³J(H2H3) = 8.7 Hz), respectively; and singlets at 7.25 and 6.6 ppm assigned to the HC=N and H5 resonances, respectively. The resonances for the remaining acetate-bridged compounds were assigned accordingly, all showing absence of the H6 signal. In all cases, a singlet resonance *ca.* 2.0 ppm was for the two equivalent methyl acetate protons, consistent with a *trans* geometry of the metallated moieties.¹²⁹

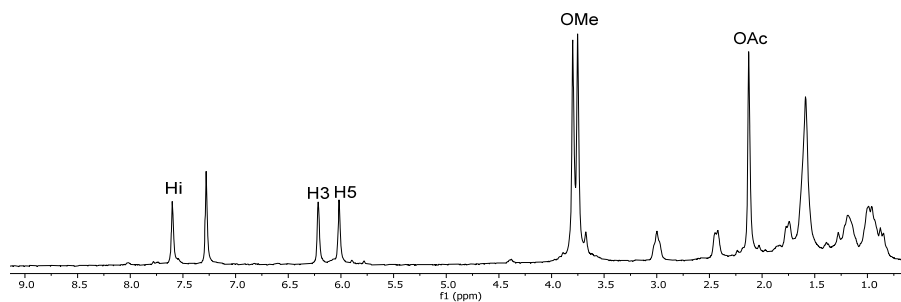
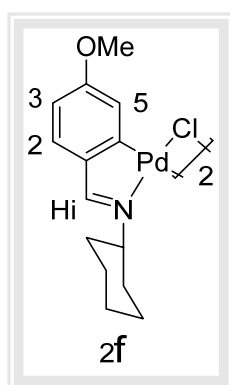


Figure 74. ¹H NMR of compound **1d** in CDCl₃.

¹²⁹ J. M. Vila, M. Gayoso, M. Pereira, J. Ortigueira, M.L. Torres, *J. Organomet. Chem.*, 547 (1997) 297.

7.2.3 Study of compounds **2c-2j**

The ^1H NMR spectra of compounds **2c-2j** were recorded in CDCl_3 and the signal was quite similar to those for compounds **1c-1j**, with the absence of the methyl acetate resonances.



The ^1H NMR spectra of compound **2f** showed a singlet at 7.74 ppm assigned to the $\text{HC}=\text{N}$ proton; doublets at 7.12 and 6.57 ppm were assigned to the H2 and H3 protons ($^3J(\text{H2H3}) = 8.5$ Hz). A broad singlet at 6.97 ppm was for the H5 proton. The ^1H NMR spectra for compounds **2g-2j** reflect the compound spin system originated by the coupling of the H3, H4, and H5 protons showing the corresponding broad signals, although in some cases, simpler patterns were obtained, such as for compound **2g**, where a broad signal at 6.53 was assigned to H4 and a broad signal at 7.0 ppm, was assigned to H3 and H5 protons. Likewise, the ^1H NMR spectra of compound **2h** showed two doublets at 7.34 ppm [$^3J(\text{H3H4}) = 7.9$ Hz], and 7.17 ppm [$^3J(\text{H5H4}) = 7.8$ Hz] assigned to the H3 and H5 protons, respectively and triplet signal at 6.87 ppm [$^3J(\text{H4H3}) = 7.9$ Hz], was assigned to H4 proton. For compound **2j** the analogous resonances appeared broad singlets at 7.18 ppm and at 7.0 ppm, was for H3 and H5, and at 6.72 ppm, was for H4.

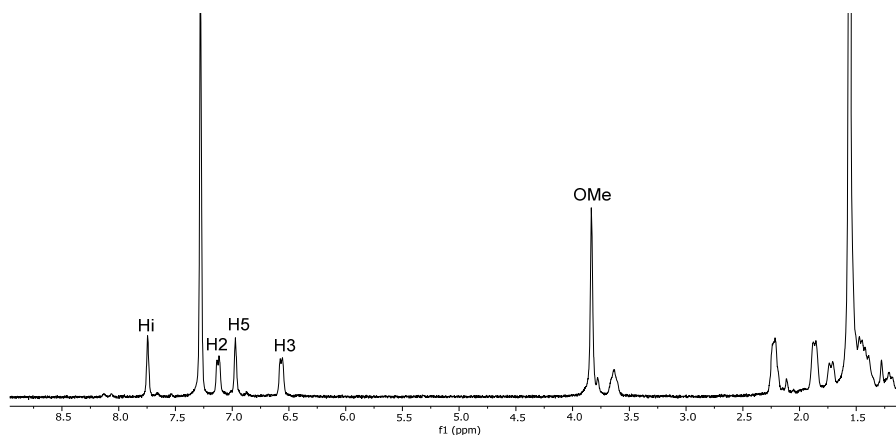
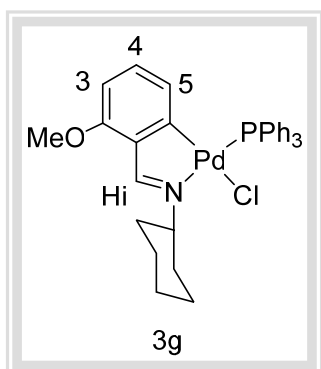


Figure 75. ^1H NMR of compound 2f in CDCl_3 .

7.2.4 Study of compounds **3c-3j**



The ^1H NMR spectra of compounds **3c-3j** were recorded in CDCl_3 and showed signals at similar positions as in the parent dinuclear chloride-bridged compound, with the most noteworthy differences being in the upfield shift of the H5 and C(4)OMe resonances due to shielding from the phosphine phenyl rings. Also, the $\text{HC}=\text{N}$ and H5 signals were split from coupling to the ^{31}P nucleus and were assigned *ca.* 8.62-8.0 and 6.36-5.62 ppm, respectively.¹³⁰ As previously described,¹³¹ this upfield change could be due to a change in the electronic flow from the d8 palladium atom. As an example, in the ^1H NMR spectra of compound

¹³⁰ J.M. Vila, M.T. Pereira, E. Gayoso, M. Gayoso, *Transition Metal Chemistry*, 11 (1986) 342-346.

¹³¹ M.A. Gutierrez, G.R. Newkome, J. Selbin, *Journal of Organometallic Chemistry*, 202 (1980) 341-350.

3g compound, a doublet at 8.59 ppm ($^4J(\text{PHi}) = 8.9$ Hz) was ascribed to the HC=N proton. A triplet at 6.0 ppm ($^4J(\text{H5P}) = 6.9$ Hz) was for the H5, also coupled to the phosphor nuclei. A doublet and a triplet at 6.40 and 6.51 ($^3J(\text{H3H4}) = 8.0$ Hz) ppm, were assigned to the H3 and H4 protons, respectively.

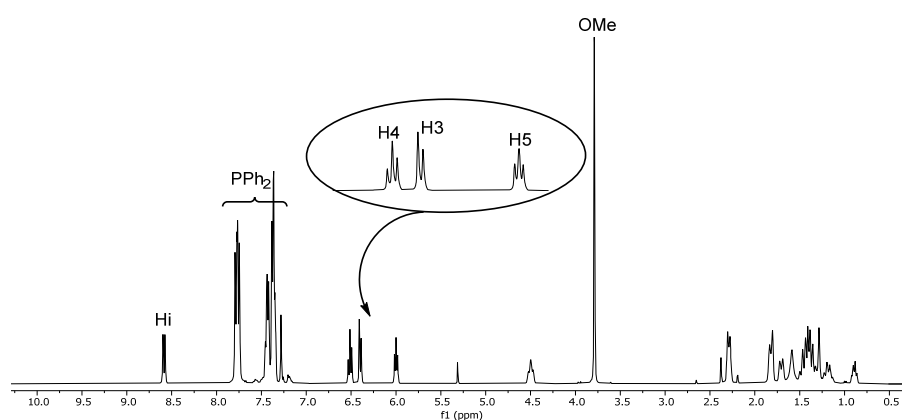


Figure 76. ^1H NMR of compound **3g** in CDCl_3 .

In the $^{31}\text{P}\{-^1\text{H}\}$ NMR spectrum, a singlet was assigned to the ^{31}P nucleus shifted to a lower field *ca.* 43 ppm; this value is in agreement with a phosphorus *trans* to nitrogen arrangement.

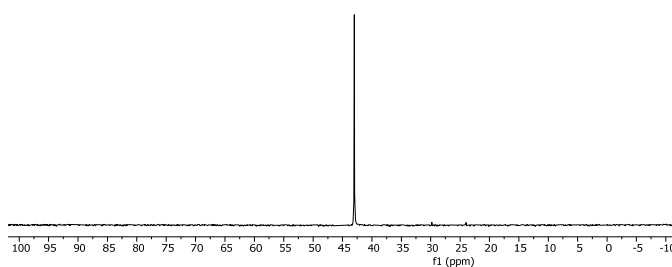
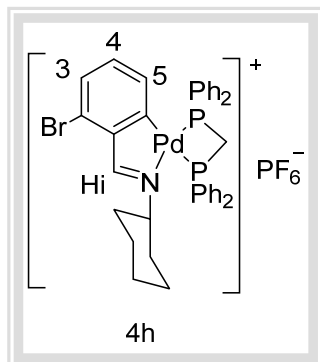


Figure 77. $^{31}\text{P}\{-^1\text{H}\}$ NMR of compound **3g** in CDCl_3 .

7.2.5 Study of compounds **4c-4j** and **3k**



The compounds were obtained as 1:1 electrolytes after reaction of the halide-bridged compounds **2c-2j** with Ph₂PCH₂PPh₂ (dppm) and ammonium hexafluorophosphate. At variance with the compounds **3c-3j**, they are void of any chloride ligand. The ¹H NMR spectra of compounds were recorded in CDCl₃, showed similar chemical shifts and coupling constant values as for compounds **3c-3j** except for H5, which has coupled with two phosphorus atoms. As an example, the spectrum of compound **4h** is described. In the ¹H NMR spectra of compound **4h**, a doublet resonance at 8.76 ppm was assigned to the HC=N (⁴J(PHi) = 5.5 Hz) coupled to the ³¹P nucleus *trans* to nitrogen. A doublet at 6.64 ppm (³J(H5H4) = 7.5 Hz) was assigned to the H5 proton coupled to H4. A doublet and a triplet at 7.22 ppm (³J(H3H4) = ³J(H4H5) = 7.5 Hz) and 6.72 ppm (³J(H4H3) = 7.5 Hz), were assigned to the H3 and H4 protons, respectively.

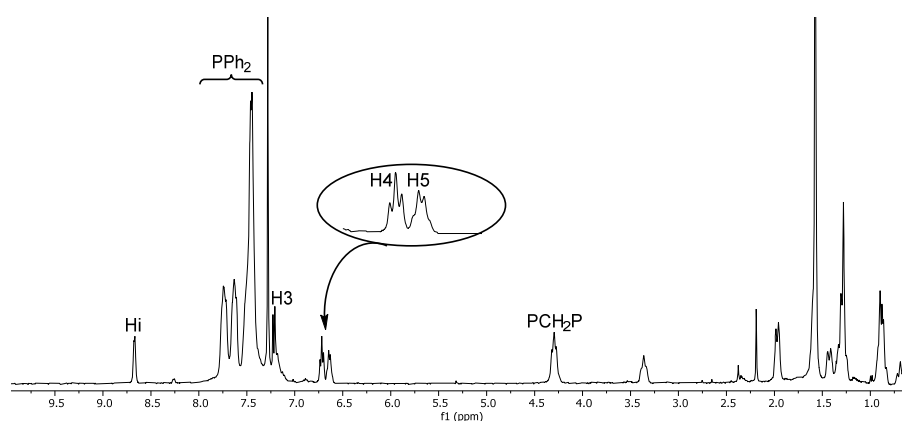
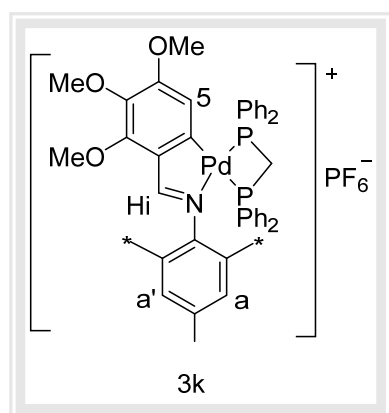


Figure 78. ¹H NMR of compound **4h** in CDCl₃.



In the ^1H NMR spectra of compound **3k**, the $\text{HC}=\text{N}$ proton showed a doublet resonance at 8.20 ppm [$^4J(\text{PHi}) = 7.6$ Hz] is coupled to ^{31}P nucleus trans to nitrogen. The proton H5 observed a doublet of doublets at 6.0 ppm ($^4J(\text{H5P}_{\text{trans}}) = 10.4$ Hz, $^4J(\text{H5P}_{\text{cis}}) = 7.6$ Hz, 1H). The two protons Ha and Ha' showed a singlet at 6.68 ppm. The $\text{OMe}(\text{C4})$ NMR resonance is shifted to a lower frequency, due to the shielding effect of the phosphine phenyl ring. One of the two inequivalent OMe groups would be unaffected by the phosphine's phenyl ring, they would have two separate resonances in an antiparallel configuration. At the high field, a signal at 2.25 ppm (3H) and another at 2.18 ppm (6H) correspond to the methyl groups Me and Me*, which are equivalent.

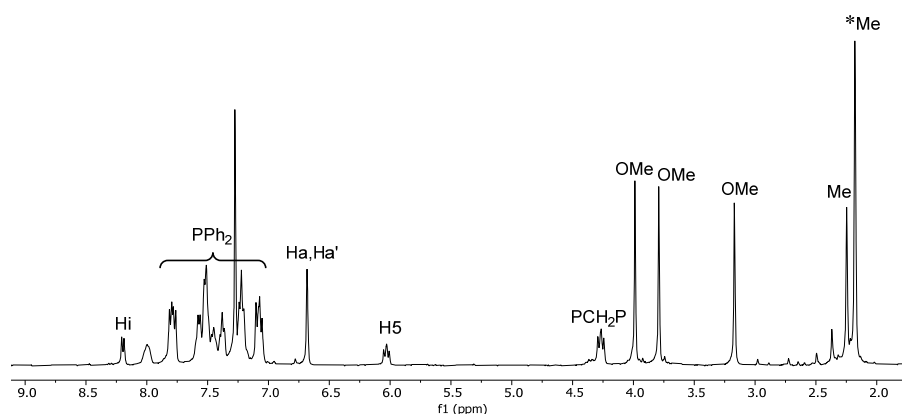


Figure 79. ^1H NMR of compound **3k** in CDCl_3 .

In the $^{31}\text{P}\{-^1\text{H}\}$ NMR spectra two doublets were assigned to the two non-equivalent phosphorus nuclei. The doublets were assigned based on the assumption that a ligand with a higher *trans* influence causes the resonance of the phosphorus atoms *trans* to it to shift to a lower frequency. Moreover, the lower frequency doublet corresponds to the phosphorus nucleus *trans* to the phenyl carbon C(6), while the higher frequency doublet corresponds to the phosphorus nucleus *trans* to the imine nitrogen.

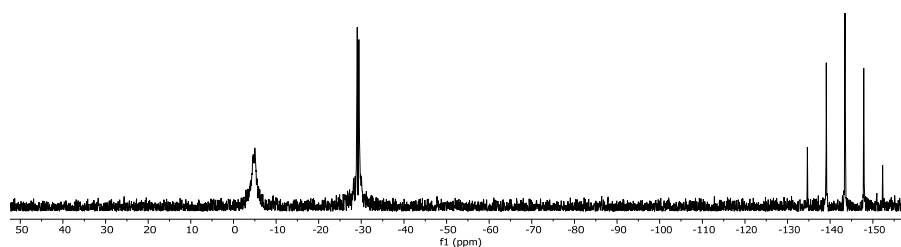


Figure 80. $^{31}\text{P}\{-^1\text{H}\}$ NMR of compound 4h in CDCl_3 .

7.2.6 Cyclopalladated compounds using Michael Additions complexes.

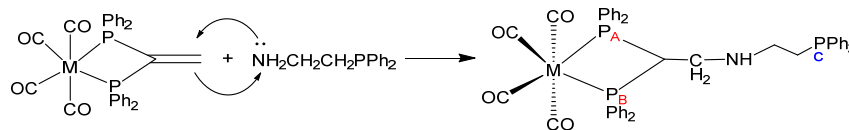
7.2.6.1 Study of $\text{M}(\text{CO})_4[\text{Ph}_2\text{PCH}(\text{CH}_2\text{-NH}-(\text{CH}_2)_2\text{PPh}_2)\text{PPh}_2]\text{-P,P}$ (M = Mo, W).

In organometallic chemistry and catalysis,¹³² metal carbonyl complexes and their phosphine derivatives are essential. Because the catalytic activity is linked to the potential for one ligand to be replaced by another, ligand replacement mechanisms have gotten a lot of

¹³² J. Collman, L. Hegedus, J. Norton, R. Finke, University Science Books: Mill Valley, CA, 94941 (1987) 921-919.

attention.¹³³ Many investigations have focused on CO substitution by various ligands in $M(\text{CO})_6$ ($M = \text{Cr}, \text{Mo}, \text{and W}$).¹³⁴

A variety of amines, hydrazines, or carbon nucleophiles can be added to the vinylidene double bond in $[M(\text{CO})_4(\text{vdpp-PP}')]^{\cdot}$.¹³⁵ Moreover, the ligand 1,1-bis(diphenylphosphino)ethene (vdpp), was of importance in our work because the vinylidene double bond in vdpp provides the opportunity for the preparation of metal ligands by Micheal addition reaction. Furthermore, $M(\text{CO})_4\text{vdpp}$ ($M = \text{Mo or W}$) were coordinated to the nucleophilic of primary amine that also includes one donor atom to give $M(\text{CO})_4[\text{Ph}_2\text{PCH}(\text{CH}_2\text{-NH}(\text{CH}_2)_2\text{PPh}_2)\text{PPh}_2]\text{-P,P}$ ($M = \text{Mo}, \text{W}$).



$M = \text{W}, \text{Mo}$

Scheme 6. The reaction of $M(\text{CO})_4\text{vdpp}$ with aminophosphine ligand.

The $^{31}\text{P}\{-^1\text{H}\}$ NMR spectrum of $\text{W}(\text{CO})_4[\text{Ph}_2\text{PCH}(\text{CH}_2\text{-NH}(\text{CH}_2)_2\text{PPh}_2)\text{PPh}_2]\text{-P,P}$ showed two singlets at -2.0 ppm, which was assigned to phosphorous ($\text{P}_\text{A}+\text{P}_\text{B}$) and its satellite signals. The signals of aminophosphine (P_C) showed at -20.3 and -20.9 ppm. In addition, the signals of oxidized P were observed at 31 and 32 ppm (Figure 81). The ^1H NMR spectrum showed a triplet at 4.9 ppm assigned to the

¹³³ L.M. Pignolet, Springer Science & Business Media, **2013**.

¹³⁴ D. Armitage, G. Wilkinson, by G. Wilkinson, FGA Stone, and EW Abel, Pergamon, New York, 2 (**1982**) 99.

¹³⁵ A.M. Herring, S.H. Koskimies, B.L. Shaw, *Journal of organometallic chemistry*, 338 (**1980**) 13-17.

PCHP proton (${}^2J_{HP} = 8.2$ Hz). The ${}^{31}\text{P}\{-\text{H}\}$ NMR spectrum of the $\text{Mo}(\text{CO})_4[\text{Ph}_2\text{PCH}(\text{CH}_2\text{-NH}-(\text{CH}_2)_2\text{PPh}_2)\text{PPh}_2]\text{-P,P}$ consisted of two singlets at δ 22.0 ppm assigned to the phosphorous ($\text{P}_\text{A}+\text{P}_\text{B}$), and two singlets at -20.35 and -20.9 ppm assigned to the aminophosphine phosphor (P_C). In addition, the signals of oxidized P were observed at 31 and 32 ppm. The ${}^1\text{H}$ NMR spectrum showed a multiplet at 4.5 ppm assigned to the *PCHP* proton.

The choice of solvent may also be important, as it may have a major impact on both the thermodynamics and kinetics of isomerization. NMR spectra were carried out in CDCl_3 , a solvent that could affect ligands by hydrogen bonding (weakly) between the solvent and phosphorous lone pairs, thus ${}^{31}\text{P}\{-\text{H}\}$ NMR presence isomers on the ligands. we concluded that perhaps the metal ligands were much purer than the NMR spectra's indicated. Nevertheless, we continued to the next reaction, and they were successful.

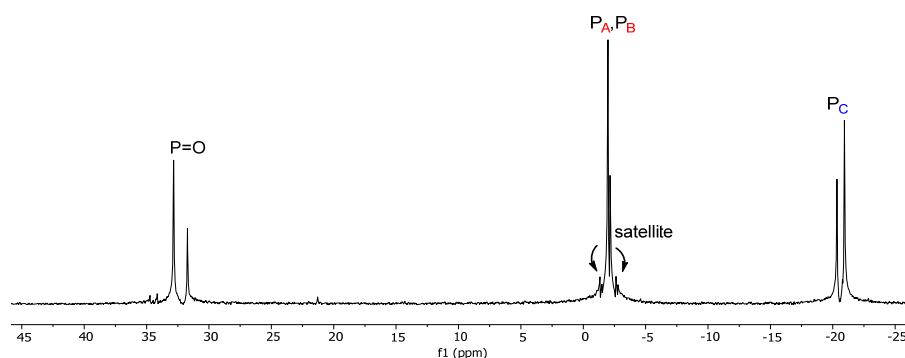


Figure 81. ${}^{31}\text{P}\{-\text{H}\}$ NMR of $\text{W}(\text{CO})_4[\text{Ph}_2\text{PCH}(\text{CH}_2\text{-NH}-(\text{CH}_2)_2\text{PPh}_2)\text{PPh}_2]\text{-P,P}$ in CDCl_3 .

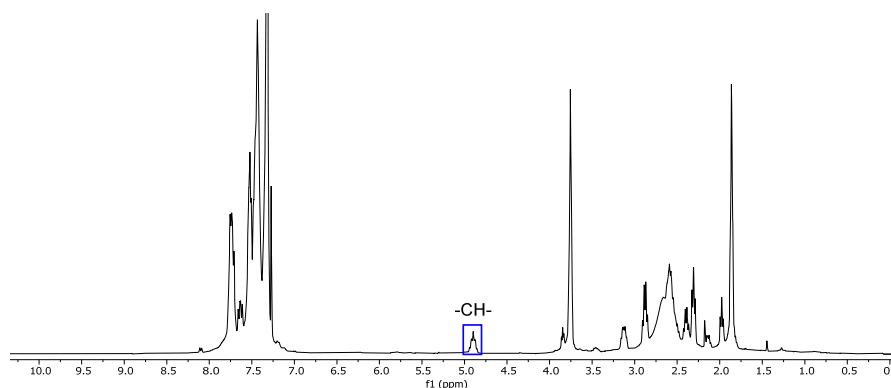
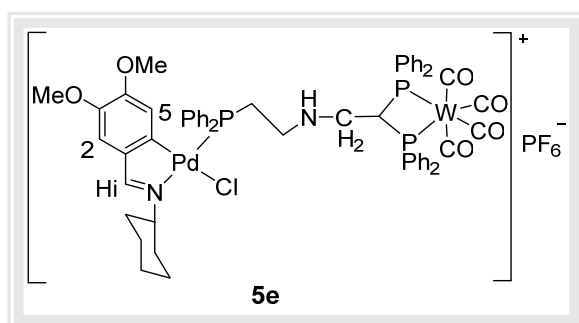


Figure 82. ^1H NMR of $\text{W}(\text{CO})_4[\text{Ph}_2\text{PCH}(\text{CH}_2\text{-NH}-(\text{CH}_2)_2\text{PPh}_2)\text{PPh}_2]\text{-P,P}$ in CDCl_3 .

7.2.6.2 Study of compounds **5c-5j** and **6c-6f**.



The ^1H NMR spectrum of **5e** showed a doublet at 6.0 ppm ($^4J(\text{H5P}) = 5.6$ Hz), which is assigned to the H5 coupled to the ^{31}P nucleus. A singlet signal of H2 proton showed at 6.93 ppm. A doublet resonance at 8.07 ppm was assigned to the $\text{HC}=\text{N}$ ($^4J(\text{HiP}) = 7.7$ Hz) coupled to the ^{31}P nucleus *trans* to nitrogen. A broad signal *ca.* 5.0 ppm is assigned to the *PCHP*. The signals for the methylene protons of cyclohexylamine were observed *ca.* 1.8–3.60 ppm. The (C4)-OMe proton signal was displaced to a lower frequency by approximately 0.8 ppm, in relation to their position in the beginning product spectrum, due to the shielding effect of the phosphine phenyl rings *cis* to the metallated carbon atom.

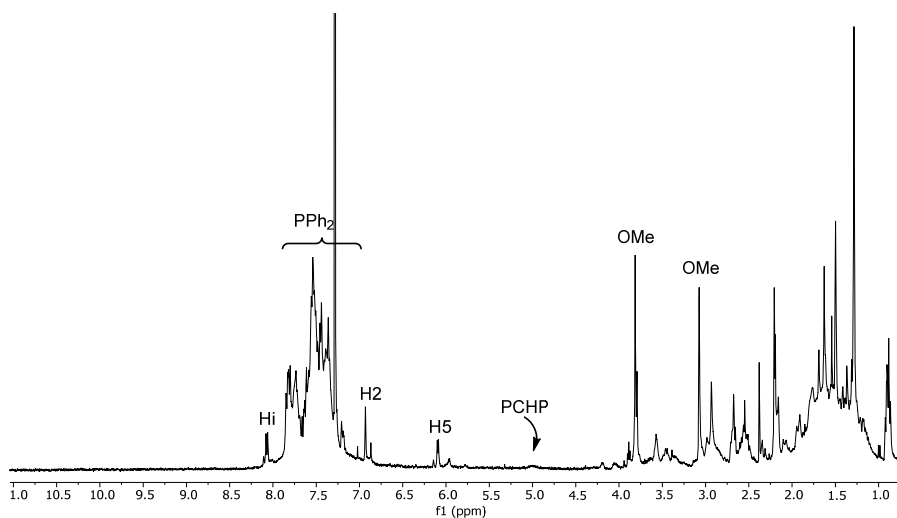
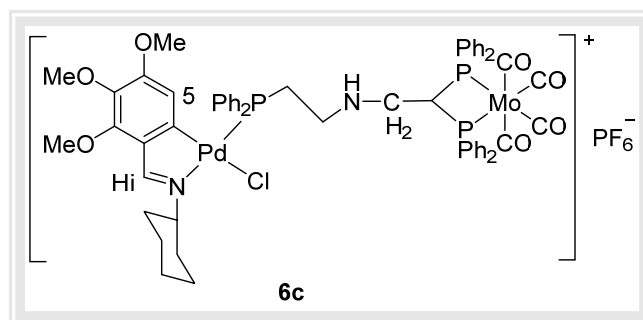


Figure 83. ^1H NMR of compound **5e** in CDCl_3 .



The ^1H NMR spectrum of **6c** showed a doublet at δ 5.86 ppm ($^4J(\text{H5P}) = 5.5$ Hz), which is assigned to the H5 coupled to the ^{31}P nucleus. A doublet resonance at 8.36 ppm was assigned to the $\text{HC}=\text{N}$ nucleus ($^4J(\text{HiP}) = 8.1$ Hz) coupled to the ^{31}P nucleus *trans* to nitrogen. The PCHP proton was not observed. The signals for the methylene protons were observed *ca.* 1.9–2.77 ppm, assigned to cyclohexylamine. The methoxy groups of (C2) and (C3) showed singlets at 3.9 and 3.7, respectively. Whereas methoxy group (C4) shifted to a lower frequency.

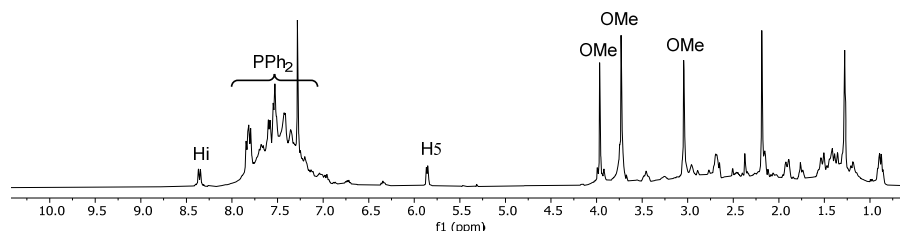


Figure 84. ^1H NMR of compound **6c** in CDCl_3 .

The $^{31}\text{P}\{-^1\text{H}\}$ NMR spectra of compound **5e** showed a singlet *ca.* 51 ppm, which was assigned to a phosphor atom bonded to palladium. Signal exhibition in a highly downfield shift for the complexes indicates that the phosphor atom of the aminophosphine ligand is coordinated with the transition metal. A singlet at -0.2 ppm, was assigned to vdpp phosphorous. In addition, presence signals at 32 and 36 ppm. The $^{31}\text{P}\{-^1\text{H}\}$ NMR spectra of compound **6c** showed a singlet *ca.* 51 ppm, which was assigned to phosphor bonded to palladium. Whereas other derivatives **6d-6f** showed in addition to 51 ppm, another singlet *ca.* 35 ppm.

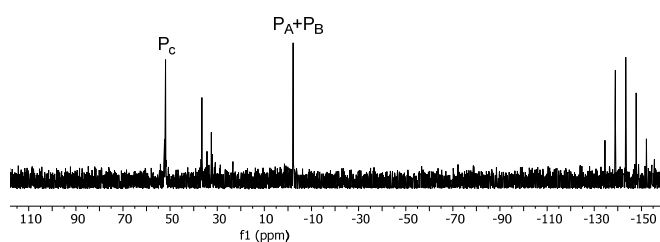
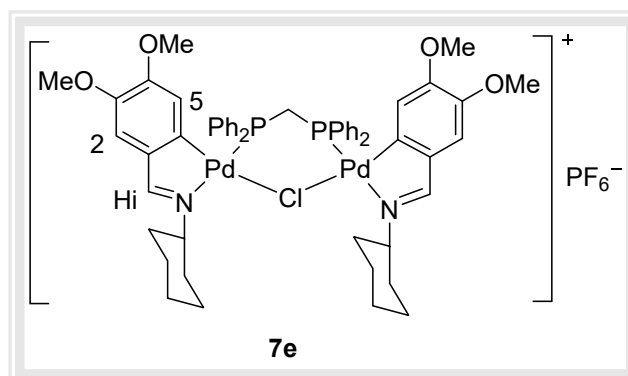


Figure 85. $^{31}\text{P}\{-^1\text{H}\}$ NMR of compound **5e** in CDCl_3 .

7.2.7 Study of compounds **7e** and **7f**.

Treatment of the chloride bridged dinuclear compounds **2e** and **2f** with the diphosphine (dppm) ligand and NH_4PF_6 in molar ratio 1:1 gave the dinuclear compounds in a bridging mode where a diphosphine ligand and a halogen atom connect the two metal centers.



The ^1H NMR and $^{31}\text{P}\{-^1\text{H}\}$ NMR spectra of compounds were recorded in CDCl_3 . In the ^1H NMR spectra, the $\text{HC}=\text{N}$ resonance appeared as a singlet signal at 8.76 ppm. A doublet at 5.64 ppm ($^4J(\text{H5P}) = 6.6$ Hz), was assigned to proton H5 coupled to a ^{31}P nucleus. A singlet signal of H2 showed at 6.9 ppm. The C(4)OMe group was shifted to a lower frequency, due to the shielding effect of the phenyl ring. Because one of the inequivalent C(4)OMe groups would not be influenced by the phosphine's phenyl ring in an antiparallel arrangement, two different resonances for the two inequivalent C(4)OMe groups would be seen. The $^{31}\text{P}\{-^1\text{H}\}$ NMR spectra showed a singlet *ca.* 30 ppm, indicating that the two ^{31}P nuclei are equivalent.

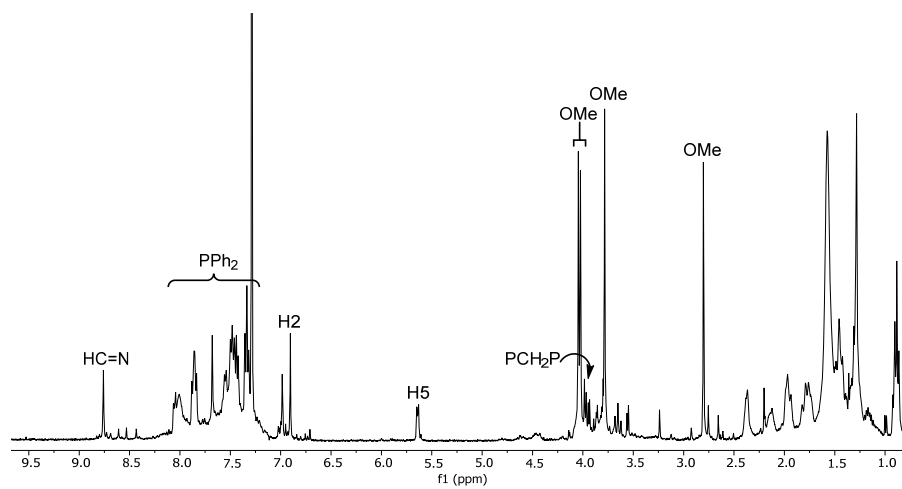


Figure 86. ^1H NMR of compound 7e in CDCl_3 .

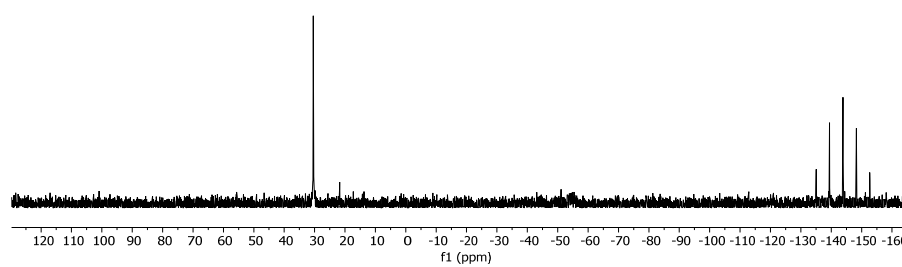


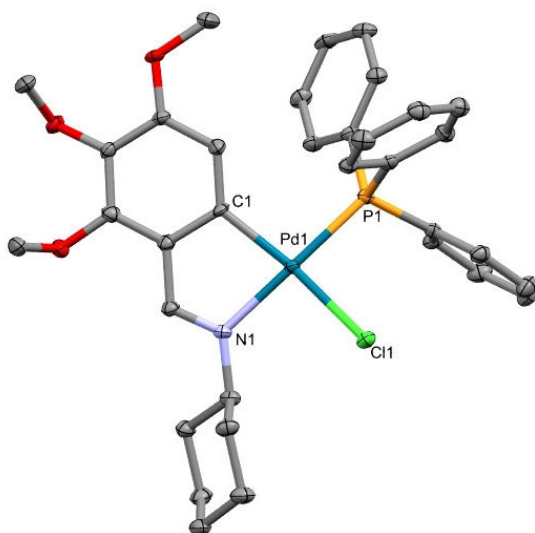
Figure 87. $^{31}\text{P}\{-^1\text{H}\}$ NMR of compound 7e in CDCl_3 .

7.3 Study of X-ray diffraction

7.3.1 Crystal structures of cyclometallated **3c**, **3d** and **3j**.

Suitable crystals of compounds **3c**, **3d** and **3j** were obtained by slowly evaporating a CH₂Cl₂/n-hexane solution. The molecular structures are shown in Figures 88, 89, and 90. Crystallographic data are given in Table 37, Table 38, and Table 39 shows selected bond lengths and angles. For the crystal structure of **3j**, two distinct molecules were generated per asymmetric unit, corresponding to two distinct conformers.

A nitrogen atom from the imine group, an *ortho* carbon atom from the metallated phenyl ring, a chlorine atom, and a phosphorus atom from a triphenylphosphine ligand constitute the coordination sphere around each palladium atom.



The sum of angles at palladium is *ca.* 360°, with the most noteworthy deviation due to chelation in the somewhat reduced "bite" angle C1-Pd(1)-N(1) of 81.4° for **3c** and **3d** compounds, and 81.12° for **3j**.

Figure 88. Crystal structure of compound **3c**.

The Pd(1)-P(1) bond distance, 2.262(14) Å for **3c**, 2.264(8) Å for **3d**, and 2.260(2) Å for **3j**, is less than the sum of the single-bond radii for palladium and phosphorus, 2.41 Å, implying a partial double bond between the two atoms.

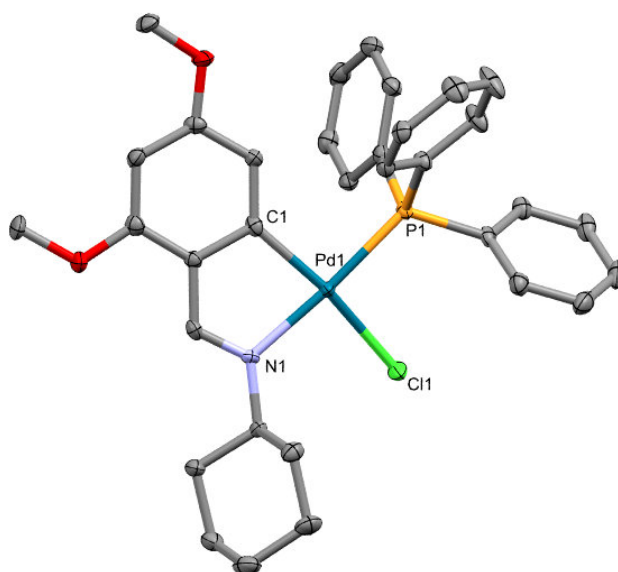


Figure 89. Crystal structure of compound **3d**.

The bond lengths of Pd(1)-Cl(1) and Pd(1)-C(1), 2.379(13), 2.027 (5) Å for **3c**, 2.365(8), 2.026(3) Å for **3d**, and 2.370(18), 2.034 (9) for **3j**, respectively, are in accordance with previously reported data.¹³⁶ The molecules in the crystal structure **3j** are linked together by hydrogen bonds, or C–H···F interactions. The intermolecular interactions distance between the fluorine (F1) and (F2) with the hydrogen of

¹³⁶ (a) A. Fernández, E. Pereira, J.J. Fernández, M. López-Torres, A. Suárez, R. Mosteiro, M.T. Pereira, J.M. Vila, *New Journal of Chemistry*, 26 (2002) 895-901.

(b) M. López-Torres, A. Fernández, J.J. Fernández, A. Suárez, S. Castro-Juiz, M.T. Pereira, J.M. Vila, *Journal of organometallic chemistry*, 655 (2002) 127-133.

phosphine benzyl ring are 2.451 Å, 2.547 Å, respectively. In addition, the bond angles $\delta(\text{C16-H16}\cdots\text{F1})$ and $\delta(\text{C50-H50}\cdots\text{F2})$ are 108.44° and 121.31° , respectively.

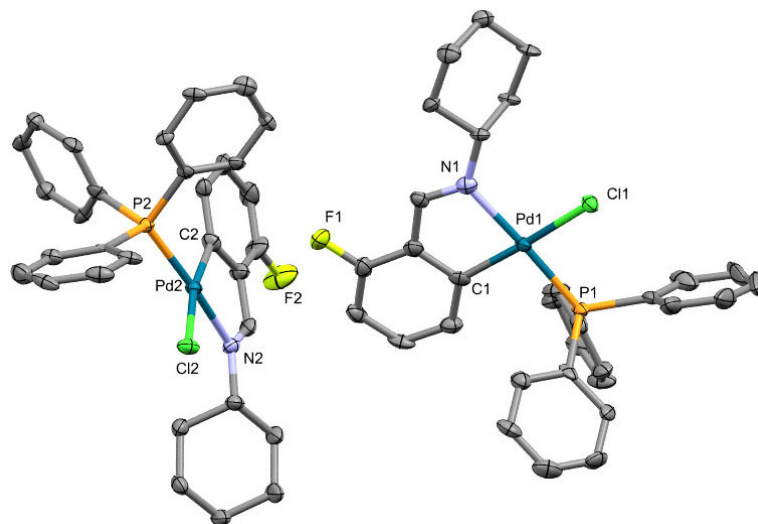


Figure 90. Symmetric and asymmetric view structure of compound 3j.

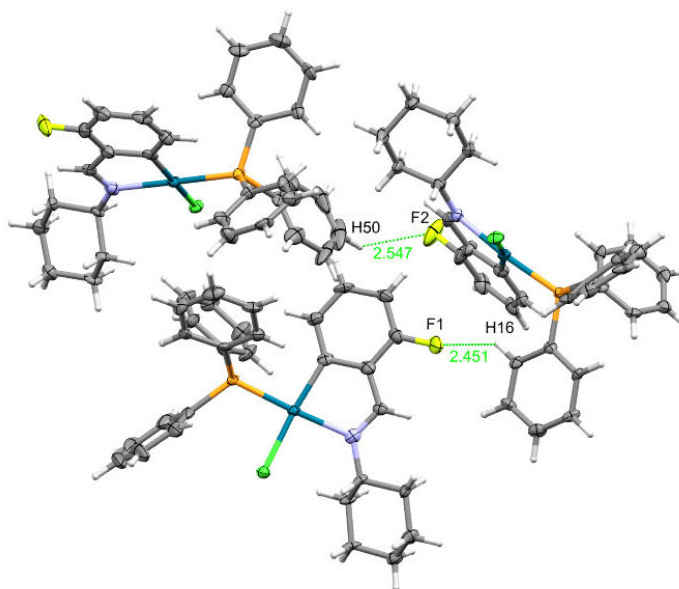


Figure 91. Intermolecular interactions (C-H...F) for compound 3j.

Table 36. C–F interactions (Å, °) of compound 3j.

Y–H···X	Y–H	H···A	Y–X	<(Y–H···A) ^o
C16–H16–F1 ^a	0.950	2.451	2.894	108.44
C50–H50–F2 ^b	0.950	2.547	3.147	121.31

Symmetry operations ^ax, y, z, ^b1.5 – x, – 0.5 + y, 0.5 – z.

Table 37. Compound 3c was obtained from X-ray single-crystal diffraction studies. Bond lengths are given in [Å] and angles in [°].

Pd1-N1	2.112(5)	C1-Pd1-N1	81.41(2)
Pd1-C1	2.027(5)	C1-Pd1-P1	97.15(16)
Pd1-P1	2.262(14)	N1-Pd1-C11	93.07(13)
Pd1-C11	2.379(13)	P1-Pd1-C11	89.95(5)

Table 38. Compound 3d obtained from X-ray single-crystal diffraction studies. Bond lengths are given in [Å] and angles in [°].

Pd1-N1	2.094(3)	C1-Pd1-N1	81.40(12)
Pd1-C1	2.026(3)	C1-Pd1-P1	94.44(10)
Pd1-P1	2.264(8)	N1-Pd1-C11	91.92(8)
Pd1-C11	2.365(8)	P1-Pd1-C11	92.19(3)

Table 39. Compound 3j obtained from X-ray single-crystal diffraction studies. Bond lengths are given in [Å] and angles in [°].

Pd(1)-N(1)	2.120(5)	C(1)-Pd(1)-N(1)	81.9(3)
Pd(1)-C(1)	2.020(7)	P(1)-Pd(1)-Cl(1)	90.31(7)
Pd(1)-P(1)	2.260(2)	Cl(1)-Pd(1)-N(1)	93.1(2)
Pd(1)-Cl(1)	2.364(2)	P(1)-Pd(1)-C(1)	94.8(2)
Pd(2)-N(2)	2.111(5)	C(2)-Pd(2)-N(2)	81.42(3)
Pd(2)-C(2)	2.018(7)	P(2)-Pd(2)-Cl(2)	91.96(7)
Pd(2)-P(2)	2.264(2)	N(2)-Pd(2)-P(2)	173.2(2)
Pd(2)-Cl(2)	2.366(2)	C(2)-Pd(2)-Cl(2)	170.1(2)
N(1)-Pd(1)-P(1)	176.5(2)	N(2)-Pd(2)-Cl(2)	91.9(2)

Table 40. Crystal's data and structures refinement for compound 3c and 3d.

Crystal structure	3c	3d
Molecular formula	C ₃₄ H ₃₇ ClNO ₃ PPd	C ₃₃ H ₃₅ ClNO ₂ PPd
Formula weight	680.46	650.44
Temperature/K	100.00	100.00
Crystal system	Orthorhombic	Monoclinic
Space group	P2 ₁ /n	Cc
a/Å	22.5430(14)	9.5967(4)
b/Å	9.7727(5)	22.4611(10)
c/Å	13.6276(9)	13.9324(5)
α/°	90	90
β/°	90	101.5830(10)
γ/°	90	90
Volume/Å ³	3002.2(3)	2942.0(2)
Z	4	1
ρ _{calc} /cm ³	1.505	0.367
μ/mm ⁻¹	0.797	0.202
F(000)	1400.0	334.0
Crystal size/mm ³	0.08 × 0.03 × 0.02	0.12 × 0.09 × 0.06
Radiation	MoKα (λ = 0.71073)	MoKα (λ = 0.71073)
θ range for data collection/°	4.542 to 56.558	4.696 to 56.672
Index ranges	-30 ≤ h ≤ 30, -13 ≤ k ≤ 13, -18 ≤ l ≤ 18	-12 ≤ h ≤ 12, -29 ≤ k ≤ 29, -17 ≤ l ≤ 18
Reflections collected	120820	45580
Independent reflections	7453 [R _{int} = 0.0977, R _{sigma} = 0.0378]	6621 [R _{int} = 0.0465, R _{sigma} = 0.0303]
Data/restraints/parameters	7453/1/373	6621/2/355
Goodness-of-fit on F ²	1.047	1.040
Final R indexes [I ≥ 2σ (I)]	R ₁ = 0.0383, wR ₂ = 0.0714	R ₁ = 0.0226, wR ₂ = 0.0449
Final R indexes [all data]	R ₁ = 0.0524, wR ₂ = 0.0786	R ₁ = 0.0256, wR ₂ = 0.0463
Largest diff. peak/hole / e Å ⁻³	0.64/-0.91	0.26/-0.44
Flack parameter	0.487(11)	-0.041(10)

Table 41. Crystal's data and structures refinement for compound 3j.

Crystal structure	3j
Molecular formula	C ₃₁ H ₃₀ ClFNPPd
Formula weight	608.430
Temperature/K	100.00
Crystal system	monoclinic
Space group	P2 ₁ /n
a/Å	25.2382(19)
b/Å	9.3553(8)
c/Å	25.294(2)
α/°	90
β/°	95.345(2)
γ/°	90
Volume/Å ³	5946.2(8)
Z	8
ρ _{calc} /cm ³	1.359
μ/mm ⁻¹	0.793
F(000)	2475.3
Crystal size/mm ³	0.14 × 0.04 × 0.02
Radiation	Mo Kα (λ = 0.71073)
θ range for data collection/°	4.36 to 53.36
Index ranges	-31 ≤ h ≤ 31, -11 ≤ k ≤ 11, -31 ≤ l ≤ 31
Reflections collected	257548
Independent reflections	12382 [R _{int} = 0.1679, R _{sigma} = 0.0581]
Data/restraints/parameters	12382/0/650
Goodness-of-fit on F ²	1.060
Final R indexes [I ≥ 2σ (I)]	R ₁ = 0.1001, wR ₂ = 0.1840
Final R indexes [all data]	R ₁ = 0.1130, wR ₂ = 0.1900
Largest diff. peak/hole / e Å ⁻³	1.54/-4.01

7.3.2 Crystal structures of cyclometallated **4e**, **4f**, **4h** and **3k**.

Suitable crystals of compounds **4e**, **4f**, **4h**, and **3k** were obtained by slowly evaporating a CH₂Cl₂/n-hexane solution. The molecular structure for **4e**, **4h**, and **3k** are shown in the Figures below. Crystallographic data are given in the Tables show selected bond lengths and angles with calculated standard deviations. Whilst the formed crystal for **4f** generated two unique molecules per asymmetric unit, corresponding to two separate conformers and existing two molecules of CH₂Cl₂.

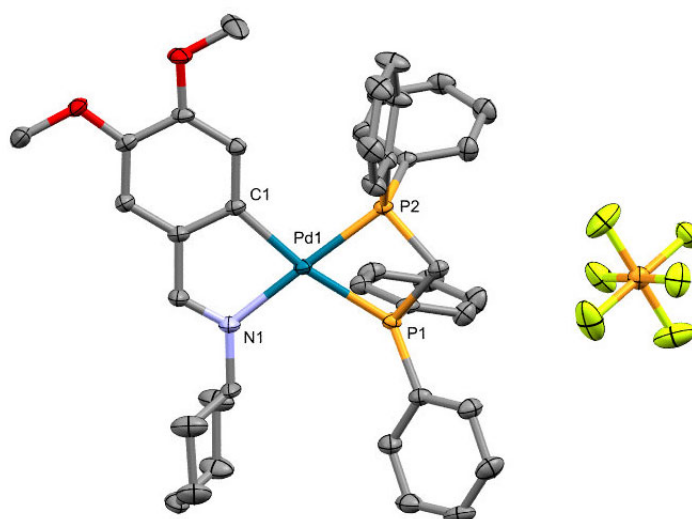


Figure 92. Crystal structure of compound **4e**.

The palladium atom is in a square-planar geometry bonded to two chelating ligands: bidentate [C,N] Schiff base ligand and a Ph₂PCH₂PPh₂-P,P diphosphine. The sum of angles at the metal center is ca. 360°, with the most significant distortion in the somewhat reduced "bite" angle C(1)-Pd(1)-N(1), 80.9(8)° for **4e**, 80.97(11)° for **4h**, 80.47(11)° for **3k** and 81.25(18)° for **4f** upon chelation.

The P(1)–Pd(1)–P(2) bond angle 71.04(2)° for 4e, 72.12(3)° for 4h, 70.88(3)° for 3k and 71.78(4)° for 4f reflect the strain of the four-membered chelate ring of the phosphine. The Pd(1)–N(1) bond length, *ca.* 2.088(2) Å for 4e, 2.120(2) Å for 4h, 2.096(2) Å for 3k and 2.115(4) Å for 4f is longer than the single bond expected value of 2.011 Å, consequent on the trans effect of the phosphine ligand.¹³⁷ The Pd(1)–C(1) bond length, of 2.038(2) Å for 4e, 2.033(3) Å for 4h, 2.036(3) Å for 3k and 2.034(5) Å for 4f is in agreement with the partial multiple-bond character of the Pd–C bond.¹³⁸

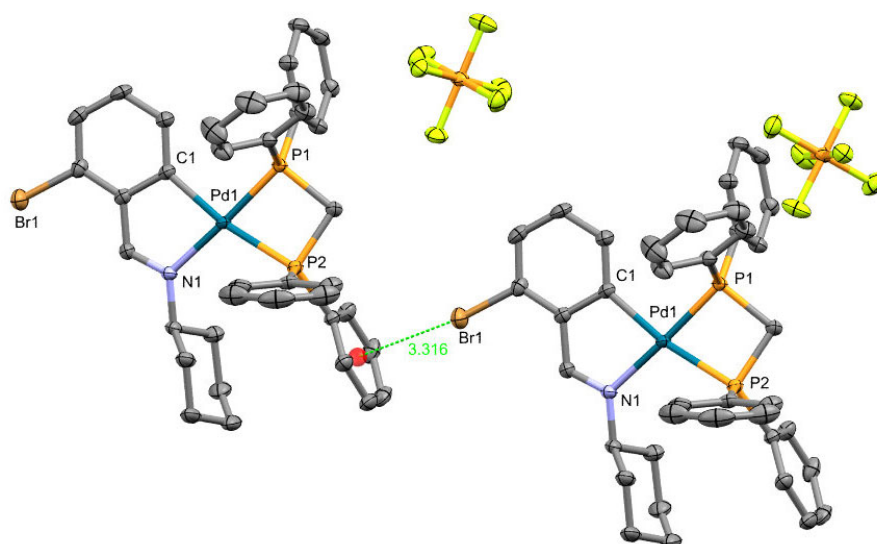


Figure 93. Intermolecular Br1... π interaction of crystal structure of compound 4h.

¹³⁷ (a) T. Suzuki, A. Morikawa, K. Kashiwabara, *Bulletin of the Chemical Society of Japan*, 69 (1996) 2539-2548. (b) S. Chakladar, P. Paul, A.K. Mukherjee, S.K. Dutta, K.K. Nanda, D. Podder, K. Nag, *Journal of the Chemical Society, Dalton Transactions*, (1992) 3119-3124.

¹³⁸ J. Vila, M. Pereira, J. Ortigueira, M. López-Torres, Castin eiras, A.; Lata, D.; Fernández, JJ; Fernández, A, *J. Organomet. Chem*, 556 (1998) 31-39.

In the crystal structure of 4h, there are intermolecular interactions between the bromine atoms and the π electrons phenyl ring. The bond length interaction between centroid Cg1 of phenyl ring and Br1 is 3.316(5) Å. For more information, see Table 42.

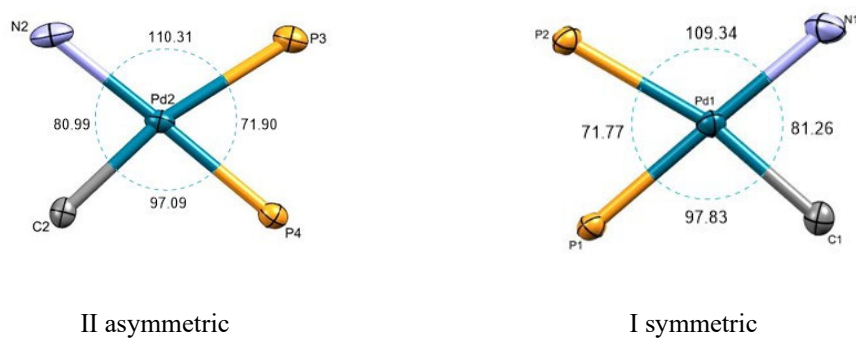


Figure 94. The bonds angles of symmetric and asymmetric conformers of compound 4f.

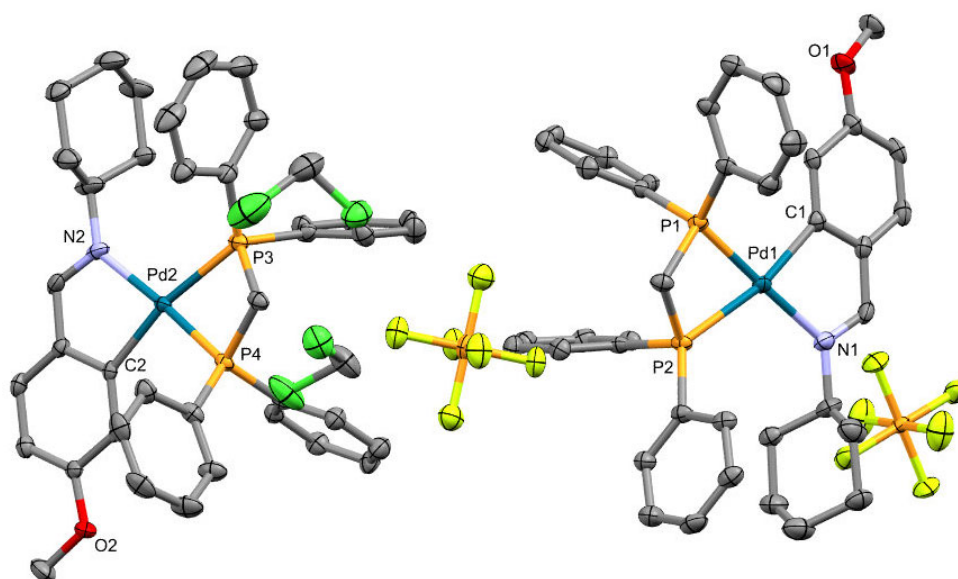


Figure 95. View of symmetric and asymmetric structures of compound 4f.

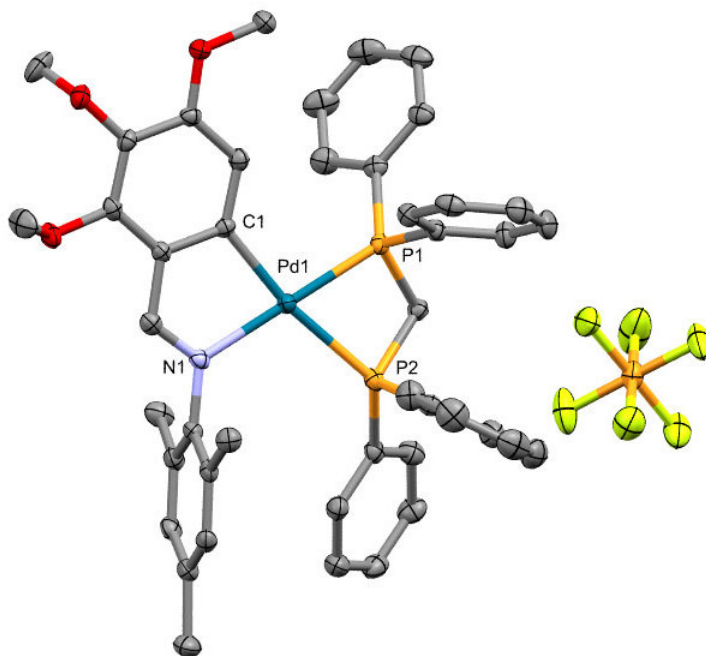


Figure 96. Crystal structure of compound 3k.

Table 42. C—Br interactions (Å, °) of compound 4h.

Y—X---Cg	Y—X	X---Cg	Y---Cg	$\angle(Y—X---Cg)^{\circ}$
C5—Br1---Cg1	1.884	3.316	5.173	167.86

Symmetry operation $-1 + x, y, z$.

Table 43. Compound 4e was obtained from X-ray single-crystal diffraction studies. Bond lengths are given in [Å] and angles in [°].

Pd(1)-N(1)	2.088(2)	C(1)-Pd(1)-N(1)	80.98(8)
Pd(1)-C(1)	2.038(2)	P(1)-Pd(1)-P(2)	71.04(2)
Pd(1)-P(1)	2.252(6)	N(1)-Pd(1)-P(2)	107.98(6)
Pd(1)-P(2)	2.388(6)	P(1)-Pd(1)-C(1)	100.15(7)
N(1)-Pd(1)-P(1)	178.06(6)	C(1)-Pd(1)-P(2)	169.76(6)

Table 44. Compound 4h was obtained from X-ray single-crystal diffraction studies. Bond lengths are given in [Å] and angles in [°].

Pd(1)-N(1)	2.120(2)	C(1)-Pd(1)-N(1)	80.97(11)
Pd(1)-C(1)	2.033(3)	P(1)-Pd(1)-P(2)	72.12(3)
Pd(1)-P(1)	2.245(8)	N(1)-Pd(1)-P(2)	111.02(7)
Pd(1)-P(2)	2.383(2)	P(1)-Pd(1)-C(1)	96.17(9)
N(1)-Pd(1)-P(1)	176.10(7)	C(1)-Pd(1)-P(2)	166.53(9)

Table 45. Compound 3k was obtained from X-ray single-crystal diffraction studies. Bond lengths are given in [Å] and angles in [°].

Pd(1)-N(1)	2.096(2)	C(1)-Pd(1)-N(1)	80.47(11)
Pd(1)-C(1)	2.036(3)	P(1)-Pd(1)-P(2)	70.88(3)
Pd(1)-P(1)	2.251(8)	N(1)-Pd(1)-P(2)	108.80(7)
Pd(1)-P(2)	2.408(8)	P(1)-Pd(1)-C(1)	99.86(9)
N(1)-Pd(1)-P(1)	179.49(7)	C(1)-Pd(1)-P(2)	170.54(9)

Table 46. Compound 4f was obtained from X-ray single-crystal diffraction studies. Bond lengths are given in [Å] and angles in [°].

Pd(1)-N(1)	2.115(4)	C(1)-Pd(1)-N(1)	81.25(18)
Pd(1)-C(1)	2.034(5)	P(1)-Pd(1)-P(2)	71.78(4)
Pd(1)-P(1)	2.245(12)	P(2)-Pd(1)-N(1)	109.34(12)
Pd(1)-P(2)	2.376(12)	P(1)-Pd(1)-C(1)	97.82(14)
Pd(2)-N(2)	2.125(4)	C(2)-Pd(2)-N(2)	81.08(17)
Pd(2)-C(2)	2.036(4)	P(3)-Pd(2)-P(4)	71.89(4)
Pd(2)-P(3)	2.388(13)	N(2)-Pd(2)-P(3)	110.24(12)
Pd(2)-P(4)	2.240(12)	C(2)-Pd(2)-P(4)	97.08(12)
N(1)-Pd(1)-P(1)	177.92(16)	N(2)-Pd(2)-P(4)	173.97(15)

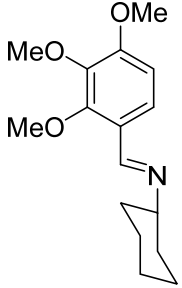
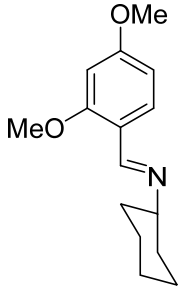
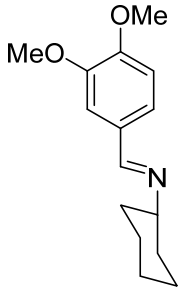
Table 47. Crystal's data and structures refinement for compounds 4e and 4h.

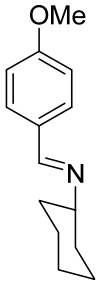
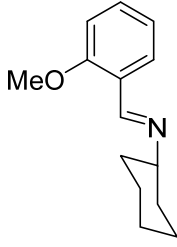
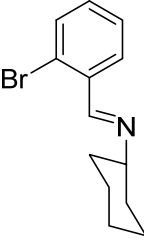
Crystal structure	4e	4h
Molecular formula	C ₄₀ H ₄₂ F ₆ NO ₂ P ₃ Pd	C ₃₈ H ₃₇ BrF ₆ NP ₃ Pd
Formula weight	882.11	900.955
Temperature/K	100.00	100.00
Crystal system	Triclinic	monoclinic
Space group	P-1	P2 ₁ /c
a/Å	12.5158(8)	12.3331(7)
b/Å	12.9085(9)	13.8140(8)
c/Å	13.9286(9)	22.5392(14)
α/°	71.877(2)	90
β/°	81.955(2)	104.621(2)
γ/°	69.474(2)	90
Volume/Å ³	2001.7(2)	3715.6(4)
Z	2	4
ρ _{calc} /cm ³	1.472	1.611
μ/mm ⁻¹	0.647	1.763
F(000)	910.0	1805.6
Crystal size/mm ³	0.09 × 0.07 × 0.06	0.13 × 0.06 × 0.04
Radiation	MoKα (λ = 0.71073)	Mo Kα (λ = 0.71073)
θ range for data collection/°	4.724 to 56.562	4.38 to 58.26
Index ranges	-16 ≤ h ≤ 16, -17 ≤ k ≤ 17, -18 ≤ l ≤ 18	-16 ≤ h ≤ 16, -18 ≤ k ≤ 18, -30 ≤ l ≤ 30
Reflections collected	52381	213238
Independent reflections	9938 [R _{int} = 0.0523, R _{sigma} = 0.0379]	10000 [R _{int} = 0.0928, R _{sigma} = 0.0314]
Data/restraints/parameters	9938/0/501	10000/0/452
Goodness-of-fit on F ²	1.036	1.059
Final R indexes [I ≥ 2σ (I)]	R ₁ = 0.0356, wR ₂ = 0.0801	R ₁ = 0.0384, wR ₂ = 0.0877
Final R indexes [all data]	R ₁ = 0.0456, wR ₂ = 0.0847	R ₁ = 0.0555, wR ₂ = 0.0982
Largest diff. peak/hole / e Å ⁻³	0.96/-0.58	0.90/-1.76

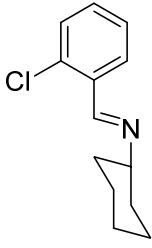
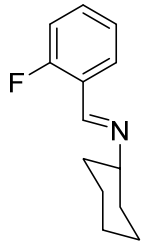
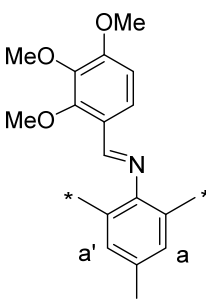
Table 48. Crystal data and structure refinement for compounds 3k and 4f.

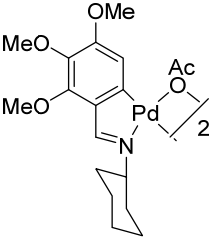
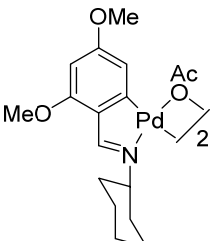
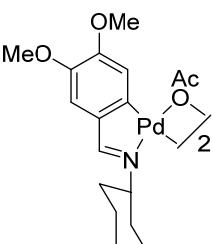
Crystal structure	3k	4f
Empirical formula	C ₄₄ H ₄₄ F ₆ NO ₃ P ₃ Pd	C ₃₉ H ₄₀ F ₆ NOP ₃ Pd 2(CH ₂ Cl ₂)
Formula weight	948.11	852.09
Temperature/K	100.00	100.00
Crystal system	monoclinic	Triclinic
Space group	P2 ₁ /n	P-1
a/Å	14.2798(8)	12.0121(8)
b/Å	14.0263(8)	18.4207(14)
c/Å	21.2483(11)	21.3521(16)
α/°	90	107.573(2)
β/°	98.393(2)	104.718(2)
γ/°	90	103.530(2)
Volume/Å ³	4210.3(4)	4101.6(5)
Z	4	4
ρ _{calc} /cm ³	1.496	1.459
μ/mm ⁻¹	0.622	0.742
F(000)	1936.0	1835.0
Crystal size/mm ³	0.33 × 0.07 × 0.02	0.23 × 0.04 × 0.03
Radiation	MoKα (λ = 0.71073)	MoKα (λ = 0.71073)
2θ range for data collection/°	4.092 to 55.752	3.83 to 52.746
Index ranges	-18 ≤ h ≤ 18, -18 ≤ k ≤ 18, -27 ≤ l ≤ 25	-15 ≤ h ≤ 15, -23 ≤ k ≤ 23, -26 ≤ l ≤ 26
Reflections collected	91837	151568
Independent reflections	10043 [R _{int} = 0.0905, R _{sigma} = 0.0485]	16747 [R _{int} = 0.0685, R _{sigma} = 0.0386]
Data/restraints/parameters	10043/0/530	16747/0/946
Goodness-of-fit on F ²	1.038	1.124
Final R indexes [I >= 2σ (I)]	R ₁ = 0.0446, wR ₂ = 0.0966	R ₁ = 0.0603, wR ₂ = 0.1214
Final R indexes [all data]	R ₁ = 0.0641, wR ₂ = 0.1068	R ₁ = 0.0731, wR ₂ = 0.1269
Largest diff. peak/hole / e Å ⁻³	1.54/-1.47	1.25/-1.13

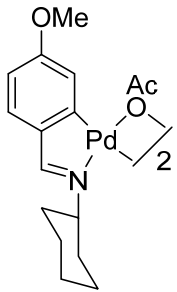
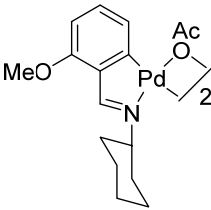
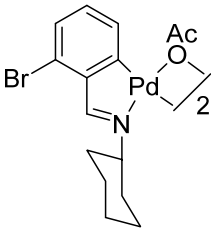
7.4 Data additional

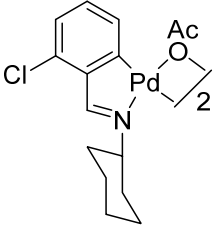
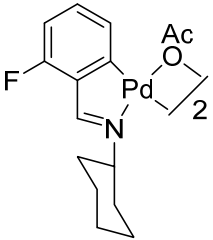
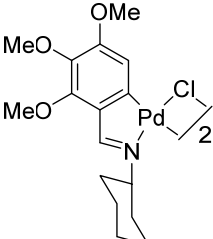
<p>ligand c</p> 	<p>Yield 90 %.</p> <p>IR = $\nu(\text{C}=\text{N})$ 1637cm^{-1}</p> <p>^1H NMR (400 MHz, CDCl_3) δ 8.58 (s, 1H, Hi), 7.73 (d, $^3J(\text{H6H5}) = 8.8$ Hz, 1H, H6), 6.72 (d, $^3J(\text{H5H6}) = 8.8$ Hz, 1H, H5), 3.89 (s, 3H, OMe), 3.90 (s, 3H, OMe), 3.94 (s, 3H, OMe), 3.21 (m, $^3J(\text{HH}) = 10.5$ Hz, 1H, N-CH-Cy), 2.01–1.18 (m, 10H, Cy).</p>
<p>ligand d</p> 	<p>Yield 93 %.</p> <p>IR = $\nu(\text{C}=\text{N})$ 1640 cm^{-1}.</p> <p>^1H NMR (400 MHz, CDCl_3) δ 8.65 (s, 1H, Hi), 7.92 (d, $^3J(\text{H6H5}) = 8.8$ Hz, 1H, H6), 6.52 (d, $^3J(\text{H5H6}) = 8.8$ Hz, 1H, H5), 6.44 (s, 1H, H3), 3.84 (s, 6H, OMe), 3.18 (m, $^3J(\text{HH}) = 9.7$, 1H, N-CH-Cy), 2.11–1.20 (m, 10H, Cy).</p>
<p>ligand e</p> 	<p>Yield 92 %.</p> <p>IR = $\nu(\text{C}=\text{N})$ 1635 cm^{-1}.</p> <p>^1H NMR (400 MHz, CDCl_3) δ 8.22 (s, 1H, Hi), 7.42 (s, 1H, H2), 7.14 (d, $^3J(\text{H6H5}) = 8.4$, 1H, H6), 6.87 (d, $^3J(\text{H5H6}) = 8.4$, 1H, H5), 3.94 (s, 3H, OMe), 3.90 (s, 3H, OMe), 3.16 (m, $^3J(\text{HH}) = 10.8$ Hz, 1H, N-CH-Cy), 1.90–1.18 (m, 10H, Cy).</p>

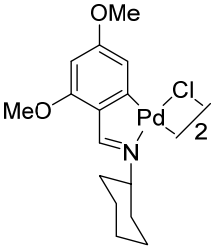
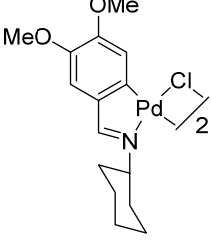
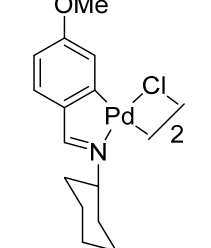
<p>ligand f</p> 	<p>Yield 95 %.</p> <p>IR = $\nu(\text{C}=\text{N})$ 1643 cm^{-1}.</p> <p>^1H NMR (400 MHz, CDCl_3) δ 8.26 (s, 1H, Hi), 7.68 (d, $^3J(\text{H}2\text{H}6) = 8.3$ Hz, 2H, H2, H6), 6.92 (d, $^3J(\text{H}3\text{H}5) = 8.3$ Hz, 2H, H3, H5), 3.84 (s, 3H, OMe), 3.17 (m, $^3J(\text{HH}) = 10.0$ Hz, 1H, N-CH-Cy), 1.89–1.17 (m, 10H, Cy).</p>
<p>ligand g</p> 	<p>Yield 96 %.</p> <p>^1H NMR (400 MHz, CDCl_3) δ 8.77 (s, 1H, Hi), 7.97 (d, $^3J(\text{H}6\text{H}5) = 8.1$ Hz, 1H, H6), 7.37 (t, $^3J(\text{H}4\text{H}3) = 8.1$ Hz, 1H, H4), 6.98 (t, $^3J(\text{H}5\text{H}6) = 8.1$ Hz, 1H, H5), 6.91 (d, $^3J(\text{H}3\text{H}4) = 8.1$ Hz, 1H, H3), 3.88 (s, 3H, OMe), 3.24 (tt, $^3J(\text{HH}) = 10.7$ Hz, 4.0 Hz, 1H, N-CH-Cy), 1.93–1.19 (m, 10H, Cy).</p>
<p>ligand h</p> 	<p>Yield 87 %.</p> <p>^1H NMR (400 MHz, CDCl_3) δ 8.68 (s, 1H, Hi), 8.03 (dd, $^3J(\text{H}6\text{H}5) = 7.8$ Hz, $^4J(\text{H}6\text{H}4) = 2.3$ Hz, 1H, H6), 7.56 (d, $^3J(\text{H}3\text{H}4) = 7.8$ Hz, 1H, H3), 7.33 (t, $^3J(\text{H}5\text{H}6) = 7.8$ Hz, 1H, H5), 7.24 (t, $^3J(\text{H}4\text{H}3) = 7.8$ Hz, 1H, H4), 3.31 (m, $^3J(\text{HH}) = 10.4$ Hz, 1H, N-CH-Cy), 1.94–1.20 (m, 10H, Cy).</p>

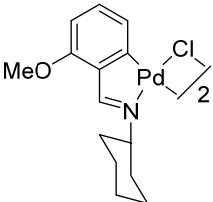
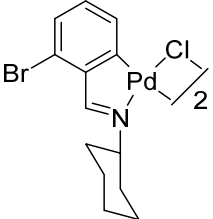
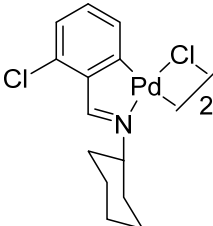
<p>ligand i</p> 	<p>Yield 91 %.</p> <p>$^1\text{H NMR}$ (400 MHz, CDCl_3) δ 8.76 (s, 1H, Hi), 8.05 (d, $^3J(\text{H6H5}) = 7.4$ Hz, 1H, H6), 7.37 (m, 2H, H4, H5), 7.32 (d, $^3J(\text{H3H4}) = 7.4$ Hz, 1H, H3), 3.30 (m, $^3J(\text{HH}) = 9.9$ Hz, 1H, N-CH-Cy), 1.97–1.18 (m, 10H, Cy).</p>
<p>ligand j</p> 	<p>Yield 96 %.</p> <p>IR = $\nu(\text{C}=\text{N})$ 1629 cm^{-1}.</p> <p>$^1\text{H NMR}$ (400 MHz, CDCl_3) δ 8.64 (s, 1H, Hi), 8.01 (t, $^3J(\text{H6H5}) = 7.7$ Hz, 1H, H6), 7.38 (d, $^3J(\text{H3H4}) = 8$ Hz, 1H, H3), 7.17 (t, $^3J(\text{H5H6}) = 7.7$, 1H, H5), 7.07 (dd, $^3J(\text{H4H3}) = 8$ Hz, $^4J(\text{H4F}) = 10.7$ Hz, 1H, H4), 3.27 (m, $^3J(\text{HH}) = 10.0$ Hz, 1H, N-CH-Cy), 2.02–1.14 (m, 10H, Cy).</p>
<p>ligand k</p> 	<p>Yield 95 %.</p> <p>IR = $\nu(\text{C}=\text{N})$ 1630 cm^{-1}.</p> <p>$^1\text{H NMR}$ (400 MHz, CDCl_3) δ 8.49 (s, 1H, Hi), 8.00 (d, $^3J(\text{H6H5}) = 8.8$ Hz, 1H, H6), 6.91 (s, 2H, Ha, Ha'), 6.84 (d, $^3J(\text{H5H6}) = 8.8$ Hz, 1H, H5), 3.96 (s, 3H, OMe), 3.94 (s, 6H, OMe), 2.30 (s, 3H, Me), 2.15 (s, 6H, Me*).</p>

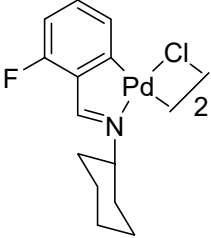
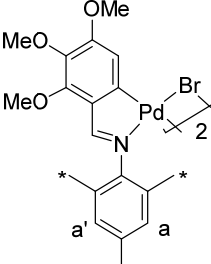
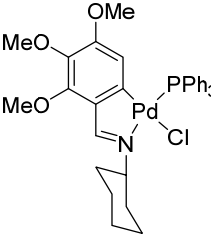
<p>compound 1c</p> 	<p>Yield 51%.</p> <p>IR = $\nu(\text{C}=\text{N})$ 1602 cm^{-1}, $\nu_{\text{as}}(\text{COO})$ = 1590 cm^{-1}, $\nu_{\text{s}}(\text{COO})$ = 1415 cm^{-1}.</p> <p>^1H NMR (400 MHz, CDCl_3) δ 7.57 (s, 2H, Hi), 6.36 (s, 2H, H5), 3.90 (s, 6H, OMe), 3.88 (s, 6H, OMe), 3.78 (s, 6H, OMe), 2.99 (m, 2H, N-CH-Cy), 2.14 (s, 6H, OAc), 0.8–2.50 (m, 20H, Cy).</p>
<p>compound 1d</p> 	<p>Yield 40 %.</p> <p>IR = $\nu(\text{C}=\text{N})$ 1610 cm^{-1}, $\nu_{\text{as}}(\text{COO})$ = 1590 cm^{-1}, $\nu_{\text{s}}(\text{COO})$ = 1430 cm^{-1}.</p> <p>^1H NMR (400 MHz, CDCl_3) δ 7.60 (s, 2H, Hi), 6.21 (s, 2H, H5), 6.02 (s, 2H, H3), 3.80 (s, 6H, OMe), 3.75 (s, 6H, OMe), 2.99 (m, $^3J(\text{HH})$ = 11.9 Hz, 2H, N-CH-Cy), 2.13 (s, 6H, OAc), 0.8– 2.45 (m, 20H, Cy).</p>
<p>compound 1e</p> 	<p>Yield 42 %.</p> <p>IR = $\nu(\text{C}=\text{N})$ 1605 cm^{-1}, $\nu_{\text{as}}(\text{COO})$ = 1580 cm^{-1}, $\nu_{\text{s}}(\text{COO})$ = 1420 cm^{-1}.</p> <p>^1H NMR (400 MHz, CDCl_3) δ 7.32 (s, 2H, Hi), 6.72 (s, 2H, H2), 6.60 (s, 2H, H5), 3.90 (s, 6H, OMe), 3.81 (s, 6H, OMe), 2.95 (m, $^3J(\text{HH})$ = 11.6 Hz, 2H, N-CH-Cy), 2.15 (s, 6H, OAc), 0.8–2.44 (m, 20H, Cy).</p>

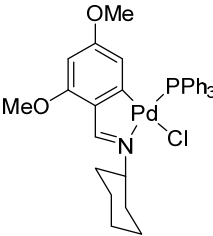
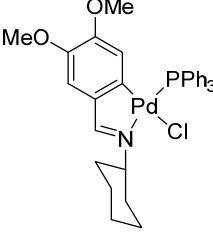
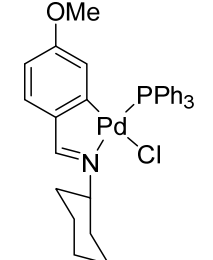
<p>compound 1f</p> 	<p>Yield 35 %.</p> <p>IR = $\nu(\text{C}=\text{N})$ 1609 cm^{-1}, $\nu_{\text{as}}(\text{COO})$ = 1570 cm^{-1}, $\nu_{\text{s}}(\text{COO})$ = 1414 cm^{-1}.</p> <p>^1H NMR (400 MHz, CDCl_3) δ 7.25 (s, 2H, Hi), 7.00 (d, $^3J(\text{H}2\text{H}3)$ = 8.2 Hz, 2H, H2), 6.60 (s, 2H, H5), 6.49 (dd, $^3J(\text{H}3\text{H}2)$ = 8.2 Hz, $^4J(\text{H}3\text{H}5)$ = 3.2 Hz, 2H, H3), 3.79 (s, 6H, OMe), 3.00 (m, $^3J(\text{HH})$ = 12.2 Hz, 2H, N-CH-Cy), 2.14 (s, 6H, OAc), 0.7–2.5 (m, 20H, Cy).</p>
<p>compound 1g</p> 	<p>Yield 36 %.</p> <p>IR = $\nu(\text{C}=\text{N})$ 1606 cm^{-1}, $\nu_{\text{as}}(\text{COO})$ = 1560 cm^{-1}, $\nu_{\text{s}}(\text{COO})$ = 1410 cm^{-1}.</p> <p>^1H NMR (400 MHz, CDCl_3) δ 7.73 (s, 2H, Hi), 6.96 (t, $^3J(\text{H}4\text{H}3)$ = 8.3 Hz, 2H, H4), 6.66 (d, $^3J(\text{H}3\text{H}4)$ = 8.3 Hz, 2H, H3), 6.47 (d, $^3J(\text{H}5\text{H}4)$ = 8.3 Hz, 2H, H5), 3.77 (s, 6H, OMe), 3.05 (m, $^3J(\text{HH})$ = 11.6 Hz, 2H, N-CH-Cy), 2.13 (s, 6H, OAc), 0.8–2.45 (m, 20H, Cy).</p>
<p>compound 1h</p> 	<p>Yield 53 %.</p> <p>IR = $\nu(\text{C}=\text{N})$ 1580 cm^{-1}, $\nu_{\text{as}}(\text{COO})$ = 1557 cm^{-1}, $\nu_{\text{s}}(\text{COO})$ = 1402 cm^{-1}.</p> <p>^1H NMR (400 MHz, CDCl_3) δ 7.71 (s, 2H, Hi), 7.12 (d, $^3J(\text{H}3\text{H}4)$ = 7.7 Hz, 2H, H3), 7.01 (d, $^3J(\text{H}5\text{H}4)$ = 7.7 Hz, 2H, H5), 6.86 (t, $^3J(\text{H}4\text{H}3)$ = 7.7 Hz, 2H, H4), 2.96 (m, 2H, N-CH-Cy), 2.14 (s, 6H, OAc), 0.8–2.45 (m, 20H, Cy).</p>

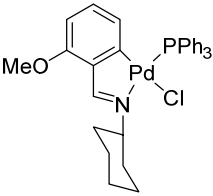
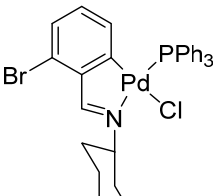
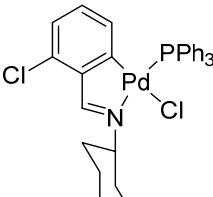
<p>compound 1i</p> 	<p>Yield 30 %.</p> <p>IR = $\nu(\text{C}=\text{N})$ 1577 cm^{-1}, $\nu_{\text{as}}(\text{COO})$ = 1558 cm^{-1}, $\nu_{\text{s}}(\text{COO})$ = 1406 cm^{-1}.</p> <p>^1H NMR (400 MHz, CDCl_3) δ 7.74 (s, 2H, Hi), 6.96 (s, 6H, H3, H4, H5), 2.99 (t, $^3J(\text{HH})$ = 12.0 Hz, 2H, N-CH-Cy), 2.14 (s, 6H, OAc), 0.8–2.50 (m, 20H, Cy).</p>
<p>compound 1j</p> 	<p>Yield 35 %.</p> <p>IR = $\nu(\text{C}=\text{N})$ 1615 cm^{-1}, $\nu_{\text{as}}(\text{COO})$ = 1574 cm^{-1}, $\nu_{\text{s}}(\text{COO})$ = 1408 cm^{-1}.</p> <p>^1H NMR (400 MHz, CDCl_3) δ 7.68 (s, 2H, Hi), 7.03 (d, $^3J(\text{H3F})$ = 6.5 Hz, 2H, H3), 6.92 (br s, 2H, H5), 6.66 (m, 2H, H4), 3.04 (m, 2H, N-CH-Cy), 2.15 (s, 6H, OAc), 0.8–2.5 (m, 20H, Cy).</p>
<p>compound 2c</p> 	<p>Yield 50 %.</p> <p>IR = $\nu(\text{C}=\text{N})$ 1597 cm^{-1}, $\nu(\text{Pd}-\text{Cl}_{\text{trans-N}})$ 332 cm^{-1}, $\nu(\text{Pd}-\text{Cl}_{\text{trans-C}})$ 278 cm^{-1}.</p> <p>^1H NMR (400 MHz, CDCl_3) δ 7.96 (s, 2H, Hi), 6.73 (s, 2H, H5), 3.95 (s, 6H, OMe), 3.89 (s, 6H, OMe), 3.78 (s, 6H, OMe), 3.58 (m, 2H, N-CH-Cy), 1.17–2.17 (m, 20H, Cy).</p>

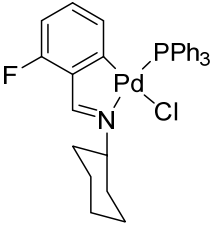
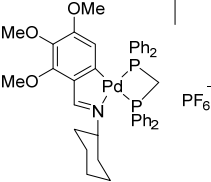
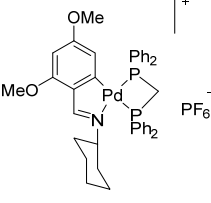
<p>compound 2d</p> 	<p>Yield 54 %.</p> <p>IR = $\nu(\text{C}=\text{N})$ 1599 cm^{-1}, $\nu(\text{Pd}-\text{Cl}_{\text{trans-N}})$ 293 cm^{-1}, $\nu(\text{Pd}-\text{Cl}_{\text{trans-C}})$ 268 cm^{-1}.</p> <p>^1H NMR (400 MHz, CDCl_3) δ 8.01 (s, 2H, Hi), 6.60 (s, 2H, H5), 6.08 (s, 2H, H3), 3.83 (s, 6H, OMe), 3.78 (s, 6H, OMe), 3.60 (s, 2H, N-CH-Cy), 1.17–2.19 (m, 20H, Cy).</p>
<p>compound 2e</p> 	<p>Yield 59 %.</p> <p>IR = $\nu(\text{C}=\text{N})$ 1595 cm^{-1}, $\nu(\text{Pd}-\text{Cl}_{\text{trans-N}})$ 322 cm^{-1}, $\nu(\text{Pd}-\text{Cl}_{\text{trans-C}})$ 266 cm^{-1}.</p> <p>^1H NMR (400 MHz, CDCl_3) δ 7.73 (s, 2H, Hi), 6.98 (s, 2H, H2), 6.79 (s, 2H, H5), 3.92 (s, 6H, OMe), 3.82 (s, 6H, OMe), 3.61 (m, 2H, N-CH-Cy), 2.19–1.0 (m, 20H, Cy).</p>
<p>compound 2f</p> 	<p>Yield 43 %.</p> <p>IR = $\nu(\text{C}=\text{N})$ 1600 cm^{-1}, $\nu(\text{Pd}-\text{Cl}_{\text{trans-N}})$ 320 cm^{-1}, $\nu(\text{Pd}-\text{Cl}_{\text{trans-C}})$ 262 cm^{-1}.</p> <p>^1H NMR (400 MHz, CDCl_3) δ 7.74 (s, 2H, Hi), 7.12 (d, $^3J(\text{H}2\text{H}3) = 8.5$ Hz, 2H, H2), 6.97 (s, 2H, H5), 6.57 (d, $^3J(\text{H}3\text{H}2) = 8.5$ Hz, 2H, H3), 3.83 (s, 6H, OMe), 3.64 (m, 2H, N-CH-Cy), 2.23–1.21 (m, 20H, Cy).</p>

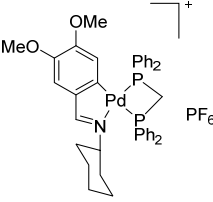
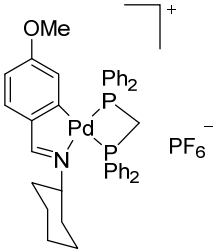
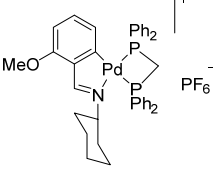
<p>compound 2g</p> 	<p>Yield 45 %.</p> <p>IR = $\nu(\text{C}=\text{N})$ 1599 cm^{-1}, $\nu(\text{Pd}-\text{Cl}_{\text{trans-N}})$ 350 cm^{-1}, $\nu(\text{Pd}-\text{Cl}_{\text{trans-C}})$ 278 cm^{-1}.</p> <p>^1H NMR (400 MHz, CDCl_3) δ 8.16 (s, 2H, Hi), 7.00 (br s, 4H, H3, H5), 6.53 (br s, 2H, H4), 3.80 (s, 6H, OMe), 2.21 (m, $^3J(\text{HH}) = 12.2$ Hz, 2H, N-CH-Cy), 1.24–2.21 (m, 20H, Cy).</p>
<p>compound 2h</p> 	<p>Yield 53 %.</p> <p>IR = $\nu(\text{C}=\text{N})$ 1606 cm^{-1}, $\nu(\text{Pd}-\text{Cl}_{\text{trans-N}})$ 340 cm^{-1}, $\nu(\text{Pd}-\text{Cl}_{\text{trans-C}})$ 270 cm^{-1}.</p> <p>^1H NMR (400 MHz, CDCl_3) δ 8.20 (s, 2H, Hi), 7.34 (d, $^3J(\text{H3H4}) = 7.9$ Hz, 2H, H3), 7.17 (d, $^3J(\text{H5H4}) = 7.8$ Hz, 2H, H5), 6.86 (t, $^3J(\text{H4H3}) = 7.9$ Hz, 2H, H4), 3.71 (m, 2H, N-CH-Cy). 1.28–2.25(m, 20H, Cy).</p>
<p>compound 2i</p> 	<p>Yield 50 %.</p> <p>IR = $\nu(\text{C}=\text{N})$ 1609 cm^{-1}, $\nu(\text{Pd}-\text{Cl}_{\text{trans-N}})$ 340 cm^{-1}, $\nu(\text{Pd}-\text{Cl}_{\text{trans-C}})$ 274 cm^{-1}.</p> <p>^1H NMR (400 MHz, CDCl_3) δ 8.21 (s, 2H, Hi), 6.97 (s, 3H, H3, H4, H5), 3.71 (m, 2H, N-CH-Cy), 1.0 – 2.25 (m, 20H, Cy).</p>

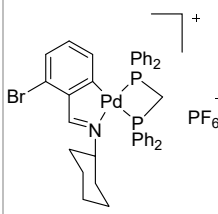
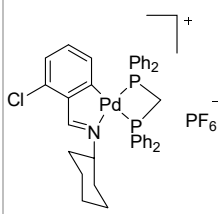
<p>compound 2j</p> 	<p>Yield 45 %.</p> <p>IR = $\nu(\text{C}=\text{N})$ 1615 cm^{-1}, $\nu(\text{Pd}-\text{Cl}_{\text{trans-N}})$ 348 cm^{-1}, $\nu(\text{Pd}-\text{Cl}_{\text{trans-C}})$ 287 cm^{-1}</p> <p>^1H NMR (400 MHz, CDCl_3) δ 8.12 (s, 2H, Hi), 7.18 (br s, 2H, H3), 7.05 (br s, 2H, H5), 6.72 (t, $^3J = 7.8$ Hz, 2H, H4), 3.72 (m, 2H, N-CH-Cy), 1.27 –2.25 (m, 20H, Cy).</p>
<p>compound 2k</p> 	<p>Yield 73 %.</p> <p>IR = $\nu(\text{C}=\text{N})$ 1598 cm^{-1}, $\nu(\text{Pd}-\text{Br}_{\text{trans-N}})$ 195 cm^{-1}, $\nu(\text{Pd}-\text{Br}_{\text{trans-C}})$ 160 cm^{-1}.</p> <p>^1H NMR (400 MHz, CDCl_3) δ 7.81 (s, 1H, Hi), 6.86 (s, 2H, Ha, Ha'), 5.93 (s, 1H, H5), 3.94 (s, 6H, OMe), 3.89 (s, 3H, OMe), 2.54 (s, 3H, Me), 2.27 (s, 6H, Me[*]).</p>
<p>compound 3c</p> 	<p>Yield 50 %.</p> <p>IR = $\nu(\text{C}=\text{N})$ 1569 cm^{-1}, $\nu(\text{Pd}-\text{Cl})$ 298 cm^{-1}.</p> <p>^1H NMR (400 MHz, CDCl_3) δ 8.26 (d, $^4J(\text{PHi}) = 9.1$ Hz, 1H, Hi), 7.67 (t, $^3J(\text{HH}) = 7.6$ Hz, 6H, PPh₃), 7.35 (t, $^3J(\text{HH}) = 7.6$ Hz, 3H, PPh₃), 7.29 (d, $^3J(\text{HH}) = 7.6$ Hz, 6H, PPh₃), 5.65 (d, $^4J(\text{H5P}) = 6.4$ Hz, 1H, H5), 4.33 (m, $^3J(\text{HH}) = 11.1$ Hz, 1H, N-CH-Cy), 3.86 (s, 3H, OMe), 3.61 (s, 3H, OMe), 2.72 (s, 3H, OMe), 2.17–0.79 (m, 10H, Cy).</p> <p>^{31}P NMR (δ ppm, CDCl_3) δ 42.86.</p>

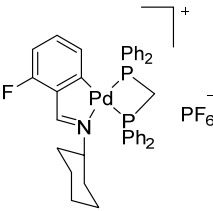
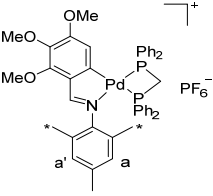
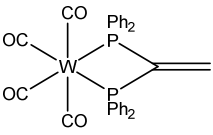
<p>compound 3d</p> 	<p>Yield 52 %. IR = $\nu(\text{C}=\text{N})$ 1577 cm^{-1}, $\nu(\text{Pd}-\text{Cl})$ 301 cm^{-1}. ^1H NMR (400 MHz, CDCl_3) δ 8.44 (d, $^4J(\text{PHi}) = 9.3$ Hz, 1H, Hi), 7.78 (m, 6H, PPh_3), 7.44 (t, $^3J(\text{HH}) = 7.0$ Hz, 3H, PPh_3), 7.37 (t, $^3J(\text{HH}) = 7.0$ Hz, 6H, PPh_3), 5.95 (d, $^4J(\text{H3H5}) = 2.1$ Hz, 1H, H3), 5.62 (dd, $^4J(\text{H5P}) = 6.6$ Hz, $^4J(\text{H5H3}) = 2.1$ Hz, 1H, H5), 4.42 (m, 1H, N-CH-Cy), 3.75 (s, 3H, OMe), 2.88 (s, 3H, OMe), 0.87–2.27 (m, 10H, Cy). ^{31}P NMR (δ ppm, CDCl_3) δ 43.08.</p>
<p>compound 3e</p> 	<p>Yield 62 %. IR = $\nu(\text{C}=\text{N})$ 1583 cm^{-1}, $\nu(\text{Pd}-\text{Cl})$ 295 cm^{-1}. ^1H NMR (400 MHz, CDCl_3) δ 8.05 (d, $^4J(\text{PHi}) = 9.1$ Hz, 1H, Hi), 7.73 (t, $^3J(\text{HH}) = 9.2$ Hz, 5H, PPh_3), 7.50–7.30 (m, 10H, PPh_3), 6.87 (s, 1H, H2), 5.97 (d, $^4J(\text{H5P}) = 6.5$ Hz, 1H, H5), 4.42 (m, $^3J(\text{HH}) = 11.9$ Hz, 1H, N-CH-Cy), 3.79 (s, 3H, OMe), 2.85 (s, 3H, OMe), 0.90–2.26 (m, 10H, Cy). ^{31}P NMR (δ ppm, CDCl_3) δ 43.80.</p>
<p>compound 3f</p> 	<p>Yield 59 %. IR = $\nu(\text{C}=\text{N})$ 1580 cm^{-1}, $\nu(\text{Pd}-\text{Cl})$ 296 cm^{-1}. ^1H NMR (400 MHz, CDCl_3) δ 8.06 (d, $^4J(\text{PHi}) = 10$ Hz, 1H, Hi), 7.86–7.70 (m, 6H, PPh_3), 7.49–7.42 (m, 3H, PPh_3), 7.39 (d, $^3J(\text{HH}) = 7.6$ Hz, 6H, PPh_3), 7.20 (dd, $^3J(\text{H3H2}) = 8.3$ Hz, $^4J(\text{H3H5}) = 2.3$ Hz, 1H, H3), 6.43 (d, $^3J(\text{H2H3}) = 8.3$ Hz, 1H, H2), 6.00 (d, $^4J(\text{H5P}) = 6.6$ Hz, 1H, H5), 4.45 (m, 1H, N-CH-Cy), 2.97 (s, 3H, OMe), 0.88–2.26 (m, 10H, Cy). ^{31}P NMR (δ ppm, CDCl_3) δ 43.41.</p>

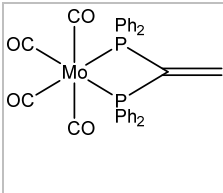
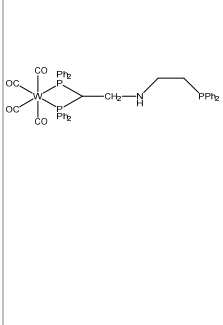
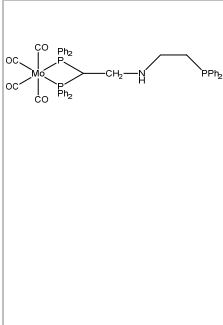
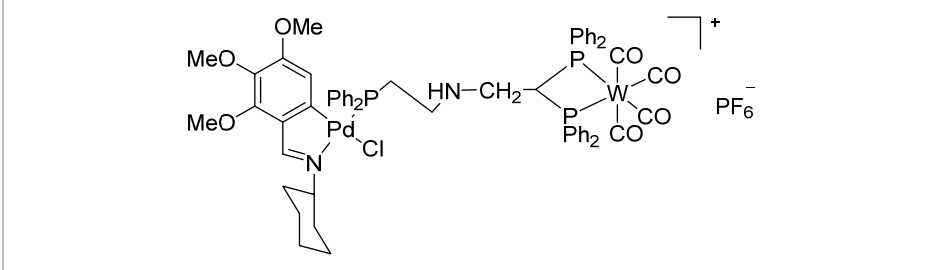
<p>compound 3g</p> 	<p>Yield 50 %. IR = $\nu(\text{C}=\text{N})$ 1560 cm^{-1}, $\nu(\text{Pd}-\text{Cl})$ 300 cm^{-1}.</p> <p>^1H NMR (400 MHz, CDCl_3) δ 8.59 (d, $^4J(\text{PHi}) = 8.9$ Hz, 1H, Hi), 7.84–7.73 (m, 6H, PPh_3), 7.46–7.39 (m, 3H, PPh_3), 7.37 (m, 6H, PPh_3), 6.51 (t, $^3J(\text{H4H3}) = 8.0$ Hz, 1H, H4), 6.40 (d, $^3J(\text{H3H4}) = 8.0$ Hz, 1H, H3), 6.00 (t, $^4J(\text{H5P}) = 6.9$ Hz, 1H, H5), 4.50 (m, 1H, N-CH-Cy), 3.79 (s, 3H, OMe), 0.87–2.30 (m, 10H, Cy). ^{31}P NMR (δ ppm, CDCl_3) δ 43.0.</p>
<p>compound 3h</p> 	<p>Yield 40 %. IR = $\nu(\text{C}=\text{N})$ 1574 cm^{-1}, $\nu(\text{Pd}-\text{Cl})$ 306 cm^{-1}.</p> <p>^1H NMR (400 MHz, CDCl_3) δ 8.62 (d, $^4J(\text{PHi}) = 8.4$ Hz, 1H, Hi), 7.76 (d, $^3J(\text{HH}) = 7.5$ Hz, 6H, PPh_3), 7.45 (d, $^3J(\text{HH}) = 7.5$ Hz, 3H, PPh_3), 7.39 (d, $^3J(\text{HH}) = 7.5$ Hz, 6H, PPh_3), 7.01 (m, 1H, H4), 6.34 (d, N = 2.5 Hz, 2H, H3 and H5), 4.52 (m, $^3J(\text{HH}) = 12.3$ Hz, 1H, N-CH-Cy), 0.8–2.30 (m, 10H, Cy).</p> <p>^{31}P NMR (δ ppm, CDCl_3) δ 42.58.</p>
<p>compound 3i</p> 	<p>Yield 30 %. IR = $\nu(\text{C}=\text{N})$ 1574 cm^{-1}, $\nu(\text{Pd}-\text{Cl})$ 300 cm^{-1}.</p> <p>^1H NMR (400 MHz, CDCl_3) δ 8.62 (d, $^4J(\text{PHi}) = 5.2$ Hz, 1H, Hi), 7.73 (d, $^3J(\text{HH}) = 7.6$ Hz, 6H, PPh_3), 7.53–7.39 (m, 9H, PPh_3), 6.84 (d, $^3J(\text{H3H4}) = 7.9$ Hz, 1H, H3), 6.44 (t, $^3J(\text{H4H3}) = ^3J(\text{H4H5}) = 7.9$ Hz, 1H, H4), 6.30 (d, $^3J(\text{H5H4}) = 7.9$ Hz, 1H, H5), 4.53 (m, $^3J(\text{HH}) = 11.6$ Hz, 1H, N-CH-Cy), 0.9–2.30 (m, 10H, Cy). ^{31}P NMR (δ ppm, CDCl_3) δ 42.80.</p>

<p>compound 3j</p> 	<p>Yield 42 %. IR = $\nu(\text{C}=\text{N})$ 1580 cm^{-1} $\nu(\text{Pd}-\text{Cl})$ 305 cm^{-1}.</p> <p>^1H NMR (400 MHz, CDCl_3) δ 8.49 (d, $^4J(\text{PHi}) = 8.6$ Hz, 1H, Hi), 7.84–7.67 (m, 6H, PPh_3), 7.49–7.32 (m, 9H, PPh_3), 6.55 (t, $^3J(\text{H3H4}) = 6.5$ Hz, 2H, H3, H4), 6.16 (t, $^3J(\text{H5H4}) = ^4J(\text{H5P}) = 6.5$ Hz, 1H, H5), 4.54 (m, $^3J(\text{HH}) = 11.2$ Hz, 1H, N-CH-Cy), 0.87–2.30 (m, 10H, Cy). ^{31}P NMR (δ ppm, CDCl_3) δ 42.90.</p>
<p>compound 4c</p> 	<p>Yield 56 %. IR = $\nu(\text{C}=\text{N})$ 1565 cm^{-1}.</p> <p>^1H NMR (400 MHz, CDCl_3) δ 8.39 (d, $^4J(\text{PHi}) = 7.6$ Hz, 1H, Hi), 7.79–7.36 (m, 20H, PPh_2), 5.94 (t, $^4J(\text{H5P}) = 9.7$ Hz, 1H, H5), 4.30 (t, $^2J(\text{HP}) = 10.1$ Hz, 2H, PCH_2P), 4.00 (s, 3H, OMe), 3.76 (s, 3H, OMe), 3.23 (m, 1H, N-CH-Cy), 3.09 (s, 3H, OMe), 2.37–0.57 (m, 10H, Cy). ^{31}P NMR (δ ppm, CDCl_3) δ -4.33 (d, $J = 62.9$ Hz), -27.53 (d, $J = 62.9$ Hz), -141.31 (heptuplet, PF_6^-).</p>
<p>compound 4d</p> 	<p>Yield 67 %. IR = $\nu(\text{C}=\text{N})$ 1574 cm^{-1}.</p> <p>^1H NMR (400 MHz, CDCl_3) δ 8.42 (d, $^4J(\text{PHi}) = 7.9$ Hz, 1H, Hi), 7.80–7.32 (m, 20H, PPh_2), 6.05 (s, 1H, H3), 5.78 (br s, 1H, H5), 4.23 (m, 2H, PCH_2P), 3.76 (s, 3H, OMe), 3.18 (s, 3H, OMe), 0.6–2.33 (m, 11H, Cy). ^{31}P NMR (δ ppm, CDCl_3) δ -4.56 (d, $J = 59.6$ Hz), -27.78 (d, $J = 59.6$ Hz), -145.73 (heptuplet, PF_6^-).</p>

<p>compound 4e</p> 	<p>Yield 68 %. IR = $\nu(\text{C}=\text{N})$ 1580 cm^{-1}.</p> <p>^1H NMR (400 MHz, CDCl_3) δ 8.16 (br s, 1H, Hi), 7.82–7.35 (m, 20H, PPh_2), 7.05 (s, 1H, H2), 6.15 (br s, 1H, H5), 4.27 (m, 2H, PCH_2P), 3.84 (s, 3H, OMe), 3.27 (m, 1H, N-CH-Cy), 3.10 (s, 3H, OMe), 0.6–2.36 (m, 10H, Cy). ^{31}P NMR (δ ppm, CDCl_3) δ -2.88 (d, $J = 58.8$ Hz), -27.33 (d, $J = 58.8$ Hz), -141.28 (heptuplet, PF_6^-).</p>
<p>compound 4f</p> 	<p>Yield 82 %. IR = $\nu(\text{C}=\text{N})$ 1574 cm^{-1}.</p> <p>^1H NMR (400 MHz, CDCl_3) δ 8.15 (d, $^4J(\text{PHi}) = 7.6$ Hz, 1H, Hi), 7.80–7.38 (m, 20H, PPh_2), 7.37 (d, $^3J(\text{H2H3}) = 8.3$ Hz, 1H, H2), 6.59 (dd, $^3J(\text{H3H2}) = 8.3$ Hz, $^4J(\text{H3H5}) = 2.3$ Hz, 1H, H3), 6.22 (ddd, $^4J(\text{H5H3}) = 2.3$ Hz, $^4J(\text{H5P}_{\text{cis}}) = 8.1$ Hz, $^4J(\text{H5P}_{\text{trans}}) = 10.4$ Hz, 1H, H5), 4.28 (dd, $^2J(\text{HP}) = 11.3, 8.1$ Hz, 2H, PCH_2P), 3.30 (s, 3H, OMe), 3.27 (m, 1H, N-CH-Cy), 0.6–2.20 (m, 10H, Cy). ^{31}P NMR (δ ppm, CDCl_3) δ -4.12 (d, $J = 61.0$ Hz), -27.74 (d, $J = 61.0$ Hz), -141.29 (heptuplet, PF_6^-).</p>
<p>compound 4g</p> 	<p>Yield 50 %. IR = $\nu(\text{C}=\text{N})$ 1565 cm^{-1}.</p> <p>^1H NMR (400 MHz, CDCl_3) δ 8.62 (d, $^4J(\text{PHi}) = 7.6$ Hz, 1H), 7.81–7.38 (m, 20H), 6.89 (t, $^3J(\text{H4H3}) = ^3J(\text{H4H5}) = 7.9$ Hz, 1H, H4), 6.62 (d, $^3J(\text{H3H4}) = 7.9$ Hz, 1H, H3), 6.28 (d, $^3J(\text{H5H4}) = 7.9$ Hz, 1H, H5), 4.22 (t, $^2J(\text{HP}) = 9.8$ Hz, 2H, PCH_2P), 3.83 (s, 3H, OMe), 3.31 (m, 1H, N-CH-Cy), 0.6–1.99 (m, 10H, Cy). ^{31}P NMR (162 MHz, CDCl_3) δ -4.65 (d, J</p>

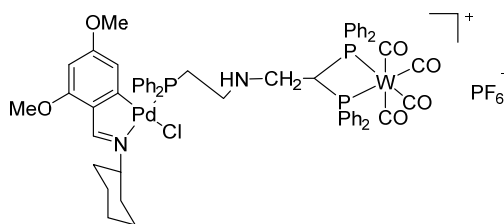
	<p>= 59.9 Hz), -28.50 (d, $J = 59.9$ Hz), -141.31 (heptuplet, PF_6^-).</p>
<p>compound 4h</p> 	<p>Yield 92 %.</p> <p>IR = $\nu(\text{C}=\text{N})$ 1560 cm^{-1}.</p> <p>^1H NMR (400 MHz, CDCl_3) δ 8.67 (d, $^4J(\text{PHi}) = 5.5$ Hz, 1H, Hi), 7.83–7.34 (m, 20H, PPh_2), 7.22 (d, $^3J(\text{H3H4}) = 7.5$ Hz, 1H, H3), 6.72 (t, $^3J(\text{H4H3}) = ^3J(\text{H4H5}) = 7.5$ Hz 1H, H4), 6.64 (d, $^3J(\text{H5H4}) = 7.5$ Hz, 1H, H5), 4.30 (t, $^2J(\text{HP}) = 9.9$ Hz, 2H, PCH_2P), 3.38 (m, $J = 12.5$ Hz, 1H, N-CH-Cy), 0.6–2.20(m, 10H, Cy).</p> <p>^{31}P NMR (δ ppm, CDCl_3) δ -4.82 (d, $J = 61.0$ Hz), -29.22 (d, $J = 61.0$ Hz), -141.28 (heptuplet, PF_6^-).</p>
<p>compound 4i</p> 	<p>Yield 82%.</p> <p>IR = $\nu(\text{C}=\text{N})$ 1562 cm^{-1}.</p> <p>^1H NMR (400 MHz, CDCl_3) δ 8.67 (br s, 1H, Hi), 7.82–7.33 (m, 20H, PPh_2), 7.03 (d, $^3J(\text{H3H4}) = 7.8$ Hz, 1H, H3), 6.81 (t, $^3J(\text{H4H5}) = ^3J(\text{H4H3}) = 7.8$ Hz, 1H, H4), 6.59 (d, $^3J(\text{H5H4}) = 7.8$ Hz, 1H, H5), 4.29 (br s, 2H, PCH_2P), 3.41 (m, 1H, N-CH-Cy), 0.6–2.37 (m, 10H, Cy).</p> <p>^{31}P NMR (δ ppm, CDCl_3) δ -3.50 (d, $J = 69.7$ Hz), -28.96 (d, $J = 69.7$ Hz), -143.48 (heptuplet, PF_6^-).</p>

<p>compound 4j</p> 	<p>Yield 71 %.</p> <p>IR = $\nu(\text{C}=\text{N})$ 1588 cm^{-1}.</p> <p>^1H NMR (400 MHz, CDCl_3) δ 8.53 (br s, 1H, Hi), 7.81–7.33 (m, 20H, PPh₂), 6.93 (t, $^3J(\text{H4H3}) = 5.7$ Hz, 1H, H4), 6.76 (t, $^3J(\text{H3F}) = ^3J(\text{H3H4}) = 9.2$ Hz, 1H, H3), 6.49 (d, $^3J(\text{PH5}) = 7.6$ Hz, 1H, H5), 4.30 (br s, 2H, PCH₂P), 3.47–3.31 (m, 1H, N-CH-Cy), 0.6–2.20 (m, 10H, Cy).</p> <p>^{31}P NMR (δ ppm, CDCl_3) δ -4.96 (d, $J = 67.0$ Hz), -29.35 (d, $J = 67.0$ Hz), -152.28 (heptuplet, PF_6^-).</p>
<p>compound 3k</p> 	<p>Yield 85 %.</p> <p>IR = $\nu(\text{C}=\text{N})$ 1565 cm^{-1}.</p> <p>^1H NMR (400 MHz, CDCl_3) δ 8.20 (d, $^4J(\text{PHi}) = 7.6$ Hz, 1H, Hi), 8.06–6.99 (m, 20H, PPh₂), 6.68 (s, 2H, Ha, Ha'), 6.03 (dd, $^4J(\text{H5P}_{\text{trans}}) = 10.4$ Hz, $^4J(\text{H5P}_{\text{cis}}) = 7.6$ Hz, 1H, H5), 4.27 (dd, $^2J(\text{HP}) = 12.0$ Hz, 8.0 Hz, 2H, PCH₂P), 3.99 (s, 3H, OMe), 3.79 (s, 3H, OMe), 3.17 (s, 3H, OMe), 2.25 (s, 3H, Me), 2.18 (s, 6H, Me*). ^{31}P-$\{^1\text{H}\}$ NMR (CDCl_3, δ ppm) -6.0 (d, $J = 66.5$), -30 (d, $J = 66.5$), -141 (heptuplet, PF_6^-).</p>
	<p>^1H NMR (400 MHz, CDCl_3) δ 7.59–7.29 (m, 20H, PPh₂), 5.58 (t, $J = 24.8$ Hz, 2H, PC(CH₂)P).</p> <p>^{31}P NMR (162 MHz, CDCl_3) δ 8.80.</p>

	$^1\text{H NMR}$ (400 MHz, CDCl_3) δ 7.61 – 7.29 (m, 20H, PPh_2), 5.63 (m, 2H, $\text{PC}(\text{CH}_2)\text{P}$). $^{31}\text{P NMR}$ (162 MHz, CDCl_3) δ 29.14.
	$^1\text{H NMR}$ (400 MHz, CDCl_3) δ 7.81 – 7.28 (m, 30H, PPh_2), 4.90 (t, $^2J = 8.2$ Hz, 1H, PCHP), 2.88–2.31 (m, 4H, CH_2CH_2), 1.98 (t, $^3J(\text{HH}) = 7.4$ Hz, 2H, CH_2). $^{31}\text{P NMR}$ (162 MHz, CDCl_3) δ ca. 32, 31, -1.98, -20.4, -20.93.
	$^1\text{H NMR}$ (400 MHz, CDCl_3) δ 7.72–7.23 (m, 30H, PPh_2), 4.57 (m, 1H, PCHP), 2.78–2.20 (m, 4H, CH_2CH_2), 1.87 (t, $J = 7.5$ Hz, 2H, CH_2). $^{31}\text{P NMR}$ (162 MHz, CDCl_3) δ 32.65, 31.56, 22.36, -20.36, -20.97.
compound 5c	
	
Yield 86 %. IR = $\nu(\text{C}=\text{N})$ 1571 cm^{-1} , $\nu(\text{C}\equiv\text{O})$ 1862 (w s), 1885, 2021 cm^{-1} , $\nu(\text{Pd}-\text{Cl})$ 293 cm^{-1} .	
$^1\text{H NMR}$ (400 MHz, CDCl_3) δ 8.27 (d, $^4J(\text{PHi}) = 8.1$ Hz, 1H, Hi), 7.78–7.21 (m, 30H, PPh_2), 5.76 (d, $^4J(\text{H5P}) = 5.8$ Hz, 1H, H5), 4.74 (br s, 1H, PCHP), 3.87 (s, 3H, OMe), 3.63 (s, 3H, OMe), 3.47 (m, 1H,	

N-CH-Cy), 2.95 (s, 3H, OMe), 2.40–2.60 (m, 4H, CH₂-CH₂), 1.83 (d, ³J(HH) = 13.3 Hz, 2H, CH₂), 0.75–1.70 (m, 10H, Cy).
³¹P NMR (162 MHz, CDCl₃) δ 51.47 (s, PPh₂), 35.92 (s), -2.18 (s, PCHP), -143.40 (heptuplet, PF₆⁻).

compound 5d

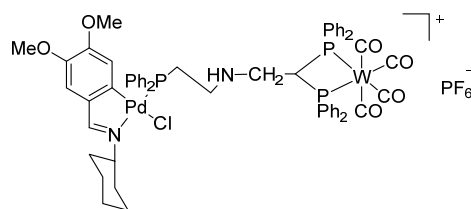


Yield = 96 %. IR = ν(C=N) 1579 cm⁻¹, ν(C≡O) 1864 (w s), 1885, 2012 cm⁻¹, ν(Pd-Cl) 292 cm⁻¹.

¹H NMR (400 MHz, CDCl₃) δ 8.34 (d, ⁴J(PHi) = 8.3 Hz, 1H, Hi), 7.79 – 7.21 (m, 30H, PPh₂), 5.92 (s, 1H, H3), 5.65 (d, ⁴J(H5P) = 5.9 Hz, 1H, H5), 4.82 (br s, 1H, PCHP), 3.67 (s, 3H, OMe), 3.50 (m, 1H, N-CH-Cy), 3.05 (s, 3H, OMe), 2.64 – 2.31 (m, 4H, CH₂-CH₂), 1.81 (d, ³J(HH) = 12.4 Hz, 2H, CH₂), 0.78 – 1.70 (m, 10H, Cy).

³¹P NMR (162 MHz, CDCl₃) δ 50.98 (s, PPh₂), 35.59 (s), -2.17 (s, PCHP), -141.17 (heptuplet, PF₆⁻).

compound 5e

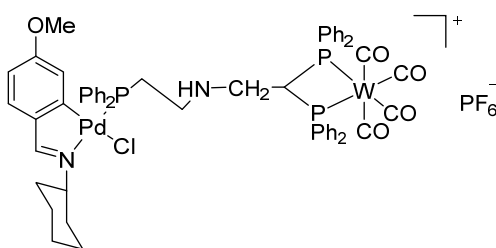


Yield = 94 %. IR = ν(C=N) 1586 cm⁻¹, ν(C≡O) 1865 (w s), 1888, 2012 cm⁻¹, ν(Pd-Cl) 294 cm⁻¹.

^1H NMR (400 MHz, CDCl_3) δ 8.07 (d, $^4J(\text{PHi}) = 7.7$ Hz, 1H, Hi), 7.89–7.31 (m, 30H, PPh_2), 6.93 (s, 1H, H2), 6.09 (d, $^4J(\text{H5P}) = 5.6$ Hz, 1H, H5), 4.99 (br s, 1H, PCHP), 3.80 (s, 3H, OMe), 3.57 (m, 1H, N-CH-Cy), 3.07 (s, 3H, OMe), 2.76–2.45 (m, 4H, $\text{CH}_2\text{-CH}_2$), 1.93 (d, $^3J(\text{HH}) = 13.6$ Hz, 2H, CH_2), 0.87–1.90 (m, 10H, Cy).

^{31}P NMR (162 MHz, CDCl_3) δ 51.97 (s, PPh_2), 36.50 (s), -2.21 (s, PCHP), -145.55 (heptuplet, PF_6^-).

compound **5f**

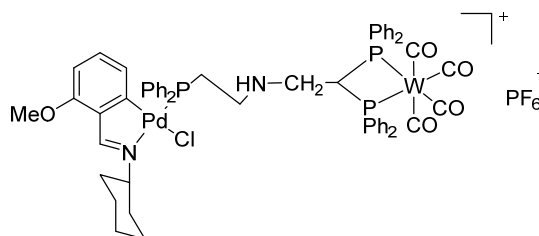


Yield 88 %. IR = $\nu(\text{C=N})$ 1580 cm^{-1} , $\nu(\text{C}\equiv\text{O})$ 1862 (w s), 1891, 2015 cm^{-1} , $\nu(\text{Pd-Cl})$ 296 cm^{-1} .

^1H NMR (400 MHz, CDCl_3) δ 7.97 (d, $^4J(\text{PHi}) = 7.3$ Hz, 1H, Hi), 7.77–7.20 (m, 30H, PPh_2), 6.41 (dd, $^3J(\text{H3H2}) = 8.3$ Hz, $^4J(\text{H3H5}) = 2.4$ Hz, 1H, H3), 6.06 (br s, 1H, H5), 4.82 (d, $^3J(\text{HH}) = 12.3$ Hz, 1H, PCHP), 3.50 (m, 1H, N-CH-Cy), 3.15 (s, 3H, OMe), 2.61–2.38 (m, 4H, $\text{CH}_2\text{-CH}_2$), 1.80 (d, $^3J(\text{HH}) = 10.4$ Hz, 2H, CH_2), 0.77–1.70 (m, 10H, Cy).

^{31}P NMR (162 MHz, CDCl_3) δ 51.22 (s, PPh_2), 35.87 (s), -2.20 (s, PCHP), -141.17 (heptuplet, PF_6^-).

compound **5g**

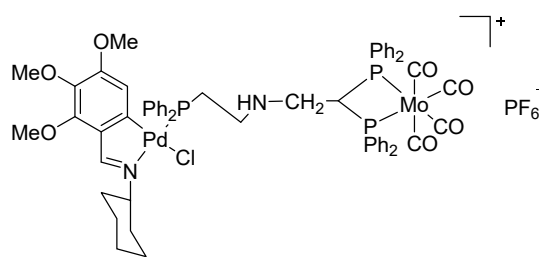


Yield 76 %. IR = $\nu(\text{C}=\text{N})$ 1572 cm^{-1} , $\nu(\text{C}\equiv\text{O})$ 1861 (w s), 1885, 2014 cm^{-1} , $\nu(\text{Pd}-\text{Cl})$ 298 cm^{-1} .

^1H NMR (400 MHz, CDCl_3) δ 8.58 (d, $^4J(\text{PHi}) = 8.1$ Hz, 1H, Hi), 7.89–7.30 (m, 30H, PPh_2), 6.72 (t, $^3J(\text{H4H3}) = 8.0$ Hz, 1H, H4), 6.50 (d, $^3J(\text{H3H4}) = 8.0$ Hz, 1H, H3), 6.18 (dd, $^3J(\text{H5H4}) = 8.0$, $^4J(\text{PH5}) = 5.5$ Hz, 1H, H5), 4.92 (m, 1H, PCHP), 3.87 (s, 3H, OMe), 3.24 (m, 1H, N-CH-Cy), 2.44–2.65 (m, 4H, CH_2CH_2), 1.92 (d, $^3J(\text{HH}) = 11.7$ Hz, 2H, CH_2), 0.88–1.78 (m, 10H, Cy).

^{31}P NMR (162 MHz, CDCl_3) δ 50.72 (s, PPh_2), 35.64 (s), -2.21 (s, PCHP), -145.57 (heptuplet, PF_6^-).

compound **6c**



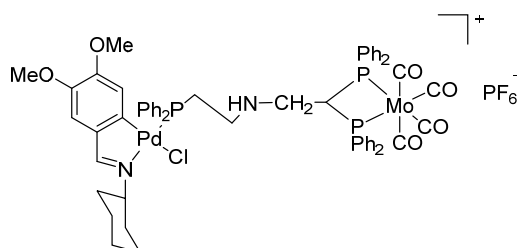
Yield 75 %. IR = $\nu(\text{C}=\text{N})$ 1571 cm^{-1} , $\nu(\text{C}\equiv\text{O})$ 1832, 1877, 1900, 2015 cm^{-1} , $\nu(\text{Pd}-\text{Cl})$ 302 cm^{-1} .

^1H NMR (400 MHz, CDCl_3) δ 8.36 (d, $^4J(\text{PHi}) = 8.2$ Hz, 1H, Hi), 8.00–7.29 (m, 30H, PPh_2), 5.86 (d, $^4J(\text{H5P}) = 5.4$ Hz, 1H, H5), 3.96 (s, 3H, OMe), 3.74 (s, 3H, OMe), 3.46 (m, 1H, N-CH-Cy), 3.04 (s,

3H, OMe), 2.76–2.39 (m, 4H, CH₂CH₂), 1.91 (d, ³J(HH) = 14.2 Hz, 2H, CH₂), 0.8–1.88 (m, 10H, Cy).

³¹P NMR (162 MHz, CDCl₃) δ 51.53 (s, PPh₂), -141.20 (heptuplet, PF₆⁻).

Compound 6d

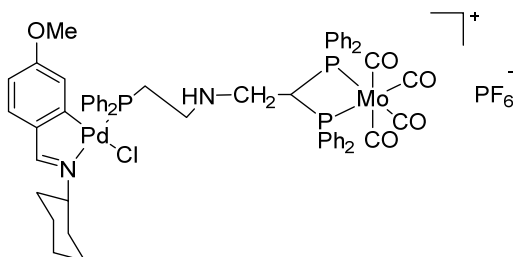


Yield 88 %. IR = $\nu(\text{C}=\text{N})$ 1589 cm⁻¹, $\nu(\text{C}\equiv\text{O})$ 1833, 1877, 1894, 2018 cm⁻¹, $\nu(\text{Pd}-\text{Cl})$ 294 cm⁻¹.

¹H NMR (400 MHz, CDCl₃) δ 8.09 (d, ⁴J(PHi) = 7.00 Hz, 1H, Hi), 7.89–7.30 (m, 30H, PPh₂), 6.82 (s, 1H, H2), 5.96 (d, ⁴J(H5P) = 5.5 Hz, 1H, H5), 4.25 (br s, 1H, PCHP), 3.80 (s, 3H, OMe), 3.58 (m, 1H, N-CH-Cy), 3.06 (s, 3H, OMe), 2.75–2.43 (m, 4H, CH₂CH₂), 1.90 (d, ³J(HH) = 11.2 Hz, 2H, CH₂), 0.89–1.88 (m, 10H, Cy).

³¹P NMR (162 MHz, CDCl₃) δ 52.33 (s, PPh₂), 32.28 (s), -143.29 (heptuplete, PF₆⁻).

compound 6e

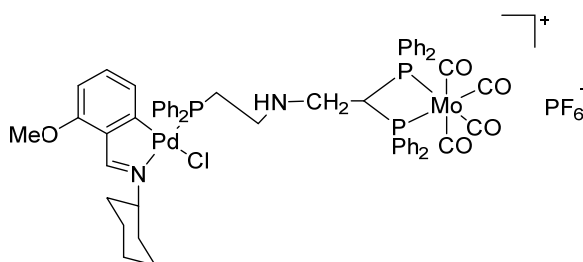


Yield 81 %. IR = $\nu(\text{C}=\text{N})$ 1577 cm⁻¹, $\nu(\text{C}\equiv\text{O})$ 1833 (w s), 2015 cm⁻¹, $\nu(\text{Pd}-\text{Cl})$ 295 cm⁻¹.

^1H NMR (400 MHz, CDCl_3) δ 8.08 (d, $^4J(\text{PHi}) = 8.0$ Hz, 1H, Hi), 7.87–6.99 (m, 30H, PPh_2), 6.57 (d, $^3J(\text{H}_2\text{H}_3) = 8.0$ Hz, 1H, H₂), 6.51 (dd, $^3J(\text{H}_3\text{H}_2) = 8.0$, $^4J(\text{H}_3\text{H}_5) = 2.3$ Hz, 1H, H₃), 6.14 (dd, $^4J(\text{H}_3\text{H}_5) = 2.2$ Hz, $^4J(\text{H}_5\text{P}) = 6.0$ Hz, 1H, H₅), 4.99 (m, 1H, PCHP), 3.63 (m, 1H, N-CH-Cy), 3.24 (s, 3H, OMe), 2.67 (d, $^3J(\text{HH}) = 10.2$ Hz, 2H, CH_2), 2.51 (d, $^3J = 4.8$ Hz, 2H, CH_2), 1.91 (d, $^3J(\text{HH}) = 12.2$ Hz, 2H, CH_2), 0.88–2.06 (m, 10H, Cy).

^{31}P NMR (162 MHz, CDCl_3) δ 51.60 (s, PPh_2), 35.25 (s, PCHP), -145.73 (heptuplet, PF_6^-).

compound **6f**

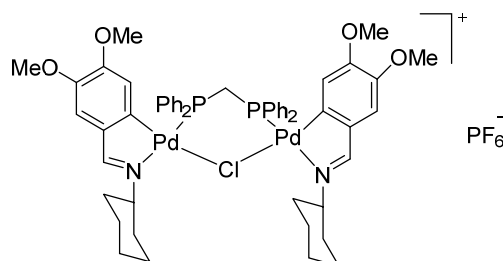


Yield 73 %. IR = $\nu(\text{C}=\text{N})$ 1572 cm^{-1} , $\nu(\text{C}\equiv\text{O})$ 1833, 1897, 1900, 2018 cm^{-1} , $\nu(\text{Pd}-\text{Cl})$ 300 cm^{-1} .

^1H NMR (400 MHz, CDCl_3) δ 8.58 (d, $^4J(\text{PHi}) = 8.1$ Hz, 1H, Hi), 7.91–7.28 (m, 30H, PPh_2), 6.72 (t, $^3J(\text{H}_4\text{H}_3) = 8.0$ Hz, 1H, H₄), 6.49 (d, $^3J(\text{H}_3\text{H}_4) = 8.0$ Hz, 1H, H₃), 6.15 (t, $^3J(\text{H}_5\text{P}) = 6.8$ Hz, 1H, H₅), 4.95 (m, 1H, PCHP), 3.81 (s, 3H, OMe), 3.50 (m, 1H, N-CH-Cy), 2.68–2.39 (m, 4H, CH_2CH_2), 1.92 (d, $^3J(\text{HH}) = 12.4$ Hz, 2H, CH_2), 0.87–2.02 (m, 10H, Cy).

^{31}P NMR (162 MHz, CDCl_3) δ 50.72 (s, PPh_2), 35.05 (s, PCHP), -141.17 (heptuplet, PF_6^-).

compound **7e**

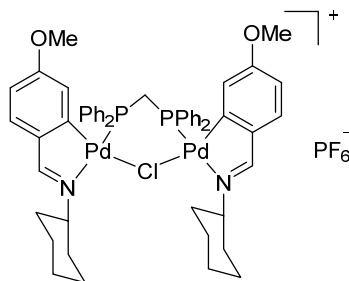


Yield: 62 %. IR = $\nu(\text{C}=\text{N})$ 1586 cm^{-1} , $\nu(\text{Pd}-\text{Cl})$ 260 cm^{-1} .

^1H NMR (400 MHz, CDCl_3) 8.76 (s, 2H, Hi), 8.0 – 7.30 (m, 20H, PPh_2), 6.98 (s, 1H, H2), 6.90 (s, 1H, H2), 5.64 (d, $^4J(\text{H5P}) = 6.6$ Hz, 2H, H5), 4.04 (s, 3H, OMe), 4.02 (s, 3H, OMe), 3.9 (m, 2H, PCH_2P), 3.78 (s, 3H, OMe), 3.65 (m, 1H, N-CH-Cy), 2.80 (s, 3H, OMe), 0.85 – 2.37 (m, 20H, Cy).

^{31}P NMR (162 MHz, CDCl_3) 30.4 (s), -141.66 (heptuplet, PF_6^-).

compound **7f**



Yield: 70 %. IR = $\nu(\text{C}=\text{N})$ 1580 cm^{-1} , $\nu(\text{Pd}-\text{Cl})$ 266 cm^{-1} .

^1H NMR (400 MHz, CDCl_3) 8.55 (d, $^4J(\text{PHi}) = 9.1$ Hz, 2H, Hi), 7.20 – 8.0 (m, 20H, PPh_2), 7.0 (d, $^3J(\text{H2H3}) = 8.3$ Hz, 2H, H2), 6.45 (dd, $^3J(\text{H3H2}) = 8.3$ Hz, $^4J(\text{H3H5}) = 2.3$ Hz, 2H, H3), 5.66 (d, $^4J(\text{H5P}) = 4.4$ Hz, 2H, H5), 4.43 (m, 2H, PCH_2P), 3.90 (s, 3H, OMe), 3.68 (m, 2H, N-CH-Cy), 3.0 (s, 3H, OMe), 0.85-2.36 (m, 20H, Cy).

^{31}P NMR (162 MHz, CDCl_3) 29.5 (s), -141.66 (heptuplet, PF_6^-).

CHAPTER 8

Palladacycles with tridentate [C, N, S] Schiff bases imine ligands.

8.1 Short biographies

Palladacycles with a $\sigma(\text{Pd}/\text{Csp}^2)$ or $\sigma(\text{Pd}/\text{Csp}^3)$ bond and a bidentate [C, X] [X = N, P, O] ligand or a tridentate [C, X, Y] or [X, C, Y] [X, Y = N, P, O] ligand have been described.^{139,140} Few articles focus on cyclopalladated compounds with tridentate [C, N, S] ligands,^{141,142,143} other than the thiosemicarbazone complexes. For example, palladacycles are generated exclusively by the activation of $\sigma(\text{Csp}^2, \text{phenyl-H})$ bonds of benzylthio- or benzosulfinyl substituted azobenzenes (Figure 97).^{144,145} Furthermore, cyclopalladated compounds containing a [Csp³, N, S] chelating ligand are even more scarce.¹⁴⁶

¹³⁹ J. Vicente, J.-A. Abad, W. Förtsch, P.G. Jones, A.K. Fischer, *Organometallics*, 20 (2001) 2704-2715.

¹⁴⁰ (a) C. Cativiela, L.R. Falvello, J.C. Ginés, R. Navarro, E.P. Urriolabeitia, *New Journal of Chemistry*, 25 (2001) 344-352. (b) M.A. Stark, G. Jones, C.J. Richards, *Organometallics*, 19 (2000) 1282-1291.

¹⁴¹ S. Chattopadhyay, C. Sinha, P. Basu, A. Chakravorty, *Organometallics*, 10 (1991) 1135-1139.

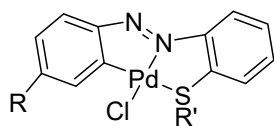
¹⁴² C. Sinha, D. Bandyopadhyay, A. Chakravorty, *Inorganic Chemistry*, 27 (1988) 1173-1178.

¹⁴³ C.K. Pal, S. Chattopadhyay, C. Sinha, A. Chakravorty, *Journal of organometallic chemistry*, 439 (1992) 91-99.

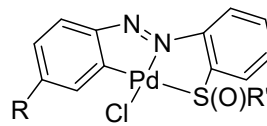
¹⁴⁴ K. Kamaraj, D. Bandyopadhyay, *Organometallics*, 18 (1999) 438-446.

¹⁴⁵ P. Wadhvani, D. Bandyopadhyay, *Organometallics*, 19 (2000) 4435-4436.

¹⁴⁶ C. López, S. Pérez, X. Solans, M. Font-Bardia, *Journal of organometallic chemistry*, 650 (2002) 258-267.



R = Me, R' = Me (1a)
 R = Me, R' = CH₂Ph (1b)
 R = Me, R' = CH₂CH₂Cl (1c)
 R = Cl, R' = CH₂Ph (1d)



R = H, R' = Me (2a), CH₂Ph (2b)
 R = 4-Me, R' = Me (2c)
 R = 5-Me, R' = Me (2d)

Figure 97. cyclopalladated compounds containing tridentate [C, N, S] ligands.

The sulfur atom forms a strong bond with the metal ion, palladium(II) or platinum(II), making the ligands excellent pincer species that protect three of the metal ion's four coordination positions, leaving only the fourth coordination site open for further reaction with nucleophiles like tertiary phosphines. In contrast to the breakage of the oxygen- or nitrogen-metal links of the chelate ring reported in the situations of semicarbazone or Schiff base ligands, the palladium(II) or platinum(II) sulfur bond remains uncleaved even when powerfully chelating diphosphines are used. Another fascinating aspect of these ligands is the tetrameric nature of the compounds formed when the ligand is treated with the appropriate metal salt; these are cyclometallated thiosemicarbazone Pd₄ or Pt₄ compounds, which also form polymers via hydrogen bonding.¹⁴⁷

¹⁴⁷ M.T. Pereira, J.M. Antelo, L.A. Adrio, J. Martinez, J.M. Ortigueira, M. Lopez-Torres, J.M. Vila, *Organometallics*, 33 (2014) 3265-3274.

As part of the work aimed at synthesizing and characterizing palladacycles *via* the (Csp², phenyl-H) bond activation of tridentate [C, N, S] Schiff base ligands, the mononuclear compounds [Pd{2-Cl-C₆H₃-CH=N-C₆H₄-SMe}Cl], [Pd{3-Br-C₆H₃-CH=N-C₆H₄-SMe}Cl] and [Pd{4-Br-C₆H₃-CH=N-C₆H₄-SMe}Cl] have been prepared and characterized. C-H activation was carried out using Li₂[PdCl₄], which gave mononuclear species, with terminal palladium-chloride bonds. In addition to studying their reactivity versus phosphine ligands.

8.1.1 Synthesis of the Schiff base ligand **l-n**.

The synthesized products are Schiff bases, which are made in a single step from the condensation of the primary amine and the corresponding aldehyde.¹⁴⁸

In 100 mL Schlenk round bottom flask, the appropriate amount of 4-Br-benzaldehyde (**l**), 3-Br-benzaldehyde (**m**), and 2-Cl-benzaldehyde (**n**) was added with the corresponding amount of 2-methylthioaniline in ethanol (40 cm³). The resulting solution was refluxed for 4 hours with magnetic stirring, after which it was cooled to room temperature and the solvent evaporated, to give a yellow solid for **l** and **m**, and green for **n**.

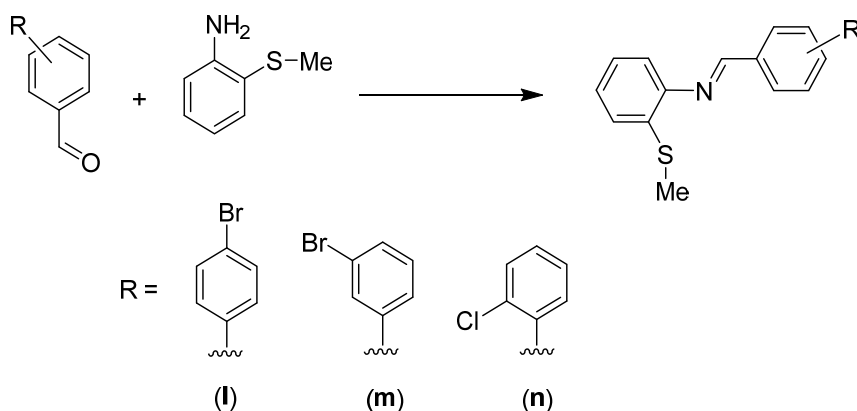


Table 49. Quantities of materials used to prepare [C, N, S] ligands.

	Aldehyde's		2-methylthioaniline	
	g	mmol	g	mmol
l	0.5	2.70	0.376	2.70
m	0.5	2.70	0.376	2.70
n	0.5	3.55	0.495	3.55

8.1.2 Synthesis of cyclopalladated compounds **1l-1n**.

In a 100 mL Schlenk round flask, palladium chloride was added to lithium chloride in methanol (40 cm³) for 3 hours under nitrogen. Then, the appropriate amount of the corresponding ligand (1.2 equivalent) was then added, and the mixture was refluxed for 1 hour at 70 °C. After which, it was cooled to room temperature, and sodium acetate (15 equivalents; 6.09 mmol) was added. Yellow **1l**, orange, **1m**, and **1n**, precipitates were formed, which were centrifuged, washed with methanol, and dried in a vacuum.

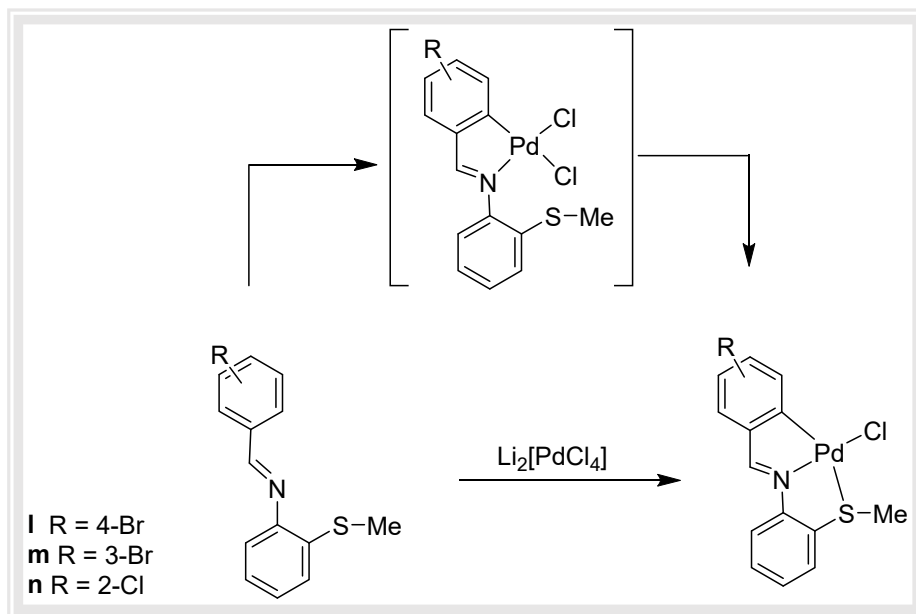
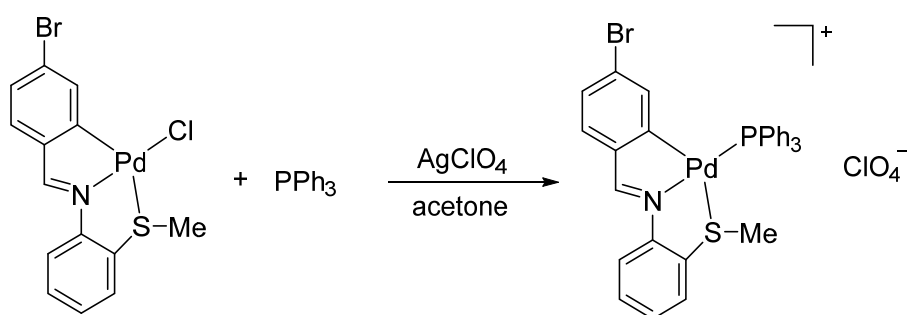


Table 50. Quantities of materials used to prepare cyclometallated compounds containing [C, N, S] ligands.

compound	ligand		Li ₂ [PdCl ₄]	
	g	mmol	g	mmol
1l	0.1	0.32	0.104	0.40
1m	0.1	0.32	0.104	0.40
1n	0.1	0.38	0.117	0.45

8.1.3 Synthesis of cyclopalladated compound with triphenylphosphine ligand **2l**.

In a 50 mL round bottom flask, 0.01 g (0.02 mmol) of compound **1l** was added to acetone (10 cm³). The appropriate amount 0.004 g (0.02 mmol) of AgClO₄ was added and mixed for 4 hours. Then, the solution was centrifuged to separate the AgCl, which was then treated with 0.005 g (0.02 mmol) triphenylphosphine (PPh₃) and was agitated at room temperature for 24 hours. The obtained residue was recrystallized in CH₂Cl₂/n-hexane and vacuum dried. Yield 60 %.



8.1.4 Synthesis of cyclopalladated compound with dppm ligand **2n**.

In a 50 mL round bottom flask, 0.01 g (0.02 mmol) of compound **1n** was added to acetone (10 cm³). For 4 hours, the appropriate amount of 0.005 g (0.02 mmol) AgClO₄ was added. The solution was then centrifuged to isolate the AgCl, which was subsequently treated with 0.009 g (0.02 mmol) of dppm and agitated at room temperature for 24 hours. The resultant residue was recrystallized in CH₂Cl₂/n-hexane and vacuum dried. Yield 50%.

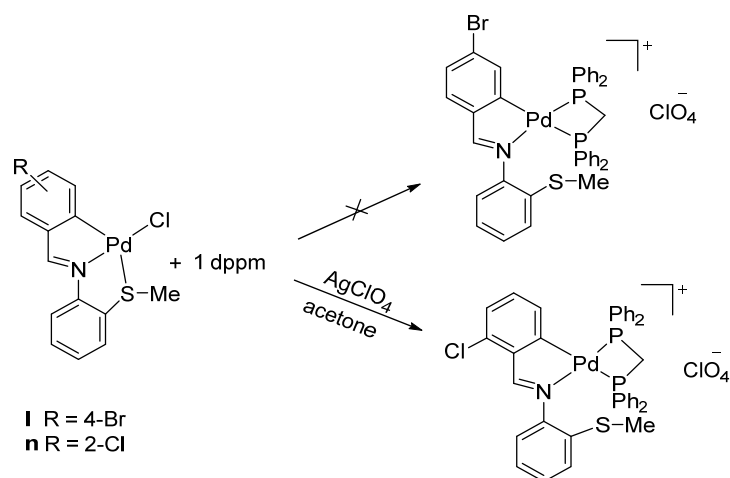


Table 51. Quantities of materials used to prepare cyclometallated compounds [C, N, S] with dppm ligand.

compound	dppm		AgClO ₄	
	g	mmol	g	mmol
1n	0.02	0.049	0.018	0.049

8.2 NMR Studying

Schiff bases (imines) are one of the most commonly used families of organic compounds.^{149,150,151} The formation of the Schiff base ligand (alternatively imines) was performed in a slightly basic or an acidic

¹⁴⁹ S. Patai, (1970).

¹⁵⁰ R. Holm, G. Everett Jr, A. Chakravorty, *Progress in Inorganic Chemistry*, (1966) 83-214.

¹⁵¹ P.A. Vigato, S. Tamburini, *Coordination Chemistry Reviews*, 248 (2004) 1717-2128.

medium.¹⁵² Due to their significant biological activities,¹⁵³ Schiff bases have piqued the interest of organic chemists.

8.2.1 Study of compounds **l-n**.

In the ¹H NMR spectra of **l-n**, a singlet *ca.* 8.50-8.80 ppm was assigned to the HC=N proton of the imine group. The number, position, and multiplicity of the corresponding signals of the benzylidene aromatic ring are determined by the different substitutions in each. It's also worth noting that the HC=N and H6 resonances appear at a lower field than expected due to the anisotropic shielding effect of the C=N double bonds (*vide supra*). Other resonances such as the SMe and amine aromatic protons signals were assigned accordingly.

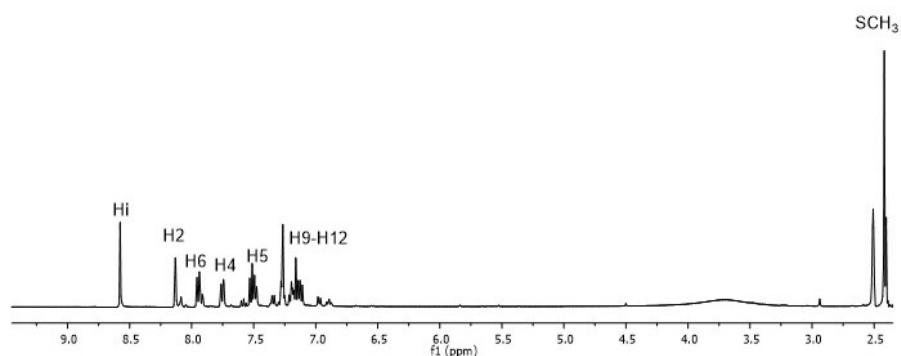
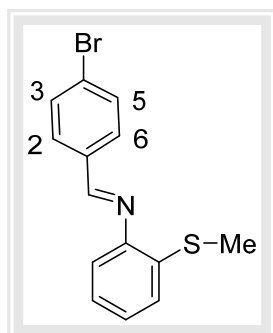


Table 52. ¹H NMR spectrum of ligand **m** in dmsd₆.

¹⁵² A. Karakaş, H. Ünver, A. Elmali, *Journal of Molecular Structure*, 877 (2008) 152-157.

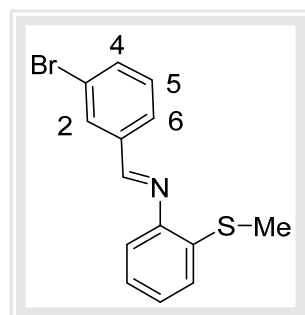
¹⁵³ K. Deyuan, Q. Chen, X. Yuyuan, Z. Xigeng, *Chinese Journal of Medicinal Chemistry*, 10 (2000) 13-17.

ligand **l**



Yield 75 %. IR = $\nu(\text{C}=\text{N})1625 \text{ cm}^{-1}$.

^1H NMR (400 MHz, $\text{dms}\text{-d}_6$) δ (ppm) = 8.57 (s, 1H, Hi), 7.89 (d, $N = 8.5 \text{ Hz}$, 2H, H2, H6), 7.75 (d, $N = 8.5 \text{ Hz}$, 2H, H3, H5), 7.24 (m, 4H, H9, H10, H11, H12), 2.4 (s, 3H, SCH_3).

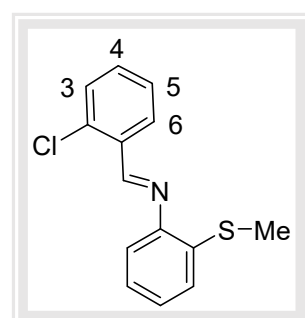


ligand **m**

Yield 85 %. IR = $\nu(\text{C}=\text{N}) 1628 \text{ cm}^{-1}$.

^1H NMR (400 MHz, $\text{dms}\text{-d}_6$) δ 8.58 (s, 1H, Hi), 8.13 (s, 1H, H2), 7.95 (d, $^3J_{\text{H}_6\text{H}_5} = 8.0 \text{ Hz}$, 1H, H6), 7.75 (d, $^3J_{\text{H}_4\text{H}_5} = 8.0 \text{ Hz}$, 1H, H4), 7.50 (m, 1H, H5), 7.27 (m, 4H, H9, H10, H11, H12), 2.42 (s, 3H, SCH_3).

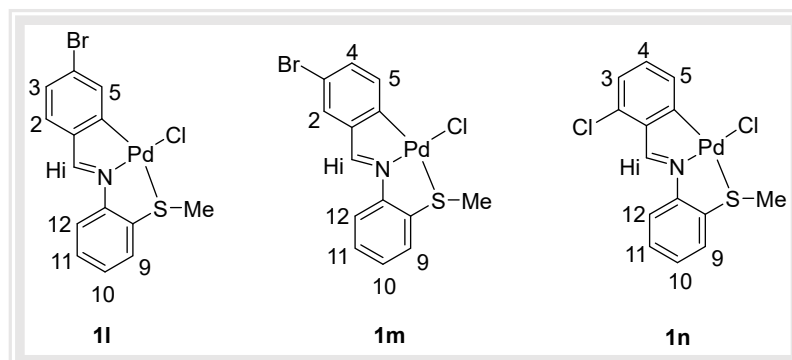
ligand **n**



Yield 95 %. IR = $\nu(\text{C}=\text{N}) 1623 \text{ cm}^{-1}$.

^1H NMR (400 MHz, $\text{dms}\text{-d}_6$) δ 8.81 (s, 1H, Hi), 8.19 (dd, $^3J_{\text{H}_6\text{H}_5} = 7.8 \text{ Hz}$, $^4J_{\text{H}_6\text{H}_4} = 1.8 \text{ Hz}$, 1H, H6), 7.59 (dd, $^3J_{\text{H}_3\text{H}_4} = 7.8 \text{ Hz}$, $^4J_{\text{H}_3\text{H}_5} = 1.8 \text{ Hz}$, 1H, H3), 7.53 (m, 1H, H4), 7.38 (m, 1H, H5), 7.29 (m, 4H, H9, H10, H11, H12), 2.41 (s, 3H, SCH_3).

8.2.2 Study of compounds **1l-1n**.



The ^1H NMR characterization of compounds **1l-1n** was carried out with a chlorine ligand terminal in deuterated DMSO- d_6 for (**1l**), and acetone- d_6 for (**1m** and **1n**). In all cases, the HC=N resonance was shifted to a down field upon coordination of the nitrogen atom to palladium.¹⁵⁴ Thus, singlet signals at 9.35 (**1l**) 9.23 (**1m**), and 9.30 (**1n**) were ascribed.

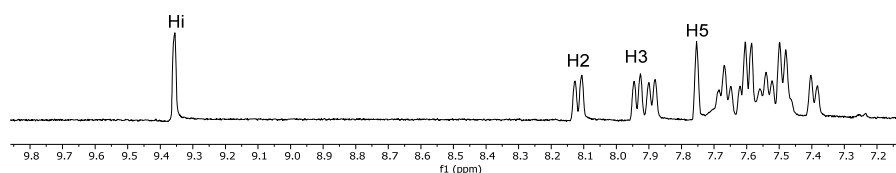
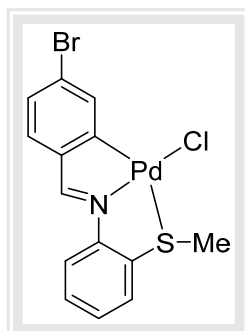


Figure 98. ^1H NMR spectrum of compound **1l** in dmsd $_6$.

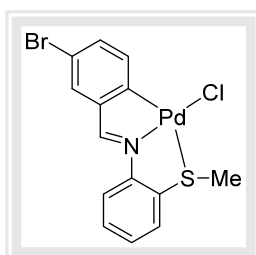
The variation in the integration and multiplicity of the protons signals in the aromatic zone confirms the activation of the C-H bond, which leads to the formation of the metallacycle; in all cases the C(6)-H resonances are absent. The aromatic proton resonances were assigned accordingly. The proton H5 of **1l-1n** forms as a singlet for **1l**, doublet for **1m** and multiplet for **1n**, at 7.75 ppm, 7.33 ppm and 7.32 ppm, respectively.

compound 1l



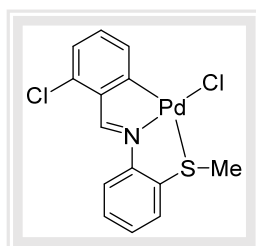
Yield 88 %, IR = $\nu(\text{C}=\text{N})$ 1550 cm^{-1} , $\nu(\text{Pd}-\text{Cl}_{\text{trans-N}})$ 315 cm^{-1} . ^1H NMR (400 MHz, $\text{dms}\text{-d}_6$) δ 9.35 (s, 1H, Hi), 8.12 (d, $^3J_{\text{H}_2\text{H}_3} = 7.7$ Hz, 1H, H2), 7.94 (d, $^3J_{\text{H}_3\text{H}_2} = 7.7$ Hz, 1H, H3), 7.89 (d, $^3J = 7.9$ Hz, 1H), 7.75 (s, 1H, H5), 7.67 (t, $^3J_{\text{H}_{10}\text{H}_{11}} = ^3J_{\text{H}_{10}\text{H}_9} = 8.0$ Hz, 1H, H10), 7.59 (d, $^3J_{\text{H}_9\text{H}_{10}} = 8.0$ Hz, 1H, H9) 7.54 (t, $^3J_{\text{H}_{11}\text{H}_{10}} = ^3J_{\text{H}_{11}\text{H}_{12}} = 8.0$ Hz, 1H, H11), 7.49 (d, $^3J_{\text{H}_{12}\text{H}_{11}} = 8.0$ Hz, 1H, H12) 7.39 (d, $^3J = 8.0$ Hz, 1H), 2.89 (s, 3H, SCH_3).

compound 1m



Yield 75 %, IR = $\nu(\text{C}=\text{N})$ 1563 cm^{-1} , $\nu(\text{Pd}-\text{Cl}_{\text{trans-N}})$ 310 cm^{-1} . ^1H NMR (400 MHz, acetone-d_6) δ 9.23 (s, 1H, Hi), 8.06 (d, $^3J_{\text{H}_4\text{H}_5} = 8.1$ Hz, 1H, H4), 7.85 (d, $^3J_{\text{H}_5\text{H}_4} = 8.1$ Hz, 1H, H5), 7.74 (s, 1H, H2), 7.68 (m, 1H, H10), 7.50 (d, $^3J_{\text{H}_9\text{H}_{10}} = 7.9$ Hz, 1H, H9), 7.40 (m, 1H, H11), 7.33 (d, $^3J_{\text{H}_{12}\text{H}_{11}} = 7.9$ Hz, H12), 7.08 (d, $^3J = 8.1$ Hz, 1H). 2.87 (s, 3H, SCH_3).

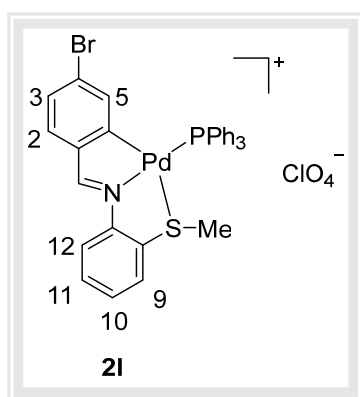
compound 1n



Yield 80 %, IR = $\nu(\text{C}=\text{N})$ 1565 cm^{-1} , $\nu(\text{Pd}-\text{Cl}_{\text{trans-N}})$ 314 cm^{-1} . ^1H NMR (400 MHz, acetone-d_6) δ 9.30 (s, 1H, Hi), 8.22 (d, $^3J_{\text{H}_3\text{H}_4} = 8.0$ Hz, 1H, H3), 7.85 (d, $^3J_{\text{H}_5\text{H}_4} = 8.0$ Hz, 1H, H5), 7.69 (d, $^3J_{\text{H}_9\text{H}_{10}} = 7.6$ Hz, 1H, H9), 7.60 (t, $^3J_{\text{H}_4\text{H}_5} = ^3J_{\text{H}_4\text{H}_3} = 8.0$ Hz, 1H, H4), 7.56 (m, 1H, H10), 7.20 (t, $^3J_{\text{H}_{11}\text{H}_{12}} = ^3J_{\text{H}_{11}\text{H}_{10}} = 7.7$ Hz, 1H, H11), 7.11 (d, $^3J_{\text{H}_{12}\text{H}_{11}} = 7.7$ Hz, 1H, H12), 2.80 (s, 3H, SCH_3).

8.2.3 Study of compound **21**.

The reactivity of compound **11** in comparison to PPh_3 was investigated. Compound **21** was created when compound **11** was treated with PPh_3 . This compound is formed when the Pd-S link is cleaved and a PPh_3 is incorporated into the palladium coordination sphere.



In the ^1H NMR spectrum, the presence of one PPh_3 ligand attached to the palladium in a trans-arrangement to the nitrogen is compatible with the position and multiplicity of signals. The $\text{HC}=\text{N}$ was coupled with the ^{31}P nucleus and given a value *ca.* 9.48 ppm (d, $^4J(\text{PHi}) = 8.3$ Hz) and a doublet at 6.57 ppm (d, $^4J(\text{PH5}) = 4.9$ Hz), is assigned to proton H5 coupling with the ^{31}P nucleus, due to the so-called transphobia effect, this is the usual outcome of the reaction between [C, N] cyclopalladated compounds and phosphine ligands.¹⁵⁵ A doublet at 7.37 and 7.45 (d, $^3J(\text{H2H3}) = 7.5$ Hz, 1H) was assigned to the proton H2

In the ^1H NMR spectrum, the presence of one PPh_3 ligand attached to the palladium in a trans-arrangement to the nitrogen is compatible with the position and multiplicity of signals. The $\text{HC}=\text{N}$ was coupled with the ^{31}P nucleus and given a value *ca.* 9.48 ppm (d, $^4J(\text{PHi}) = 8.3$ Hz) and a doublet at 6.57 ppm (d, $^4J(\text{PH5}) = 4.9$ Hz), is assigned to proton H5 coupling with the ^{31}P nucleus, due to the so-called transphobia effect, this is the usual outcome of the reaction between [C, N] cyclopalladated compounds and phosphine ligands.¹⁵⁵ A doublet at 7.37 and 7.45 (d, $^3J(\text{H2H3}) = 7.5$ Hz, 1H) was assigned to the proton H2

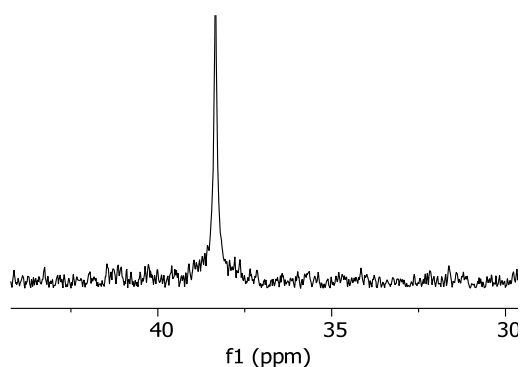


Figure 99. $^{31}\text{P}\{-^1\text{H}\}$ NMR of compound **21** in CDCl_3 .

¹⁵⁵ J. Vicente, J.A. Abad, A.D. Frankland, M.C. Ramírez de Arellano, *Chemistry–A European Journal*, 5 (1999) 3066-3075.

and H3. The overlapping protons of 2-(methylthio)aniline with phosphine protons ranged from 7.54 to 8.16 ppm. The $^{31}\text{P}\{-^1\text{H}\}$ NMR showed a singlet *ca.* 38.5 ppm.

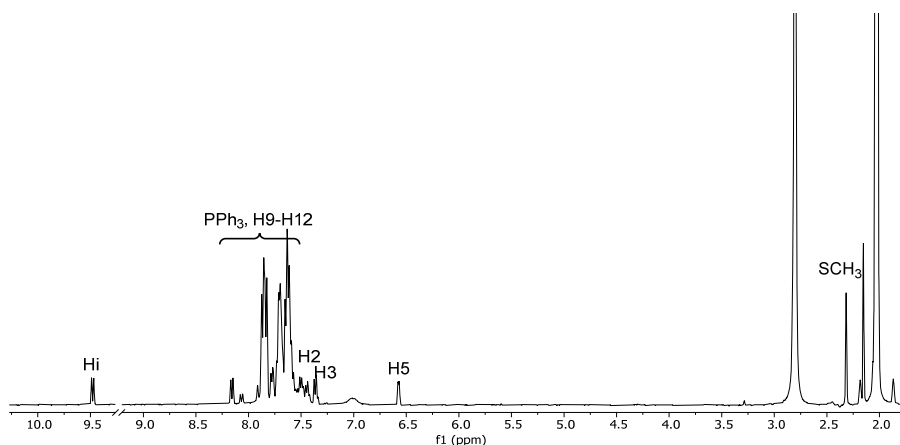
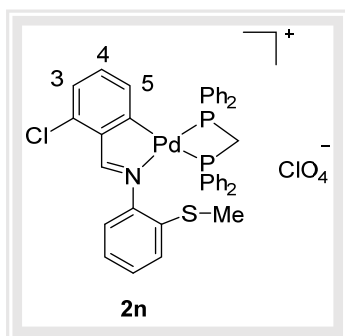


Figure 100. ^1H NMR of compound 2l in acetone- d_6 .

8.2.4 Study of compound 2n.

The reactivity of compounds 1l and 1n with dppm were investigated, and it was observed that the coordination complex dichloro-(1,1-bis(diphenylphosphino)methane-*P,P*)-palladium(II) was formed in



compound 2l, whereas compound 2n was found to be a non-pure compound.

In the ^1H NMR spectrum of 2n, a singlet signal at 9.08 ppm was assigned to the $\text{HC}=\text{N}$. A doublet at 6.33 ppm ($^4J = 8.3$ Hz) was assigned to the H5 proton coupled with the ^{31}P nucleus. Protons H3 and H4 overlapping with protons 2-(methylthio)aniline and phosphine protons ranged from 6.82 to 8.0 ppm. The CH_2 of the phosphine group, which provides an

AA'XX' pattern by connecting to the two-phosphorus nucleus, showed as a multiplet at 4.40 ppm.

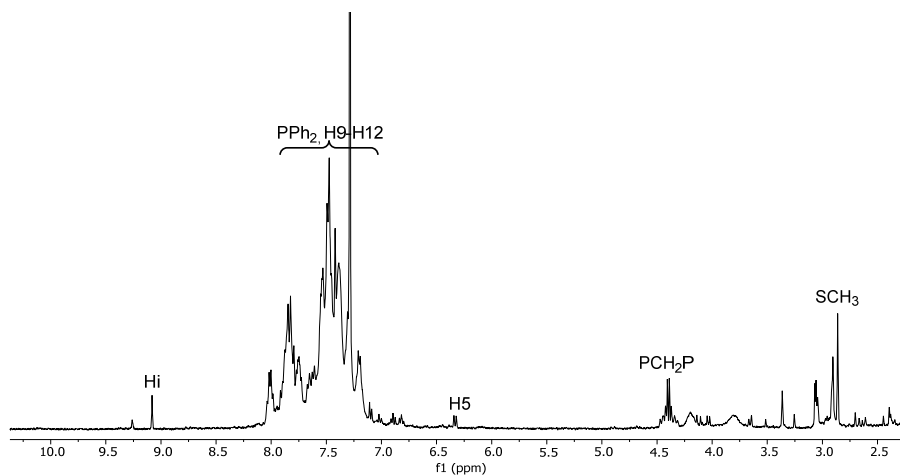


Figure 101. ^1H NMR of compound 2n in acetone- d_6 .

The $^{31}\text{P}\{-^1\text{H}\}$ NMR showed two doublets at 51.44 and *ca.* 24 ppm ($J = ca.$ 25 Hz), assigned to the chelating coordination mode of the diphosphine ligand. In addition to singlets *ca.* 31, 14, and -54 ppm.

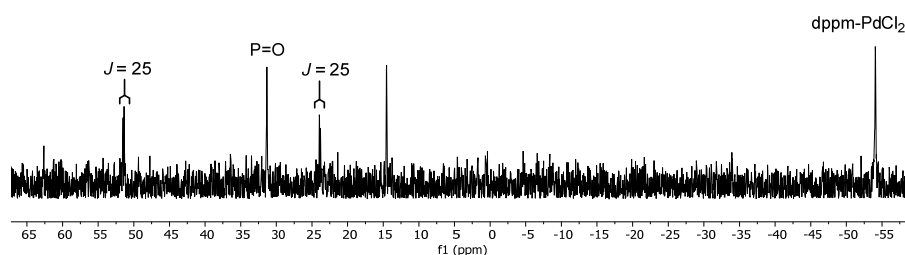


Figure 102. $^{31}\text{P}\{-^1\text{H}\}$ NMR of compound 2n in CDCl_3 .

8.3 Study of X-ray diffraction

8.3.1 Study structure of compounds **1l** and **1n**.

The crystal structure of compounds **1l** and **1n**, as determined by X-ray diffraction, confirms the spectroscopic data. The structures are made up of discrete molecules of $[\text{Pd}\{4\text{-Br-C}_6\text{H}_4\text{-(H)C=N(C}_6\text{H}_4\text{-2-SMe)}\}\text{Cl}]$ in **1l** separated by van der Waals contacts. Asymmetric unit of the crystal structure of **1n** yielded two unique molecules.

The structure shows four fused rings, with three sharing the palladium atom. The organometallic metallated ring $[\text{Pd}(1)\text{C}(6)\text{C}(1)\text{N}(1)\text{C}(7)]$ shares a carbon-carbon bond with the benzylidene ring, whilst the coordination ring $[\text{Pd}(1)\text{N}(1)\text{C}(8)\text{C}(13)\text{S}(1)]$ shares a carbon-carbon bond with the imine aromatic ring molecule has a tetracyclic system formed by an aryl ring that shares a C-C bond with the chelate ring. The palladium atom is bonded to the four different donor atoms chlorine, sulfur, imine nitrogen, and the C6 atom of the phenyl ring, in a slightly distorted square-planar environment. The Pd(1)-C(6) and Pd(1)-N(1) bond lengths are comparable to those reported earlier.¹⁵⁶ The Pd(1)-S(1) bond distance of 2.3802(8) Å is somewhat longer than expected, due to the *trans* influence of the phenyl carbon atom.¹⁵⁷ The angles are within the reported literature values, in the range 81.73(17)-96.99(4).

¹⁵⁶ O. Kennard, F. Allen, *Des. Autom. News*, 8 (1993) 31-37.

¹⁵⁷ T. Appleton, H. Clark, L. Manzer, *Coordination Chemistry Reviews*, 10 (1973) 335-422.

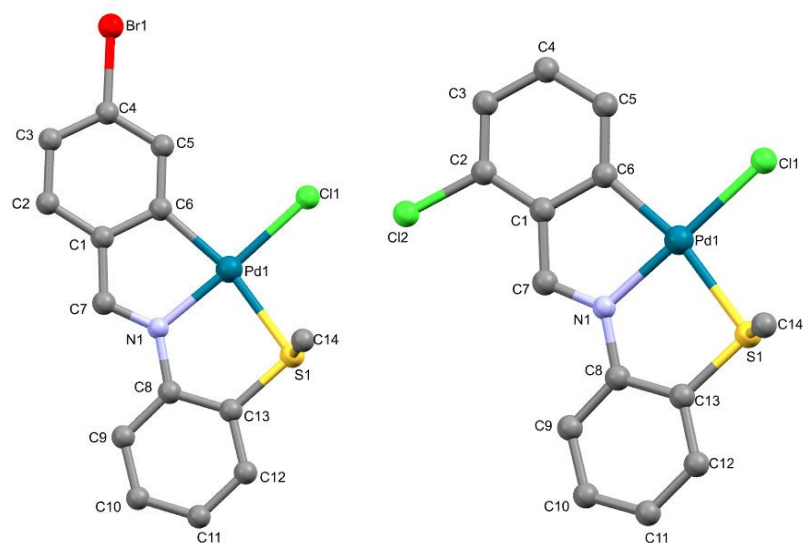


Figure 103. Crystal structures of compounds **1l** and **1n**.

The lengths of the C=N bond length, 1.293(5) Å in **1l**, and 1.307(6) Å in **1n** also show a value to those found in related palladacycles derived from Schiff bases.¹⁵⁸ The distance between the Cl and the H(10) atom in compound **1n** [2.908 Å]^{159,160} also points to a weak Cl \cdots H–C(10) intramolecular interaction.

¹⁵⁸ (a) J. Albert, M. Gomez, J. Granell, J. Sales, X. Solans, *Organometallics*, 9 (1990) 1405-1413.

(b) A.-S.S.H. Elgazwy, *Monatshefte für Chemie-Chemical Monthly*, 139 (2008) 1285-1297.

¹⁵⁹ A.v. Bondi, van der Waals volumes and radii, *The Journal of physical chemistry*, 68 (1964) 441-451.

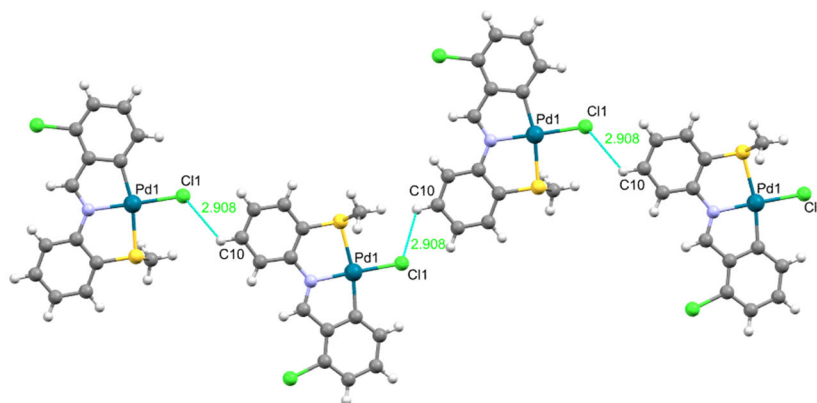


Figure 104. The intermolecular interaction between Cl and the H10 of compound 1n.

The structures of compound 1n display stacking π - π interactions, which were observed between phenyl rings of the ligand. The distances Cg1-Cg2 [3.860 Å], Cg2-Cg3 [3.769 Å] and Cg3-Cg4 [3.695 Å].

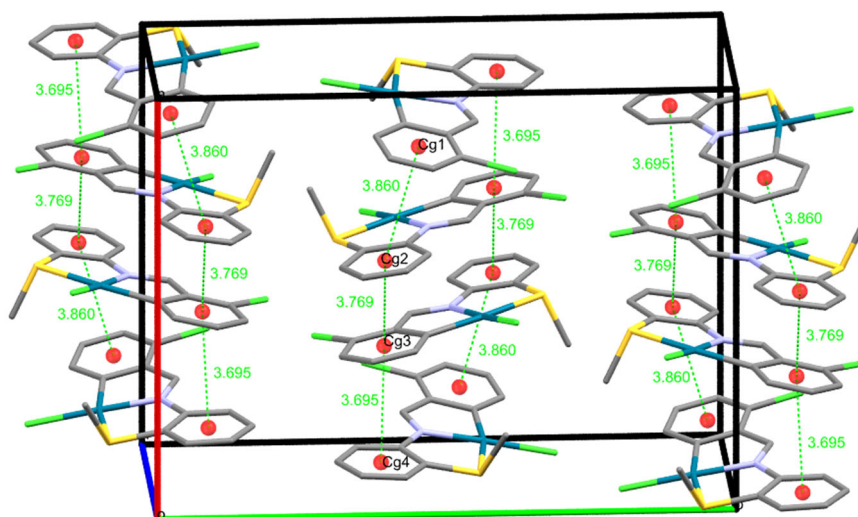


Figure 105. π - π interactions between phenyl rings of ligands in the packing crystal structures of compound 1n.

Table 53. Compound 1l was obtained from X-ray single-crystal diffraction studies. Bond lengths are given in [Å] and angles in [°].

Pd(1)-C(6)	1.992(4)	C(3)-C(2)	1.384(7)
Pd(1)-N(1)	2.013(3)	C(2)-C(1)	1.399(6)
Pd(1)-Cl(1)	2.313(11)	N(1)-C(8)	1.423(5)
Pd(1)-S(1)	2.380(11)	C(8)-C(9)	1.393(6)
N(1)-C(7)	1.293(5)	C(9)-C(10)	1.380(7)
C(7)-C(1)	1.436(6)	C(10)-C(11)	1.393(7)
C(1)-C(6)	1.418(6)	Pd(1)-N(1)-C(8)	120.04(3)
C(6)-C(5)	1.381(6)	C(6)-Pd(1)-Cl(1)	95.81(13)
C(11)-C(12)	1.389(6)	C(6)-Pd(1)-N(1)	81.73(16)
C(13)-C(8)	1.397(6)	N(1)-Pd(1)-S(1)	85.03(10)
C(5)-C(4)	1.394(6)	S(1)-Pd(1)-Cl(1)	96.99(4)
C(4)-C(3)	1.384(6)	Pd(1)-S(1)-C(13)	95.94(15)
C(12)-C(13)	1.399(6)	S(1)-C(13)-C(8)	121.00(3)

Table 54. Symmetric conformer 1n was obtained from X-ray single-crystal diffraction studies. Bond lengths are given in [Å] and angles in [°].

Pd(1)-C(6)	1.990(4)	C(8)-C(9)	1.396(6)
Pd(1)-N(1)	2.000(3)	C(9)-C(10)	1.390(6)
Pd(1)-S(1)	2.368(11)	C(10)-C(11)	1.375(6)
Pd(1)-Cl(1)	2.304(11)	C(11)-C(12)	1.383(6)
N(1)-C(7)	1.307(6)	C(12)-C(13)	1.392(6)
C(7)-C(1)	1.434(7)	C(13)-C(8)	1.400(6)
C(1)-C(2)	1.404(7)	C(6)-Pd(1)-N(1)	82.38(19)
C(2)-C(3)	1.366(6)	N(1)-Pd(1)-S(1)	85.39(10)
C(3)-C(4)	1.391(6)	C(6)-Pd(1)-Cl(1)	96.18(5)

C(4)-C(5)	1.385(6)	Cl(1)-Pd(1)-S(1)	96.11(5)
C(5)-C6	1.387(7)	Pd(1)-S(1)-C(13)	96.28(18)
C(6)-C(1)	1.425(7)	C(13)-C(8)-N(1)	117.69(5)
N(1)-C(8)	1.417(5)		

Table 55. Asymmetric conformer 1n was obtained from X-ray single-crystal diffraction studies. Bond lengths are given in [Å] and angles in [°].

Pd(2)-C(16)	1.987(4)	C(22)-C(23)	1.403(5)
Pd(2)-N(2)	2.005(3)	C(23)-C(24)	1.388(5)
Pd(2)-S(2)	2.375(9)	C(24)-C(25)	1.380(5)
Pd(2)-Cl(3)	2.304(9)	C(25)-C(26)	1.372(5)
N(2)-C(21)	1.305(5)	C(26)-C(27)	1.390(5)
C(21)-C(15)	1.444(5)	C(27)-C(22)	1.398(5)
C(15)-C(20)	1.394(5)	C(16)-Pd(2)-N(2)	82.06(14)
C(20)-C(19)	1.383(5)	N(2)-Pd(2)-S(2)	85.37(9)
C(19)-C(18)	1.378(5)	C(16)-Pd(2)-Cl(3)	95.08(11)
C(18)-C(17)	1.391(5)	Cl(3)-Pd(2)-S(2)	97.63(3)
C(17)-C(16)	1.395(5)	Pd(2)-S(2)-C(27)	96.29(12)
N(2)-C(22)	1.417(5)	C(27)-C(22)-N(2)	118.55(3)

Table 56. Crystal data and structure refinement for **1l** and **1n**.

Crystal structure	1l	1n
Molecular formula	C ₁₄ H ₁₁ BrClNPdS	C ₁₄ H ₁₁ Cl ₂ NPdS
Formula weight	447.08	402.60
Temperature/K	100.0	100.0
Crystal system	Trigonal	monoclinic
Space group	R-3	P2 ₁ /c
a/Å	28.1329(12)	14.3485(3)
b/Å	28.1329(12)	18.2981(3)
c/Å	9.5511(7)	10.9824(2)
α /°	90	90
β /°	90	99.9460(10)
γ /°	120	90
Volume/Å ³	6546.6(7)	2840.10(9)
Z	18	8
$\rho_{\text{calc}}/\text{cm}^3$	2.241	1.883
μ/mm^{-1}	4.333	15.236
F(000)	3888.0	1584.0
Crystal size/mm ³	0.22 × 0.04 × 0.04	0.1 × 0.05 × 0.03
Radiation	MoK α (λ = 0.71073)	CuK α (λ = 1.54184)
θ range for data collection/°	4.58 to 56.568	6.254 to 149.412
Index ranges	-37 ≤ h ≤ 37, -37 ≤ k ≤ 37, -12 ≤ l ≤ 12	-17 ≤ h ≤ 17, -22 ≤ k ≤ 22, -13 ≤ l ≤ 13
Reflections collected	55099	81659
Independent reflections	3633 [R _{int} = 0.0815, R _{sigma} = 0.0333]	5808 [R _{int} = 0.0922, R _{sigma} = 0.0355]
Data/restraints/parameters	3633/0/174	5808/0/346
Goodness-of-fit on F ²	1.044	1.038
Final R indexes [I >= 2 σ (I)]	R ₁ = 0.0394, wR ₂ = 0.0855	R ₁ = 0.0325, wR ₂ = 0.0744
Final R indexes [all data]	R ₁ = 0.0561, wR ₂ = 0.0918	R ₁ = 0.0464, wR ₂ = 0.0801
Largest diff. peak/hole / e Å ⁻³	2.11/-1.51	0.81/-0.94

CHAPTER 9

Catalysis

9.1 Introduction

Palladium(II) development began in the late 1960s with the presence of aryl compounds, either stoichiometric or catalytic, by Richard Heck via a breakthrough appealing area of palladium-catalyzed carbon-carbon bond formation reactions. In the years thereafter, many palladium compounds have enhanced C-C coupling reactions, and palladium-catalyzed coupling reactions have been widely employed and useful in organic synthesis. The Heck, Negishi, and Suzuki reactions¹⁶¹ are significant reactions that received the Nobel Prize in chemistry in 2010 "for palladium-catalyzed cross couplings in organic synthesis," showing the importance and excellence of organic chemistry.¹⁶²

The Suzuki-Miyaura is considered one of the most extensively utilized cross-coupling reactions ($R_1-MR_2n = R_1-B(OH)_2$), due to mild experimental conditions and strong stabilities of the substrate boronic acid to air, water, and elevated temperatures.¹⁶³ Palladium compounds catalyze a range of reactions, including hydrogenation, oxidation, and carbon-carbon coupling. Palladium is classed as a good catalyst, most helpful, and has a higher activity than other metals such as copper, nickel, and iron. However, palladium shares essential properties with

¹⁶¹ (a) R.F. Heck, J. Nolley Jr, *The Journal of organic chemistry*, 37 (1972) 2320-2322.

(b) E. Negishi, Anthony O. King, and Nobuhisa Okukado, *The Journal of organic chemistry*, 42 (1977) 1821-1823.

¹⁶² T.N.P.i.C. 2010, Prize Announcement, (2010).

¹⁶³ N. Miyaura, K. Yamada, *Tetrahedron Letters*, 20 (1979) 3437-3440.

other transition metals, such as the ability to readily react with nonpolar bonds seen in alkenes, alkynes, and arenes. This interaction results in simple, selective, and often reversible oxidative addition, transmetallation, and reductive elimination.

9.1.1 cross-coupling reactions

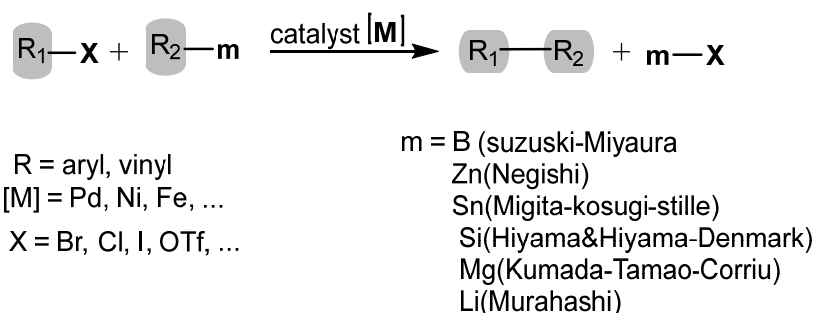
Carbon-carbon bond formation processes are critical for the synthesis of bioactive compounds, agrochemicals, and pharmaceuticals. Furthermore, they are employed to create new organic materials with novel electrical properties.¹⁶⁴ cross-coupling reactions have been one of the most important advances in organic and organometallic synthesis since catalysis was discovered.¹⁶⁵ Over the last half-century, C-C bond formation reactions have been widely investigated, and new methods for mediating reactions in a controlled and selective manner under moderate conditions have been devised employing transition metals. Many of the transformations in concern would be impossible to accomplish without the use of transition metal-based catalysts.

In the presence of a metal catalyst [M], cross-coupling reactions are characterized as carbon-carbon bond-forming reactions between an organic electrophile (R_1-X) and an organometallic nucleophile (R_2-M) (Scheme 7). Transition metal compounds of groups 8–10, in particular nickel and palladium, are commonly employed as catalysts in these processes. The fundamental reason these two metals are used in the

¹⁶⁴ P. Ruiz-Castillo, S.L. Buchwald, *Chemical reviews*, 116 (2016) 12564-12649.

¹⁶⁵ R. Jana, T.P. Pathak, M.S. Sigman, *Chemical reviews*, 111 (2011) 1417-1492.

great majority of cross-coupling reactions is due to their ease of redox state exchange, Ni(II)/Ni(0) and Pd(II)/Pd(0), which is a requirement to complete the catalytic cycle. The metal present in the nucleophile is widely used to sort C-C cross-coupling reactions. The Negishi reaction, for example, uses organo-zinc reagents, the Stille reaction uses organotin reagents, the Suzuki-Miyaura reaction uses organoboron reagents, and so on.¹⁶⁶



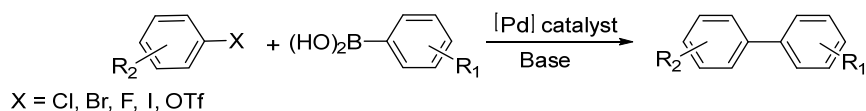
Scheme 7. General Scheme for C-C cross-coupling reactions.

9.1.2 The Suzuki-Miyaura cross-coupling reaction.

The Suzuki-Miyaura reaction is catalyzed by palladium and involves the cross-coupling of organoborane compounds ($Ar_1-B(OR)_2$) with electrophiles (Ar_2-X).^{167,168} This is one of the most effective ways to connect aryl rings with carbon-carbon bonds (Scheme 8).

¹⁶⁶ M.C. D'Alterio, È. Casals-Cruañas, N.V. Tzouras, G. Talarico, S.P. Nolan, A. Poater, *Chemistry—A European Journal*, 27 (2021) 13481-13493.

¹⁶⁷ A. Suzuki, *Chemical communications*, (2005) 4759-4763.



Scheme 8. The Suzuki-Miyaura cross-coupling reaction.

The organoboron reagents are commercially available, less poisonous, and air- and moisture-stable, which gives the Suzuki-Miyaura reaction various advantages.¹⁶⁹ Another significant feature is the ability to use water as a solvent.^{170,171} Because water is a good microwave heating solvent, the use of water as a solvent in combination with microwave heating has been studied.¹⁷² The Suzuki-Miyaura reaction's catalytic cycle is considered to begin with oxidative addition of the electrophile (Ar₂-X) to the catalyst, resulting in the intermediate Ar₂-[Pd]-X. The resulting compound is transmetalated between Ar₂-[Pd]-X and (Ar₁-B(OH)₂) to yield the disubstituted palladium species Ar₁-[Pd]-Ar₂, after which the palladium-disubstituted moiety is reductively eliminated, releasing a new coupling product (Ar₁-Ar₂) and regenerating the catalyst,

¹⁶⁸ N. Miyaura, A. Suzuki, *Journal of the Chemical Society, Chemical Communications*, (1979) 866-867.

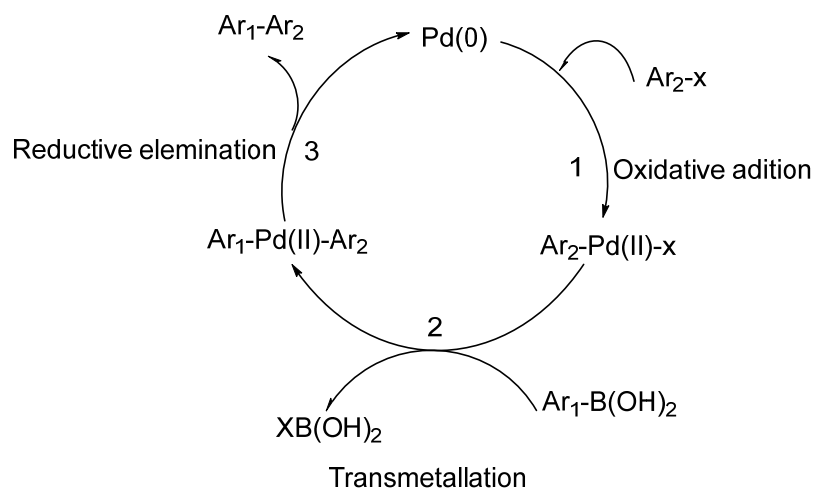
¹⁶⁹ A. Suzuki, *Angewandte chemie international edition*, 50 (2011) 6722-6737.

¹⁷⁰ C. Röhlich, A.S. Wirth, K. Köhler, *Chemistry-A European Journal*, 18 (2012) 15485-15494.

¹⁷¹ A. Fihri, D. Luart, C. Len, A. Solhy, C. Chevrin, V. Polshettiwar, *Dalton Transactions*, 40 (2011) 3116-3121.

¹⁷² N.E. Leadbeater, *Chemical Communications*, (2005) 2881-2902.

which is incorporated back into the cycle; the latter step verifies the palladacycle (Scheme 9).



Scheme 9. The Suzuki-Miyaura catalytic cycle.

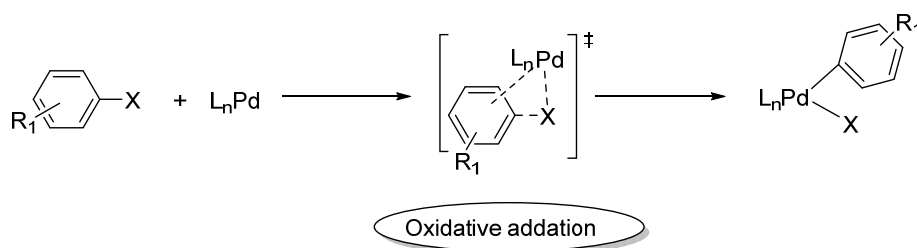
The first and last steps are shared by all cross-coupling reactions and have been thoroughly investigated using experimental and computational methods.¹⁷³ The transmetallation step, however, differs in cross-coupling reactions due to differences in the nucleophile utilized as well as the reaction conditions. Furthermore, because of the difficulties in isolating/characterizing critical intermediates, experimental evidence for this step is difficult to come by. As a result, it's not surprising that we know so little about the transmetallation step, given that it's the least researched.

¹⁷³ M. García-Melchor, M. Pacheco, C. Najera, *Acc. Chem. Res.*, 46 (2013) 2626-

Pre-activation of the active species is a crucial step that has an impact on the overall reaction. Thus, selecting a good precatalyst with bulky and electron-donating ligands will benefit the catalytic cycle by improving oxidative addition and reductive elimination while also avoiding the problem of an unwanted side reaction, β -elimination.

9.1.3 Oxidative addition

The oxidative addition step in the catalytic cycle breaks the bond between the heteroatom X and the organic R₁ group, forming two new bonds with the LPd⁰ metal compound and oxidizing the metal. The oxidation state of the metal is raised by two units as a result of the creation of these bonds. Furthermore, the strength of the C-X bond is known to affect the ease of oxidative addition; consequently, the ligand of the Pd(0) active species that is produced before the oxidative addition step is important (Scheme 10).



Scheme 10. General mechanism of oxidative addition.

The rate-determining step in the catalytic cycle is oxidative addition, which decreases relative reactivity in the order I > OTf > Br > Cl.¹⁷⁴

The oxidative addition of Pd(0) compounds is an SN₂-type mechanism, as evidenced by the unmistakable evidence of stereochemical inversion of configuration at alkyl halides carbon.¹⁷⁵ According to mechanistic research, the seemingly straightforward oxidative addition step is made up of four parallel isomerization routes leading from the cis isomer to the more stable trans isomer.¹⁷⁶

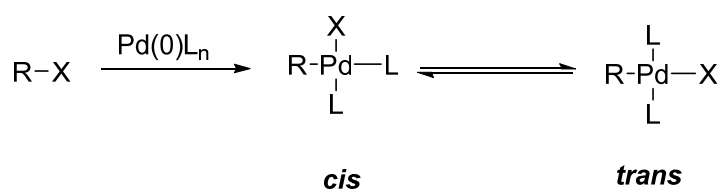


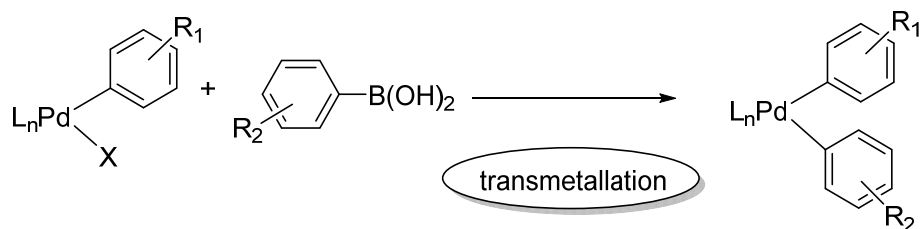
Figure 106. oxidative addition isomerization pathways from the *cis* isomer to trans isomer.

9.1.4 Transmetallation

Transmetallation is a reaction in which an organic group is transferred from one metal to another, similar to ligand exchange between metals. Furthermore, because each cross-coupling reaction uses a different nucleophile, this step is the most distinctive of C-C cross-coupling reactions. The Suzuki-Miyaura reaction is a good example of this (Scheme 11). The transmetallation step is defined as the exchange of the organoboron species' organic group (R₂-B(OH)₂) with a halogen or pseudo halogen ligand and the Pd compound (L_nPd(II)XR₁).

¹⁷⁵A.O. Aliprantis, J.W. Canary, *Journal of the American Chemical Society*, 116 (1994) 6985-6986.

¹⁷⁶A.L. Casado, P. Espinet, *Organometallics*, 17 (1998) 954-959.

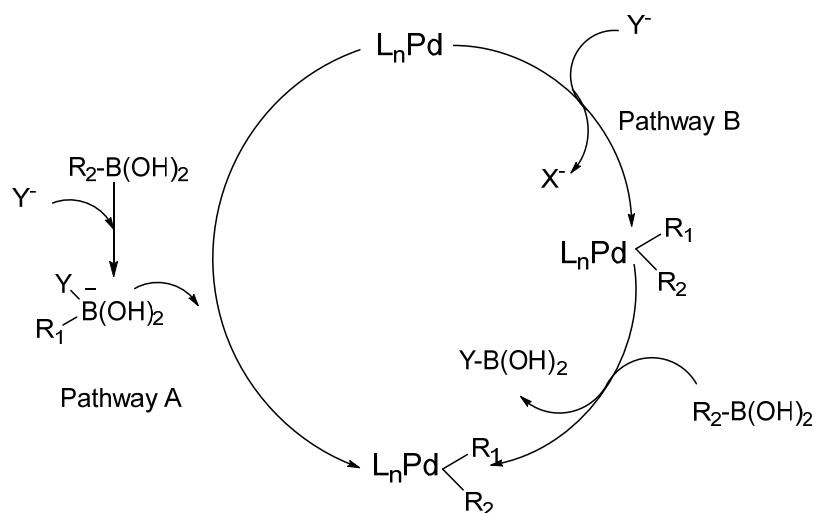


Scheme 11. General pathway for the transmetallation step.

Base promotes the transfer of the aryl or alkyl group from the organoborane to the Pd compound by initiating transmetallation. As a result, the requirement of a base¹⁷⁷ leads to two possible outcomes (Scheme 12).¹⁷⁸ In the first pathway, *pathway A*, the base attacks the organoboron compound, generating an anionic "ate compound" (an organoboronate species) that will attack the palladium halide compound nucleophilically. *Pathway B*, on the other hand, works in two steps: first, a ligand substitution occurs between the halogen and the base, and then the new compound reacts with the neutral organoborane. However, although transmetallation can occur in two ways, both lead to the same intermediate, $L_nPd-R_1R_2$, which has never been identified.

¹⁷⁷A. Chartoire, M. Lesieur, L. Falivene, A.M. Slawin, L. Cavallo, C.S. Cazin, S.P. Nolan, *Chemistry—A European Journal*, 18 (2012) 4517–4521.

¹⁷⁸S.L. Buchwald, K. Fugami, T. Hiyama, M. Kosugi, M. Miura, N. Miyaura, A. Muci, M. Nomura, E. Shirakawa, K. Tamao, *Springer*, 2003.



Scheme 12. transmetallation pathways step of Pathway A and pathway B.

9.1.5 Reductive elimination

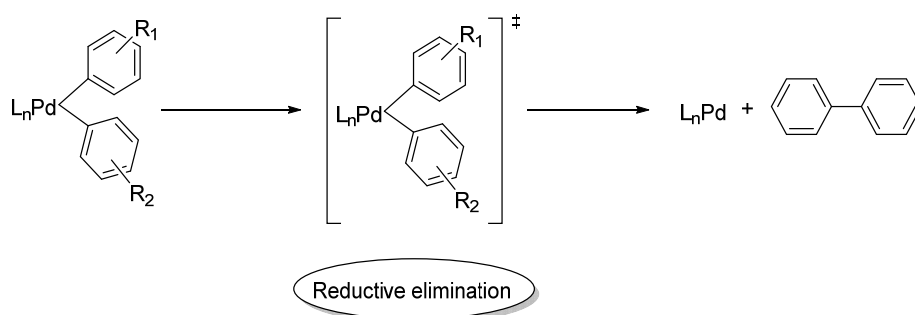
The final step in the catalytic cycle is reductive elimination, which is the inverse of oxidative addition. Thus, two bonds are broken, and one bond is created between two organic groups in the cis position, decreasing the metal from Pd(II) to Pd(0) and regenerating the active catalyst. The metal's oxidation state is decreased by two units, to be precise. Different factors, such as the properties of the ligands, influence reductive elimination, as they do in the oxidative Addition step.^{179,180,181} The ligands' effects have demonstrated that electron-donating and bulky ligands favor this step; more specifically, the

¹⁷⁹ J. Jover, N. Fey, M. Purdie, G.C. Lloyd-Jones, J.N. Harvey, *Journal of Molecular Catalysis A: Chemical*, 324 (2010) 39-47.

¹⁸⁰ R.J. Lundgren, M. Stradiotto, *Chemistry—A European Journal*, 18 (2012) 9758-9769.

¹⁸¹ Y. Lan, P. Liu, S.G. Newman, M. Lautens, K. Houk, *Chemical Science*, 3 (2012) 1987-1995.

ligands' steric hindrance reduces the duration of the transient $L_nR_1PdII R_2$ species, increasing the reaction rate.^{182,183} Furthermore, reductive elimination can take place via a variety of methods, however, in monodentate Pd(II) compounds, the mechanism is coordinated (Scheme 13). The coupling of a single C-C bond via a three-coordinated transition state is well recognized in this pathway.



Scheme 13. A mechanism for the reductive elimination step.

9.1.6 Catalysts

Suzuki coupling is most commonly used with palladium catalysts. Precursors (for example, $Pd(OAc)_2$, $Pd_2(dba)_3$, or $Pd(PPh_3)_4$) and ligands are normally found in active Pd catalysts. To improve the catalyst's reactivity and stability, it was designed to be electron-rich and spatially bulky, resulting in a high turnover number (TON) and low loading. Palladacycles (Figure 107) were designed as an example, and they have thermal stability, fast reaction times, are insensitive to

¹⁸² C. Amatore, A. Jutand, G. Le Duc, *Chemistry—A European Journal*, 17 (2011) 2492-2503.

¹⁸³ D.A. Culkin, J.F. Hartwig, *Organometallics*, 23 (2004) 3398-3416.

air and water, are minimal in cost, and are environmentally beneficial.^{184,185} illustrates the outcomes of some of the most important attempts in the production of highly active ligands for use in cross-coupling reactions throughout the last decade.

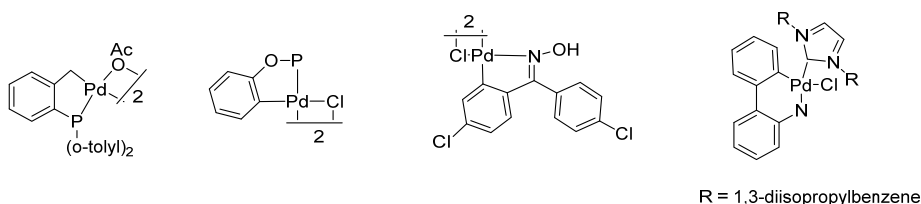


Figure 107. Palladacycle catalysts in activity.

9.1.7 Boronic acid derivatives

In general, organoboron compounds (e.g., boronic acids, boronic esters, and boronamides) include at least one carbon–boron (C–B) bond.^{186,187} Organoboron compounds have been employed in chemical synthesis for over 60 years.^{188,189} Since then, chemistries using such compounds have developed to the point where they have become one of the most diversified, well-studied, and commonly used groups of reagents in catalysis and organic synthesis.¹⁹⁰ They are now working

¹⁸⁴ O. Navarro, R.A. Kelly, S.P. Nolan, *Journal of the American Chemical Society*, 125 (2003) 16194-16195.

¹⁸⁵ D.A. Alonso, C. Nájera, M.C. Pacheco, *The Journal of organic chemistry*, 67 (2002) 5588-5594.

¹⁸⁶ I. Maluenda, O. Navarro, *Molecules*, 20 (2015) 7528-7557.

¹⁸⁷ A. Suzuki, Y. Yamamoto, *Chemistry letters*, 40 (2011) 894-901.

¹⁸⁸ J.W. Fyfe, A.J. Watson, *Chem*, 3 (2017) 31-55.

¹⁸⁹ H.C. Brown, T.E. Cole, *Organometallics*, 2 (1983) 1316-1319.

¹⁹⁰ E. Dimitrijevic, M.S. Taylor, *ACS Catalysis*, 3 (2013) 945-962.

on a variety of classic and important reactions, including hydroboration and Suzuki–Miyaura cross-couplings.¹⁹¹

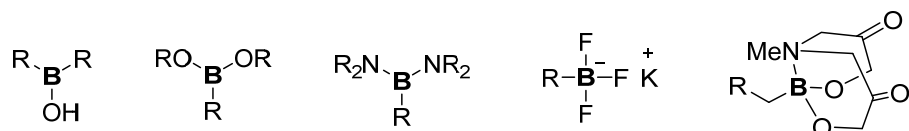


Figure 108. Derivatives of organoboron compounds in Suzuki–Miyaura cross-couplings.

9.2 Methodology

9.2.1 System of reaction

A parallel reaction system was employed with a 12-position Ralleys® reaction carousel for a quick and precise comparison of reactions carried out with different catalysts. The carousel is made up of two blocks separated by roughly 5 cm, as shown in (Figure 109 and Figure 110). The lower block slides into a plate heater, which regulates agitation speed and temperature (from ambient temperature to 220 °C) for up to twelve reactions at once. The upper block, which is chilled by a stream of water, effectively cools all tubes, reducing evaporation and solvent loss. Furthermore, its radial gas distribution system, in combination with unique waterproof covers screwed directly into each reaction tube, allows inert gas to be transported to the 12 reaction tubes, making it perfect for reactions that require an environment free

of air and humidity. The twelve reaction tubes with a volume of 5 to 20 cm³ are positioned between both bases, increasing heat transfer from the heated base to the reflux head and guaranteeing that all tubes are heated and cool at the same rate. Each tube's cap has a button for controlling gas flow and vacuum, as well as a septum for injecting or extracting solvents from the reaction tube.



Figure 109. Radleys® Reaction Carousel



Figure 110. reaction tube.

9.2.2 Method of working

9.2.2.1 The reactions procedure

In the carousel tubes, the reaction is carried out by loading the correct amounts of aryl halide, phenylboronic acid, base, and catalyst. Close the Radleys® tube and perform three vacuum/nitrogen sequences if the reaction is carried out in an inert atmosphere. After that, the right amount of solvent is added under a current of nitrogen and the mixture is stirred at the proper temperature and for the requisite amount of time.

The tubes are pulled from the carousel when the reaction time has passed and allowed to cool to ambient temperature. After cooling with 0.1 M HCl(aq), the reaction is stopped, and the linked chemical is extracted with the necessary amount of dichloromethane. Anhydrous sodium sulfate is used to eliminate any traces of water, and the organic phase is extracted, and dried under a vacuum. To determine the degree of conversion achieved, ^1H NMR is done on the residue.

9.2.2.2 Methodology of experimentation

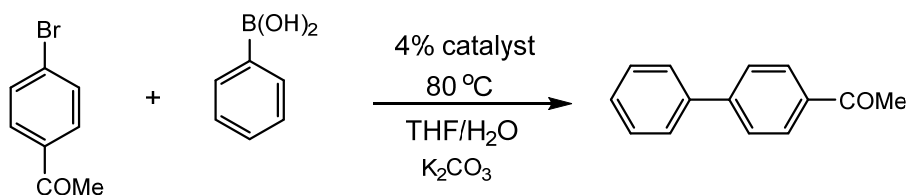


Figure 111. Scheme of reaction

In a carousel tube add 0.1 mmol of 1-(4-Bromophenyl)ethanone (20 mg), and 1.2 equivalents of phenylboronic acid (14.7 mg) to 3 cm³ of THF/H₂O (2:1). 2 potassium carbonate (K₂CO₃) equivalents (27.8 mg) with 4 % catalyst (expressed in percent of Pd). For 24 hours, the solution is heated to 80 °C. After this time, 0.1 cm³ of 0.01 M HCl is added to bring the reaction to a stop.

After cooling, the reaction was filtered to remove any precipitate and a dichloromethane extraction was performed. The organic phase is dried with anhydrous sodium sulfate, filtered, and dried in a rotary evaporator. The outcomes of the reactions are examined using ¹H NMR spectroscopy. The integral of the signal corresponds to the product versus the starting reagent.

9.2.2.3 ¹H NMR detection of reactions

The degree of conversion of the reactions is determined by ¹H NMR, which compares the intensity of the signal corresponding to the protons of the aryl halide substituent groups to the intensity of the same group corresponding to the linked product.

Following that, the ¹H NMR research is described. would be obtained for the reaction shown in Figure 113.

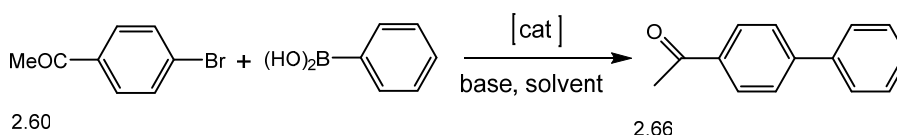


Figure 112. Example reaction for conversion calculation.

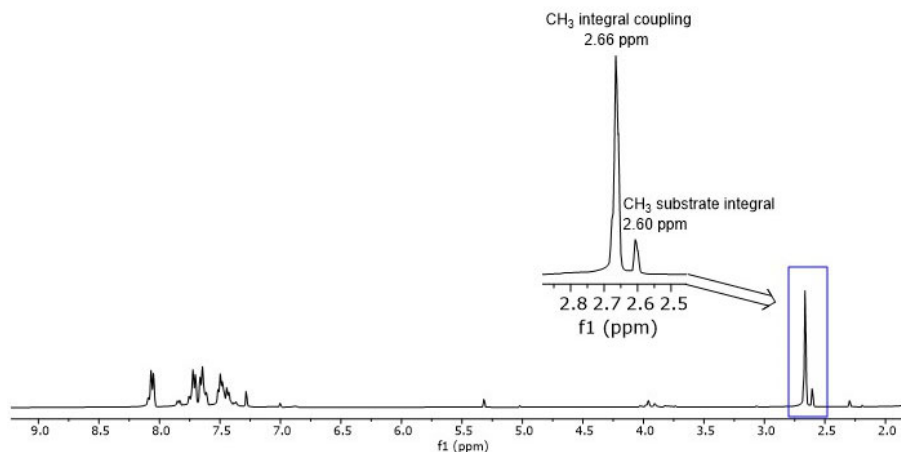


Figure 113. example of conversion calculation.

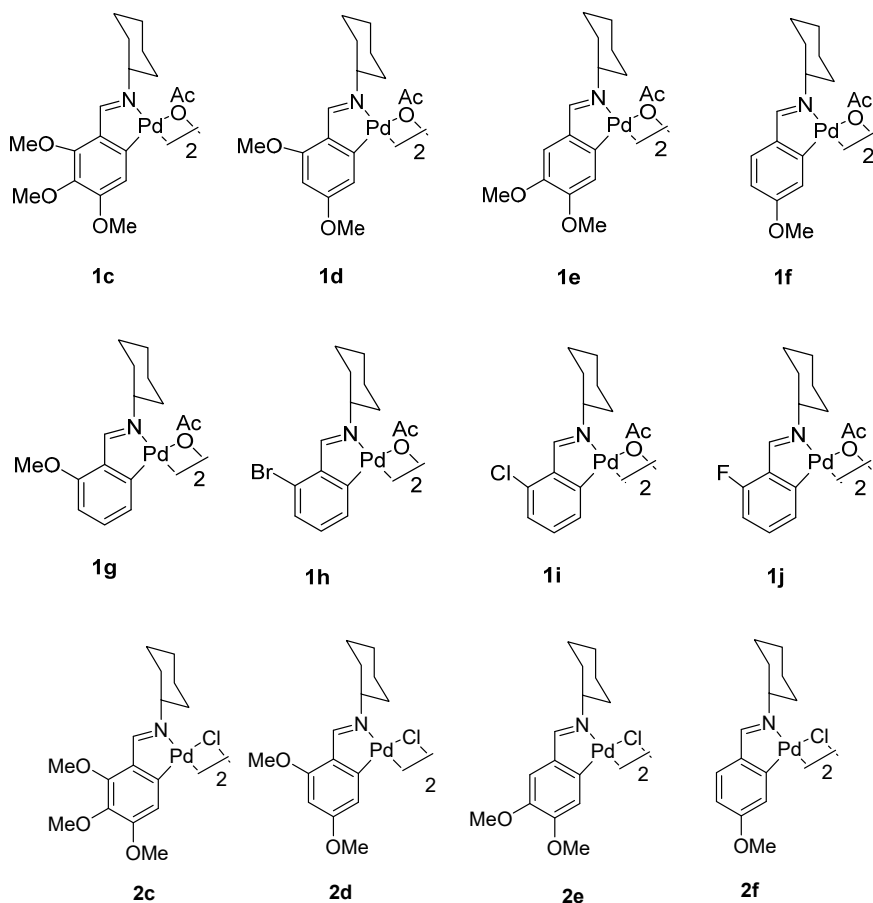
By convention, the signal corresponding to the methoxyl group of the linked product integrates for a unit, whereas the signal corresponding to the methoxyl group of the starting aryl bromide integrates for a value that is dependent on the conversion. As a result, applying the formula below to obtain the degree of conversion is sufficient:

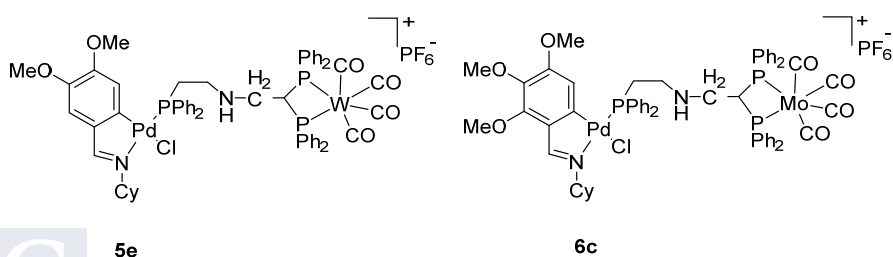
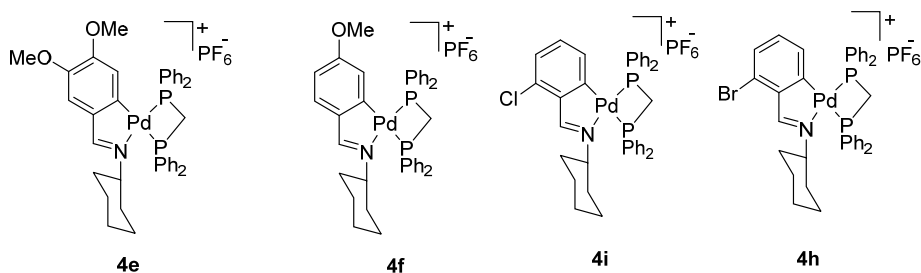
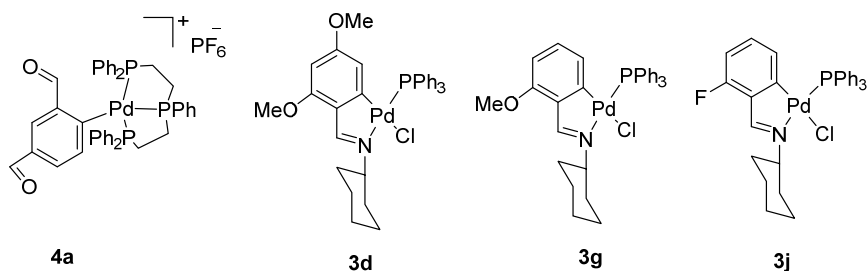
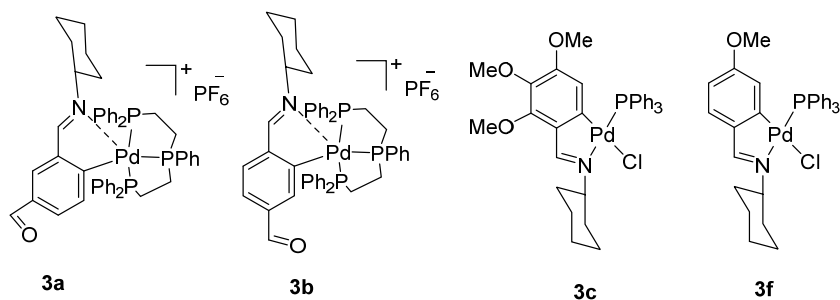
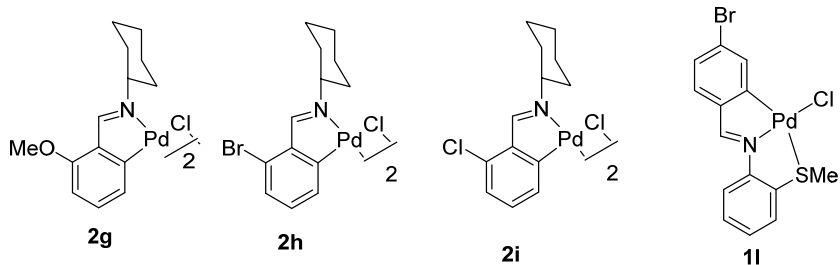
$$\% \text{ conversion} = \frac{\text{integral coupling}}{\text{substrate integral} + \text{integral coupling}} \times 100$$

As a result, in the instance of the example illustrated, we would have a conversion rate of 86%.

9.2.3 Compounds used as catalysts

The compounds were utilized as catalysts in the Suzuki reaction, as well as the results. Although a design reaction can be established, each attempt or entrance condition must be defined due to the complexity and variety of the systems used. Tests were carried out on the catalysts that most showed a higher conversion in these conditions and employed aryl bromide as substrates. The reactions in condition were carried out in the different solvents and with the same base.





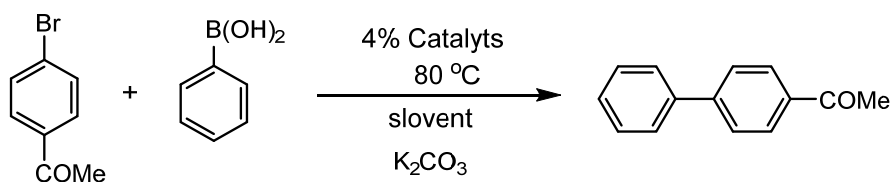


Table 57. Tests were done of the compounds in the Suzuki-Miyaura reaction's catalytic activity.

[cat]	T(°C)	T(h)	solvent	Conv. (%)
1c	80	24	THF/H ₂ O	91 %
1d	80	24	THF/H ₂ O	92 %
1e	80	24	THF/H ₂ O	98 %
1f	80	24	THF/H ₂ O	98 %
1g	80	24	THF/H ₂ O	99 %
1h	80	24	THF/H ₂ O	100 %
1i	80	24	THF/H ₂ O	100 %
1j	80	24	THF/H ₂ O	100 %
2c	80	24	THF/H ₂ O	88 %
2d	80	24	THF/H ₂ O	86 %
2e	80	24	THF/H ₂ O	88 %
2f	80	24	THF/H ₂ O	88 %
2g	80	24	THF/H ₂ O	95 %
2h	80	24	THF/H ₂ O	95 %
2i	80	24	THF/H ₂ O	94 %
3a	80	24	EtOH/H ₂ O	95 %
3b	80	24	EtOH/H ₂ O	92 %
3c	80	24	THF/H ₂ O	100 %
3d	80	24	THF/H ₂ O	100 %
3f	80	24	THF/H ₂ O	100 %
3g	80	24	THF/H ₂ O	100 %
3j	80	24	THF/H ₂ O	100 %
4a	80	24	EtOH/H ₂ O	2%

4e	80	17	EtOH/H ₂ O	100 %
4f	80	17	EtOH/H ₂ O	100 %
4i	80	17	EtOH/H ₂ O	100 %
4h	80	17	EtOH/H ₂ O	100 %
5e	80	24	EtOH/H ₂ O	65 %
6c	80	24	EtOH/H ₂ O	5 %
1l	80	24	EtOH/H ₂ O	99 %

The results of the catalysis tests using the compounds produced from Schiff base ligands reported are shown in table 56. conversions that were made, which were calculated using the integrals of the group signal –COMe, as well as the reaction conditions, such as time and temperature. K₂CO₃ was employed as a base in all cases. The phenylboronic acid and 4-bromoacetophenone were utilized with a THF: H₂O and EtOH: H₂O mixture as a solvent.

Based on the results, it can be concluded that the ligand from which the compound is derived has a substantial influence on its catalytic activity, which is determined by its structure and the most influential coordinating ligands in it. As a result, there have been more tests with the compounds produced from ligands **c-j** and **a-b**. The solvent's influence is taken into account, it appears that THF: H₂O and EtOH: H₂O produce the same results.

Initial catalysis studies demonstrated that compounds containing palladium linked to the PPh₃ and dppm phosphine ligands have higher catalytic activity. In all cases, reactions carried out at 80 °C provide a higher conversion even though compounds containing acetate bridge ligands **1c**, **1d**, **1e**, and **1f** have better catalytic activity than the

compounds containing chloride bridge ligands **2c**, **2d**, **2e**, and **2f**. This does not apply to compounds containing bridging acetate and chloride ligands **1g**, **1h**, **1i**, **1j**, **2g**, **2h**, **2i**, and **2j**, which have both high activities. For compound **1l**, in which the metal atom is coordinated to two five-membered chelate rings, giving high catalytic activity. Compounds **3a** and **3b**, which have a diimine ligand, also demonstrated a high conversion compared to compound **4a**, which contains two formal aldehydes and has a significantly lower activity. This indicates that imine ligand with electron-donating groups in the nitrogen moiety improves catalytic performance when the catalytic species is generated in situ with the palladium. Whereas compound **5e** occurs conversion higher than compound **6c**, this could be due to the compound's stability, which makes it difficult to interact with the substrate, resulting in lower catalytic activity.

Compounds containing PPh_3 and dppm ligands are also effective and gave a high conversion although reaction proceeds at a shorter and longer time. We concluded that most compounds in general, produced satisfactory outcomes, and with the phosphine ligands are the most efficient, due to their greater ease of synthesis and stability, they have been the compounds used to conduct a more detailed study of catalytic activity.

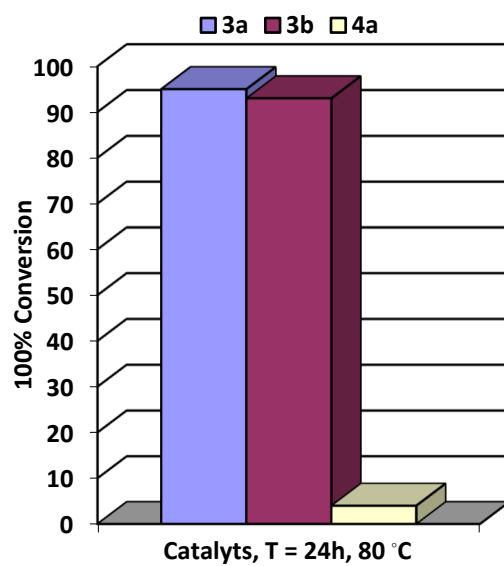


Figure 114. Graph of conversions achieved by catalysts containing nitrogen donor imine ligand and non-nitrogen donor.

CHAPTER 10

Conclusions

- 1- Cyclometallated palladium(II) compounds have been synthesized using Schiff bases **a-b** with general formulas 1,3-(CyN=CH)₂C₆H₄ and 1,4-(CyN=CH)₂C₆H₄, which have been described in **Chapter 6**.
- 2- Schiff base ligands **c-j** and **k**, whose general formulas are given in **Chapter 7** on general considerations, were used to create cyclometallated palladium(II) compounds.
- 3- The coordination compounds [N, S] are formed when ligands **l-n** react with lithium tetrachloropalladate, and the organometallic compounds [C, N, S] **1l-1n** are afforded a strong Pd-S with nucleophiles without bond cleavage.
- 4- The phosphine ligands are placed mutually in *trans* in the structures of the compounds in **Chapter 6**, and the structures confirm the existence of one, or two, non-coordinate formyl groups. The formyl groups of the molecule are parallel to the metalated phenyl ring.
- 5- Non-cyclometallated Pd(II) compounds with one or two uncoordinated formyl groups have been successfully synthesized with cyclohexylamine in molar ratio 1:1, and with aminophosphine ligand in molar ratio 1:1 or 1:2.
- 6- The compound's crystal structures have been determined **1b**, **4a**, **6b** and **7b**. In each structure, the metal atom is in a slightly distorted square planar environment, resulting in a Pd combination.
- 7- Crystal structures **3b** and **9b** have been obtained a dinuclear structure with two (HC=NCy) groups and triphos ligands are coupled to the palladium centers via the nitrogen lone pair.
- 8- The synthesis of cyclometallated palladium(II) with vdpp, dppm, and acetylacetonate ligands, all of which have one formyl group, has proven unsuccessful with aminophosphine ligand, resulting in mixed products.

- 9- Compounds containing one or two uncoordinated aminophosphines produced **9a-9b** and **10a-10b** have been unable to synthesize with the appropriate palladium and platinum salts, resulting in phosphine ligand decomposition.
- 10- Compounds generated from imine ligands **c-j** have been effectively synthesized and are summarized in **Chapter 7**. It has been demonstrated that metalation of the ligands results in compounds having a dinuclear with acetate bridge ligands. their reactivity to triphenylphosphine and diphosphine ligands has been investigated.
- 11- In its structure, Mo and W compounds with uncoordinated ligand donor atoms were formed. These compounds' reactivity with compounds **2c-2g** results in the formation of heterodinuclear compounds **5c-5g** and **6c-6f**.
- 12- The reaction of bromide bridged dimer compound **2k** with dppm gave mononuclear compound **3k** and it has been determined by X-ray diffraction.
- 13- Valid crystals for resolution by X-ray diffraction have been obtained in some cases in **Chapter 8**, and their crystalline structure has been determined.
- 14- The catalytic activity of several of the compounds generated in the Suzuki cross-coupling reaction was investigated, and it was discovered that most of them are active in the reaction. **Chapter 9** summarizes the findings.



The metallocycles are compounds that are contained within organometallic chemistry and that can have a very different nature depending on the metal as well as on the ligands attached to it. Because to this, their properties and reactivity cover

a large field of research.

In this work, the study of this type of compounds using nitrogen and phosphorus ligands, which may have very different characteristics, will be addressed. This allows the design of the synthesis of families of compounds that have the usual properties and applications of the metallocycles, such as their use as catalysts in industrial processes, the evaluation of their potential cytotoxicity or luminescent properties related mainly to metal.